THE VISCOSITY OF HUMAN BLOOD AT HIGH HEMATOCRITS

by

James Douglas Oliver III

S.B. (1981) Massachusetts Institute of Technology

SUBMITTED TO THE DEPARTMENT OF CHEMICAL ENGINEERING IN PARTIAL FULFILLMENT OF THE REQUIREMENTS FOR THE DEGREE OF

MASTER OF SCIENCE

IN CHEMICAL ENGINEERING

at the

MASSACHUSETTS INSTITUTE OF TECHNOLOGY

February 1986

Signature of Author

Department of Chemical Engineering
February 19, 1986

Certified by _____

Clark K. Colton
Thesis Supervisor

Accepted by _____

William M. Deen
Chairman, Department Graduate Committee

The Viscosity of Human Blood at High Hematocrits

by

James Douglas Oliver III

Submitted to the Department of Chemical Engineering on February 19, 1986 in partial fulfillment of the requirements for the degree of Master of Science in Chemical Engineering.

Abstract

The viscosity of human blood was measured in both plasma and saline suspensions with a Haake Rotovisco RV100 viscometer. Hematocrits of samples ranged from below physiologic to greater than 98, and shear rates ranged from 0.03 to 300 sec^{-1}. Even at high concentrations, blood retained its fluidity, with viscosity at high shear rates on the order of 50-100 cP. At high hematocrits, where cell-cell crowding is the dominant rheological mechanism, the type of suspending fluid had a negligible effect on the absolute viscosity, but led to an artificially higher relative viscosity for the saline suspensions. At lower hematocrits and lower shear rates, where aggregation and cell-protein interactions are important, the absolute viscosity of plasma suspensions was higher. The emulsive properties of the red cell, however, created a lower relative relative viscosity for plasma suspenisons than for cells in saline. The data was fit to the three-parameter Quemada equation, and empirical curves were developed to represent blood viscosity as a function of shear rate and hematocrit over the range of experimentation. Examination of the rheological parameters provided some indication as to the thresholds of influence for the important mechanisms of blood viscosity. Most noteworthy, it appears that at hematocrits of 65 to 80 and higher, the erythrocytes begin to behave as a continuous phase and blood viscosity becomes independent of the suspending fluid. The mathematical expressions are of interest in the design of clinical cross-flow membrane plasmapheresis devices, in which high concentrations are established near the filter.

Thesis Supervisor: Clark K. Colton
Title: Bayer Professor of Chemical Engineering

Acknowledgments

This is the hardest part to write, where I must attempt to thank within the space of a few paragraphs the people who have made this possible. I gratefully acknowledge the support of the GEM, Prince, and Kleberg Foundations and the Amoco Oil Corportation during the work of this thesis.

Many thanks to Professor Clark K. Colton, for his guidance and patience and his insistence on quality. Thanks also to Gail Gamboa and Barbara Driscoll for their help and for making life so pleasant around the office.

Thanks to Andrew Zydney for his always excellent advice and the best of luck to him in his career. Also to W. Mark Saltzman, fellow vampire, for sharing jokes and saving me a lot of time along the way. Mark Green of the Ceramics Laboratory was a big help in mastering the vagaries of viscometry, even if he might have gotten queasy at the sight of blood. David Yarmush's assistance with albumin labeling was greatly appreciated.

The Medical Engineering/Medical Physics program of the Division of Health Sciences and Technology consistently admits an odd assortment of people who know how to make long hours pass quickly. If they ever graduate, there will be some serious damage inflicted on the world. I also thank countless friends at M.I.T. and Harvard Medical School, too many to name here.

To my many teachers, and especially to Mrs. Bright, who kept me off the streets, I give my eternal gratitude.

Christine and Ed have put up with me for a long time and will have to continue to do so. The chances are that they'll probably never read this, so I'll admit that they have been better friends than I deserve.

My little sisters, Jeanne and June, probably don't realize how old and wise they've gotten over the past few years, or how much I depend on them, but if they ever find out, I'm in big trouble.

And finally, to my parents, for whom the words just do not exist.

Table of Contents

List of Figures

List of Tables

Chapter 1

INTRODUCTION

The study of the viscosity of blood traces its roots back to the dawn of rheology, to the pioneering days of Poiseuille [1843], and with advances in scientific instrumentation reached its peak in the 1960s with the numerous works of Merrill, Cokelet, Dintenfass, Copley, Chien, and many others. In more recent times, attention has turned to the microscopic phenomena underlying the observed physical behavior, such as the properties of the red cell membrane and the mechanisms of the cell-cell and cell-fluid interactions [Skalak *et al.*, 1981a and 1981b; Secomb *et al.*, 1983a and 1983b]. Despite the complex rheological nature of blood suspensions, they in many ways are an ideal system for the study of non-Newtonian fluid mechanics: The particles are well-defined and almost identical to one another, they deform in a well-characterized manner, and the extent of their aggregation and deformation can be controlled through the system properties. The fluid-like nature of the erythrocytes and their aggregability give blood suspensions properties similar to emulsions and polymers.

Since most blood viscosity work has been carried out with an eye toward understanding phyisological and clinical-pathological conditions, the vast majority of data exists at cell concentrations around 40-50 volume per cent. A limited amount of data for concentrated (>80%) suspensions exists (see Chapter 2) which was gathered primarily as a means of assessing properties of the red cell, but which also had applications to the pathophysiological effects of polycythemia, where hematocrits of up to 80 to 85 per cent may be recorded at high altitudes [Harris and Kellermeyer, 1970].

Recent research on extracorporal blood treatment has provided a new incentive for a greater understanding of blood viscosity in concentrated suspensions. An analysis of the ultrafiltrate flux and blood flow characteristics of cross-flow membrane plasmapheresis devices has led to conclusions that the local cell concentration near the filter is at least 95% and may be up to or greater than 98% [Zydney and Colton, 1982; Zydney, 1985]. In order to generate accurate expressions for the mass and momentum profiles, it is necessary to expand the present data base at high hematocrits and to develop a means for representing blood viscosity as a function of both hematocrit and shear rate over the broadest possible range of applicability.

The scope of this thesis, then, will be to present systematic work on blood and red cell suspension viscosity as a function of hematocrit with particular emphasis on hematocrits above 90 and shear rates in the region of interest for plasmapheresis (50-500 sec^{-1}). The data will then be fitted to mathematical models from the literature and combined with empirical formulations of the relevent parameters in order to derive an expression that will provide general usage. By examination of the parameter variation with hematocrit, an assessment of the microscopic behavior of red cell rheology can be made.

Chapter 2

BACKGROUND

2.1 Composition of Blood and Structure of the Red Blood Cell

Blood is composed of the corpuscles--erythrocytes (red blood cell, RBC), leukocytes (white blood cells, WBC), and platelets--suspended in a fluid medium, the plasma. Erythrocytes in normal human blood make up greater than 99 per cent of the corpuscular volume, outnumbering leukocytes by 500-1000 to 1 and platelets by approximately 20 to 1. Therefore, the cellular contributions to the physical characteristics of blood come almost exclusively from the red cells.

By weight, the plasma is 90 per cent water, 7 per cent proteins, 1 per cent inorganic salts and 2 per cent low molecular weight organic solutes. The plasma proteins are prinicipally albumin (4.5 gm.%, mol. wt. = 69,000), globulins (2.5 gm. %, mol. wt. = 35,000 to 1,000,000), and fibrinogen (0.3 gm. %, mol. wt. = 330,000).

The red blood cell under normal conditions is typically a biconcave disk 6-9 μm in diameter, 1 μm thick in the center and increasing to 2-2.5 μm at the periphery. The average cell volume is 90 μm^3 and the surface area is about 140 μm^2.

The red cell membrane is believed to be a two-layer structure consisting of an inner, rigid shell of proteins covered by a more fluid phospholipid bilayer (see Figure 2-1). Choline phospholipids (phosphatidyl choline and sphingomyelin) are found primarily in the outer surface of the bilayer, while the inside half is composed mostly of amino phospholipids (phosphatidyl ethanolamine and phosphatidyl serine).

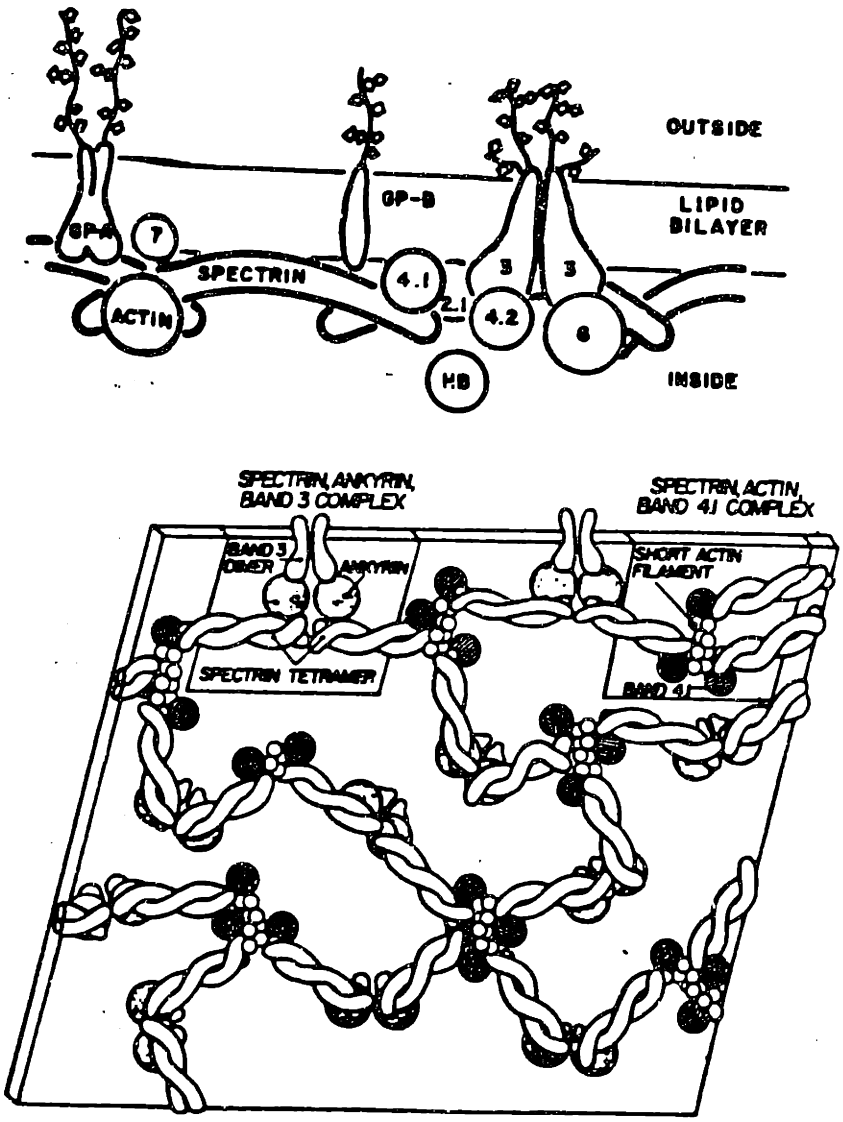

Figure 2-1: Schematic of the red cell membrane. *Top*, cross-section illustrating lipid bilayer, integral membrane proteins, and cytoskeleton proteins. *Bottom*, structure of the membrane skeleton. From Lux, [1981].

Interspersed throughout the bilayer are molecules of glycolipids and unesterified cholesterol along with integral membrane proteins which penetrate or span the bilayer. Peripheral membrane proteins (spectrin, ankyrin, red cell actin, and band 4.1) bind to or are absorbed to the integral proteins and to each other, providing an internal microfibrillar "cytoskeleton" for the membrane. The exact nature of these connections is the subject of much current research but it appears that a complex of spectrin-actin-band 4.1 is responsible for the intraskeletal connections while a spectrin-ankyrin-band 3 complex provides the bonds to the lipid bilayer [Lux, 1981].

It has been proposed that the red cell membrane can be modeled as a solid-liquid composite [Evans and Hochmuth, 1977]. The solid cytoskeleton provides the membrane's resistance to shear deformation at constant surface area. It is also responsible for the elastic reversibility and the yield behavior of the membrane [Evans and Hochmuth, 1978]. The liquid-like lipid bilayer resists changes in membrane surface area. The ratio of the elastic modulus ($\equiv \frac{\Delta force}{\Delta dimension}$) for surface area changes to that for shear deformation at constant surface area is on the order of 10^4-10^5 [Waugh and Evans, 1976; Evans *et al.*, 1976].

The cytoplasm of the erythrocyte is predominantly a 34 per cent hemoglobin-in-water solution. Adult hemoglobin (hemoglobin A) consists of four globin polypeptide chains each bound to a separate heme group. It has a molecular weight of 64,458. The main function of the red blood cell is to transport oxygen bound to the hemoglobin. The physical characteristics of blood and of the red blood cell are summarized in Appendix A.

Blood is stored in liquid state at 4 °C under mandate from the Food and Drug Administration. The time limits for classification of indated blood are also under federal regulations. For citrate phosphate dextrose, the time is 21 days; for citrate phophate dextrose-adenine$_1$ it is 35 days; and for adenine-saline$_1$ it is 42 days.

While stored, blood undergoes a variety of changes which include loss of platelets, granulocytes, plasma proteins, enzymes, and seepage of intracellular electrolytes [Sherwood, 1981]. Additionally, as cells begin to age, the content of membrane lipids decreases and the mean corpuscular hemoglobin concentration increaeses. These factors increase the viscosity of erythrocytes with time [Erslev and Atwater, 1963; Usami *et al.*, 1971].

2.2 Rheological Behavior of Blood

2.2.1 Rheological Properties of Plasma

The earliest studies of plasma viscosity indicated that it was a non-Newtonian fluid with shear-thinning properties [Copley *et al.*, 1960; Wells and Merrill, 1961; Cerny *et al.*, 1962], but subsequent data [Charm and Kurland, 1962; Copley and Scott-Blair, 1962; Merrill *et al.*, 1963a] showed that indeed plasma did conform to Newtonian behavior, with a viscosity of 1.6 cP at 20 °C. The apparent shear rate dependence of the original measurements was attributed to interactions at the fluid-air interface of cone-and-plate viscometers and of Couette viscometers without guard rings [Copley, 1971; Copley and King, 1972]. This will be addressed later in the section on viscometry (Section 3.3).

Serum, the fluid remaining after blood is allowed to clot *in vitro*, is essentially a defibrinogenated plasma solution. It shows none of the non-Newtonian behavior attributed to plasma's surface effects. Based on this observation, it has been suggested that the plasma proteins and principally fibrinogen may form an interlocking network which is irreversibly degraded at shear rates greater than 5 sec^{-1} [Charm and Kurland, 1974]. Plasma does exhibit some additional non-Newtonian characteristics such as drag reduction in turbulent flow [Chmiel, 1974].

Using a sphere-in-sphere viscometer to minimize surface effects, Chmiel and Walitza [1980] have confirmed Newtonian behavior and have described the temperature dependence of plasma viscosity by

$$\mu(T) = \mu(T_0) \cdot \exp\left(\frac{420(T_0 - T)}{(T+162)(T_0-162)}\right) \tag{2.1}$$

where T is the temperature of interest in degrees Kelvin, T_0 is the reference temperature at which the value $\mu(T_0)$ is known. This temperature dependence is much the same as that of water.

The effect of protein concentration on plasma viscosity has been looked at in some investigations, but has not beeen well characterized [Eastham and Morgan, 1965; Wells, 1965; Mayer, 1966; Mayer *et al.*, 1966; Rand *et al.*, 1970]. Serum typically has a viscosity 20% less than that of plasma. Bayliss [1952] proposes an equation for correlating plasma viscosity μ_p to total protein concentration

$$\frac{\mu_p}{\mu_w} = \frac{1}{1 - b \cdot c_{\text{protein}}} \tag{2.2}$$

where μ_w is water viscosity, b is a constant, and $c_{protein}$ is the protein concentration in gms/100 ml. Eastham and Morgan [1965] found that increasing albumin concentration to 11 per cent increased viscosity from 1.6 to 2 centipoises at 25 °C while fibrinogen at 4 percent increased the viscosity to greater than 3 centipoises. MacKenzie and co-workers [1970] found a proportional increase in viscosity with an increase in globulin concentration. In summary, there appears to be an increase in viscosity with an increase in plasma proteins, although the viscosity is least sensitive to changes in albumin concentration. There is evidence that in some clinical pathological states, such as severe leukemia or macroglobulinemia, shear-thinning behavior of plasma may be present [Dintenfass, 1965b and 1966].

2.2.2 Rheological Behavior of Red Blood Cell Suspensions

Since the plasma is essentially Newtonian, and since leukocytes and platelets have a negligible effect on flow properties, the singularities of blood rheology stem from the behavior of the erythrocytes. At low shear rates the cell reversible form stacked primary aggregates, called rouleaux, which can in turn form larger secondary aggregates (see Figure 2-2). The rouleaux disintegrate with increasing shear. The mechanism behind the aggregation phenomenon is not yet understood, although electrostatic attraction, plasma surface tension, and molecular bridging between membranes have all been proposed [Fahraeus and Lindqvist, 1931; Casteneda *et al.*, 1965; Merrill *et al.*, 1966]. Experiments suggest that fibrinogen concentration is the most important determinant of cellular aggregation [Merrill, *et al.*, 1963b and 1965b].

Skalak and co-workers [1977] have developed a general formulation for energy conservation in rouleau aggregation and disaggregation:

$$\frac{dW}{dt} = \frac{dE}{dt} + \frac{dK}{dt} + \frac{dD}{dt} - \gamma\frac{dA_c}{dt} \tag{2.3}$$

where W is work done by external forces (surface and body); E is elastic stored energy (strain energy); K is kinetic energy; D is dissipated energy (including viscous energy of solids, fluids, and the process itself); and $-\gamma\frac{dA_c}{dt}$ is the rate of energy required to separate the contact surfaces, with γ being the surface energy and A_c the common contact area. For static equilibrium it can be shown that

$$\gamma = \frac{\partial E}{\partial A_c}. \tag{2.4}$$

Using a known strain energy function, the surface energy can be estimated to be in the range of 10^{-4} dyne/cm [Skalak *et al.*, 1981b]. There is presently no method of proceeding from equation (2.3) and deriving an expression for rouleau formation and disaggregation in dynamic states [Skalak *et al.*, 1981a].

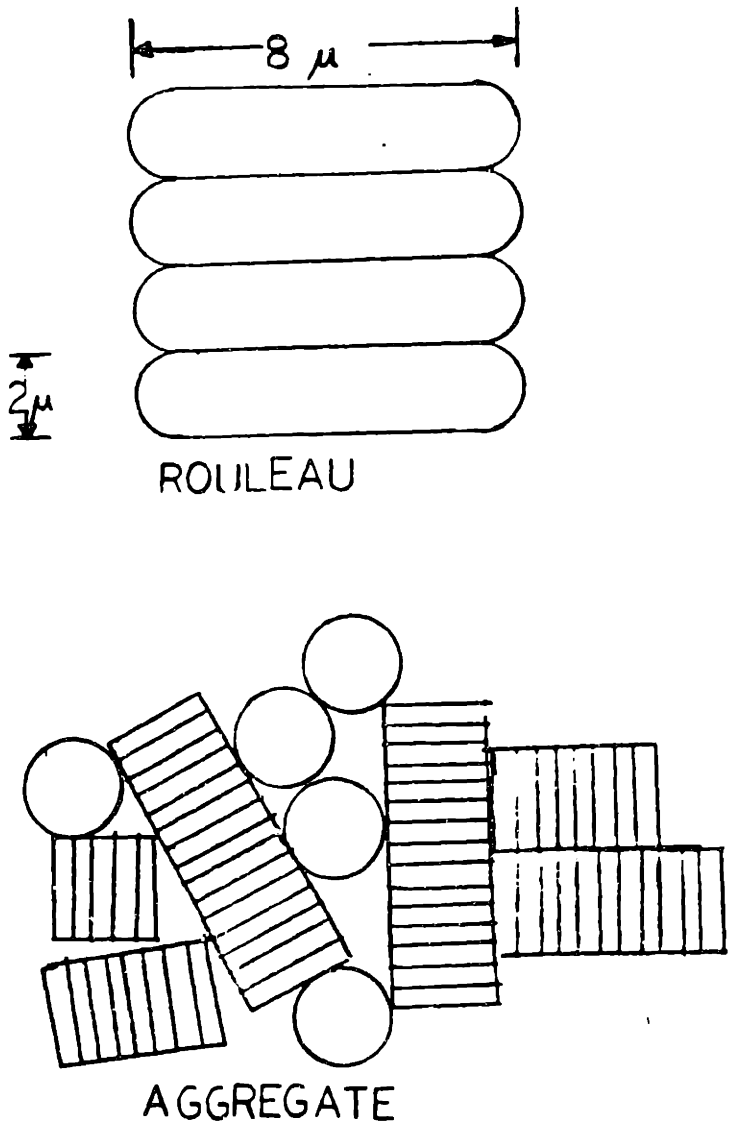

Figure 2-2: Red blood cell rouleau and aggregate.

At very high shear rates, on the order of 50-100 sec^{-1}, the cells undergo deformation and orient themselves with the flow in order to achieve the smallest possible effective volume. Since the cell membrane is highly resistant to changes in surface area but relatively receptive to shear deformation, they assume the shape of prolate ellipsoids. The membrane rotates cyclically around the cellular contents in a "tank-treading" motion, which establishes an internal velocity profile in the cytoplasm [Schmid-Schonbein *et al.*, 1971]. The circulation of fluid inside the membrane has the effect of aligning the cell along the external streamlines and it also reduces the effective volume of the cell. The increase in deformation with shear for the red cell follows the theoretical development for the behavior of a fluid drop developed by Rumscheidt and Mason [1961b].

The effects of these structural changes on the viscosity are shown schematically in Figure 2-3, from Chien [1970], where three sets of data are represented. One curve is for normal blood in plasma, one is for normal blood cells in an 11% albumin solution and the third is for gluteraldehyde-hardened blood cells in 11% albumin.

The albumin solution lacks the proteins necessary for aggregate formation, principally fibrinogen. At low shear rates, therefore, the difference in viscosity between the plasma-suspended RBC and the albumin-suspended normal RBC is due to the effects of aggregation. Similarly, at high shear rates, the difference between the hardened RBC viscosity and the normal RBC viscosity represents deformational effects. The hardened RBC in albumin solution undergo no microstructural changes and thus viscosity is relatively constant with shear rate, with a degree of shear-thickening behavior common to suspensions of rigid particles or of polymers.

For suspensions of rigid particles, the viscosity of the suspension is directly proportional to the viscosity of the continuous phase. In other words, the relative

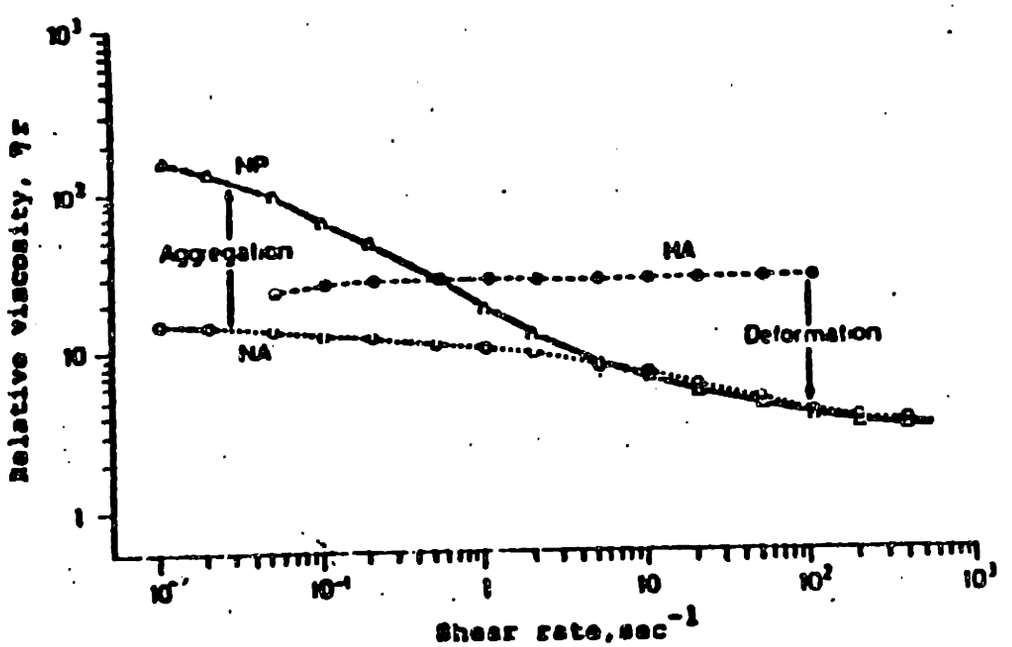

Figure 2-3: Effects of aggregation, deformation, and orientation of the red cell on viscosity.

H=45, η_f=1.2 cP. NP=normal cells in plasma. NA= normal cells in 11% albumin. HA=hardened cells in 11% albumin. From Chien, 1970.

viscosity η_r is independent of the viscosity of pure suspending fluid η_f, where $\eta_r \equiv \eta/\eta_f$. For blood suspensions, however, this is not the case: Experimental work has shown that η_r decreases with increasing η_f [Dintenfass, 1965a]. Blood in this respect is analagous to an emulsion, for which Taylor [1932] and Oldroyd [1953] have shown that, for dilute emulsions, the viscosity is a function of the ratio of the droplet viscosity to that of the non-miscible suspending fluid. Taylor's expression for the bulk viscosity of a dilute emulsion is

$$\eta_r = 1+2.5cT \tag{2.5}$$

where c is the volume fraction of the disperse phase and T is the Taylor coefficient equal to $\frac{\eta_i+0.4\eta_f}{\eta_i+\eta_f}$, where η_i, the internal viscosity, is the viscosity of the pure disperse phase of the emulsion. This coefficient results from the internal velocity profile established in the fluid drop from the shear and normal forces of the continuous phase. The higher the viscosity of the suspending fluid relative to that of the droplet, the greater is the magnitude of the effect. For $\eta_i \approx 50\eta_f$, the droplets behave as rigid particles. For blood cells, the internal viscosity is not a true liquid viscosity but also includes effects from the red cell membrane on the cytoplasm, and therefore η_i has a shear rate dependence.

Secomb and co-workers [1983a] have developed a model for the tank-treading motion of the RBC membrane. This model is based on the following observations:

1. Cell membranes labeled with Heinz bodies or latex spheres show tank-treading motion in high-viscosity dextran solutions.
2. All areas of the membrane move with uniform frequency.
3. Tank-treading motion is seen in whole blood, but not in dilute RBC/plasma suspensions.

From observations (1) and (3), they conclude that the tank-treading motion results from physical interactions with other cells or with very viscous media. This

also supports the hypothesis of a shear-thinning internal viscosity.

The effects of anticoagulation have been characterized by Rosenblum [1968], who classifies anticoagulants into those which shrink the red cell, such as citrate and oxalate, and those that do not change cell size, such as acid-citrate dextrose (ACD). The former increase blood viscosity while the latter show no effect. Cokelet [1963] was also unable to find any effect of anticoagulation with ACD other than those resulting from dilution of the plasma proteins.

The effects of plasma osmolarity were studied by Meiselman *et al.* [1967] who found that cells in hypotonic plasma solutions had an increased hematocrit, a decreased viscosity, and an increased yield stress. Previously, Rand and Burton [1964] had found that cells washed with saline had much less rigid membranes in hypertonic saline solutions. This apparent contradiction in results has been related to the loss of membrane proteins and lipoproteins from cell washing [Meiselman *et al.*, 1967].

2.3 Previous Experimental Work

2.3.1 Experimental Work on Blood Viscosity at Normal Hematocrits

The study of blood viscosity literally dates to the beginnings of viscometry itself. The French physician Jean Poiseuille, credited with the pioneering work on fluid flow through glass capillaries [1843], initially had addressed himself to the relationship of blood flow to pressure, temperature, and vessel diameter. It was only after encountering inconsistencies with blood, which he attributed to variations in blood composition, that he turned to water and other fluids.

Hagenbach [1860] first established the theoretical derivation of Poiseuille's law for laminar flow through a capillary, and first included the concept of viscosity:

$$\mu = \frac{\pi \Delta p}{8QL} R^4 \tag{2.6}$$

where Δp is the pressure difference along the capillary of length L and radius R, and Q is the volumetric flow rate of the fluid.

Attempts to correlate blood flow with this equation persisted through the remainder of the 19th century [Ewald, 1877; Lewy, 1897] but systematic work did not begin until the early 20th century with the work of duPre'Denning and Watson [1906], who studied blood anticoagulated with potassium oxalate in capillary viscometers and the effects of hematocrit, temperature, anticoagulant concentration, and the size of the capillary bore. Interestingly, they observed an increase in blood viscosity at diameters of 300 μm or less.

Other investigations in the early 1900s followed a similar tack and include studies of blood of different animals [Burton-Opitz, 1906 and 1911; Welsh, 1911; Hess, 1911 and 1920; Trevan, 1918; Langstroth, 1919; Berczeller and Wastl, 1924]. Nygaard and co-workers [1935] studied the blood viscosities from H=14 to 58 and proposed a combination of a linear and a hyperbolic equation to model the hematocrit dependence.

Of significant importance is the work of Fahraeus and Lindqvist [1931], who showed that in capillaries of diameters less than 300 μm, Poiseuille flow is not observed and the apparent viscosity of blood decreases as the tube diameter decreases, in contrast to the results of duPre'Denning and Watson. This phenomenon, known as the Fahraeus-Lindqvist effect, results from the tendency of red cells to migrate away from the vessel walls, establishing a cell-free layer of fluid around the flowing cells. This layer has a lubricating effect which grows more significant as the tube diameter decreases, resulting in detectable alterations in the bulk viscosity.

In the 1940s and 1950s activity in the field of blood rheology further increased [Copley *et al.*, 1942; Moll, 1943; Riehl, 1943; Bingham and Roepke, 1944a and 1944b], but it was not until the early 1960s that investigators were able to study blood at low rates of shear (less than 100 sec^{-1}), where its non-Newtonian behavior is evident. This became possible through the employment of cone-and-plate and concentric-cylinder (Couette) viscometers with advanced instrumentation, which were more suitable for this purpose than capillary viscometers. Dintenfass [1962a] claims the first report on the shear-thinning behavior of blood; that is, that the viscosity of blood reversibly decreases with increasing shear rate. (Dintenfass uses the term *thixotropic* throughout his work to describe this behavior, but in the classical sense thixotropy defines behavior under non-steady-state conditions: A thixotropic material is one which experiences a transient decrease in viscosity upon the application of a constant shear stress [Goodeve and Whitfield, 1938; Bird *et al.*, 1960]. Dintenfass [1968a] argues that the difference between shear-thinning and thixotropy is only a question of time scale and instrumentation limits; nevertheless, the classical definitions will be retained in this work.)

Cokelet, Merrill, and co-workers conducted extensive studies into the low-shear rate behavior of blood [Cokelet, 1963; Cokelet *et al.*, 1963, Merrill *et al.*, 1963a and 1965a]. Typical data for normal blood is shown in Figure 2-4.

Figure 2-4 is a plot of the square root of shear stress (τ) versus the square root of shear strain rate ($\dot{\gamma}$). Three regimes are noted: A region at high shear rates (greater than 100 sec^{-1}) governed by Newtonian behavior, a non-Newtonian region below 20 sec^{-1} and a transition region in-between the two. The low shear rate range (down to 0.1 sec^{-1}) is correlated to a semiempirical equation first derived by Casson [1958] to describe printing ink rheology and later proposed by Reiner and Scott-Blair [1959] to be applicable to blood:

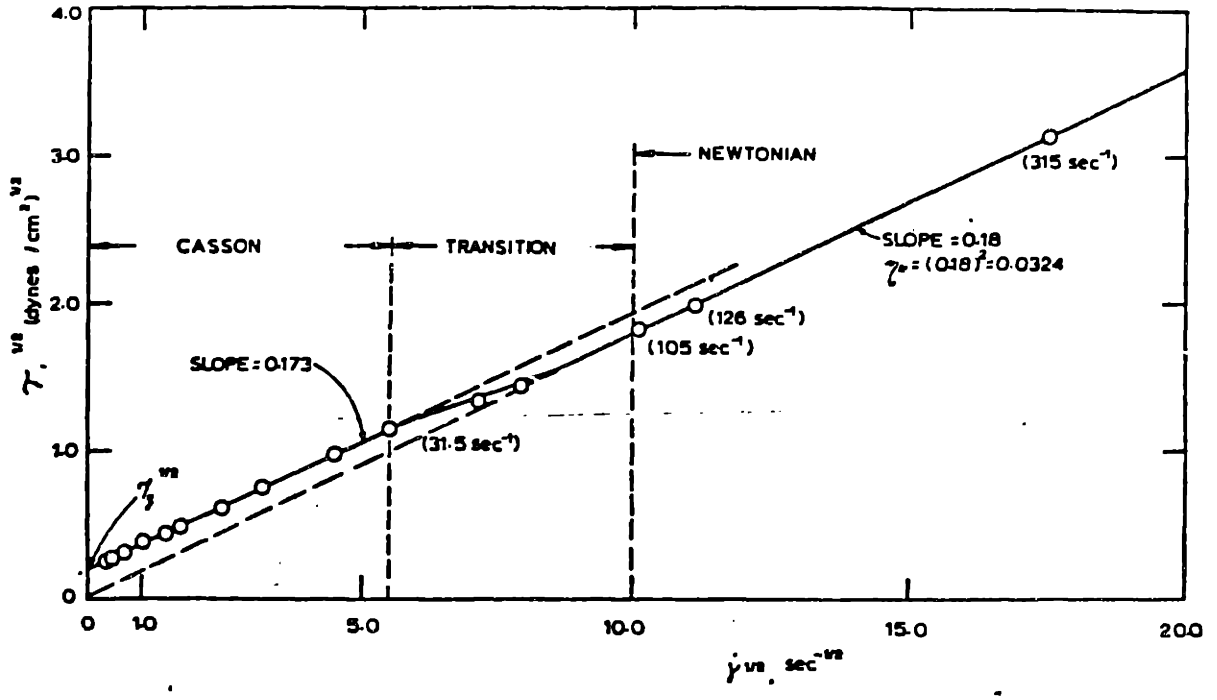

Figure 2-4: Casson plot for normal human blood.

H=40, T=37 °C. $\tau_y \approx 0.04$ dynes/cm^2. From Merrill, 1969.

$$\sqrt{\tau} = \sqrt{\tau_y} + \sqrt{\mu_N \dot{\gamma}} \qquad (2.7)$$

where τ_y is a yield shear stress and μ_N is the asymptotic Newtonian viscosity at high shear rates.

Values for τ_y have been obtained by a variety of experimental methods, all of which have the potential for introducing significant instrument artifact. These methods include extrapolation of Casson plots to zero shear rate [Cokelet *et al.*, 1963; Merrill *et al.*, 1966], torque decay [Merrill *et al.*, 1965a], pressure decay [Merrill *et al.*, 1965a], force on an oscillating plate [Benis and Lacoste, 1968], and sedimentation [Charm and Kurland, 1967]. The values for τ_y measured by these methods range from 0.003 to 0.20 dyne/cm^2.

Red cells in Ringer or isotonic saline solution or suspended in plasma suspensions lacking fibrinogen do not exhibit a yield shear stress [Cokelet, 1963; Merrill *et al.*, 1963b and 1965c]. Addition of a slight amount of fibrinogen gives conformity to the Casson equation, and the magnitude of the yield stress varies with fibrinogen concentration [Merrill *et al.* 1963b, 1965c, 1966].

The existence of a yield shear stress for blood, and thus the validity of the Casson equation, is disputed by some researchers [Chien *et al.*, 1970; Chmiel, 1974] who believe it is an artifact extrapolated from the limits of the instrumentation. Experiments conducted at shear rates from 0.1 to 5 x 10^{-3} sec^{-1} using a wide gap Couette system showed significant deviation from the Casson equation which indicated the absence of a yield shear stress [Chmiel, 1974]. The questions about yield shear stress concern a no-flow situation of principally academic interest. They are of no concern at the shear rates of interest for plasmapheresis devices and require measurements out of the range of the instrumentation used here. The yield shear stress will not be considered at any length in this work.

2.3.2 Experimental Work on Blood Viscosity at High Hematocrits

As early as 1924, there were reports that the viscosity of packed cells was 8 to 90 times that of plasma [Berczeller and Wastl, 1924]. More recently, the viscosity of packed red cells became of interest when it was realized that blood does not behave as a suspension of rigid particles [Dintenfass, 1962b]. A 65% suspension of clay or microscopic glass spheres would have a viscosity 10 to 100 times that of blood at the same cell concentration.

There is a dearth of data on blood viscosity at high hematocrits. What little data that does exist shows a considerable variance in reported values, as plotted in Figure 2-5. Chien *et al.* [1966] have the most complete base of data to date on the variation of viscosity over a wide range of hematocrits and shear rates. Three types of blood preparations--whole blood, defibrinated blood, and Ringer-suspended cells--were measured over hematocrits ranging from 0 to 95. Their data is shown in Figures 2-6 to 2-8 fitted to fifth-order polynomial curves of the form,

$$\ln(\eta) = \sum_{i=0}^{5} a_i \cdot H^i \tag{2.8}$$

whose constants a_i are given in Table 2-I. At low hematocrits ($H<5$), Newtonian behavior is observed for all suspensions. Newtonian behavior persists up to $H=15$ when fibrinogen is absent and up to $H=30$ when all plasma proteins are absent. The viscosity differences between suspensions is the greatest at low shear rates, supporting the contention that protein-mediated aggregation dominates rheology at low shear rates. Viscosity decreases when plasma proteins are removed, but at high hematocrits, the differences between the suspensions become negligible as the volume of non-cellular medium vanishes.

The work of Chien *et al.* is probably the most referred-to source in the literature and their equations the most used for examining blood viscosity as it

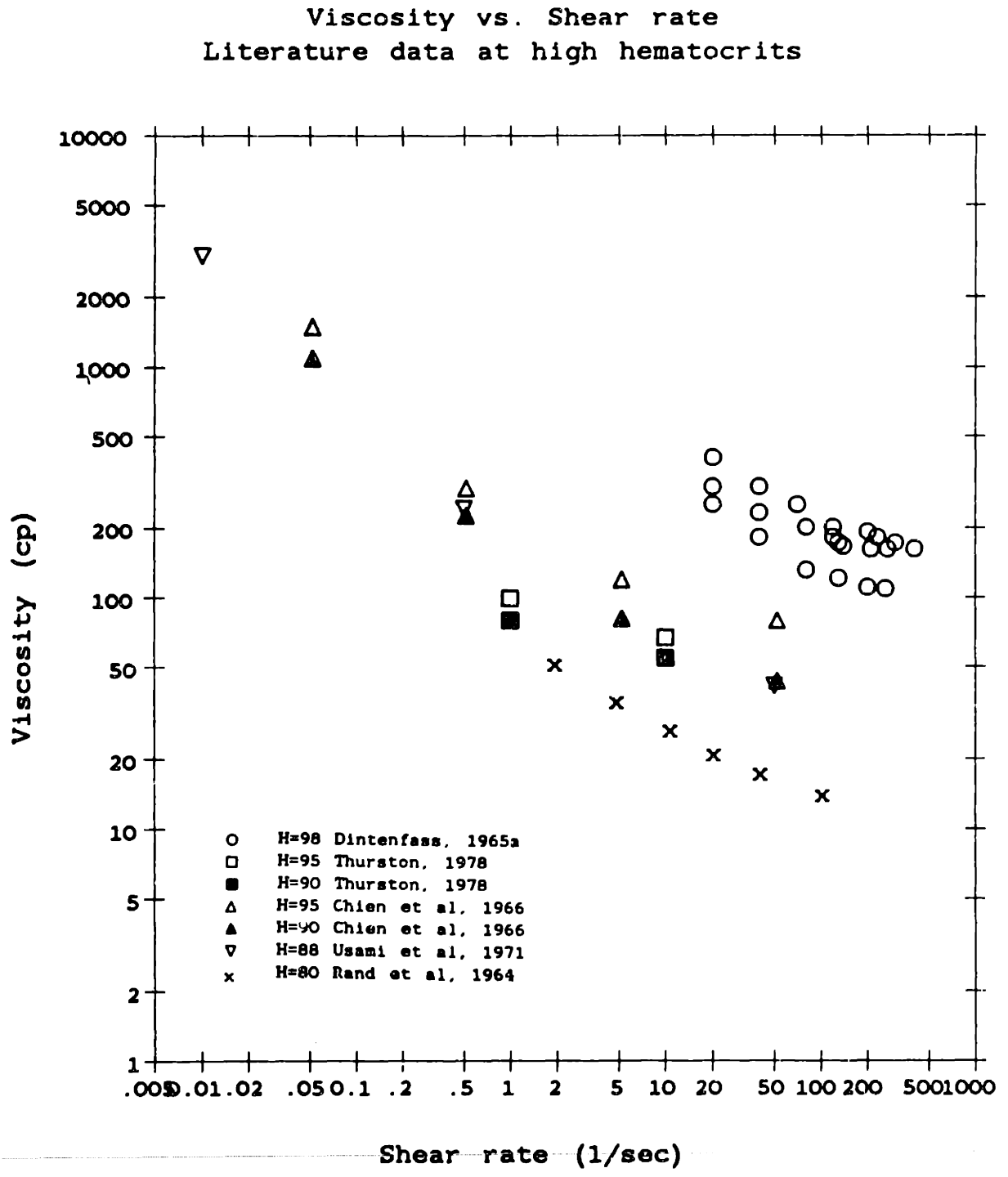

Figure 2-5: Literature data for blood viscosity at high hematocrits.

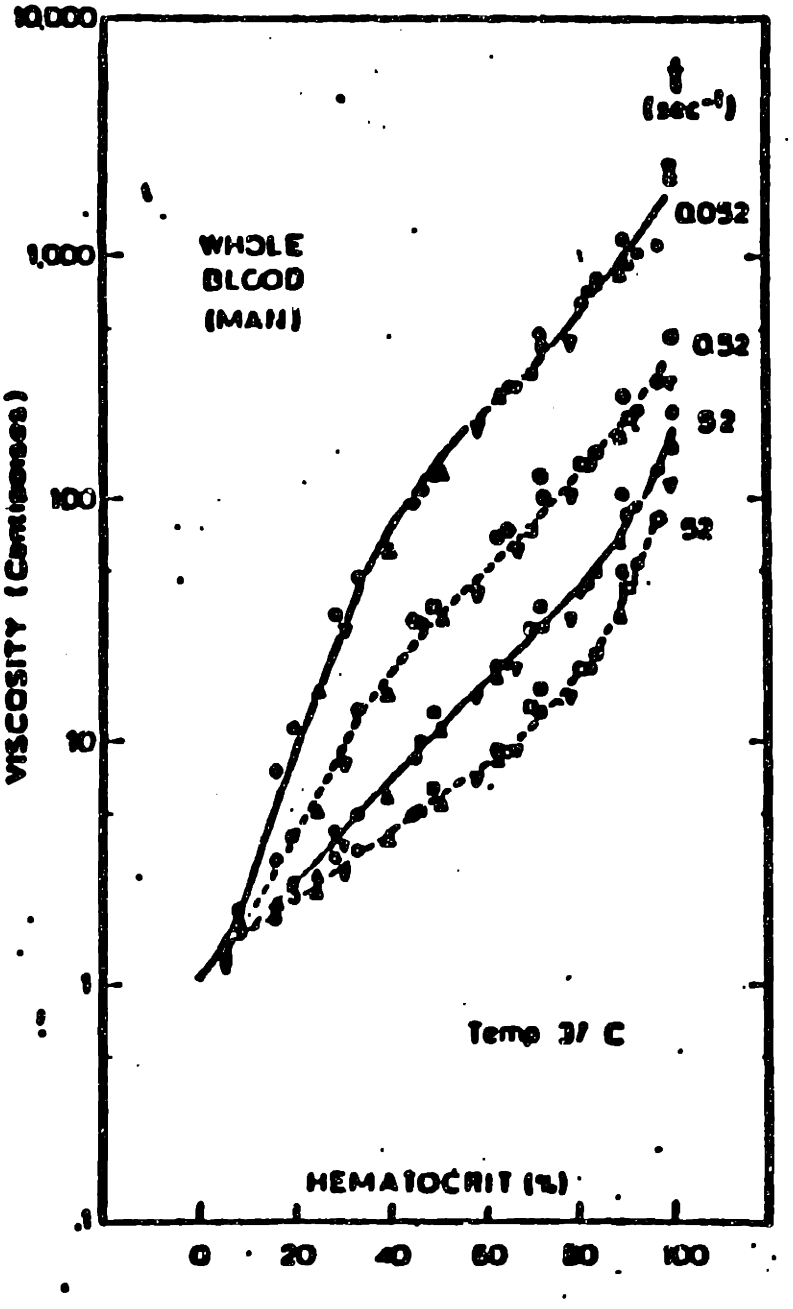

Figure 2-6: Data of Chien *et al.* [1966] for whole blood.

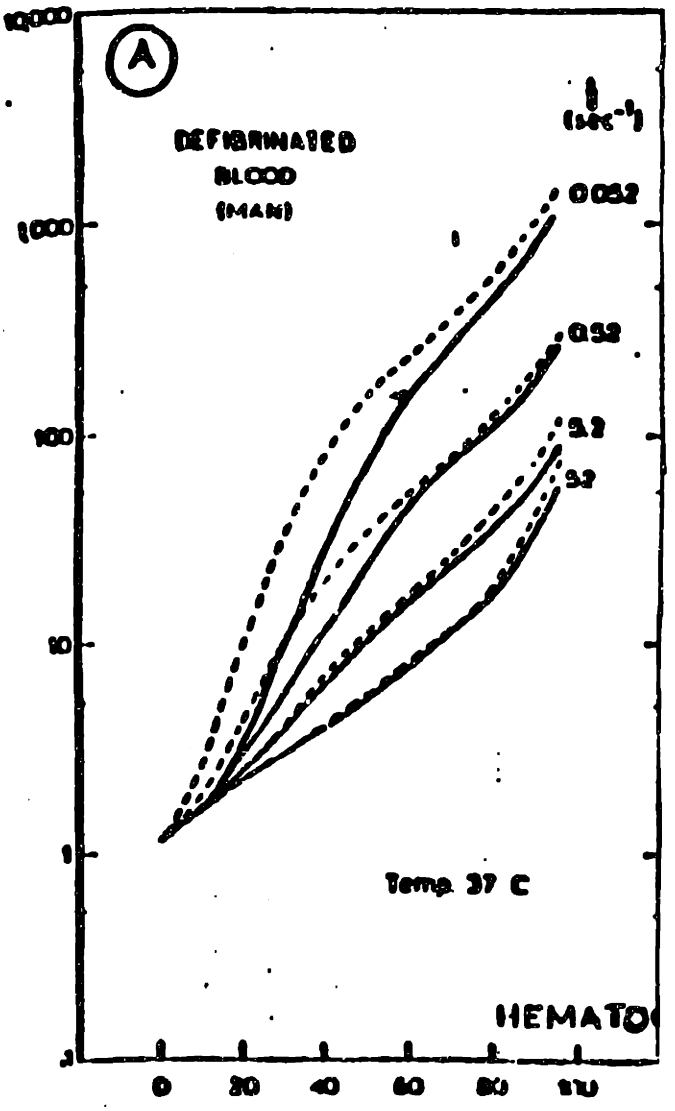

Figure 2-7: Data of Chien *et al.* [1966] for defibrinated blood. Dashed lines represent whole blood curves.

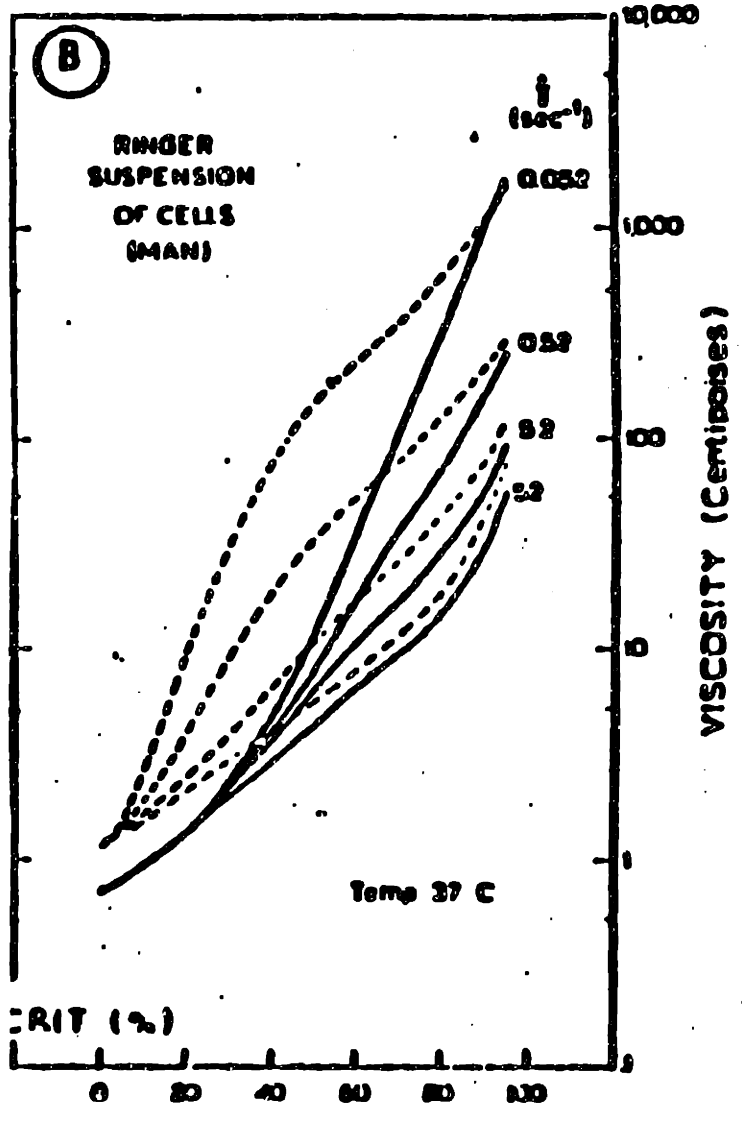

Figure 2-8: Data of Chien *et al.* [1966] for Ringer's suspenison. Dashed lines represent whole blood curves.

Constants for polynomial fit of data of Chien et al, 1966.

Solution type/ Shear rate (1/s)	a0	a1	a2	a3	a4	a5
wb 52	0.2028	2.928e-02	-1.570e-04	1.3850e-05	-2.8130e-07	1.788e-09
wb 5.2	0.1817	2.423e-02	9.850e-04	-1.3720e-05	2.9900e-08	3.530e-10
wb .52	0.1499	2.599e-02	3.598e-03	-9.4670e-05	9.5240e-07	-3.335e-09
wb .052	0.1342	4.250e-02	5.820e-03	-1.6425e-04	1.6958e-06	-6.035e-09
db 52	0.1336	5.467e-02	-1.369e-03	4.4390e-05	-5.2420e-07	2.381e-09
db 5.2	0.0813	4.245e-03	-4.300e-04	2.4560e-05	-4.0510e-07	2.097e-09
db .52	0.1260	4.130e-02	-9.300e-05	3.2280e-05	-6.0980e-07	3.147e-09
db .052	0.0681	-3.440e-03	4.383e-03	-7.3530e-05	4.4460e-07	-7.000e-10
rs 52	-0.3651	4.131e-02	-9.700e-04	4.0600e-05	-6.1720e-07	3.186e-09
rs 5.2	-0.3644	2.160e-02	3.140e-04	1.7630e-05	-4.1340e-07	2.397e-09
rs .52	-0.3658	4.237e-02	-1.508e-03	6.7960e-05	-8.9610e-07	3.908e-09
rs .052	-0.3760	3.763e-02	-6.450e-04	3.8020e-05	-4.0730e-07	1.369e-09

"wb"-whole blood "db"-defibrinated whole blood
"rs"-Ringer's suspension

Table 2-I: Constants for polynomial fit of Chien data.

From Chien *et al.*, 1966.

varies with cell concentration and shear rate. An inconsistency with the Chien polynomials is that the a_0 values for any one type of suspension are not equal, and thus non-Newtonian behavior is predicted for pure plasma and saline. The purely empirical constants from these polynomials give little insight into the physical phenomena being observed. The fact that their ranges extend only to hematocrits of 95 and shear rates of 52 sec^{-1} points out the need for more extensive data at the high-shear, high-hematocrit spectrum as well as a renewed effort to develop a set of equations satisfactory for predicting blood viscosity over a broad range of conditions.

An obvious approach to expanding the applicability of the Chien equations is to derive another set of empirical equations relating the coefficients a_i in equation (2.8) to shear rate. Constraints may be imposed such as requiring that as $H \rightarrow 0$, $\eta \rightarrow \eta_f$ for all shear rates (*i. e.*, setting a_0 to a constant for each set of curves) and that Newtonian behavior is approached at high shear rates. Such an undertaking was made as a part of this work and the results are reported on in Chapter 4.

2.4 Theoretical Models and Mathematical Correlations

Because of the complex nature of the cell-cell and cell-fluid interactions in blood and red blood cell suspensions, to date it has not been possible to explain their rheology from the standpoint of a unified theory. Such a theory would have to incorporate the various aspects of shear rate and concentration dependence described in the previous sections of this chapter. To recap:

1. As shear rates approach zero, non-Newtonian behavior results from the domination of cell-protein interactions and subsequent increased aggregation.
2. At high shear rates, cells deform and orient along the streamlines, there

is tank-treading motion of the membrane and establishment of an internal velocity profile. Newtonian behavior is observed.

3. The fluid nature of the erythrocyte makes for substantial deviations in behavior of RBC suspensions versus that of rigid particle suspensions. For blood, the relative magnitude of the viscosity is smaller at a given concentration. Even at greater than 95 volume percent, blood suspensions are quite fluid. Analogies can be drawn to emulsions, with the cellular phase represented by a non-Newtonian internal viscosity.
4. Suspensions are Newtonian in the limit of dilute concentrations.
5. At high concentrations, cell crowding effects predominate and viscosity becomes independent of the suspending fluid.

Most proposed models for blood are extensions of [illegible]es for suspensions of rigid particles or for emulsions. It is the intent here to briefly mention several approaches.

The Casson equation, equation (2.7), was originally developed to explain the behavior of mutually attractive particles which form structures that diminish in size as shear rate increases. In addition, the structure which exists at zero shear must be subjugated to a yield stress before any flow developes. The Casson equation does not explain blood rheology at low hematocrits, where no yield stress is observed.

Many empirical equations have been modifications of an equation first derived by Einstein [1906] for dilute suspensions of rigid, non-interacting particles,

$$\eta_r = \frac{1}{1-\alpha \cdot c} \tag{2.9}$$

where α is a shape factor equal to 2.5 for spheres. At hematocrits less than 5, where Newtonian behavior is observed, equation (2.9) describes whole blood adequately. Jeffrey [1923] extended Einstein's theory to particles of ellipsoid shape, from which Taylor [1932] derived his expression for emulsion viscosity, equation (2.5). Dintenfass [1968b], starting with Taylor's equation, proceeded by a method where a

concentrated emulsion is equated to a hypothetical continuous phase of equal viscosity, and then sequential addition of disperse phase to the emulsion is assumed to follow Taylor's equation. The result is

$$\eta_r = \frac{1}{(1-c\cdot T)^{2.5}} \tag{2.10}$$

Values for η_i from this equation are between 1 and 6 cP [Dintenfass, 1968b]. This is smaller than the reported 6-8 cP viscosity of a 34 per cent hemoglobin-in-water solution, which approximates the makeup of the erythrocyte cytoplasm [Quemada, 1977].

The methodology used to derive this equation is valid only at shear rates high enough to prevent aggregation, so that the cells exist as independent units. Based on attempts at using it with experimental data, it will hold for more dilute suspensions ($H<85$) only with very viscous suspending fluids. For example, in order to measure η_i at $H=38$, Dintenfass [1968b] uses a suspending fluid viscosity $\eta_f>9$ cP. The limitations of equation (2.10) would follow from the concept of a shear-thinning internal viscosity and from the previously mentioned observations of Secomb *et al.* [1983a]. Only at high shear rates would the emulsion properties of blood become apparent from deformation, orientation, and tank-treading. The tank-treading is dependent on viscous stresses from either other cells or from highly viscous media [Secomb *et al.*, 1983a].

Quemada [1977, 1978a, and 1978b] has proposed an interesting equation for concentrated suspensions based on the principle of minimum energy dissipation. His derivation is strictly valid for rigid, attracting spheres but is seen to adequately describe blood rheology. The expression for the relative viscosity as a function of both shear rate and concentration is

$$\eta_r = [1 - \frac{c}{2}\cdot(\frac{k_0 + k_\infty\cdot\sqrt{\dot{\gamma}_r}}{1 + \sqrt{\dot{\gamma}_r}})]^{-2} \tag{2.11}$$

or

$$\eta_r = [1 - \frac{c}{2}(k_\infty + \frac{k_0 - k_\infty}{1 + \sqrt{\gamma_r}})]^{-2}$$

where k_0 and k_∞ are dimensionless "intrinsic viscosities" defined as $(\frac{d\eta_r}{dc})_{c \to 0}$ at zero and high shear rate, respectively. The term in parentheses in equation (2.11) is the intrinsic viscosity $k(c,\gamma)$ at the shear rate of interest. For rigid particles, the intrinsic viscosity is inversely proportional to the packing concentration c_p, which is the maximum concentration to which the effective particles existing at the shear rate may be packed. In other words, the intrinsic viscosity is directly proportional to the volume of an effective particle. For deformable fluid particles such as erythrocytes, the intrinsic viscosity empirically includes any deviations from rigid spheres, and the relationship of intrinsic viscosity to particle volume is more qualitative. The dimensionless relative shear rate γ_r is equal to γ/γ_c where γ_c is a theoretical "critical shear rate" for aggregate formation. Aggregation is assumed to be governed by Brownian collisions while disaggregation is controlled by shear-induced collisions. In the limit of a dilute concentration of rigid spheres, γ_c is rougly equivalent to the rotational diffusion coefficient $\frac{D}{a^2}$, where D is the translational diffusivity and a is the radius of the particle. For blood cell aggregates, γ_c may be on the order of a Maxwell relaxation time $\frac{E_i}{\eta_i}$, where E_i is the elastic modulus of the aggregate. A complete derivation of the Quemada equation is given in Appendix C.

Since the Quemada expression will be employed extensively in the analysis of this work, it will be worthwhile at this point to examine this equation in some detail, first from a purely mathematical standpoint and then later in the context of the physical meaning of its parmeters. Sets of curves for the Quemada equation are

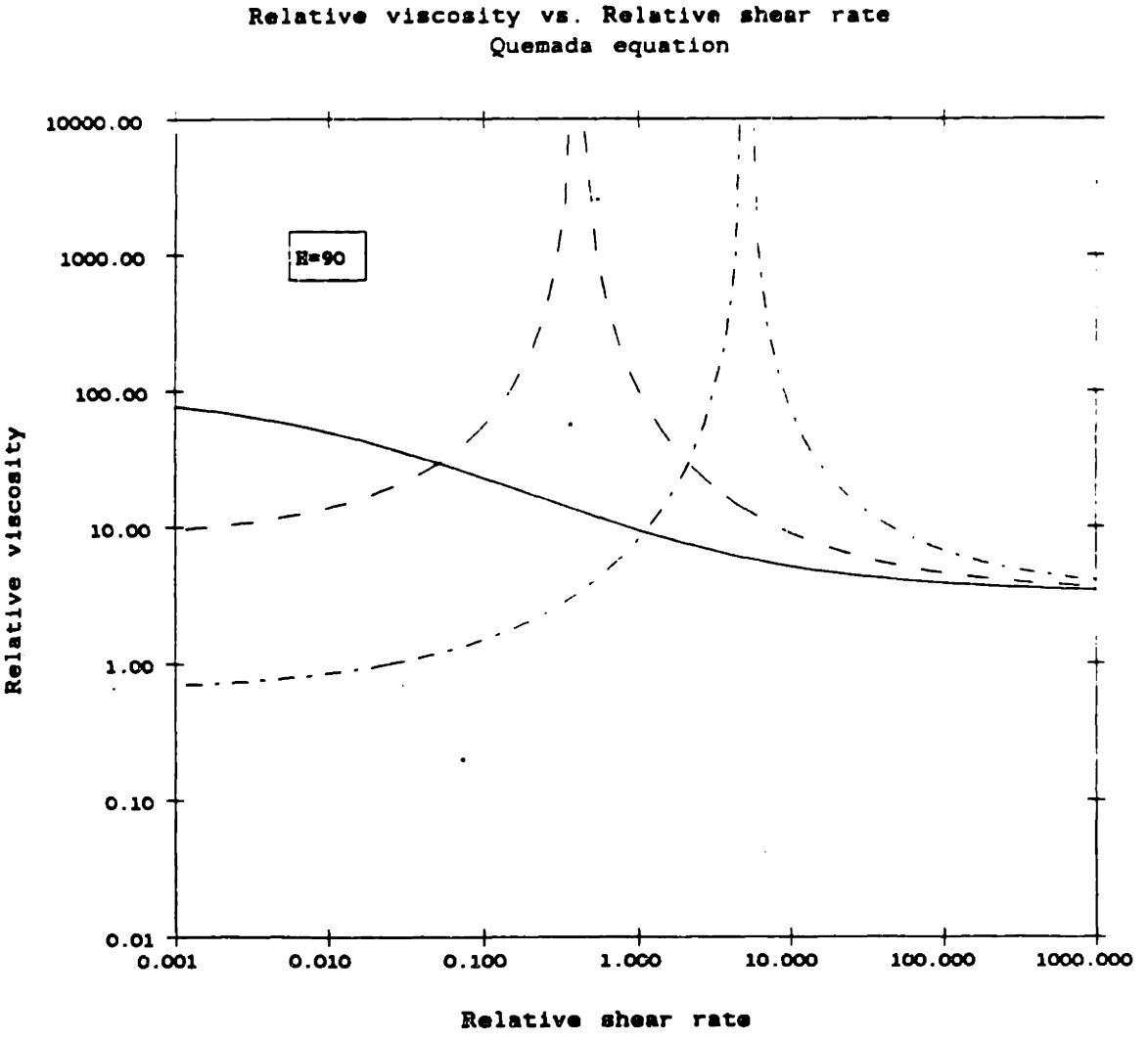

Figure 2-9: Plots of the Quemada equation at H=90.

Solid lines: $k_\infty=1$, $k_0=2$

Dashed lines: $k_\infty=1$, $k_0=3$

Dot/dashed lines: $k_\infty=1$, $k_0=5$

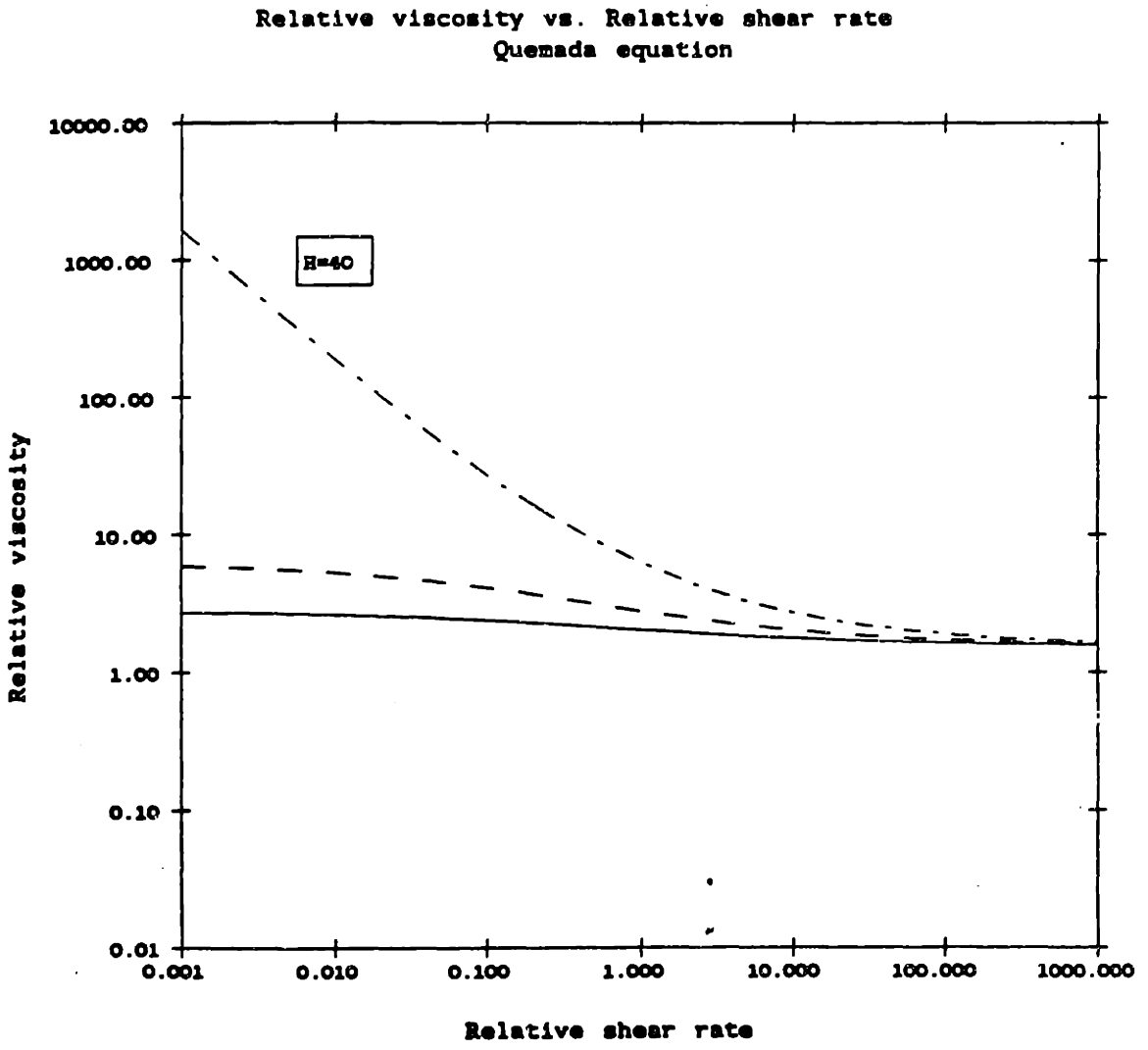

Figure 2-10: Plots of the Quemada equation at H=40.

Solid lines: $k_\infty=1$, $k_0=2$

Dashed lines: $k_\infty=1$, $k_0=3$

Dot/dashed lines: $k_\infty=1$, $k_0=5$

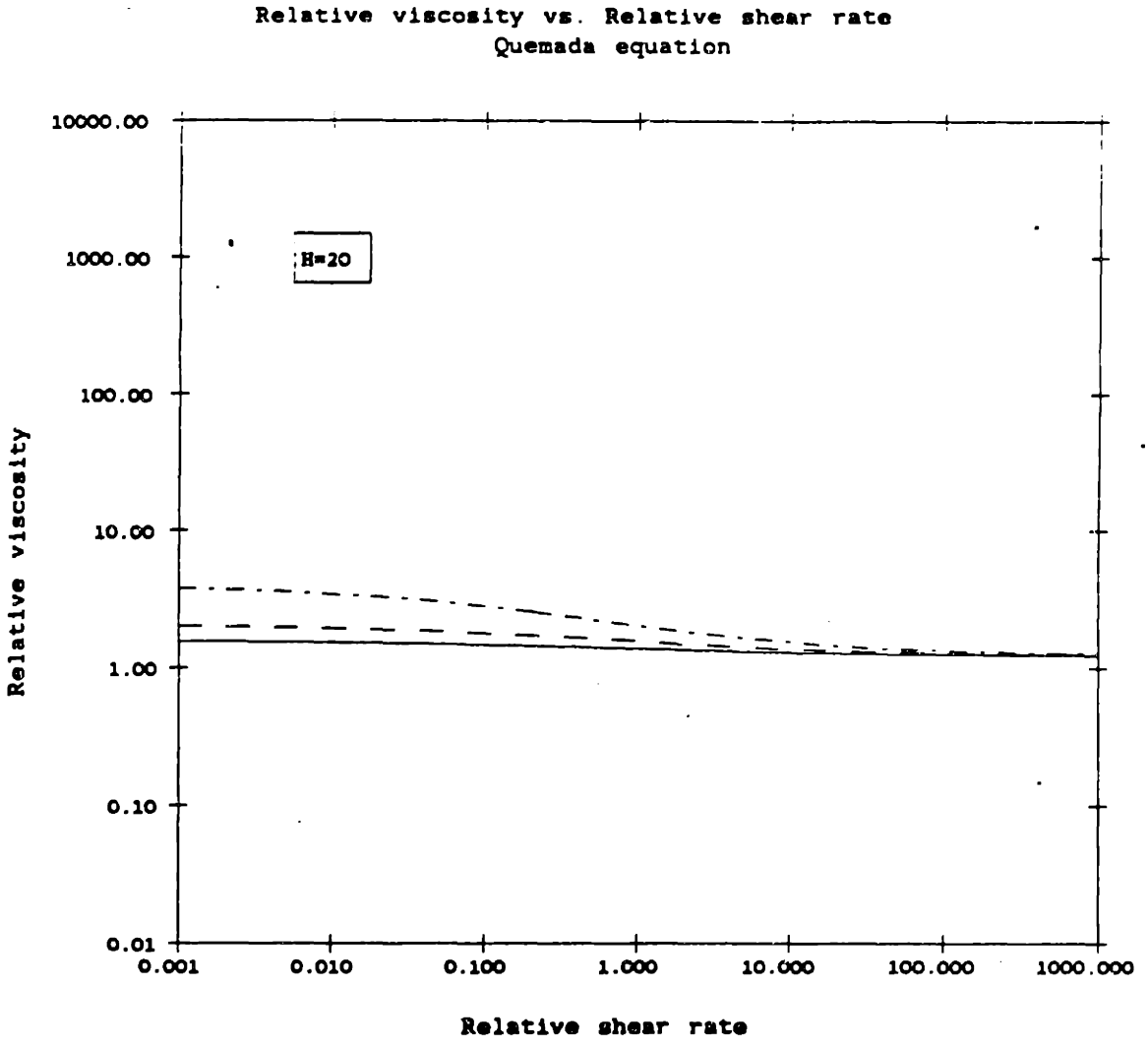

Figure 2-11: Plots of the Quemada equation at H=20.

Solid lines: $k_\infty=1$, $k_0=2$

Dashed lines: $k_\infty=1$, $k_0=3$

Dot/dashed lines: $k_\infty=1$, $k_0=5$

shown in Figures 2-9 to 2-11 for hematocrits of 90, 40, and 20. From these curves it is evident that k_∞ and k_0 provide the asymptotic values of the viscosity, while the critical shear rate scales the x-axis over the range of shear rates examined. A low value for $\dot{\gamma}_c$ shifts the relative shear rate to the right, toward the k_∞ asymptote. Alternatively, the critical shear rate can be thought of as an analogue to the Michaelis-Menten rate constant: when $\dot{\gamma} = \dot{\gamma}_c$, $k = \frac{k_0 + k_\infty}{2}$.

As shown in the graph for H=90, there exists the potential for a singular solution at high hematocrit and high k_0, where the viscosity is infinite. This occurs when the term in brackets in equation (2.11) is zero, and

$$\sqrt{\dot{\gamma}_r} = \frac{\frac{c}{2}k_0 - 1}{1 - \frac{c}{2}k_\infty}. \tag{2.12}$$

This has a real-valued solution only when $\sqrt{\dot{\gamma}_r} > 0$, and thus the criterion for the existence of a singular point is

$$\frac{1 - \frac{c}{2}k_0}{1 - \frac{c}{2}k_\infty} < 0. \tag{2.13}$$

Since $k_0 > k_\infty$ for shear-thinning suspensions, this reduces to

$$\frac{c}{2}k_0 > 1. \tag{2.14}$$

This case has no physical meaning, as viscosity would never follow this behavior, but may result when k_0 values are extrapolated from data at higher shear rates.

Quemada fit his equation to experimental data from the literature [Quemada, 1978b]. The values derived for the rheological parameters from these fits are shown in Table 2-II and the corresponding equations are plotted in Figure 2-12. He has also [Quemada, 1981] fit his equation to the data of Chien *et al.*, 1966, but unfortunately presented his results graphically, in terms of c_p, without reporting the

Source	H	k_∞	k_0	γ_c (sec^{-1})
1	41.9	1.8	4.68	0.69
2a	40	1.84	4.65	2.23
2b	45	2.07	4.33	1.8
3a	45	1.78	4.20	5.0
3b	45	1.78	3.29	25.0
3c	45	3.62	-	-
4	88	1.83	2.26	2.16

Table 2-II: Fits of literature data to Quemada equation.

Source codes: 1-Merrill *et al.*, 1965c, whole blood

2-Schmid-Schonbein *et al.*, 1971b, whole blood

3-Chien, 1970: (a) normal cells in plasma, (b) normal cells in albumin,

(c) hardened cells in albumin

4-Usami *et al.*, 1971, packed cells in plasma

η_f=1.2 cP for all samples.

From Quemada, 1978b.

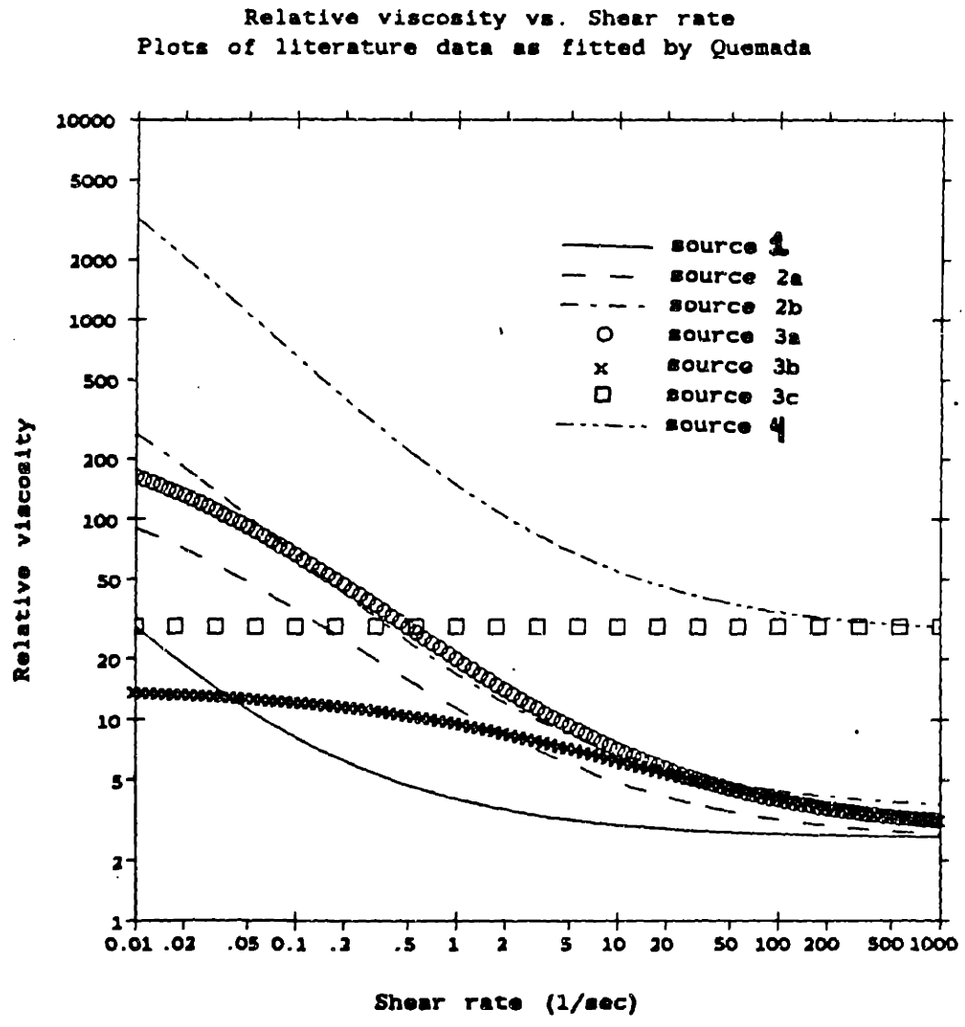

Figure 2-12: Plots of Quemada equation for literature sources given in Table 2-II.

values obtained. As part of the present work, fits were made to the Chien data and are discussed in Chapter 5.

Values for k_∞ in Table 2-II are very close to 1.8 save for the hardened cells. Ideally, k_∞ can be thought of as being affected by anything which would affect either the internal viscosity of the cell or the effective hydrodynamic volume of the cell at high shear, since k_∞ is related to the packing concentration of effective particles (see Appendix C). It should therefore hold that as long as the nature of the cells, the hematocrit, and the suspending fluid viscosity are the same, then k_∞ should be constant. The value obtained at H=88 is similar to the others in Table 2-II, but in analyzing data from Chien *et al.* [1966], Quemada [1981] noted that at low hematocrits, k_∞ decreased as hematocrit increased, reached a minimum at H=75, and then increased. His proposed explanation for this is to imagine that below hematocrits of around 40, the effective particle volume at high shear is the hydrodynamic volume of an individual cell, which is reduced by crowding effects as hematocrit increases. At about H=40, these effective volumes begin to overlap, and at H=75 an inversion phenomenon typical to emulsions happens as the continuous solution phase becomes sequestered between cells and converts into a dispersed phase, while the erythrocytes become the continuous phase.

Comparison of the values of k_0 give an indication of the effects of aggregation. The absence of plasma proteins leads to less aggregation at zero shear rate and higher packing concentrations as described in Appendix C. In fitting the data of Chien *et al.*, Quemada [1981] noted an almost linear decrease of k_0 with hematocrit, which he ascribed to successive effects of increased aggregation and then deformation, both which result in increasing the "compactness" of the red cell aggregates.

The values for $\dot{\gamma}_c$ in Table 2-II show a large jump from 5 to 25 sec^{-1} in going

from plasma to albumin suspensions. If, as in polymer chains, γ_c is assumed to be proportional to the elastic modulus E_i as shown in Appendix C, and $E_i \sim a^{-3}$ where a is the effective radius of the rouleau, then effects which decrease aggregation would increase γ_c.

In the limit as $c \rightarrow 0$, it is reasonable to assume that $\gamma_c \rightarrow \infty$ since there is less aggregation and the time constant for rotational diffusion will be small. The term in parentheses is equation (2.11) becomes $1 - \frac{c}{2} \cdot k_0$. In the fits of Quemada for the data of Chien *et al.*, however, it appears that both k_0 and k_∞ are discontinuous at the boundary of Newtonian behavior and that the Newtonian intrinsic viscosity is some intermediate value between the two.

A few other methods will be quickly touched upon. Linear viscoelastic models for blood attempt to model both the dissipative (viscous) and energy-storing (elastic) properties of blood. Thurston [1972] was the first to delve into this arena of biorheology. There have been many proposed constituitive equations for blood, but none have been found to be fully satisfactory in terms of representing all of the material function of blood (shear viscosity, normal stress differences, and oscillatory material functions). If interest is limited to just the shear viscosity, however, several models predict blood behavior reasonably well, although all previous work has been at hematocrits in the physiologic range [Walitza *et al.*, 1979; Riha, 1980]. These models are limited by their complexity and their inability to be related to physical parameters.

Princen [1983] has proposed a method of calculating yield shear stress for foams and concentrated emulsions based on a geometric analysis of the shear stress and membrane tension of hexagonally closed-packed drops. His analysis does not extend to void fractions above 10 per cent.

Secomb *et al.* [1983b] have developed very complicated expressions for the relative viscosity of packed red cells based on a model for tank-treading motion of the cells. Their model shows good agreement at high shear rates but is very poor at both lower hematocrits and low shear rates, where the tank-treading effect is less important rheologically.

Chapter 3

MATERIALS AND METHODS

3.1 Blood Sampling and Preparation

The blood samples used for the viscosity measurements were either drawn from the author or were units of whole blood or of packed cells obtained from the American Red Cross. Those drawn from the author were used in preliminary measurements and consisted of approximately 7 ml of blood drawn into Vacutainers (Becton-Dickinson no. 6460) with sodium citrate anticoagulant. Each unit was drawn into either citrate phosphate dextrose (CPD), citrate phosphate dextrose-adenine$_1$ (CPD-A$_1$), or adenine-saline$_1$ (AS$_1$) anticoagulant-preservative and was used before its expiration date. Typically these units were obtained approximately 14 days after they had been collected from donors. A unit of whole blood consists of 450 ml of blood drawn into 63 ml of anticoagulant-preservative and a unit of packed red cells consists approximately of 250 ml of blood concentrated to 60-75% cell volume. Units were stored refrigerated at 4 °C.

Saline suspensions of blood were made from the units of packed red cells. Ten 15-ml Pyrex centrifuge tubes were filled with 8 to 10 ml each of packed cells and centrifuged for four hours at 900*g* in a refrigerated centrifuge (International Equipment Company, model PR6). The supernatant and buffy coat were removed and discarded and the remaining cells (about 5-6 ml) were washed in an equal volume of Eagle's solution and centrifuged again for thirty minutes to an hour. The cells were washed and centrifuged twice more. The final centrifugation lasted for 12 hours and, after removal of the supernatant, Eagle's solution was added to adjust to

the desired hematocrit. The recipe for Eagle's solution is given in Appendix B.

Suspensions of red blood cells in plasma were prepared by spinning down 10 ml aliquots for 12 hours. The supernatant was retained and the cells were not washed in Eagle's solution. Instead, the supernatant was centrifuged for 30 minutes to settle any solid materials, which were discarded, and the plasma was used to adjust the hematocrits of the red cell samples.

3.2 Hematocrit Determination

Hematocrit determination was done by the microhematocrit method. Two 25 μl Microcap (Drummond Scientific Company) glass capillary tubes were filled one-half to two-third full with the sample in question. One end of each tube was sealed with Seal-Ease (Clay-Adams, Parisippany, NJ), and the tubes were spun in a Readacrit microcentrifuge (Clay-Adams no. 0591, Parisippany, NJ) at 6300g for 5 minutes. The length of the red cell column and the total length of material in the tube was read by graduations built into the centrifuge. For microhematocrits below 98, if agreement was not within 0.5 hematocrit units, a third measurement was done. For microhematocrits above 98, the agreement criteria between tubes was within 0.3 hematocrit units and the values were recorded to the nearest tenth.

It is well known that a column of packed red cells contains a small amount of plasma trapped between the cells, which in the case of microhematocrit determination means that the reading is higher than the actual volume percentage of cells. Methods using radioactive-labeled albumin have been employed to quantify the amount of plasma trapped [Chien *et al*, 1965; Thomas and Janes, 1968], and an attempt was made to adapt one of these methods to determine with greater accuracy the hematocrit of the high concentration samples. The nature of these samples, their high viscosity and adhesiveness to the sides of glass tubes, made it

impossible to measure out accurate volumes as required by the Chien method and the method of Thomas and Janes proved unsuitable for samples of extremely low plasma to cell ratio. Values of the plasma trapping correction factor (equal to 1 minus the porosity) for the microhematocrit method are in the range of .99 [Chien *et al*, 1965] at cell volumes of 44.5%. Since the porosity of a centrifuged column decreases with increasing length of cell column, the correction factor should be even higher for highly concentrated suspensions.

The relationship between the steady-state porosity of a centrifuged column of packed cells and the compressive pressure of centrifugation has been examined by Saltzman [1984] and Zydney *et al.* [1985]. Using a differential force balance on a layer of cells in the column, the compressive pressure π at any point in the column is given by

$$\pi = \frac{1}{(1-\epsilon)} \int_0^y (\rho_c - \rho_f)\, \omega^2 R\, d[(1-\epsilon)y] \tag{3.1}$$

where ϵ is the porosity, ρ_c and ρ_f are the cell and suspending fluid densities, respectively, ω is the rotational velocity of the centrifuge and R is the arm length of the centrifuge. An empirical expression relating compressive pressure to porosity derived by Zydney *et al.* is

$$K\pi = \left(\frac{\epsilon_0}{\epsilon}\right) + \left(\frac{\epsilon}{\epsilon_0}\right) - 2 \tag{3.2}$$

where K is a parameter fitted from experimental data and ϵ_0 is the porosity at zero compressive pressure, equal to 0.2. From experimental data at $592g$ and $925g$ K is determined to be 4.0 x 10^{-5} cm^2/dyne or 5.3 x 10^{-2} $(mm\ Hg)^{-1}$. Assumming that K is a property only of the material being centrifuged, these equations may be used to provide a value for fluid trapping in the microcentrifuge. Solution of equations (3.1) and (3.2) at $6300g$ for plasma and Eagle's suspensions are shown in Figure 3-1 for both the local porosity and the average porosity, defined as

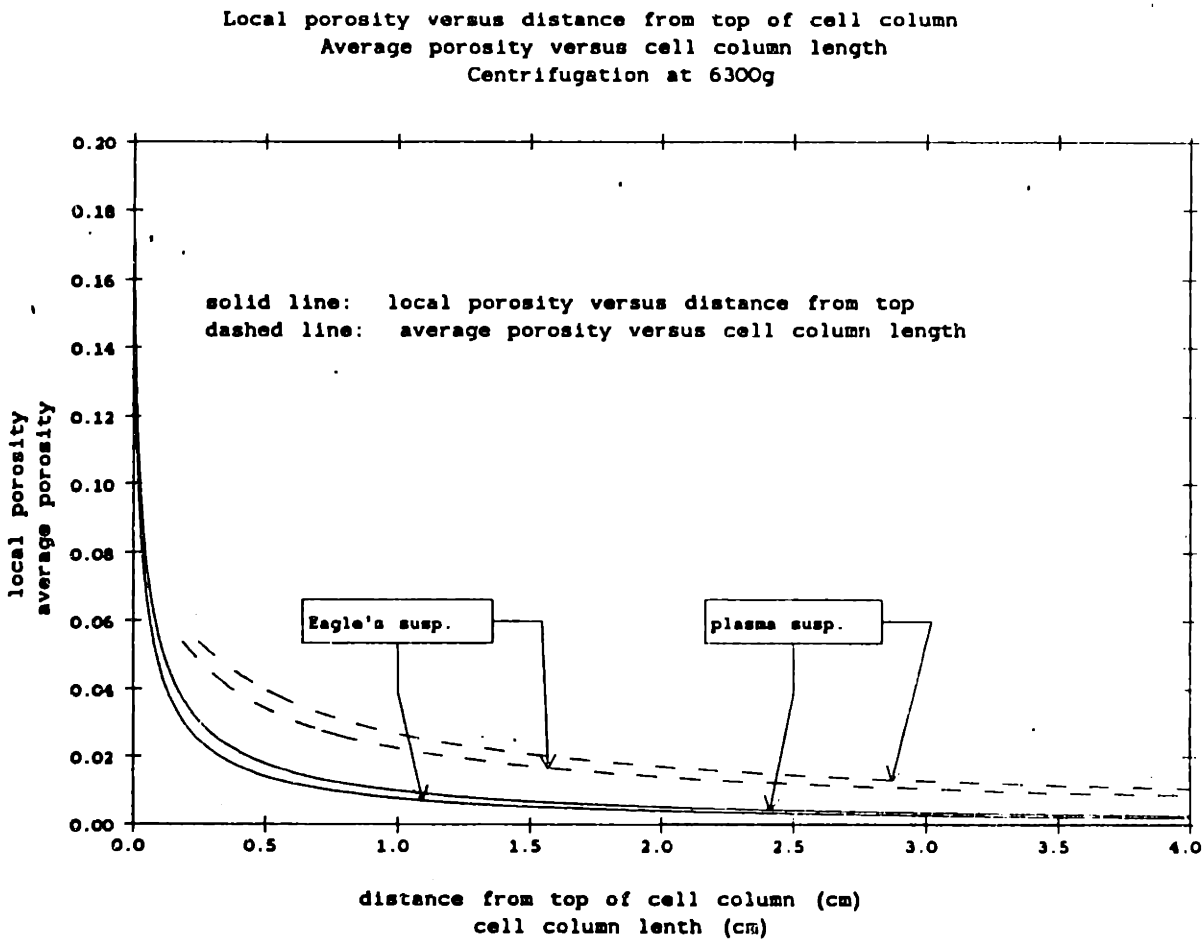

Figure 3-1: Plots of ϵ as a function of position in the cell column and of $\bar{\epsilon}$ as a function of cell column length.

$$\bar{\epsilon} = \frac{1}{L}\int_0^L \epsilon \, dy \tag{3.3}$$

Values for the average porosity at the typical microcentrifuge cell column length of 3 cm are 0.01 for Eagle's solution and 0.012 for plasma, which is in agreement with the value reported by Chien *et al.* [1965]. The microhematocrit values were multiplied by (1-$\bar{\epsilon}$) to obtain the hematocrits reported in the results. Because of these adjustments, the hematocrit H and cell volume fraction c are used interchangeably throughout this work.

3.3 Viscometry Measurements

3.3.1 Techniques of Viscometry

Before discussing the particulars of the equipment and methods used for measuring blood viscosity, it will be helpful to first review some general considerations of blood viscometry. The rotating coaxial cylinder (Couette) viscometer is in widespread use for these applications. It consists of an inner cylinder placed in an outer cup, with a gap between the two where the sample of fluid to be assessed is placed (see Figure 3-2). Either the inner or the outer cylinder may be rotated, and the viscosity of the fluid being sheared causes a momentum flux which developes a torque which is measured on the cylinder not rotated. If the gap width between the cylinders is narrow (less than 5%) compared to the radius of the cup, the fluid will undergo simple, steady, laminar shear and the velocity profile within the gap can be approximated by a straight line. The shear rate in sec^{-1} in the annulus is given by

$$\gamma = 2\omega \frac{R_o^2}{R_o^2 - R_i^2} \tag{3.4}$$

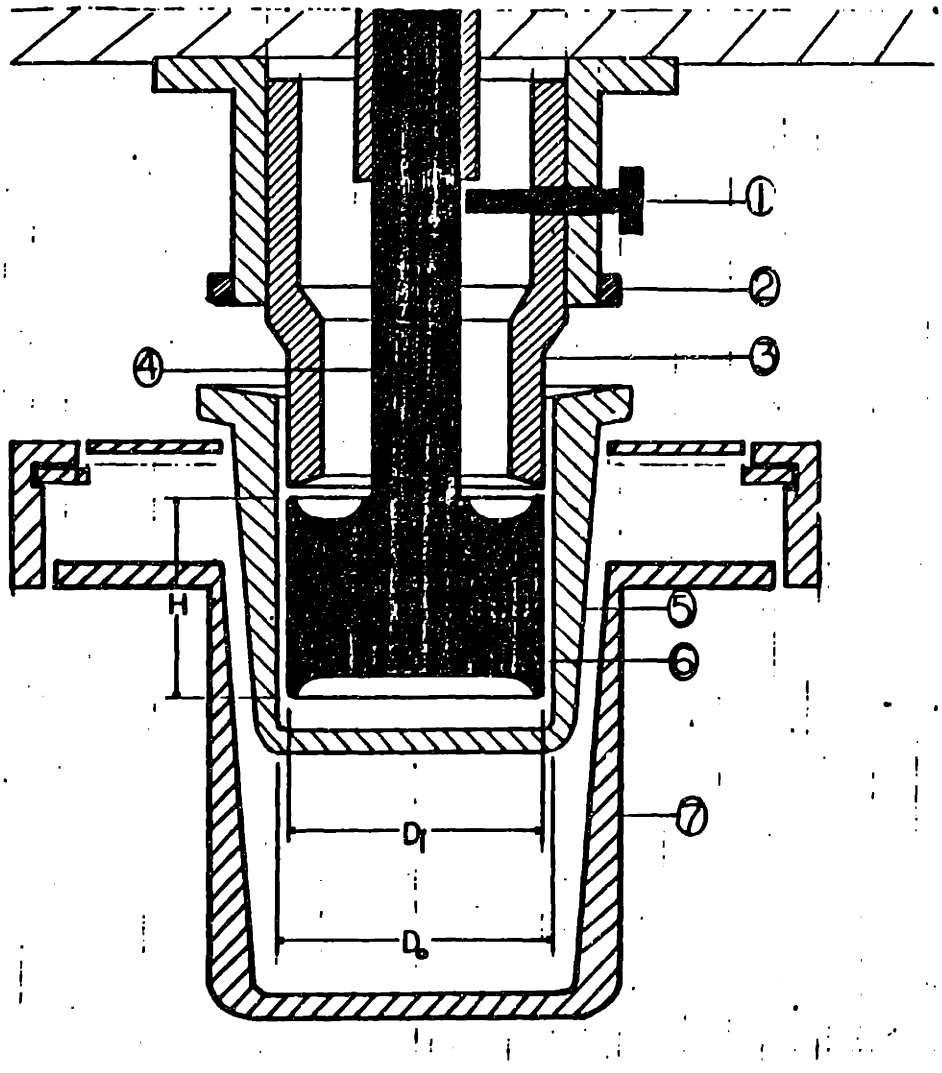

Figure 3-2: The Haake ZA30 sensor system, an example of a coaxial cylinder viscometer.

1. Knurled screw to hold inner cylinder. 2. Clamping ring to hold guard ring.

3. Guard ring. 4. Inner cylinder. 5. Outer cylinder (beaker).

6. Gap where sample is located. 7. Beaker housing

where ω is the angular velocity of the rotating cylinder in radians/sec, and R_o and R_i are the radii of the outer and inner cylinders, respectively. The torque across the gap is constant, so that if end effects are neglected, the shear stress in dyne/cm^2 exerted on the inner cylinder is given by

$$\tau = \frac{M}{2\pi h R_i^2} \tag{3.5}$$

where M is the torque exerted in g-cm and h is the length of the cylinder. Thus knowledge of ω, M, and the geometric parameters of the system leads to measurement of $\dot{\gamma}$,τ, and hence, $\eta=\tau/\dot{\gamma}$.

The interpretation of rheological data for blood is complicated by several effects, artifacts, and sources of error, some of which are common to all fluids while others are peculiar to blood. Included in the former are end and edge effects resulting from flows above and below the inner cylinder. These can be minimized by modification of the inner cylinder, either by recessing the ends or converting the bottom end into a conical configuration [Meiselman and Cokelet, 1973].

The air-fluid interface at the top of the viscometer can be a source of significant error. Even a simple Newtonian sample such as water exhibits surface effects from its high surface tension if a free meniscus develops in the gap. When plasma viscosities were intially measured [Copley *et al.*, 1960; Wells and Merrill, 1961; Cerny *et al.*, 1962] in viscometers without guard rings, shear-thinning behavior was reported due to the formation of a wax-like "skin" of lipids, lipoproteins, or denatured proteins. Employment of a guard ring such as that shown in Figure 3-2 eliminates the surface effects by preventing fluid which lies on the air-fluid interface from influencing the torque reading.

The presence of the walls of the cylinder necessarily introduces a inhomogeneity into the distribution of cells in the gap, since the center of any one

cell cannot lie closer to the wall than its radius. This wall exclusion effect was studied mathematically and experimentally by Vand [1948], who used glass spheres in coaxial and capillary viscometers. His model assumed a "rectangular" concentration profile of a layer of pure suspending fluid next to the walls and a bulk region of constant concentration which was later used by Quemada [1977] to derive his expression for blood viscosity, equation (2.11) (see Appendix C). In a monodisperse system, Vand found a particle-free layer with a width of 1.1 times the particle radius which resulted in a decrease in the measured wall shear stress below that expected for a homogeneous suspension. Cokelet *et al.* [1963] found that torque values of 2 to 5% higher could be obtained by the use of grooves 66μm deep in the walls of the cylinders. The necessity of the grooved surfaces is disputed by Chien *et al.* [1966], who note that their presence does not always prevent formation of the plasma layer [Merrill *et al.*, 1963a]. Also, it is desirable to obtain data at conditions which represent flow systems of interest (*e. g.*, blood vessels), and these do not have regularly grooved walls. The cylinders of the Haake viscometer used in this study had smooth surfaces.

The applicability of equations (3.4) and (3.5) depends on the maintenance of laminar, unidimensional (tangential) flow in the gap. If the inner cylinder is the rotor, centrifugal forces can introduce secondary flows and Taylor vortices and as the rotation rate increases, eventually lead to turbulent flow. For an annulus width of 1 mm and a outer radius of 2.5 cm, the shear rate at which secondary flow occurs for plasma at 37 °C is about 150 sec^{-1} and for blood is about 300-450 sec^{-1}. When the outer cylinder is the rotor, as in the case of the present study, inertial forces tend to stabilize the flow and the shear rate at which secondary flow begins is around 10^5 sec^{-1} [Meiselman and Cokelet, 1973].

Other considerations are more specific to blood. The difference in density

between the erythroctes (approximately 1.09 g/cm^3) and plasma (approximately 1.02 g/cm^3) results in a tendency of red cells to settle in plasma solutions. A homogeneous sample can be maintained in the coaxial cylinder viscometer by having the region above the inner cylinder covered with a pool of blood [Meiselman and Cokelet, 1973].

The torque-time curves for blood show two regimes of behavior: At shear rates above 1 sec^{-1} the torque reading rises quickly (on the order of a second) to a constant value which is maintained until the shear is stopped. At shear rates above 10 sec^{-1} the time for this rise is negligible. At rates below 1 sec^{-1} a more gradual rise to a maximum is observed followed by a decay to an equilibrium value. The time for this rise can be as long as a minute or more at shear rates of 0.01 sec^{-1}. Direct visualization of the annulus shows that at low shear rates, the red cells migrate away from the outer and possibly from the inner walls, forming a substantial cell-free layer near the walls [Cokelet *et al.*, 1963; Meiselman, 1965]. It has been hypothesized that the slow rise is due to transient effects from intiation of the shear and that the decay represents migration of the cells away from the cylinder walls, which can be represented mathematically as an exponential decay [Cokelet and Smith, 1973] (see Figure 3-3). The argument thus is that the correct torque is one which is extrapolated to zero time from the decaying exponential curve. As will be discussed in the next section, there was no torque decay at the lowest observable shear rate of the present study. A theoretical model for blood flow at low shear rates in a coaxial cylinder viscometer is given by Bloor [1982].

3.3.2 Viscometer

Rheological measurements were performed with a Haake Rotovisco RV100 with the CV100 measuring system (Haake, Inc., Saddle Brook, NJ). The instrument

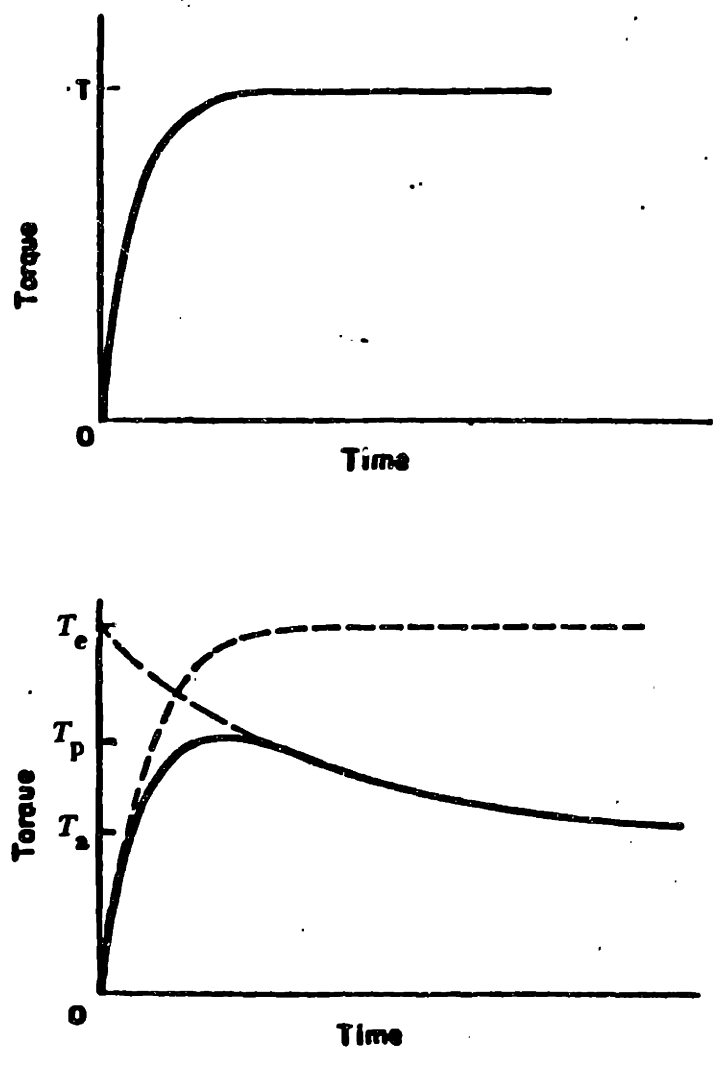

Figure 3-3: Torque-time curves for blood.

Top, shear rates greater than 1 sec $^{-1}$. *Bottom*, shear rates less than 1 sec $^{-1}$. T_a is the asymptotic equilibrium torque value measured, T_p is the peak torque, and T_e is the torque extrapolated to time zero. From Cokelet and Smith [1973].

is the property of the Ceramics Laboratory of the Department of Materials Science and Engineering at M.I.T. and is pictured in Figure 3-4. The ZA30 sensor system was used, which is a stainless steel coaxial cylinder system (see Figure 3-2, page 52). The outer cup is driven by a motor, which provides greater stabilization against secondary flows as described previously. The viscosity of the fluid being sheared causes a momentum flux which develops a torque on the inner cylinder, deflecting measuring springs in the drive unit and producing an electrical signal proportional to the torque. The relevant dimensions for the ZA30 are listed in Table 3-I. The inner cylinder slides into the measuring shaft of the unit and is held on the shaft by a knurled screw. It is mechanically positioned and centered by an air bearing in the measuring system which is supplied with compressed air from an air supply unit (Haake model LV100). The air pressure in the supply unit resevoir is maintained between 5.5 and 3.5 bar. The feed pressure to the bearing is 2.5 bar.

The top and bottom surfaces of the inner cylinder are not flat but are recessed from the outer edge to minimize end effects as shown in Figure 3-2. A guard ring, secured on the measuring shaft by a clamping ring, is employed in all measuremnets to minimize artifacts from the fluid-air interface. A refrigerated bath and circulator (Haake model F3-K) supplies a water jacket in the measuring system with a supply of distilled water, which is maintained at a constant temperature by a balance of controlled heating against continuous cooling. The water jacket is used to set sample temperature and to remove dissipated heat from the sample created by shearing.

The viscometer is linked to an HP-85 Desk Top Computer (Hewlett-Packard Corporation, Corvaillis, OR), which in turned is connected to an HP 7470A Graphics Plotter. The viscometer interface is a Haake DVM 7615 four-channel digital voltmeter with three control lines connected to an HP 82940A I/O interface.

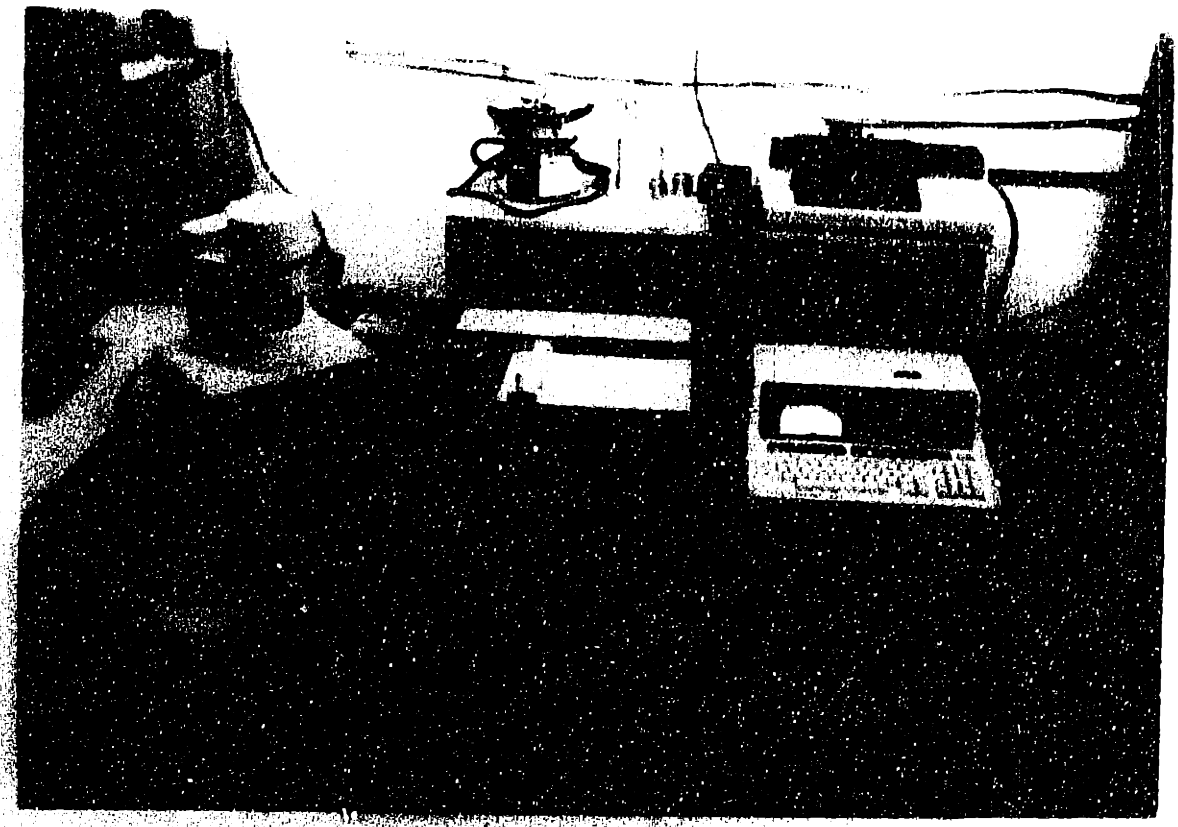

Figure 3-4: Haake Rotovisco RV100 viscometer with accesories as described in text.

1. **CV100 measuring system**
2. **RV100 viscometer**
3. **Graphics Plotter**
4. **HP-85 computer**
5. **LV100 air supply unit**

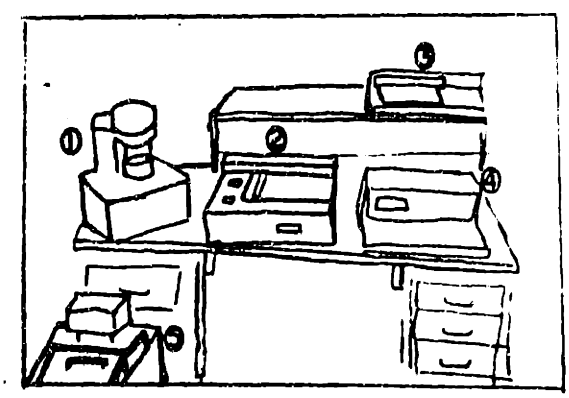

Inner cylinder diameter (D_i)	27.83 mm
Inner cylinder length (h)	26.9 mm
Outer cylinder diameter (D_o)	30 mm
Gap width	1.085 mm
Sample volume	5 ml

Table 3-I: Geometric parameters for the ZA30 sensor sytem.

A Haake rotational software cartridge (part #1077922) is used to program the computer, which can then be used to set the viscometer parameters and control the measuring operation. The viscometer may be run in either a τ vs. time mode at constant shear rate, or in a τ vs. shear rate mode with a maximum range of 0 to 300 sec^{-1}. The software reads 100 data points evenly distributed over time or over the selected range of shear rates and can print digital values or plot data on the Graphics Plotter.

3.3.3 Viscometry Methods

Enough sample to cover the inner cylinder, about 5 to 7 ml in volume, is carefully mixed and poured into the cup, which is covered with a piece of Parafilm and placed into the measuring unit for about two minutes to allow temperature equilibration at 37 ^{o}C. While the sample is warming, the guard ring and inner cylinder are mounted following the procedure recommended by the instrument instructions: The clamping ring is loosened and the guard ring slides into the housing, resting at the upper stop, and is clamped into position. The inner cylinder slides into the measuring shaft and is secured by the knurled screw. The guard ring is now loosened and allowed to rest on the upper face of the cylinder. The clamping ring is again tightened, which lifts the guard ring to a level of 0.1 to 0.2 mm above the inner cylinder. For highly viscous samples it is necessary to elevate the guard ring slightly more.

The shaft is lowered into the cup and then briefly raised up to overcome surface tension effects in the annulus and to observe whether the sample covers the gap between the guard ring and the inner cylinder. The sample is just visible at the border of the outer cylinder, providing a small pool of blood to maintain homogeneity in the annulus [Meiselman and Cokelet, 1973]. The exposed shaft is

encased with a Plexiglas housing and then the entire measuring system is covered with a large cardboard box to eliminate artifacts from outside air currents.

A fresh piece of plotting paper is placed in the recorder and calibrated. The scale parameters for the recorder are set according to the particular sensor system used. For the ZA 30 these values are 0.3 Pa/scale division for the τ axis and 3 sec^{-1}/scale division for the $\dot{\gamma}$ axis. The mode of operation is set to automatic reversal, that is, to step up continuously from 0 to 300 sec^{-1} over a period of one minute, to hold at 300 sec^{-1} for six seconds, and then to step down back to 0 sec^{-1}. (There is an associated hysteresis that is reported on in Chapter 4.) The full-scale factor for the τ axis of the recorder was set to the minimum value possible. The run is intiated.

Upon completion, a hard copy of the data points is obtained from the HP-85. Repeat measurements are made from 0 to 30 sec^{-1} and from 0 to 3 sec^{-1} with appropriate modifications in the full-scale setting for the τ axis. The sample is then removed and discarded and the cup, inner cylinder, and guard ring are washed out with hot water.

In order to insure that the shear induced by the instrument would not cause hemolysis sufficient to affect the measurements, a series of samples had their viscosities measured first at a constant shear rate of 0.3 sec^{-1}, then were subjugated to constant shear rates of 300 sec^{-1} for a period of a minute, and then viscosities were remeasured at 0.3 sec^{-1}. No significant change was noted in the values at the low shear rate. Secomb *et al.* [1983a], in the direct microscopic observation of concentrated red cells at shear rates up to 1585 sec^{-1}, did not report on any significant hemolysis.

An assessment of the torque-time curves for concentrated suspensions of blood showed no transient effects such as those seen in Figure 3-3 at shear rates of 0.3

sec^{-1}, which is the lowest constant shear rate at which the viscometer could be run. There was agreement between those viscosity values obtained in the constant shear rate mode and the corresponding value obtained with continuous variation of shear rates.

3.4 Data Analysis

The data was fitted to several functions, both linear and non-linear. A general optimization routine was written in FORTRAN and run on the VAX-11 computer of the Whitaker College Computer Facility. The program was adapted from one by Zydney [1985] and is given in Appendix D. The general principals behind the data analysis will be presented here, as developed by Zydney [1985].

Determination of the optimal set of parameters $b_1, b_2, \ldots, b_P$ for a function Y which describes a set of data of N points can be equated to minimizing E, the value of the sum of squared residuals

$$E = \sum_{i=1}^{N} [y_i - y_{i,exp}]^2 \tag{3.6}$$

where y_i is the calculated value from the function Y at the same set of conditions as the experimental value $y_{i,\,exp}$.

Minimizing E is equivalent to finding values of b_i such that the gradient of E is zero. In mathematical terms, this is represented as a set of P coupled equations

$$F_j(b) = \frac{\partial E}{\partial b_j} = 2\sum_{i=1}^{N} [y_i - y_{i,exp}]\frac{\partial y_i}{\partial b_j} = 0 \tag{3.7}$$

The method of steepest descent [Himmelblau, 1970] is used to find the set of parameters which minimize E. The set of equations represented by equation (3.7) can be solved by a Newton-Raphson iteration,

$$\mathbf{b}^{j+1} = \mathbf{b}^j - (\mathbf{A}^j)^{-1}\mathbf{F}^j \tag{3.8}$$

where **A** is the jacobian maxtrix with components

$$A_{ij} = \frac{\partial F_i}{\partial b_j} \tag{3.9}$$

The derivatives of y_i are evaluated numerically as

$$\frac{\partial y_i}{\partial b_j} = \frac{y_i(b_j+\Delta b) - y_i(b_j)}{\Delta b} \tag{3.10}$$

The derivatives of F are found in a similar fashion.

After the data has been fit to the equation, various regression parameters are calculated from the covariance matrix:

$$\mathbf{cov}(\mathrm{b}) = \frac{E}{N-P}(\mathbf{X}^t\mathbf{X})^{-1} \tag{3.11}$$

where **X** is the matrix whose elements are

$$X_{ij} = \frac{\partial y_i}{\partial b_j} \tag{3.12}$$

and $\mathbf{X}^t$ is the transpose of **X**. The variance of the fitted parameter b_i is given by the diagonal elements of the covariance matrix.

$$\mathrm{var}\,(b_i) = \mathrm{cov}\,(b_i, b_i) \tag{3.13}$$

The correlation coefficient between any two parameters b_i and b_j is

$$\rho_{ij} = \frac{\mathrm{cov}\,(b_i, b_j)}{[\,\mathrm{var}\,(b_i)\cdot \mathrm{var}\,(b_j)]^{0.5}} \tag{3.14}$$

The 95% confidence limits for a function of the fitted parameters Y=Y(b) is evaluated first by finding the variance of Y from the variances and covariances of the R parameters [Freund and Minton, 1979]:

$$\mathrm{var}\,(Y) = \sum_{i=1}^{R} \left(\frac{\partial Y}{\partial b_i}\right)^2 \cdot \mathrm{var}\,(b_i) + 2\sum_{i=2}^{R}\sum_{j<i}^{R-1} \left(\frac{\partial Y}{\partial b_i}\right)\left(\frac{\partial Y}{\partial b_j}\right) \mathrm{cov}\,(b_i, b_j) \tag{3.15}$$

where the second term on the right represents sums over all possible combinations of i and j such that i>j. The standard deviation σ_Y at any point on the function Y is given by the square root of the variance. The 95% confidence interval at any point on Y is given by

$$Y - t_{0.025}\sigma_Y < Y < Y + t_{0.025}\sigma_Y \tag{3.16}$$

where $t_{0.025}$ is the area under one tail of the Student t-distribution.

To avoid weighing the fits toward minimizing residuals at high values of η, the residuals were weighted by the reciprocal of the calculated value. The actual form of equation (3.6) used is

$$E = \sum_{i=1}^{N} \left[\frac{\eta_i - \eta_{i,exp}}{\eta_i}\right]^2 \tag{3.17}$$

Chapter 4

RESULTS

4.1 General comments

Examples of the raw data from the Haake viscometer as printed by the Graphics Plotter are shown in Figure 4-1. Each sample was run in three ranges of operation: high shear from 0 to 300 sec^{-1}, medium from 0 to 30 sec^{-1}, and low from 0 to 3 sec^{-1}. The plot of shear stress vs. shear rate in the lowest range shows two discernible artifacts: (a) a period in the step-up curve representing a start-up lag during which time the cylinder is rotating but the transducer as yet records no reading, and (b) a hysteresis between the step-up and step-down curves, with the step-down curve respresenting values on the order of 1 to 3 per cent higher than the step-up curve. This hysteresis, which existed to a smaller extent at higher shear rates, is caused by the time lag between the shear rate imposed and the shear rate measured. Its magnitude diminished as the rate of change of shear rate was decreased, but it could never be completely eliminated. The HP-85 computer printed out a hard copy of 100 data points for each run, and a representative sampling of points were selected from these lists for fitting. Approximately every fifth point from both the up and the down curves was used, averaging twenty data points obtained per run. From the up curve, no points were obtained from the region of the start-up artifact, and in compensation there was a higher rate of selection of points from the down curve in this region.

Measurement of plasma and saline viscosities at 37 ^{o}C showed a small but significant shear-thickening behavior which could have resulted from the

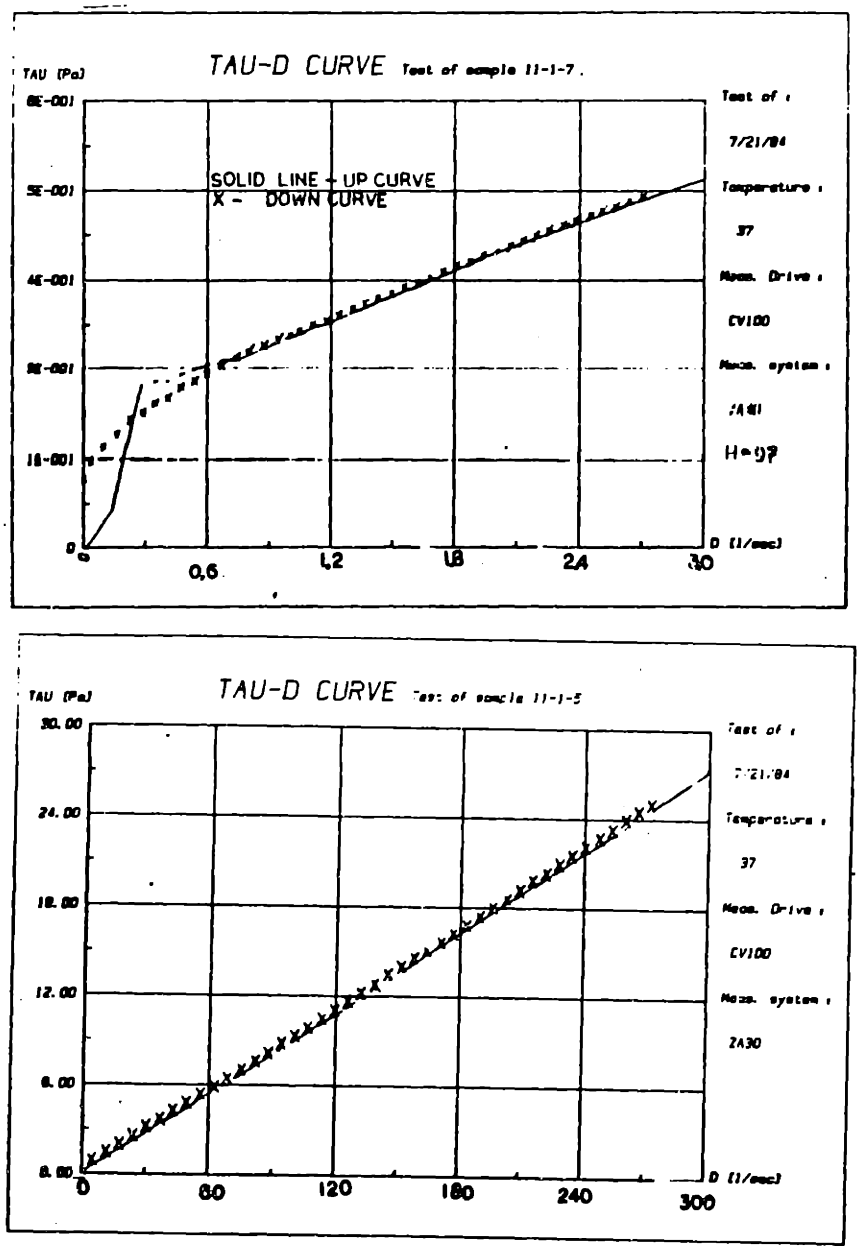

Figure 4-1: Plots of τ vs. γ from H-P Graphics Plotter interfaced with Haake viscometer, H=97.

Solid line=up curve. X=down curve.

development of secondary flows in the viscometer [Merrill, 1969]. The viscosity measured for Eagle's solution ranged from 0.85 to 0.9 cP. These values are somewhat higher than literature values of 0.69 cP for water at 37 ^{o}C, and the discrepancy is probably due to viscometer limitations in measurement of low-viscosity samples. In order to maintian consistency with other published data, 0.69 cP is used as the pure fluid viscosity for all saline solutions reported here. Plasma viscosities were more variable, ranging from 1.03 to 1.21 cP, which are comparable to typical literature vlaues of 1.2 cP. For plasma suspensions the individual plasma values were used for calculating relative viscosity.

A series of measurements using freshly drawn blood obtained from a single source (the author) was used in order to check the reproducibility of the experimental method. Viscosity differences between different samples at the same hematocrit were on the order of 5% or less at hematocrits greater than 95. At hematocrits above 97 the sensitivity to concentration was enough to require that hematocrit be measured to the nearest tenth of a unit. At lower hematocrits it was sufficient to measure hematocrit to within a unit.

Tables of the data used in this work are presented in Appendix F. For definitional purposes, throughout the remainder of this work a *unit* of blood refers to all of the blood contained in the original bag obtained from the Red Cross. Each unit provided one or more *batches* of blood. A batch of blood is defined as an amount of blood removed from a unit and processed at one particular time, which is then divided into several *samples* of varying hematocrit. Sample identification is by the batch number followed by the sample number, *e. g.*, 19-6. The unit identifications for each sample are given in Appendix F.

Variations in viscosity from batch-to-batch and from unit-to-unit were shear-dependent, with the greatest differences at very low shear rates. Different batches

from the same unit generally had comparable values at all shear rates, within 5% of each other. Samples from different units were within 5% at high shear rates, but could be separated by up to a factor of two or more at shear rates below 0.1 sec^{-1}. At shear rates above 0.1 sec^{-1}, viscosity differences were usually small. Some of the variability can be traced to the age of the blood samples, and this is expanded on later in this chapter.

4.2 Viscosity of RBC suspended in saline solution

The data for RBC suspensions in Eagle's solution are presented in Figures 4-2 to 4-25 (pages 69 to 92). Each plot is one of relative viscosity (η_r) versus shear rate ($\dot{\gamma}$) at a different hematocrit. Hematocrits range from 98.4 to 7. Relative viscosities were calculated by dividing the measured viscosity by 0.88 cp, which was used as the pure Eagle's solution viscosity for all samples. On any one figure, data from different samples are represented by different symbols. Different samples from the same unit have the same designation with regard to the symbol being open or filled. Thus, in Figure 4-10, the two batches used are from the same unit, while in Figure 4-11, the two batches are from different units. There is no correlation of symbols between different figures.

The filled triangles in each figure are data values derived from the Chien *et al.* [1966] equation, (2.8), for Ringer's solution suspensions. Since the Chien *et al.* data are for viscosity and not relative viscosity, an estimate for η_f was made by taking the average values of the polynomials at zero hematocrit. In this manner, for Ringer's saline, η_f=0.692 cP. The solid curves with error bars and the dashed curves represent fits of the data to the Quemada equation, equation (2.11), and will be discussed in detail in Chapter 5.

On visual inspection, the points on each plot may appear to be segregated into

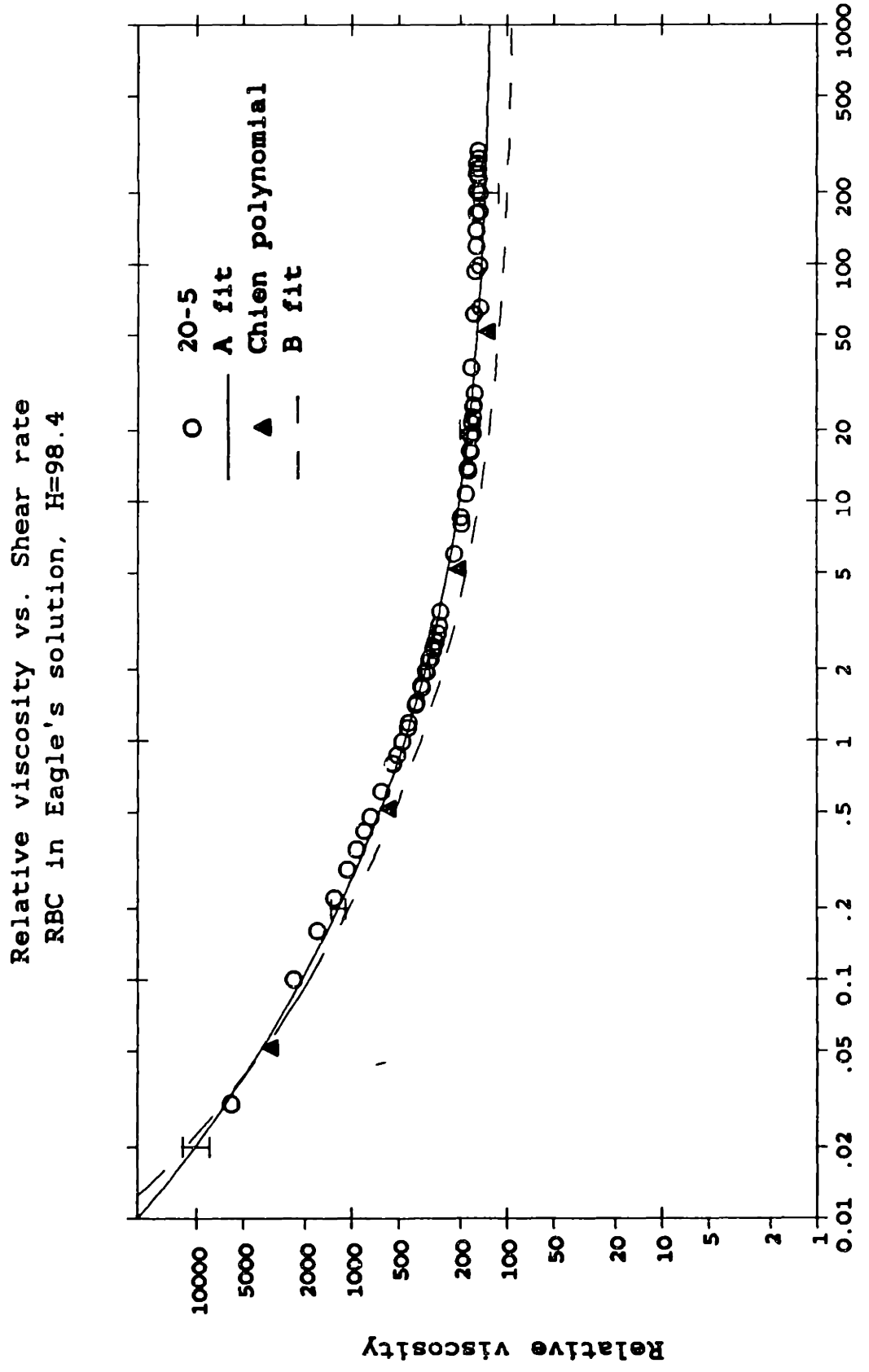

Figure 4-2: Eagle's solution data, H=98.4.

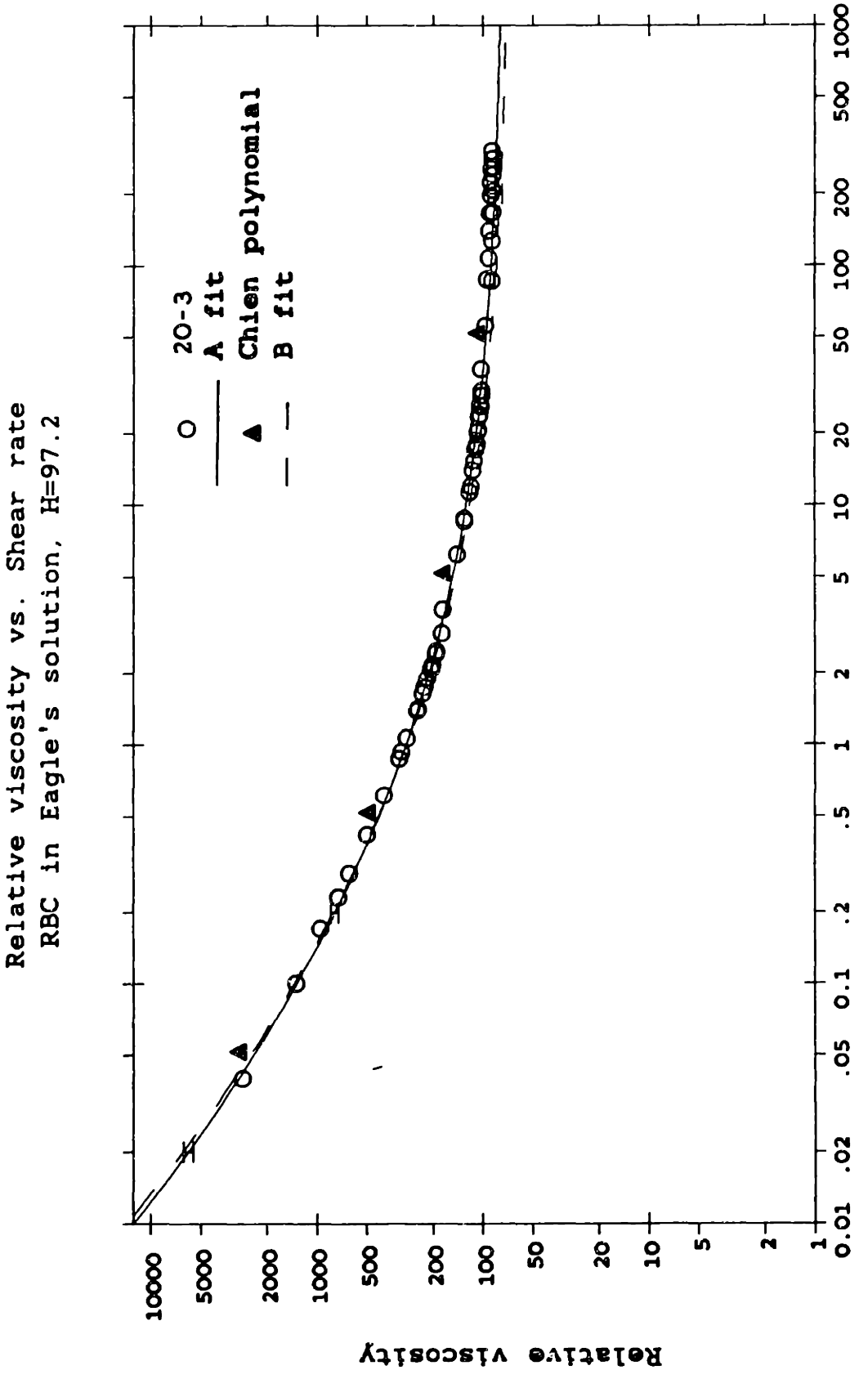

Figure 4-3: Eagle's solution data, H=97.2.

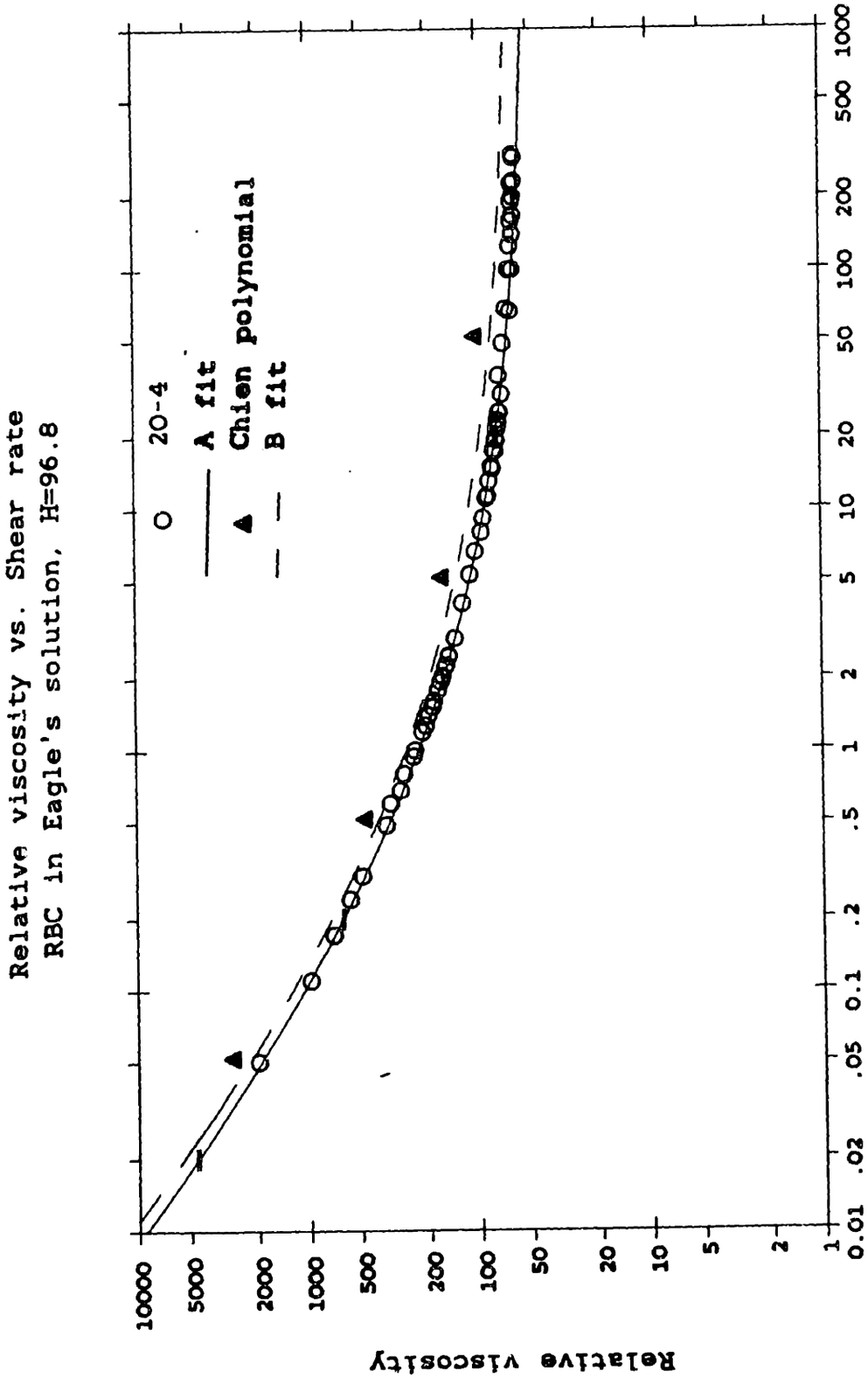

Figure 4-4: Eagle's solution data, H=96.8.

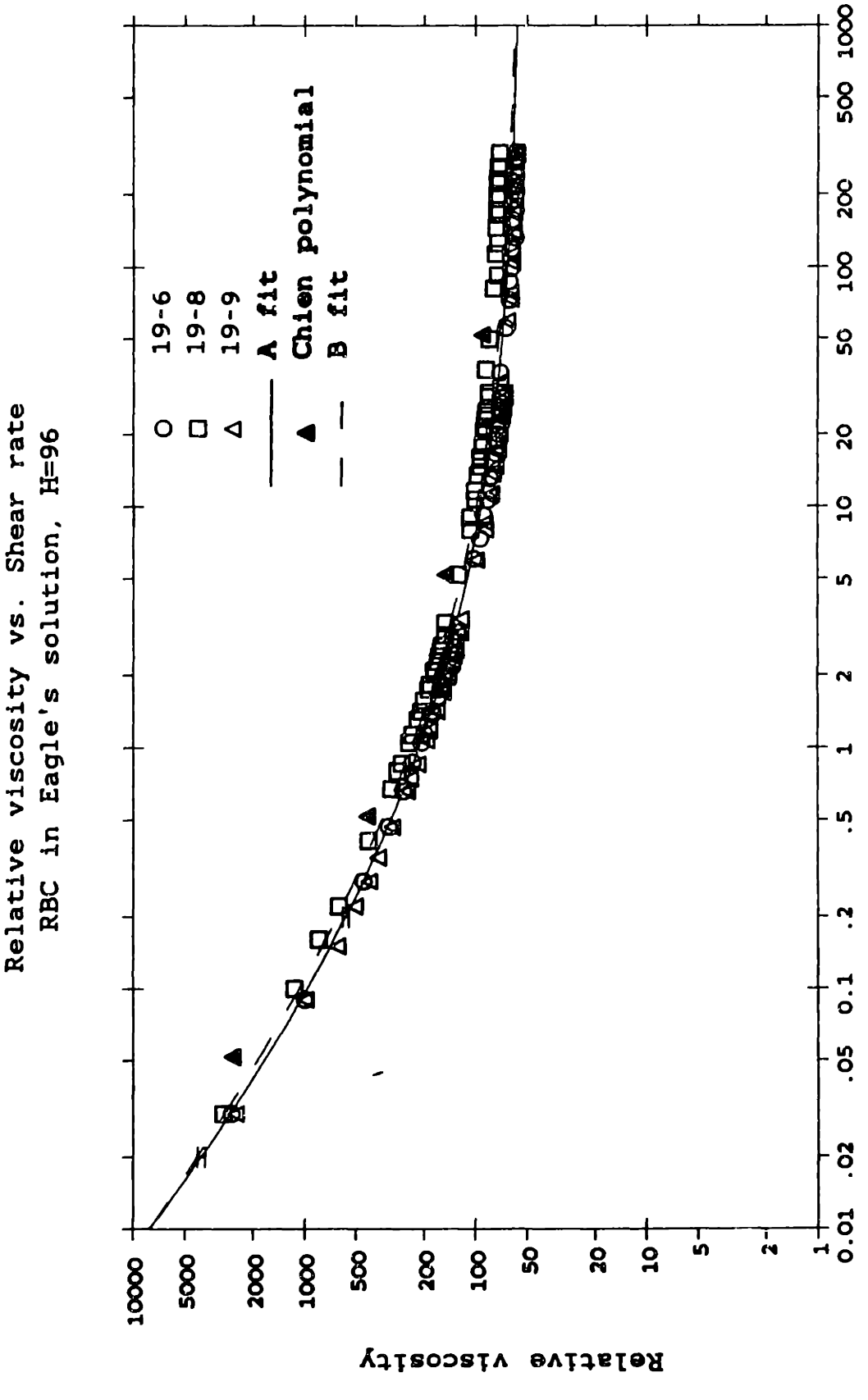

Figure 4-5: Eagle's solution data, H=96.

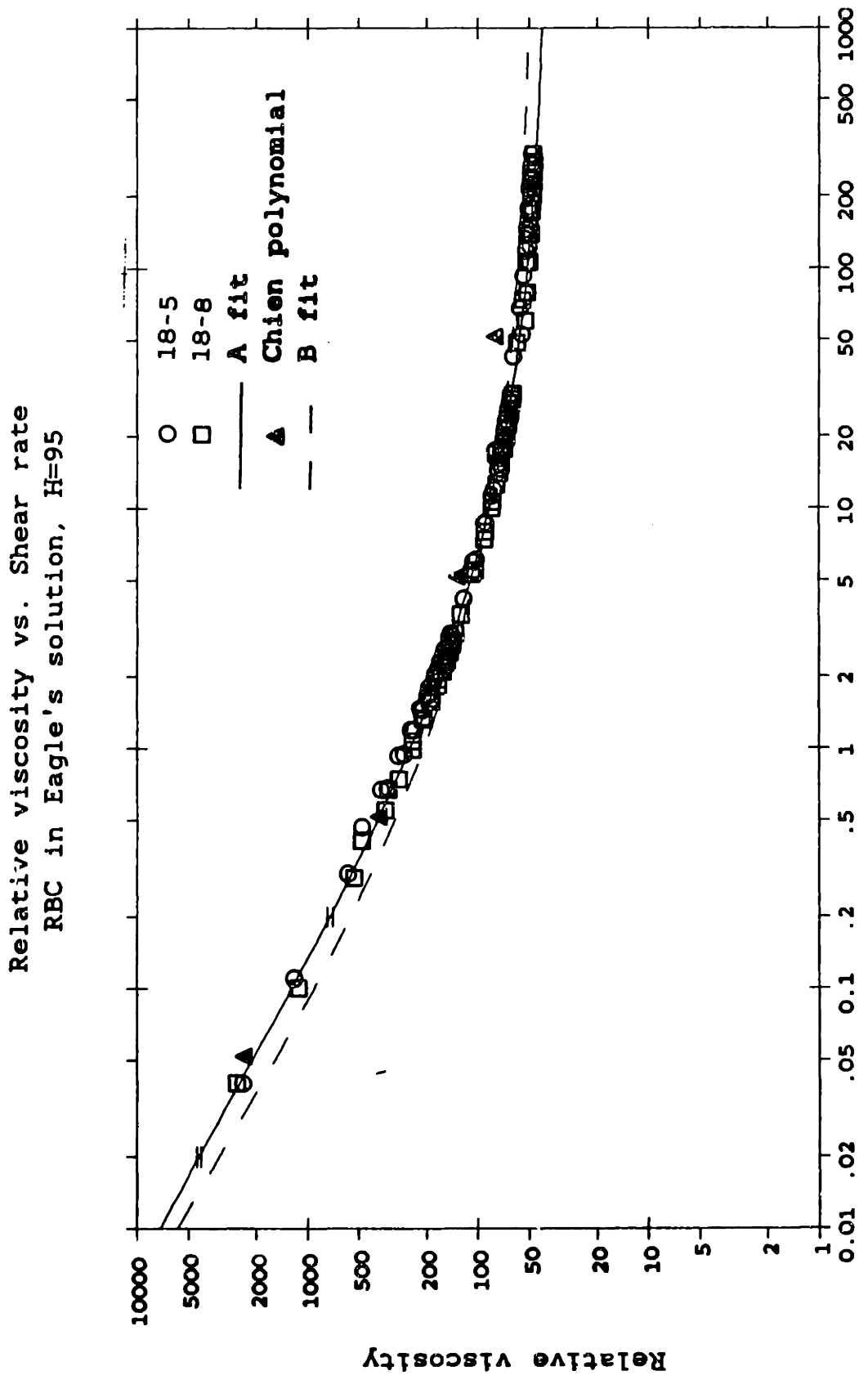

Figure 4-6: Eagle's solution data, H=95.

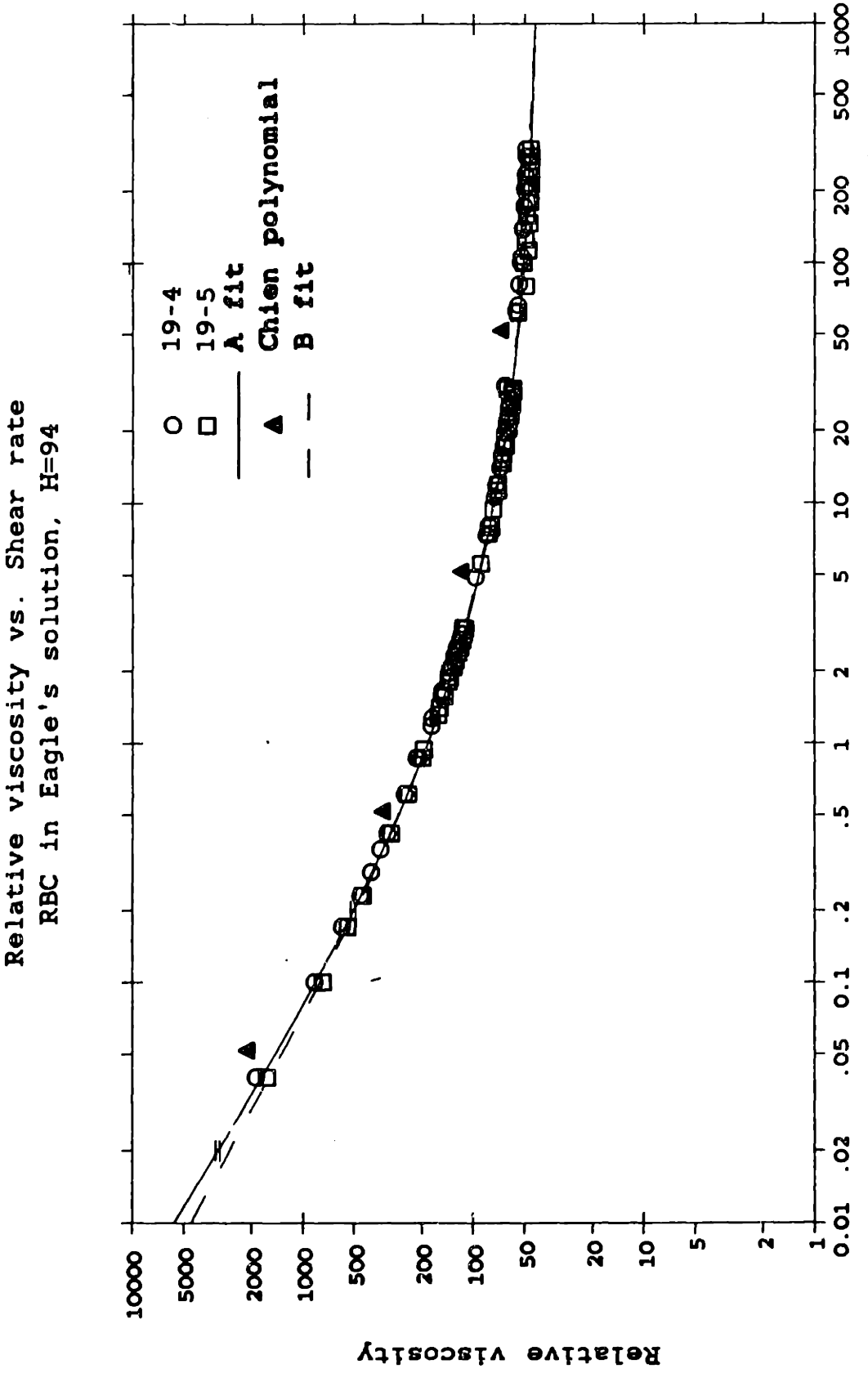

Figure 4-7: Eagle's solution data, H=94.

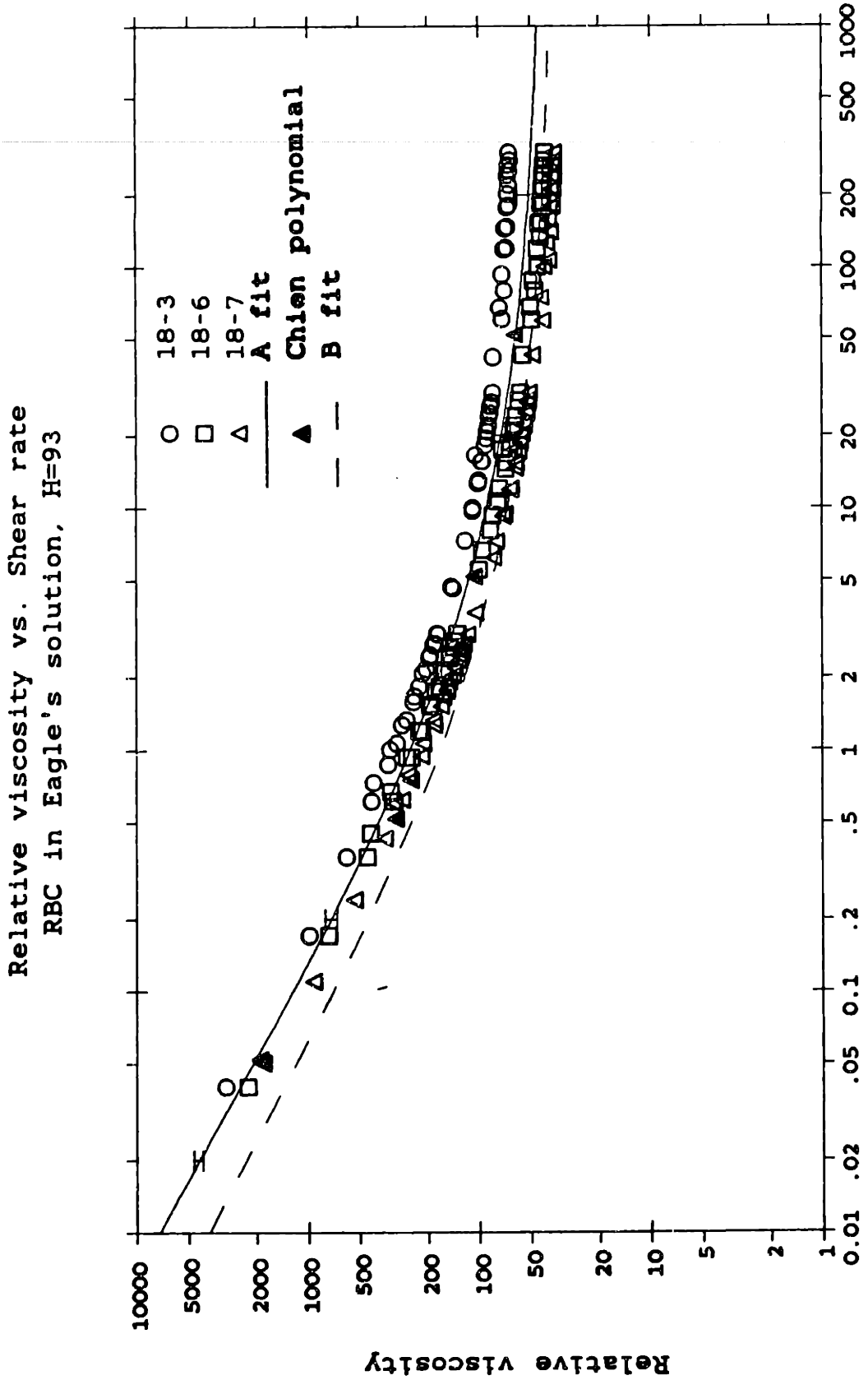

Figure 4-8: Eagle's solution data, H=93.

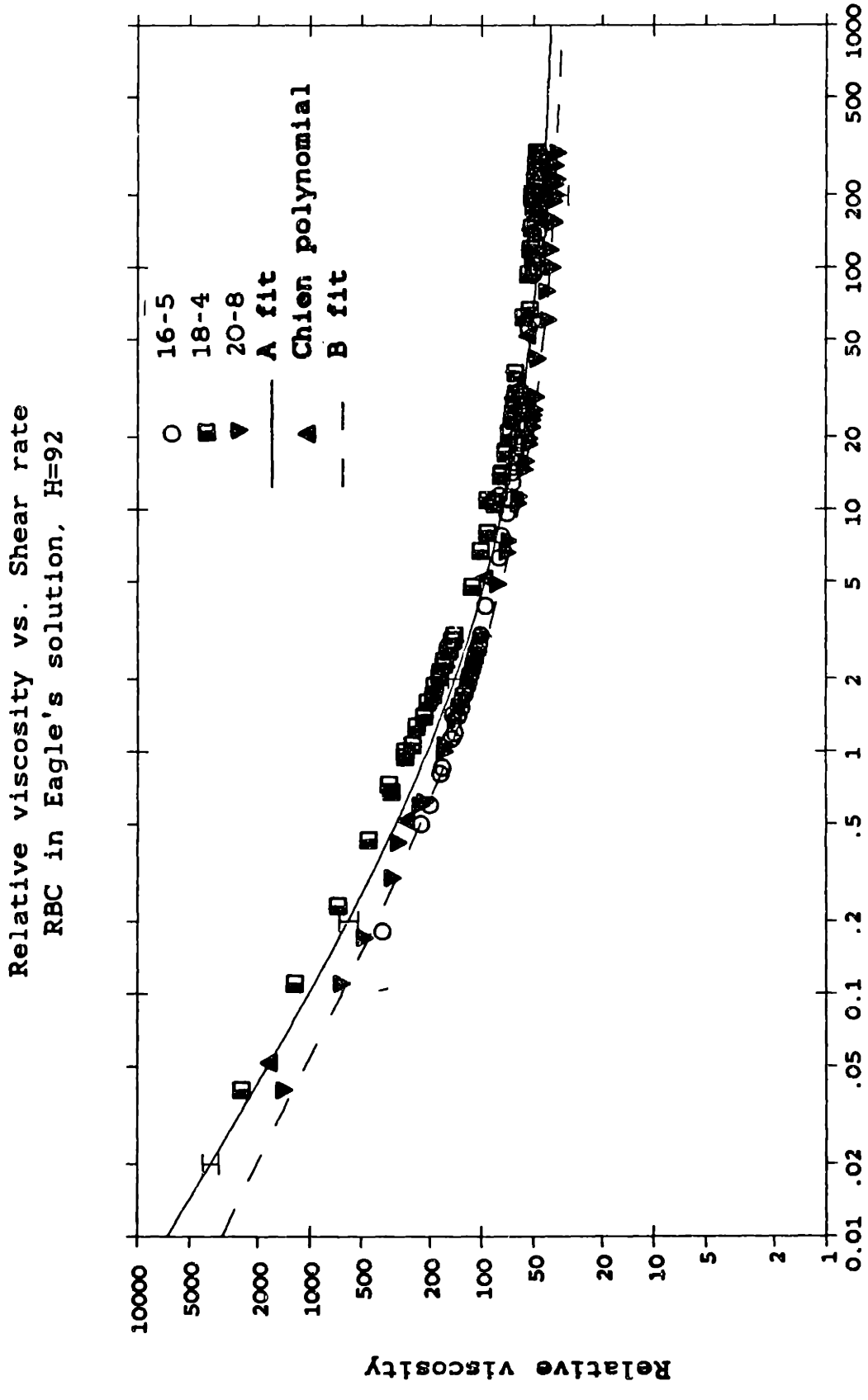

Figure 4-9: Eagle's solution data, H=92.

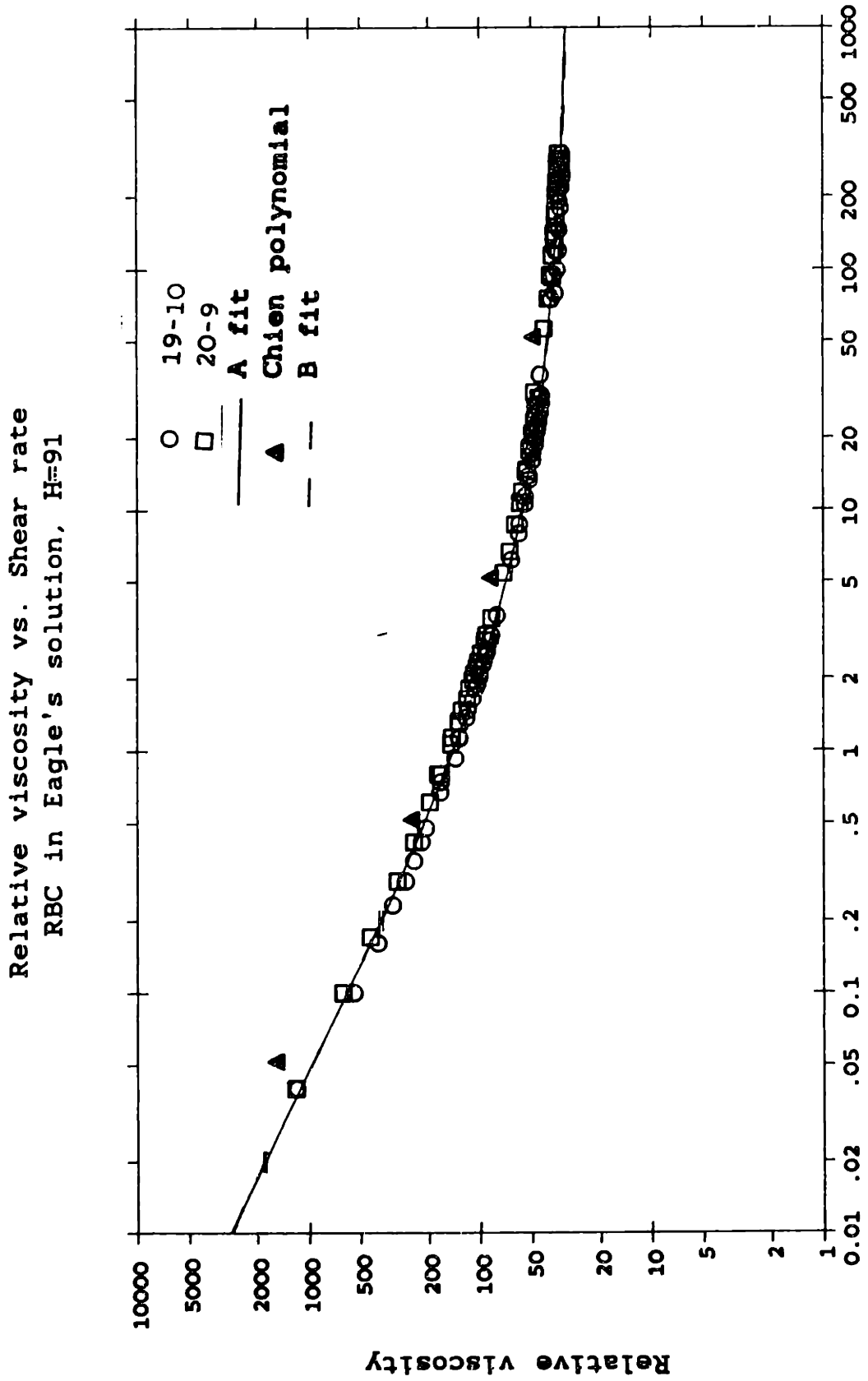

Figure 4-10: Eagle's solution data, H=91.

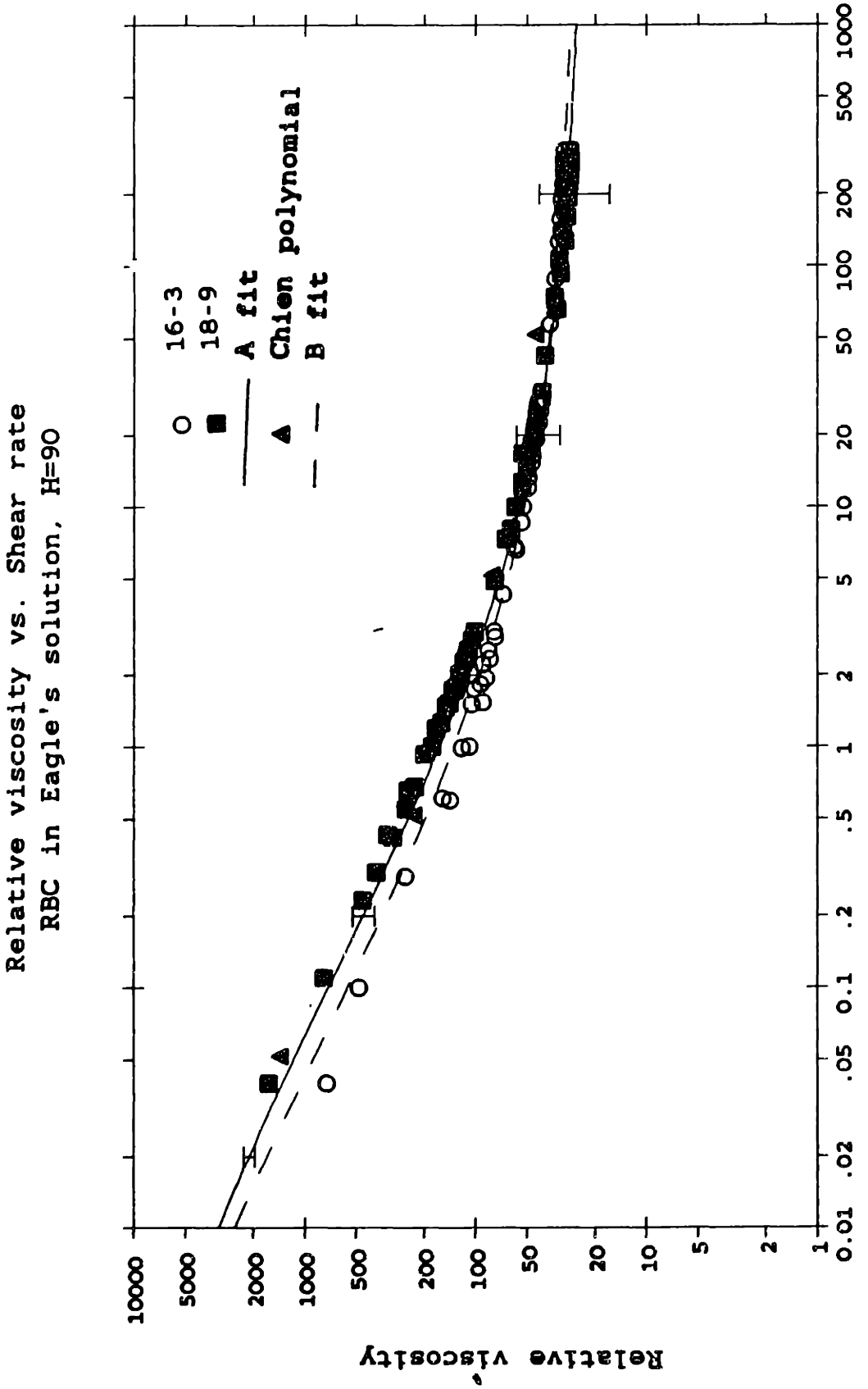

Figure 4-11: Eagle's solution data, H=90.

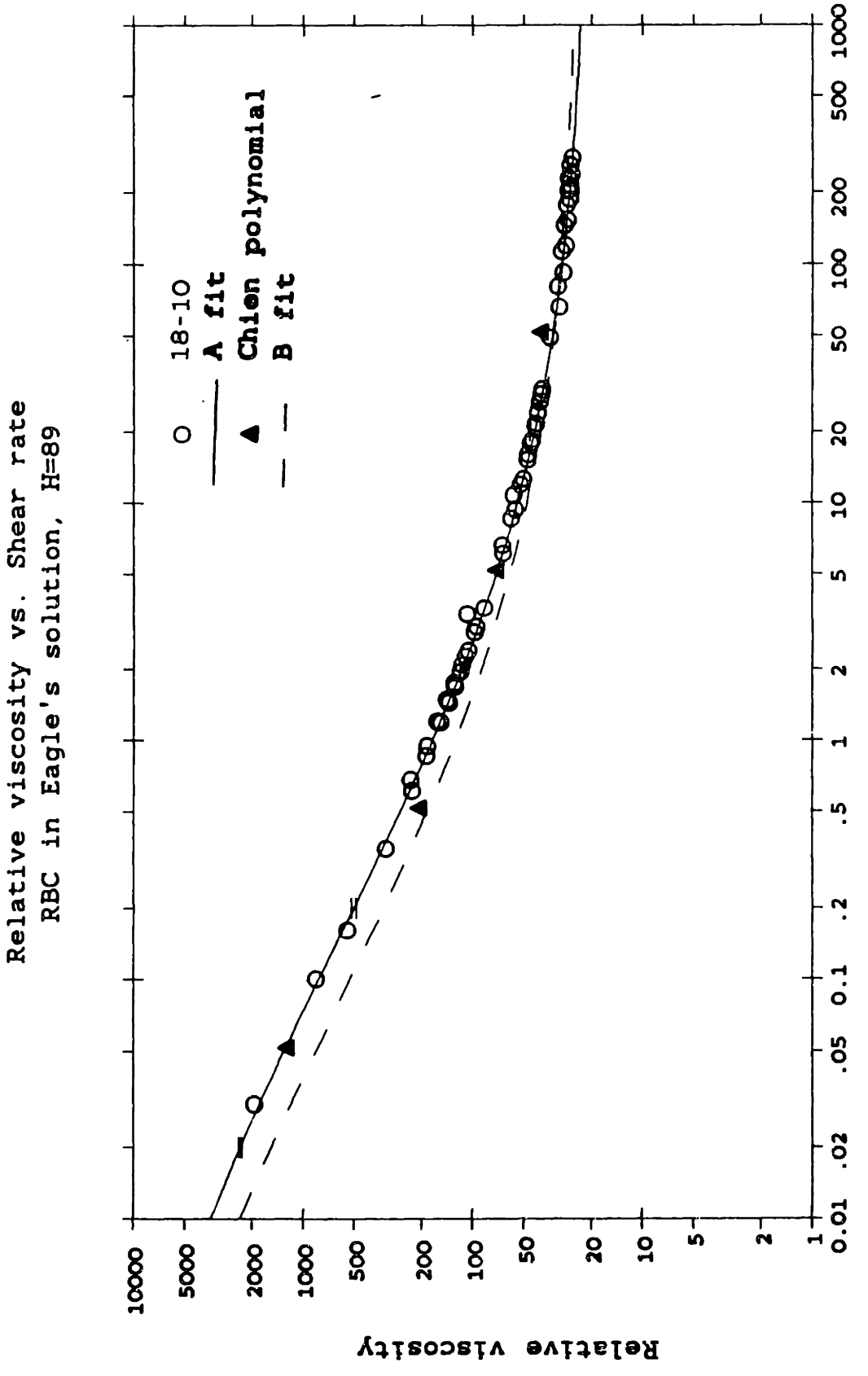

Figure 4-12: Eagle's solution data, H=89.

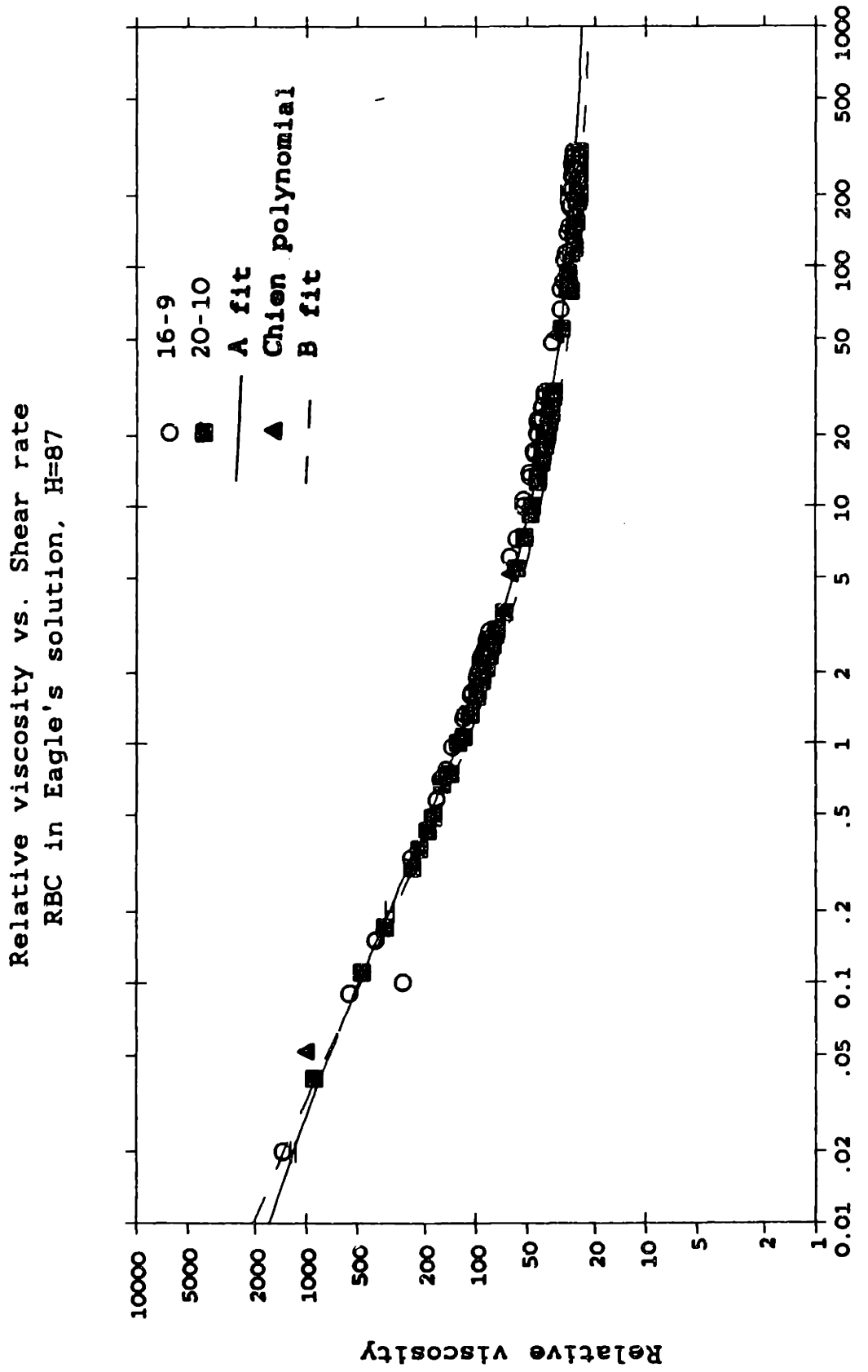

Figure 4-13: Eagle's solution data, H=87.

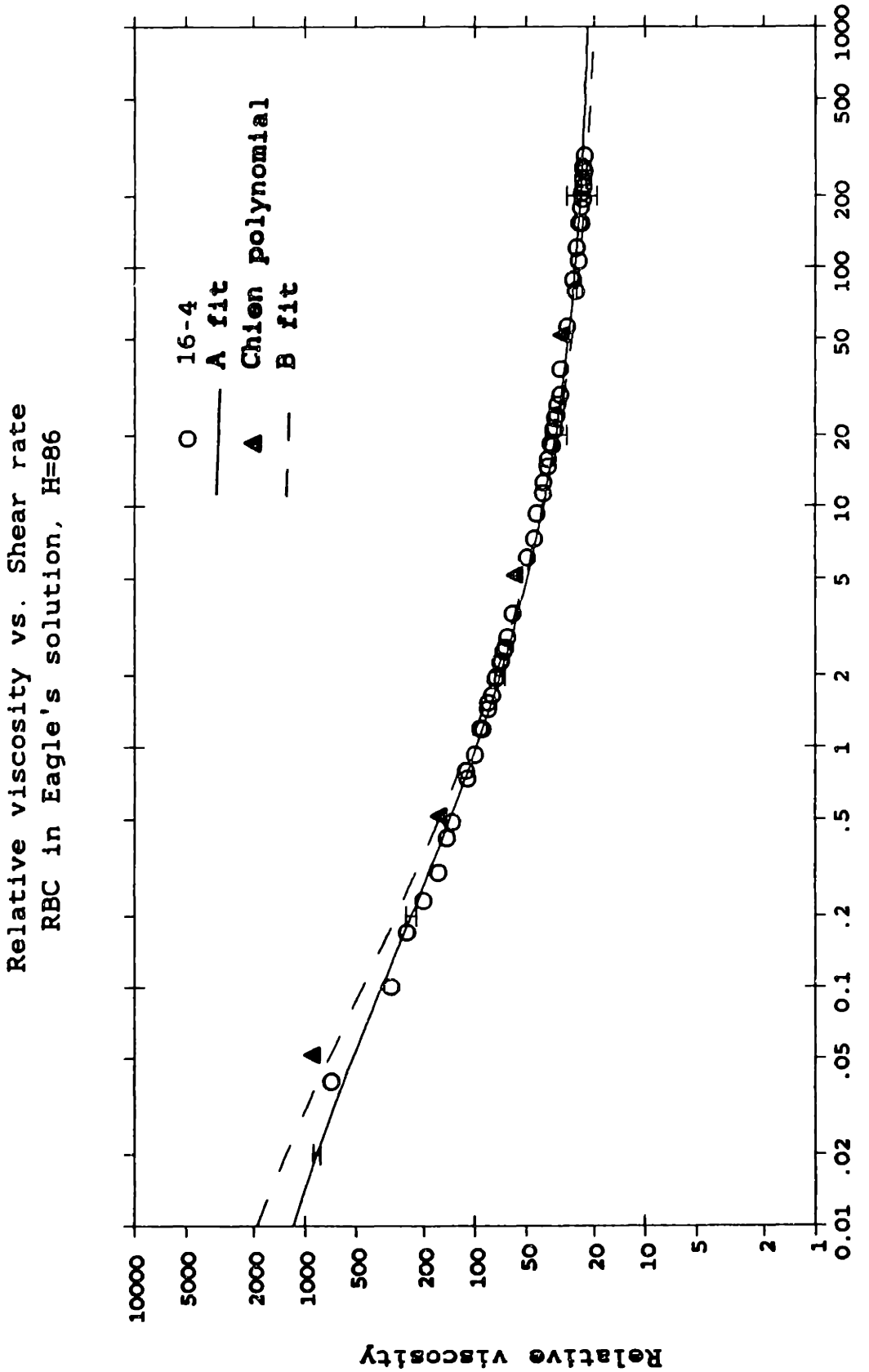

Figure 4-14: Eagle's solution data, H=86.

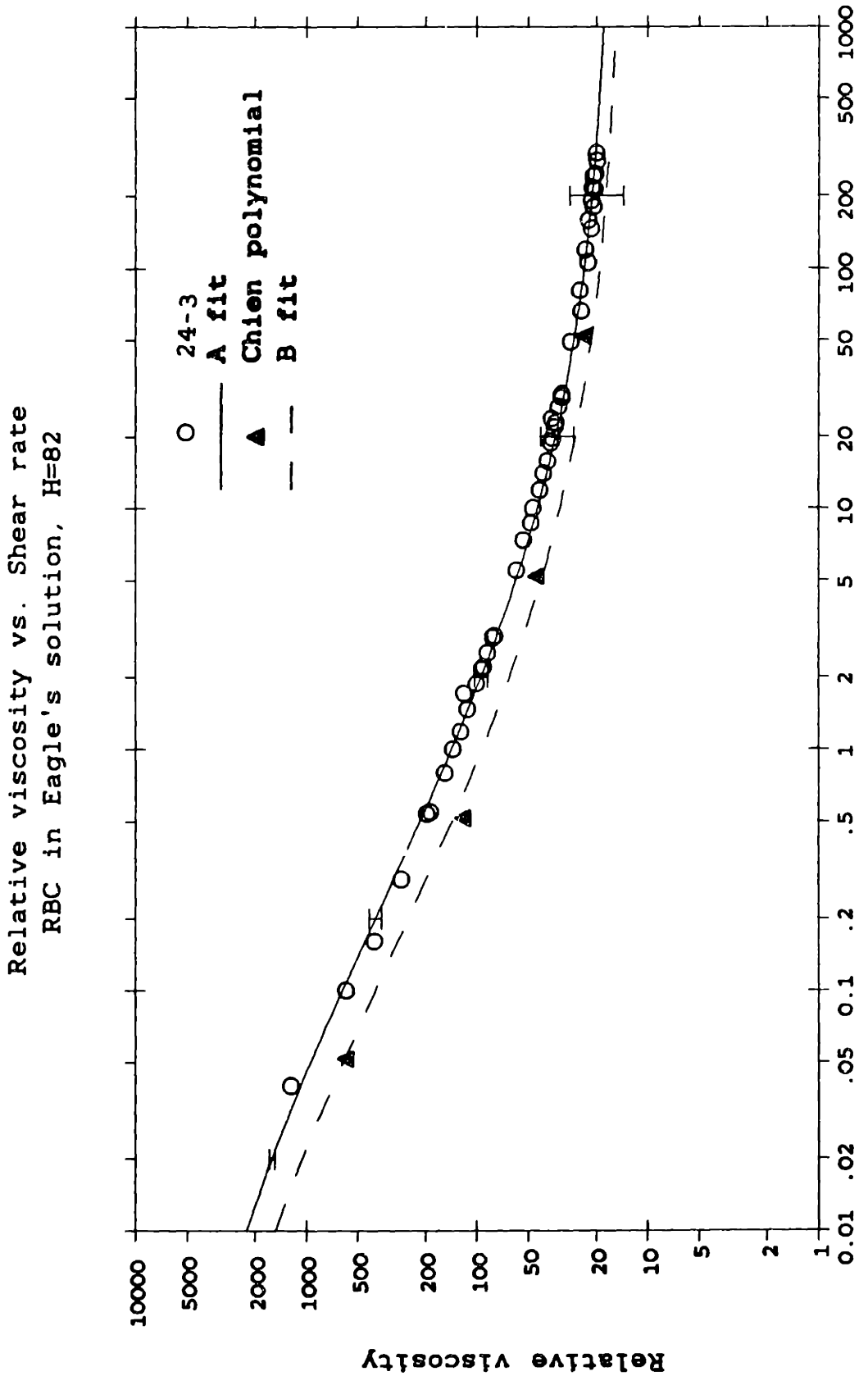

Figure 4-15: Eagle's solution data, H=82.

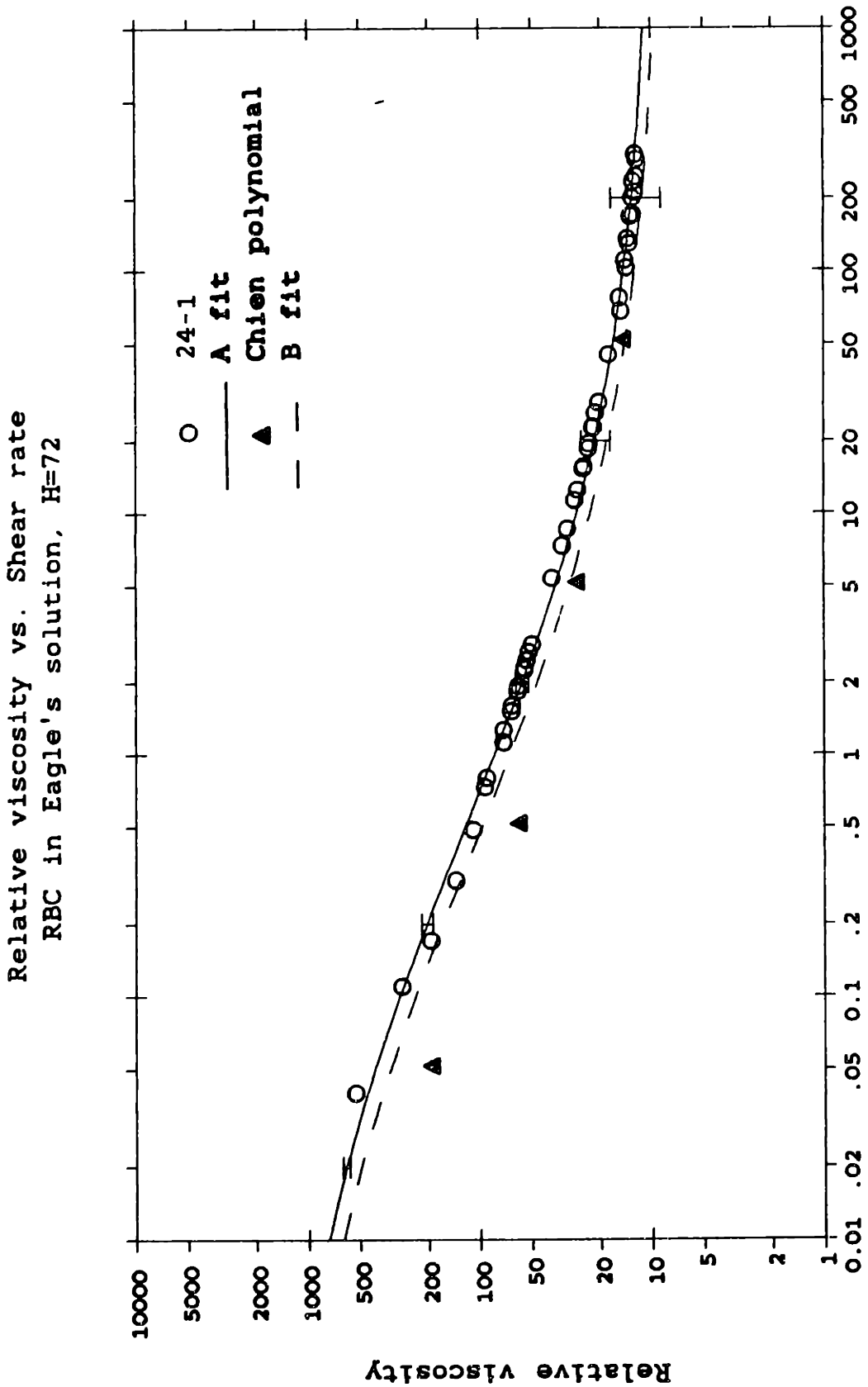

Figure 4-16: Eagle's solution data, H=72.

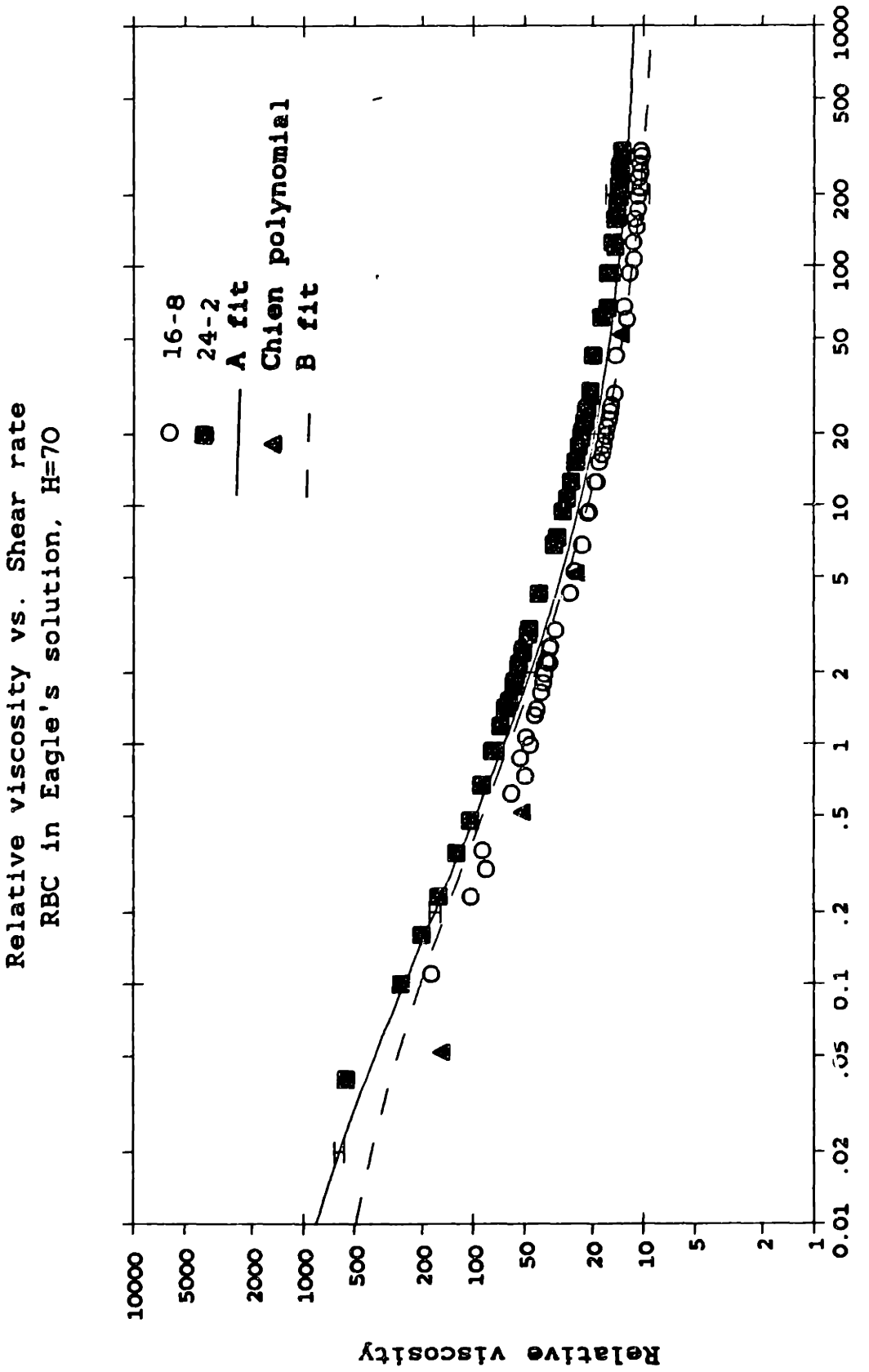

Figure 4-17: Eagle's solution data, H=70.

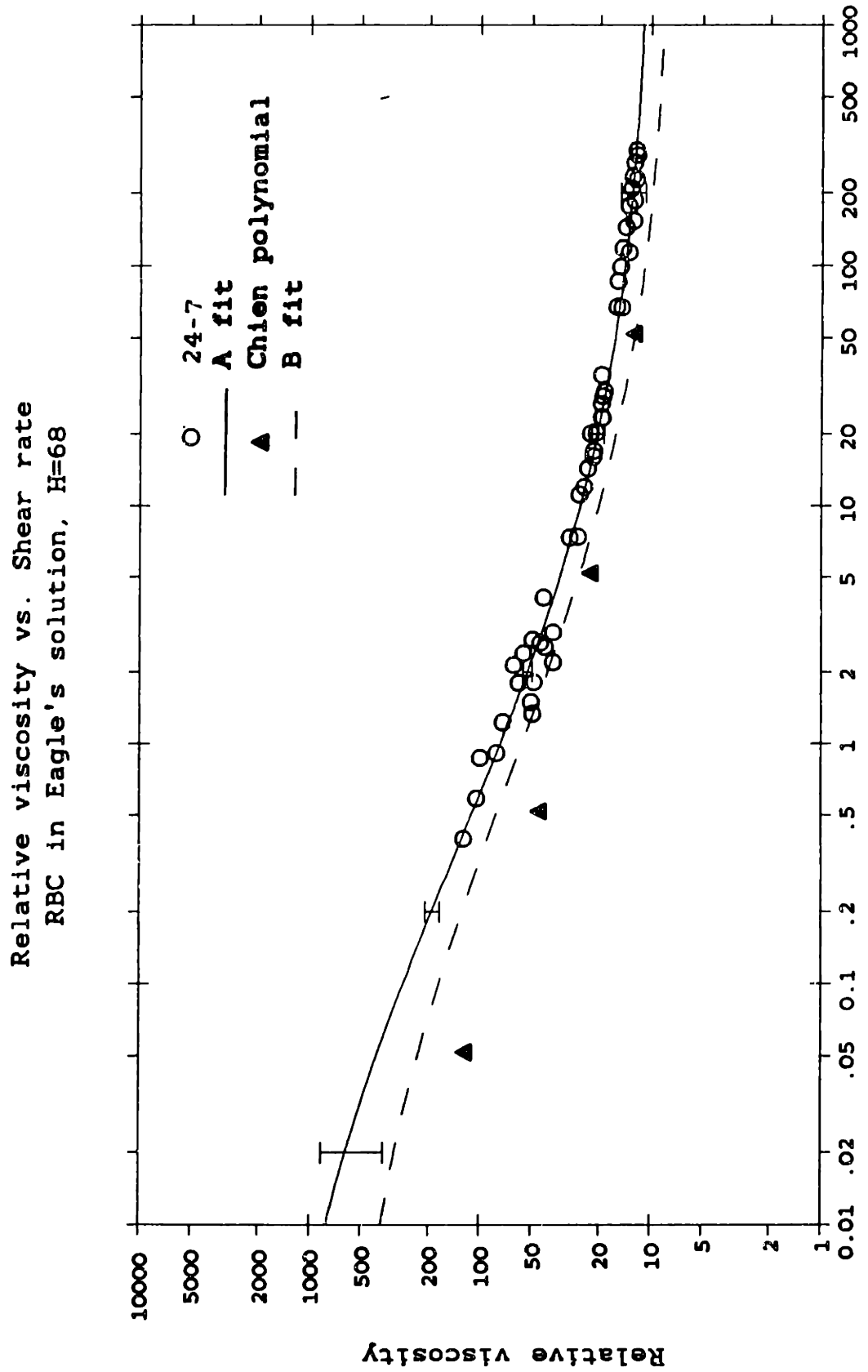

Figure 4-18: Eagle's solution data, H=68.

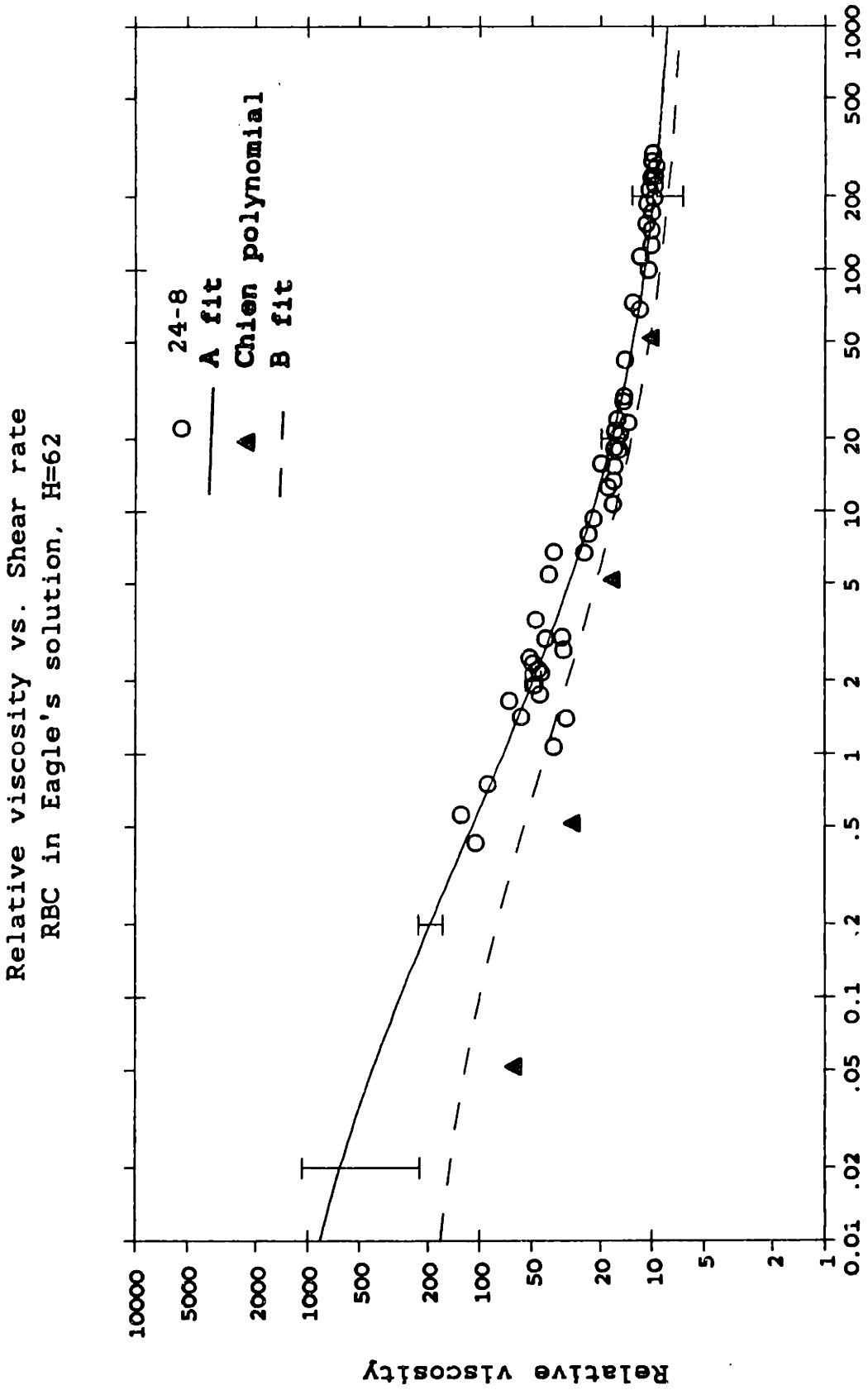

Figure 4-10: Eagle's solution data, H=62.

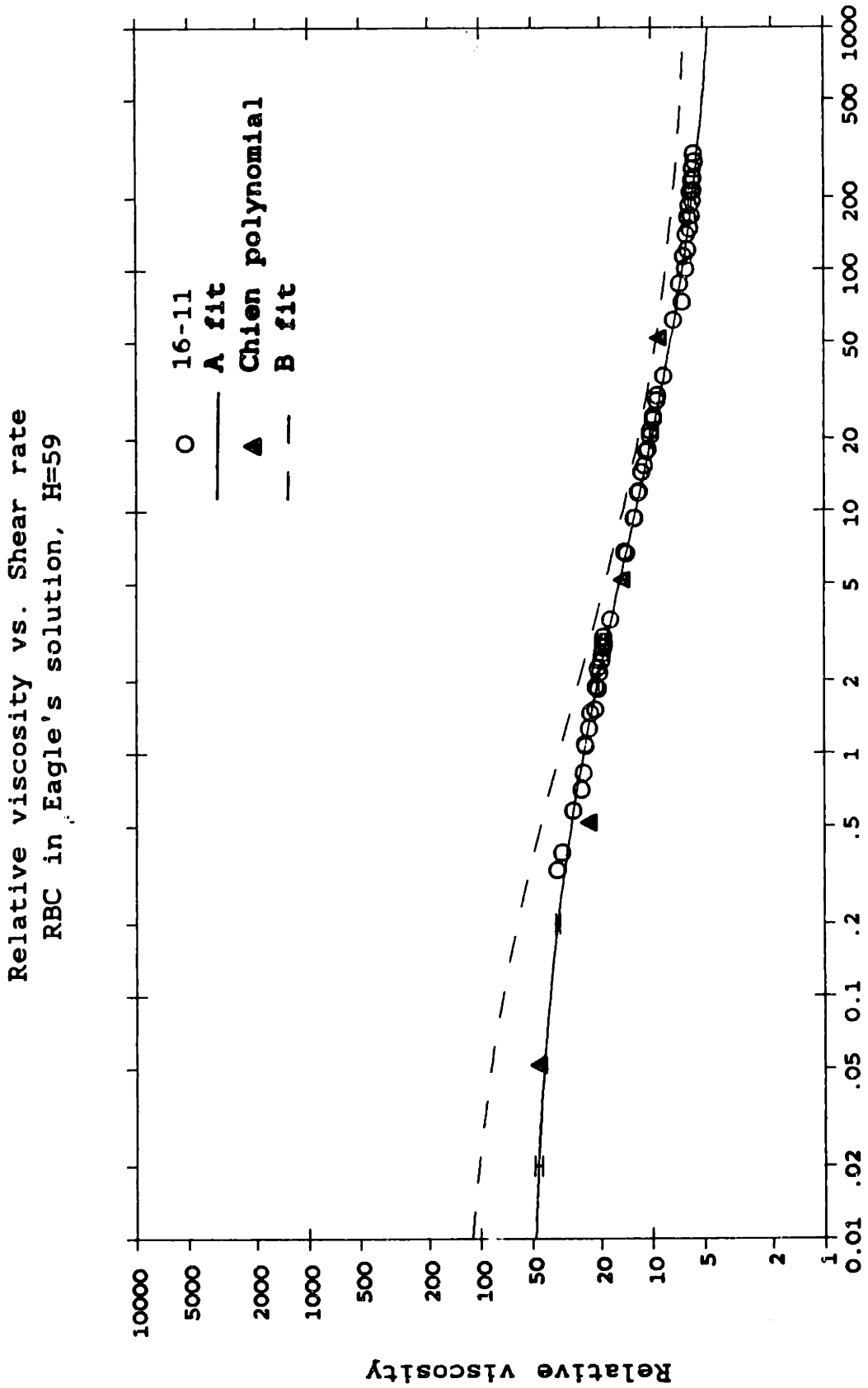

Figure 4-20: Eagle's solution data, H=59.

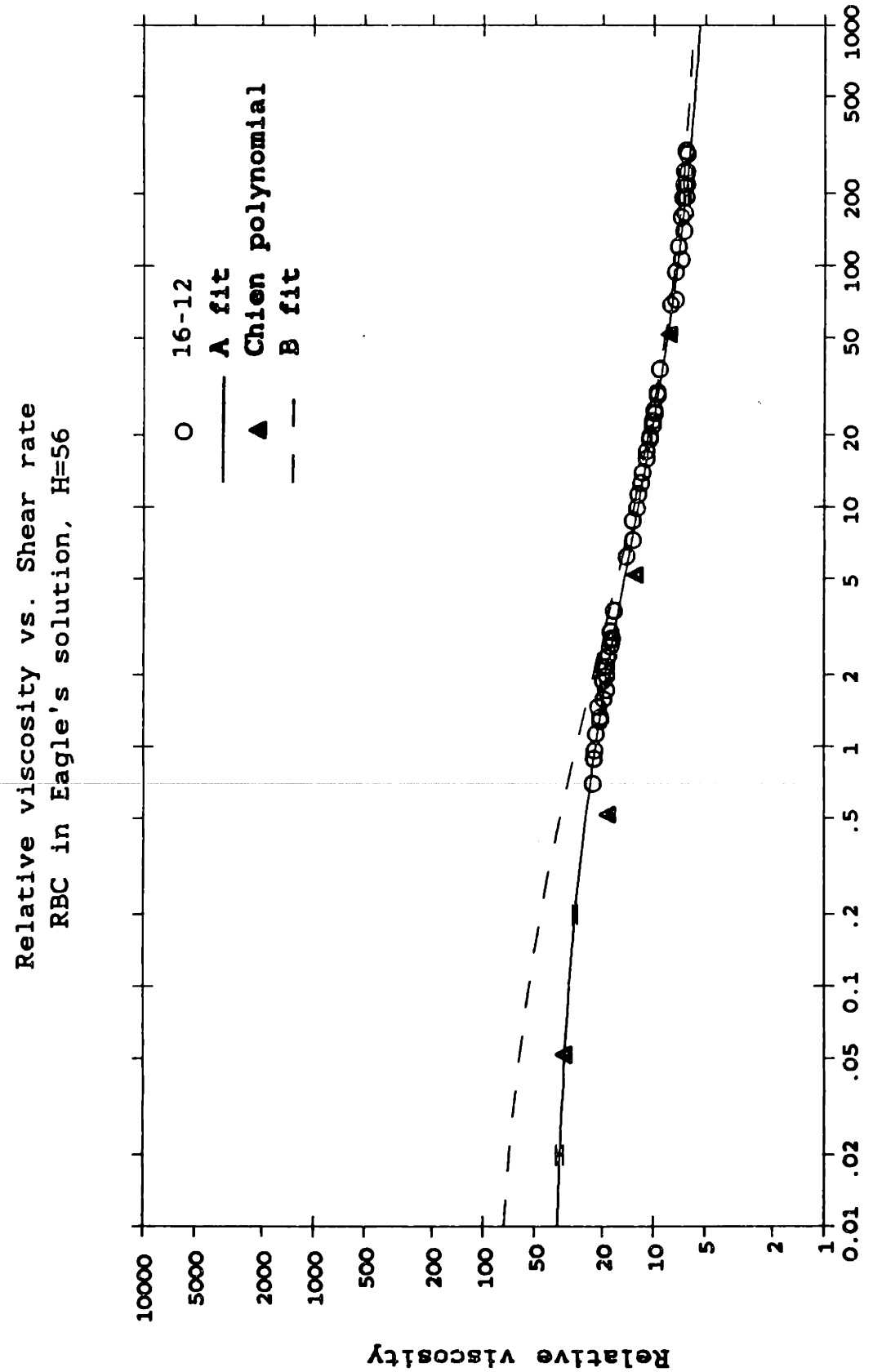

Figure 4-21: Eagle's solution data, H=56.

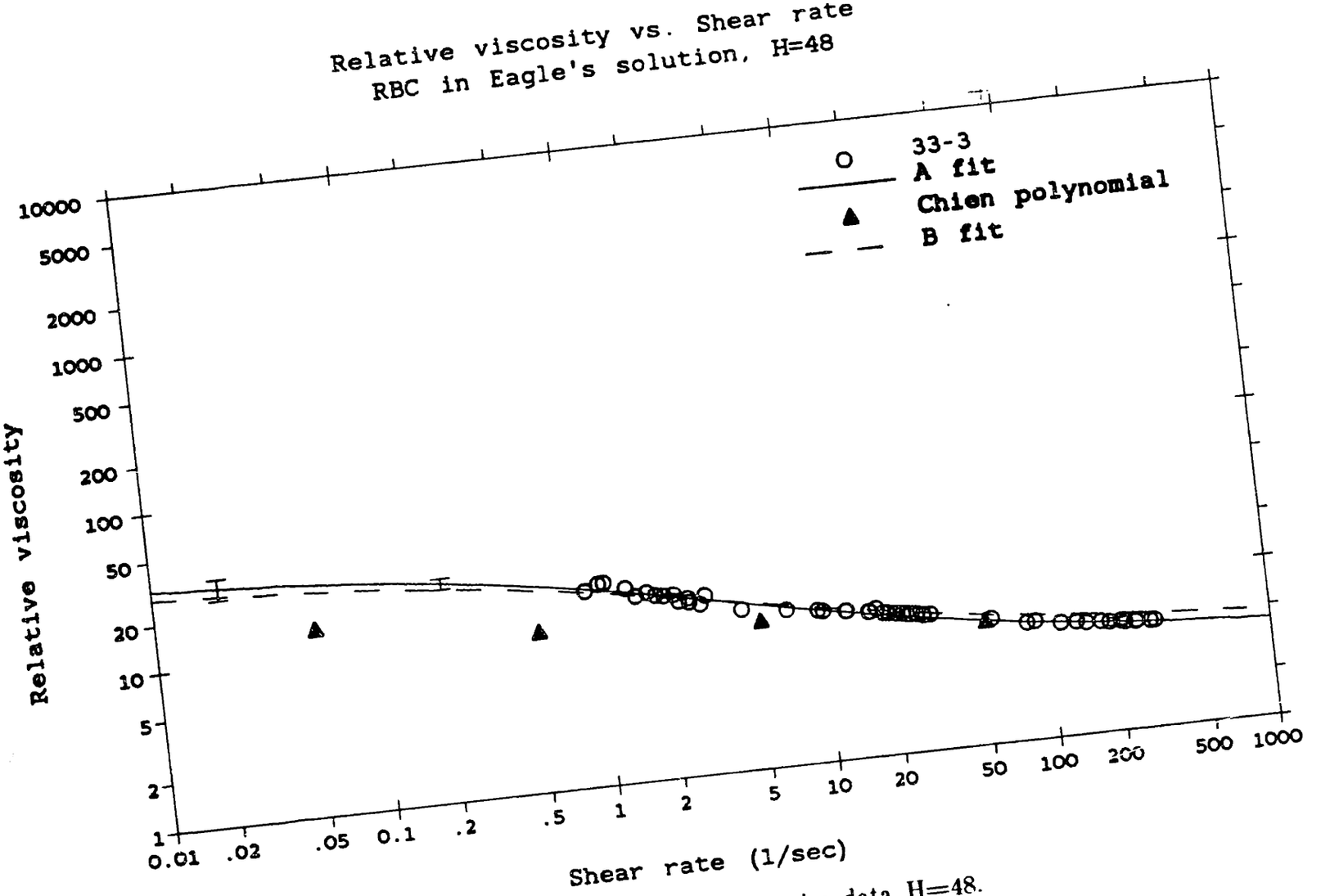

Figure 4-22: Eagle's solution data, H=48.

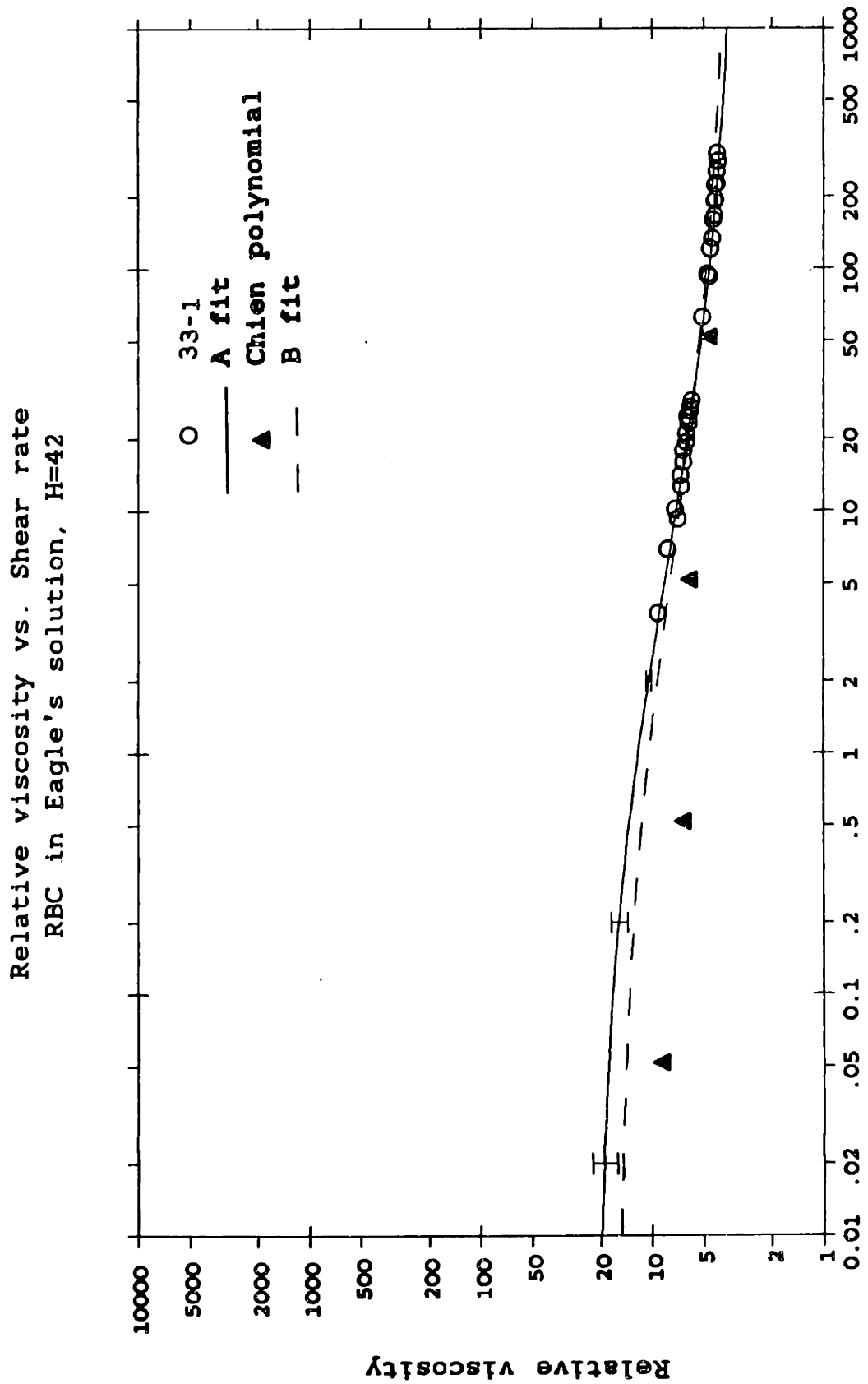

Figure 4-23: Eagle's solution data, H=42.

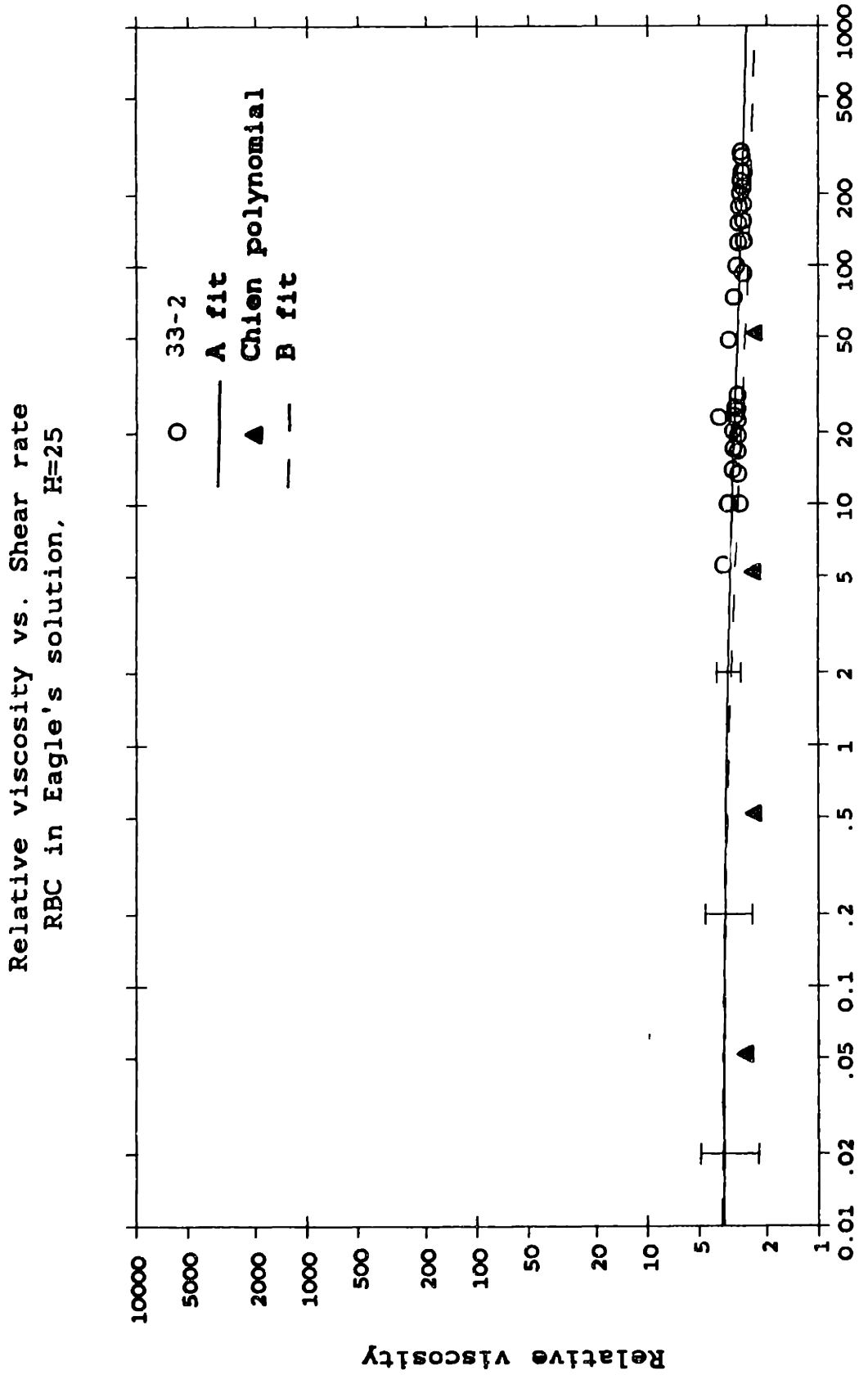

Figure 4-24: Eagle's solution data, H=25.

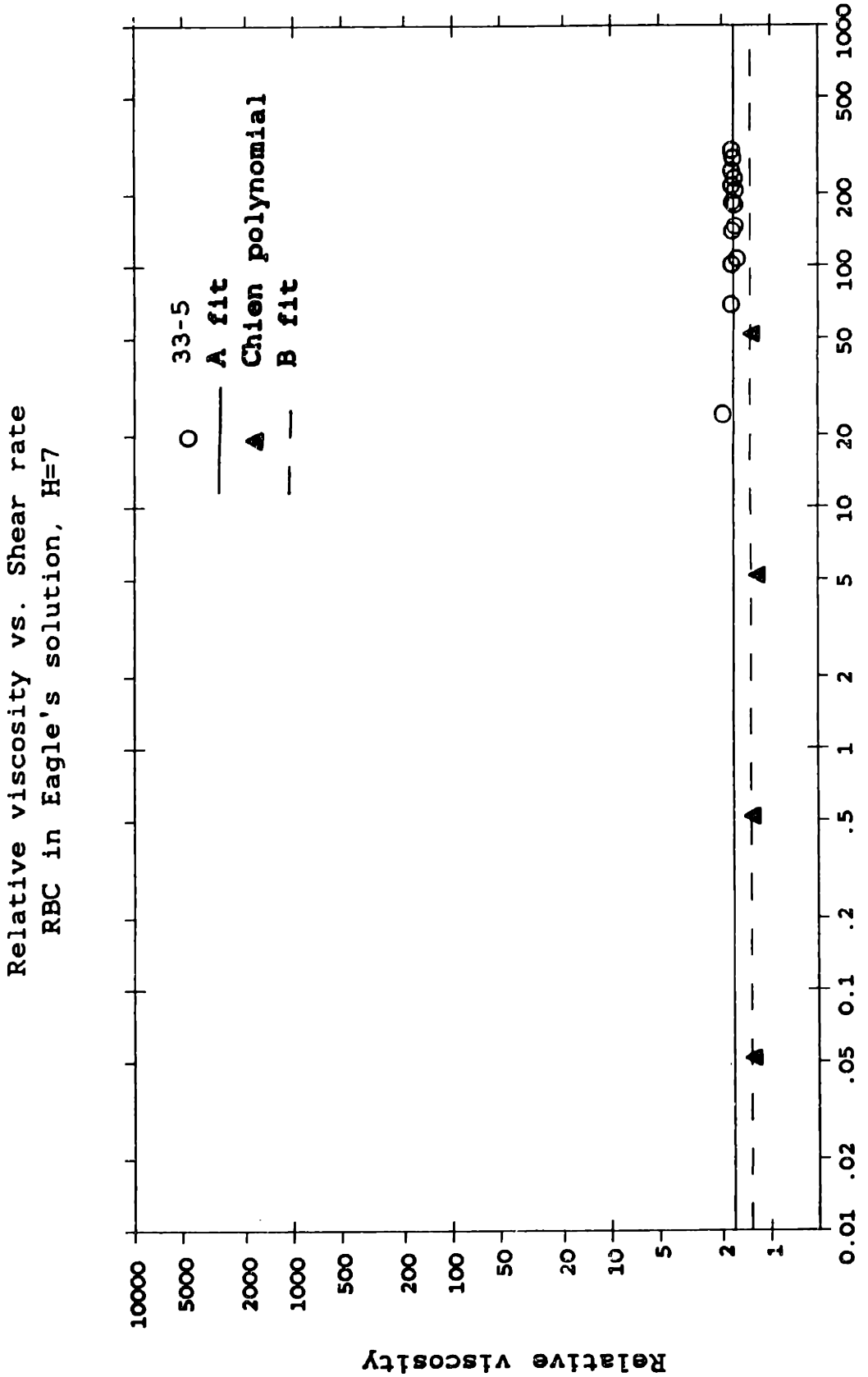

Figure 4-25: Eagle's solution data, H=7.

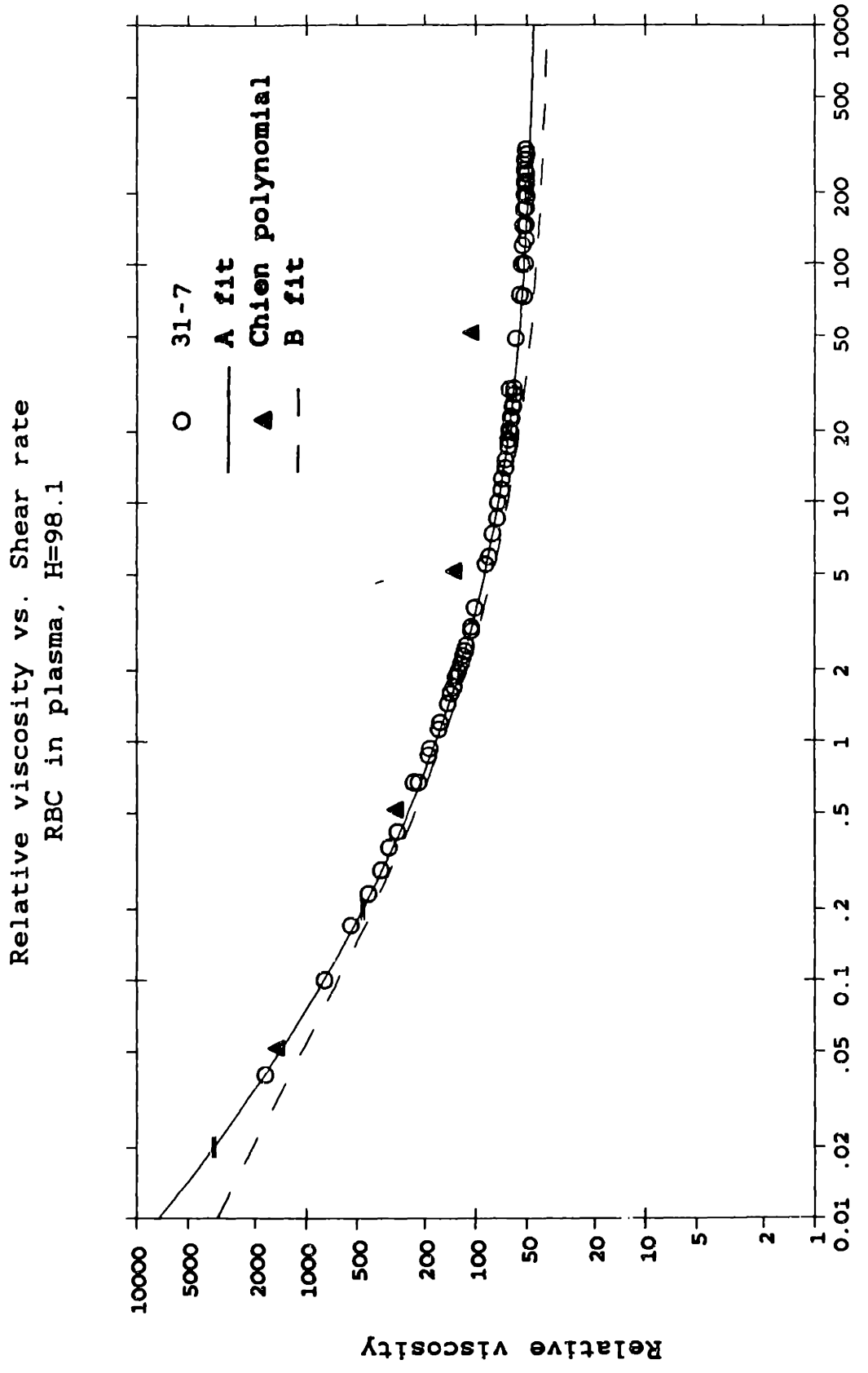

$\eta_{f,31}$=1.21 cP

Figure 4-26: Plasma data, H=98.1.

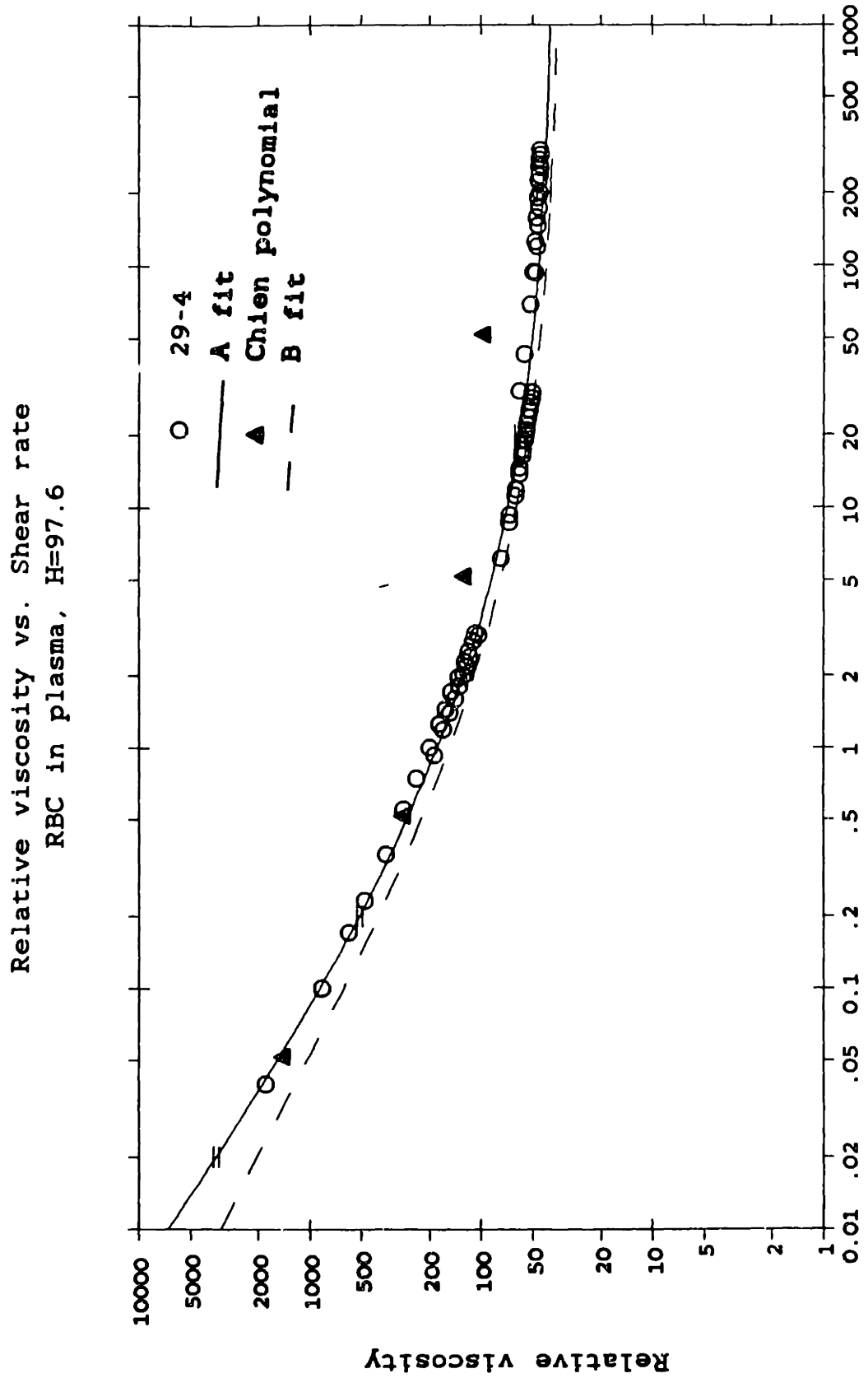

Figure 4-27: Plasma data, H=97.6.

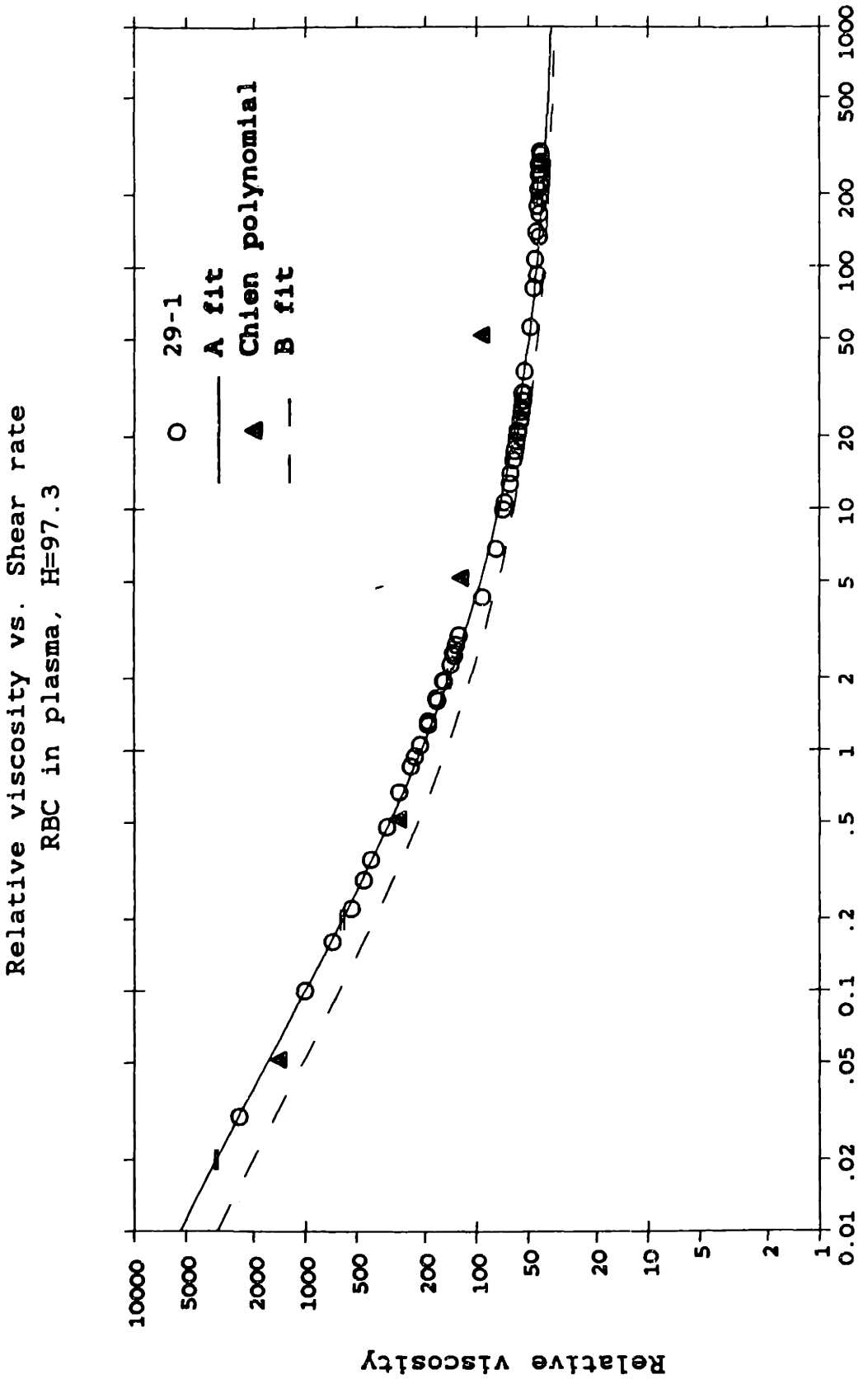

$\eta_{f,29}$=1.05 cP

Figure 4-28: Plasma data, H=97.3.

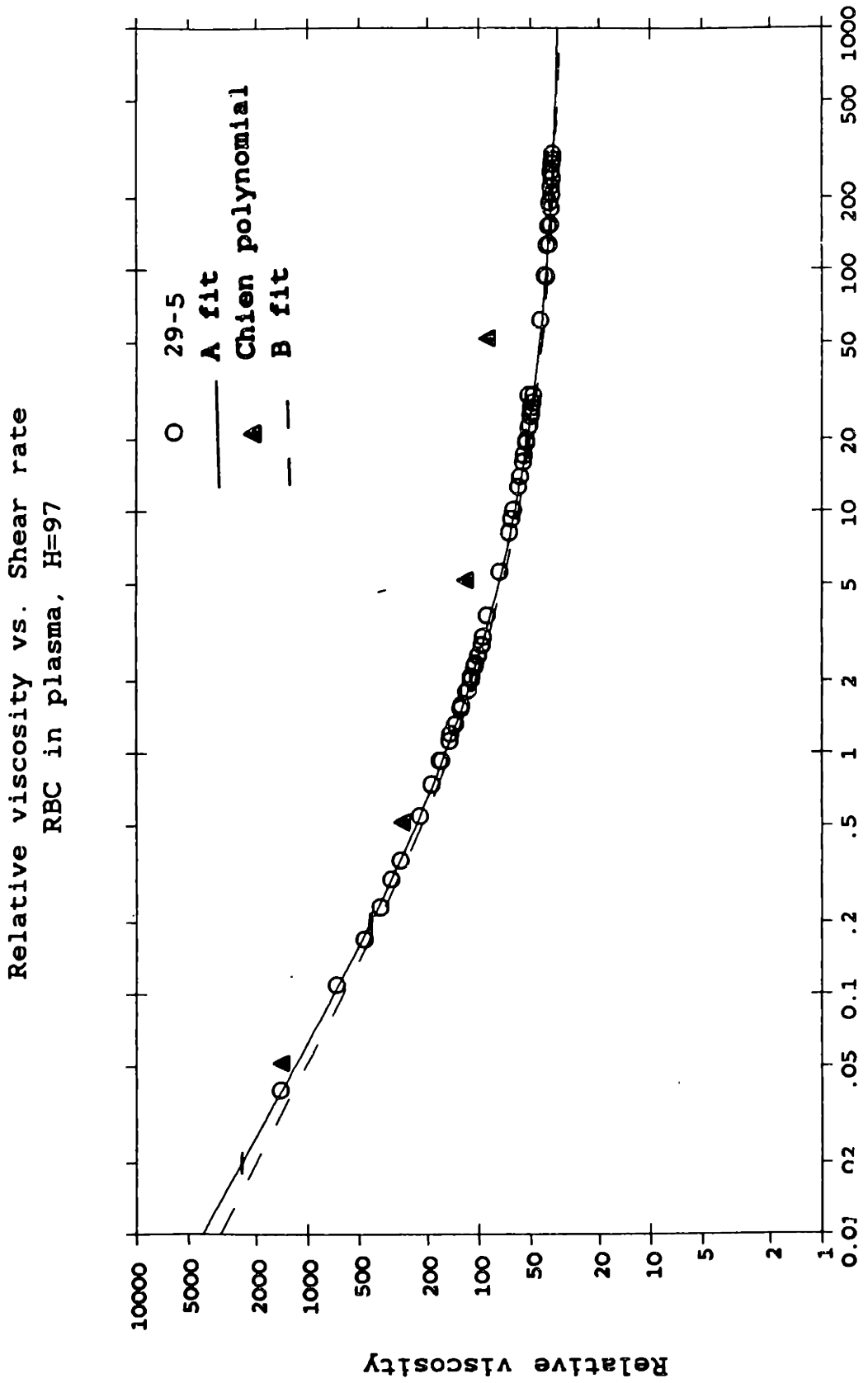

Figure 4-29: Plasma data, H=97.

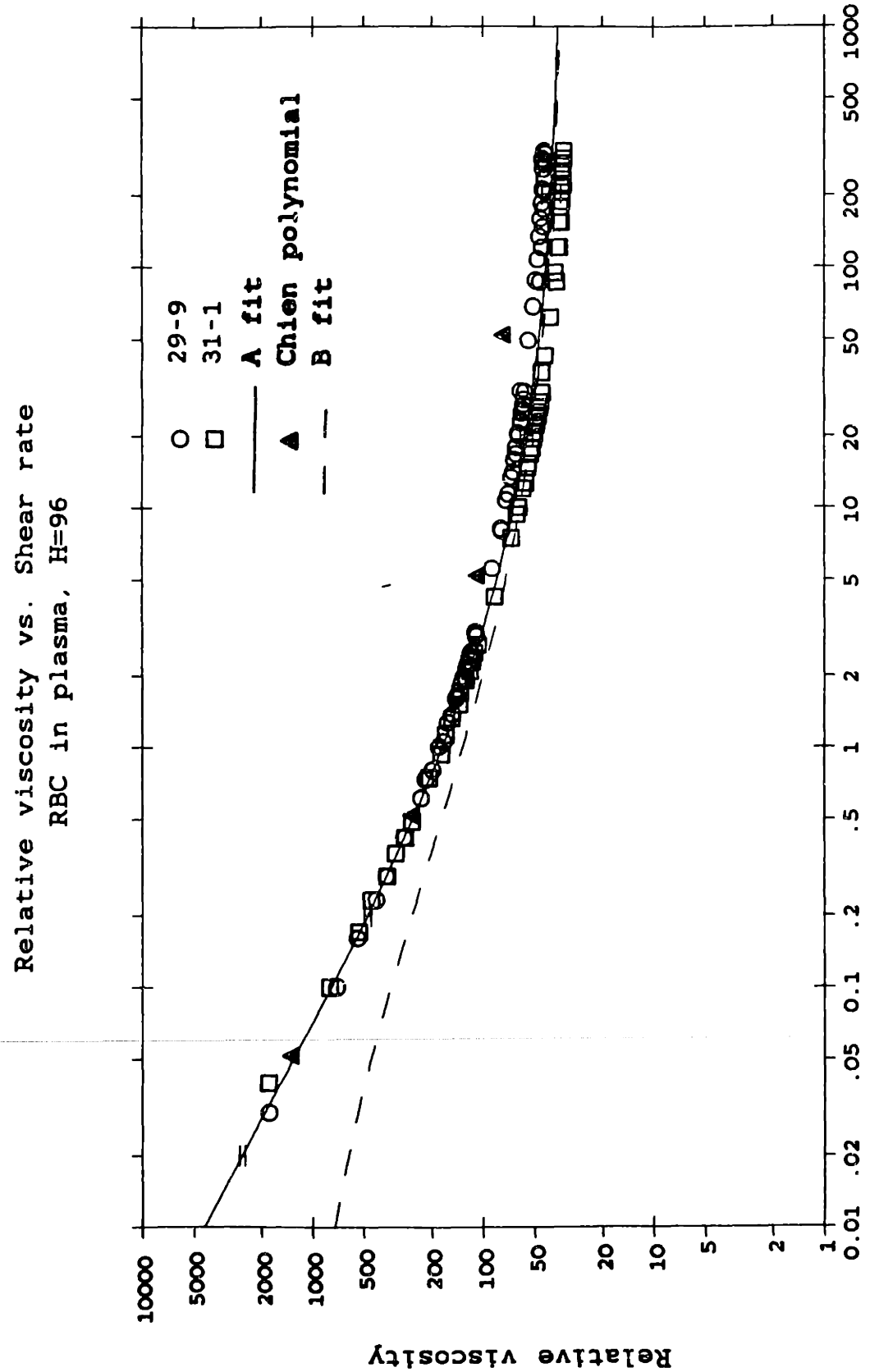

$\eta_{f,29}$=1.05 cP $\eta_{f,31}$=1.21 cP

Figure 4-30: Plasma data, H=96.

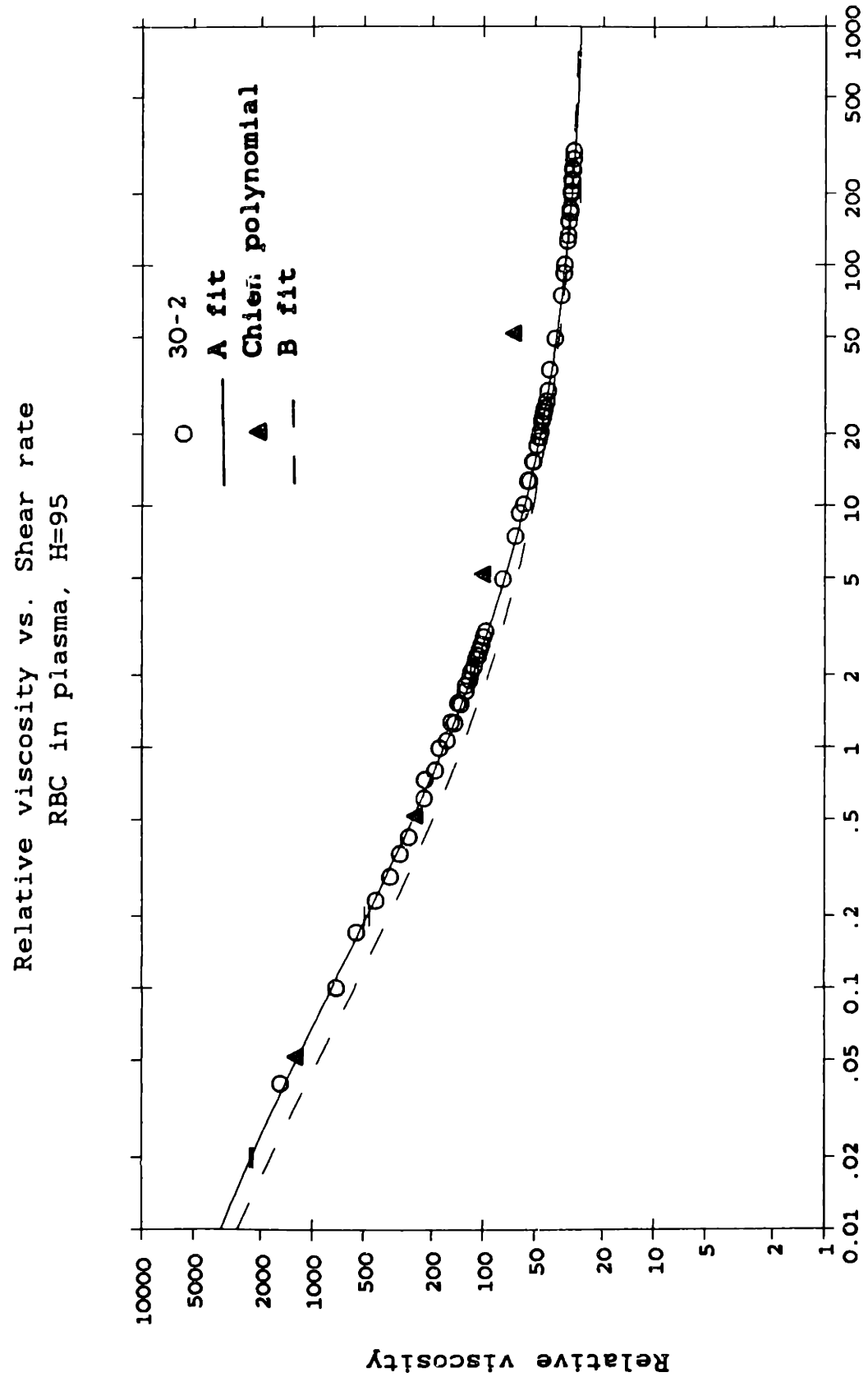

$\eta_{f,30}$=1.13 cP

Figure 4-31: Plasma data, H=95.

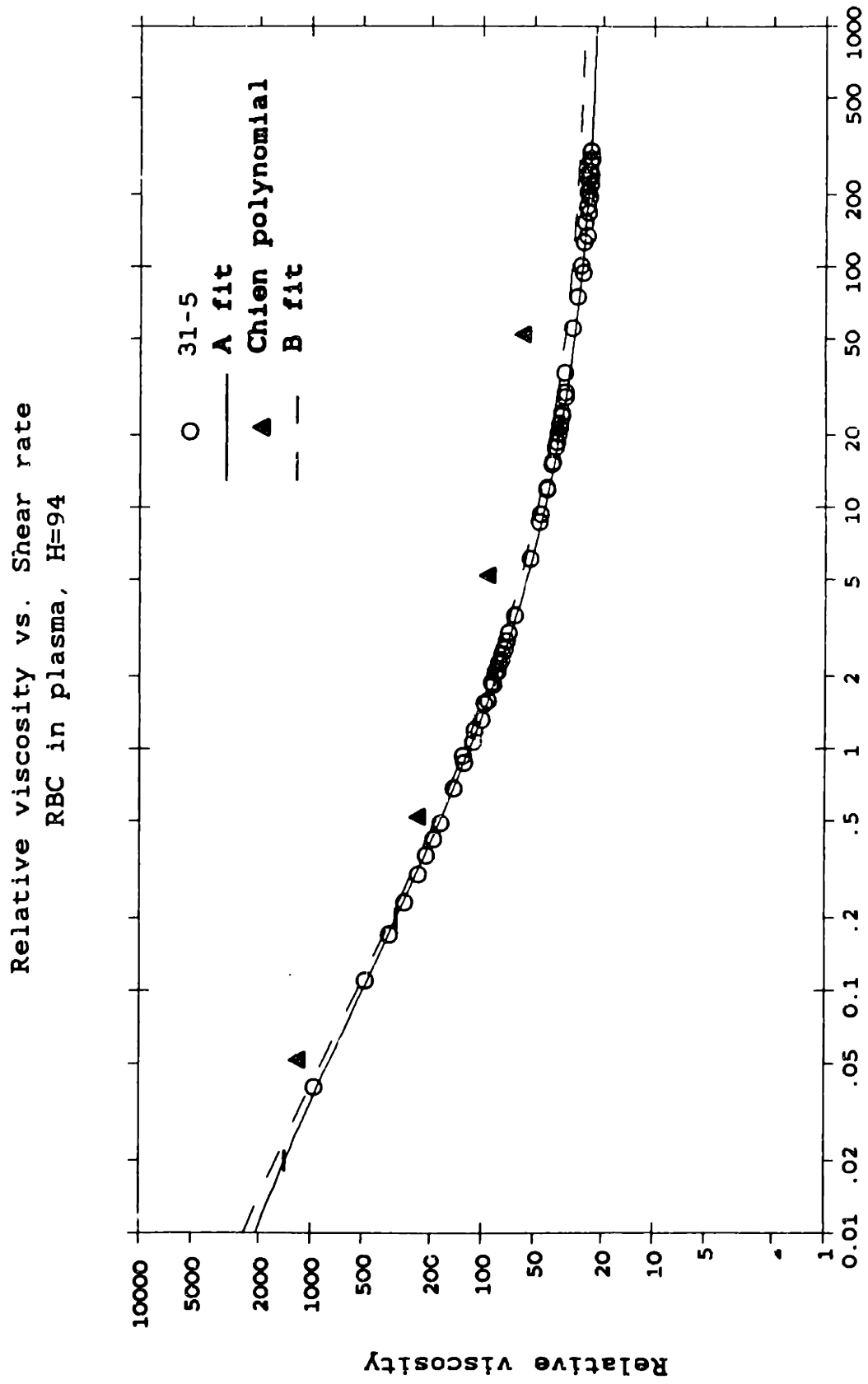

$\eta_{f,31}$=1.21 cP

Figure 4-32: Plasma data, H=94.

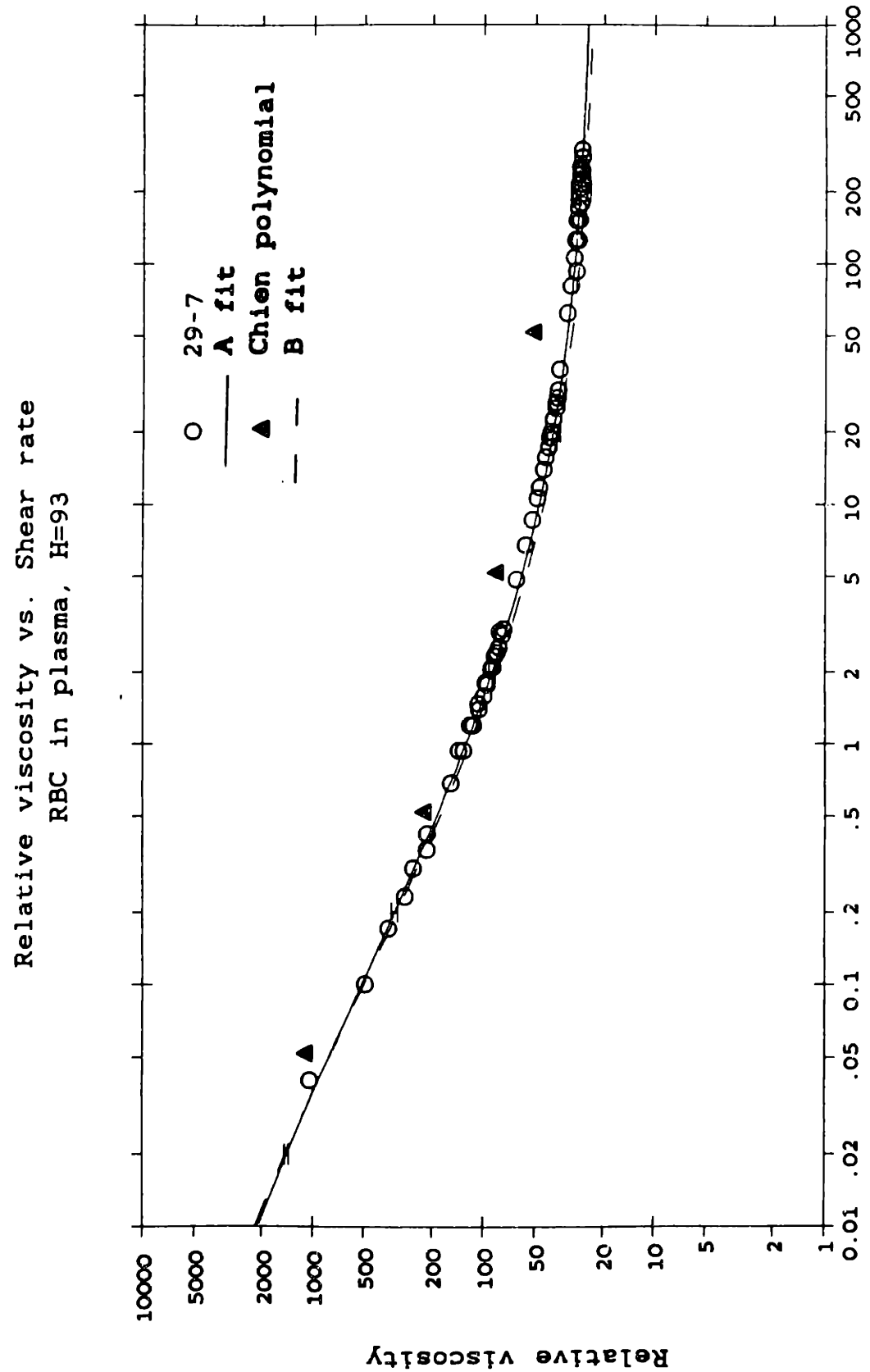

$\eta_{f,29}$=1.05 cP

Figure 4-33: Plasma data, H=93.

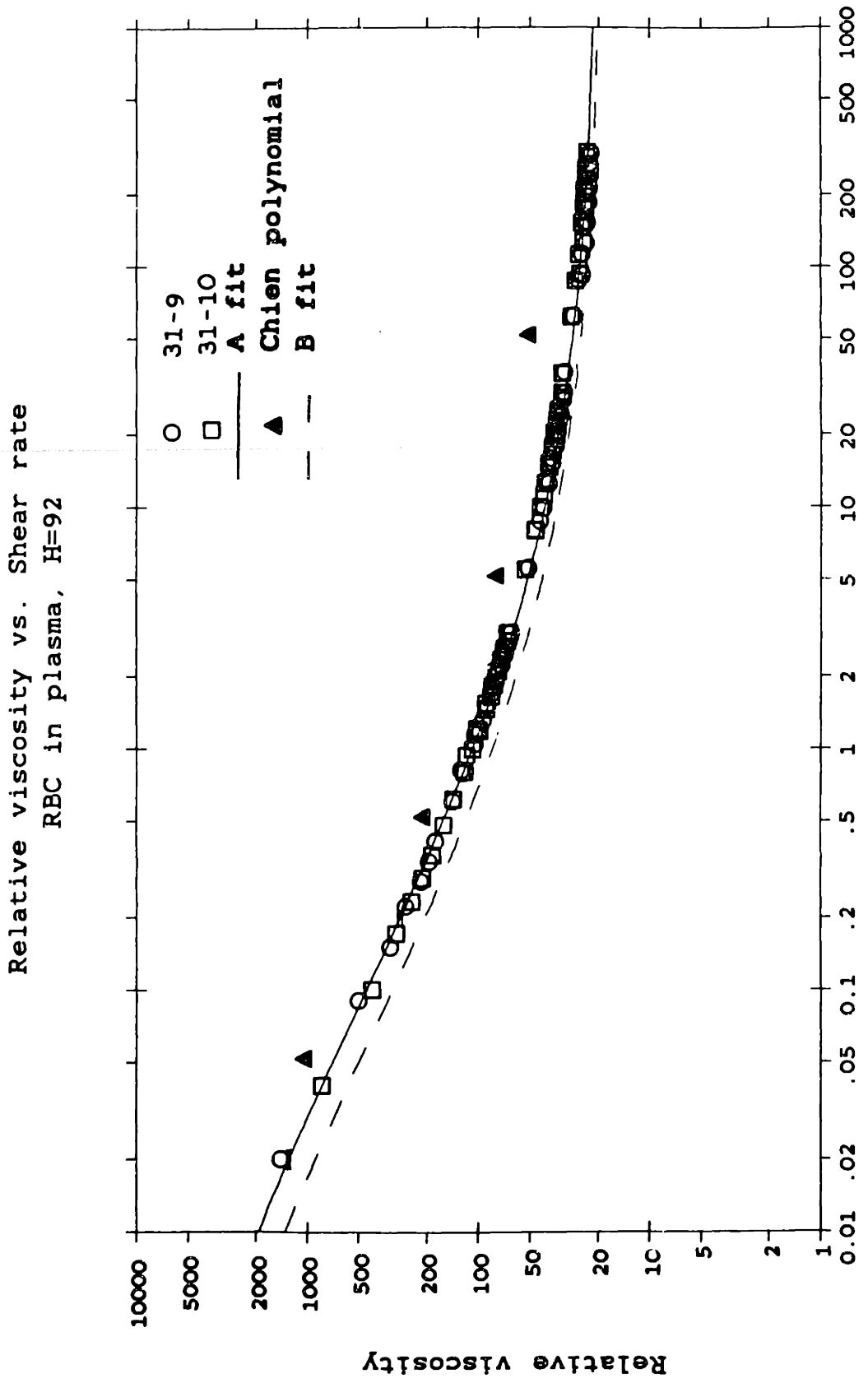

$\eta_{f,31}$=1.21 cP

Figure 4-34: Plasma data, H=92.

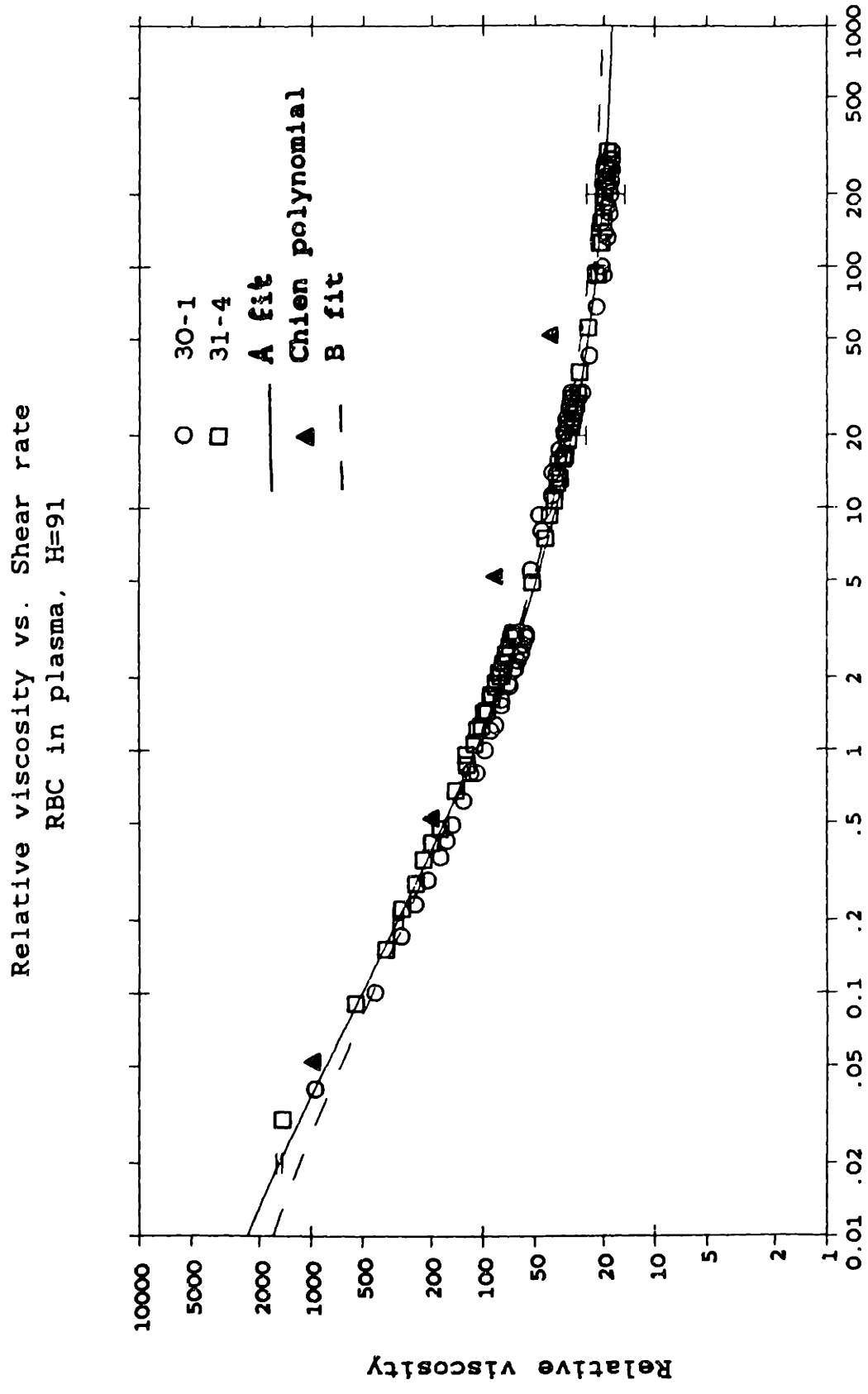

$\eta_{f,30}$=1.13 cP $\eta_{f,31}$=1.21 cP

Figure 4-35: Plasma data, H=91.

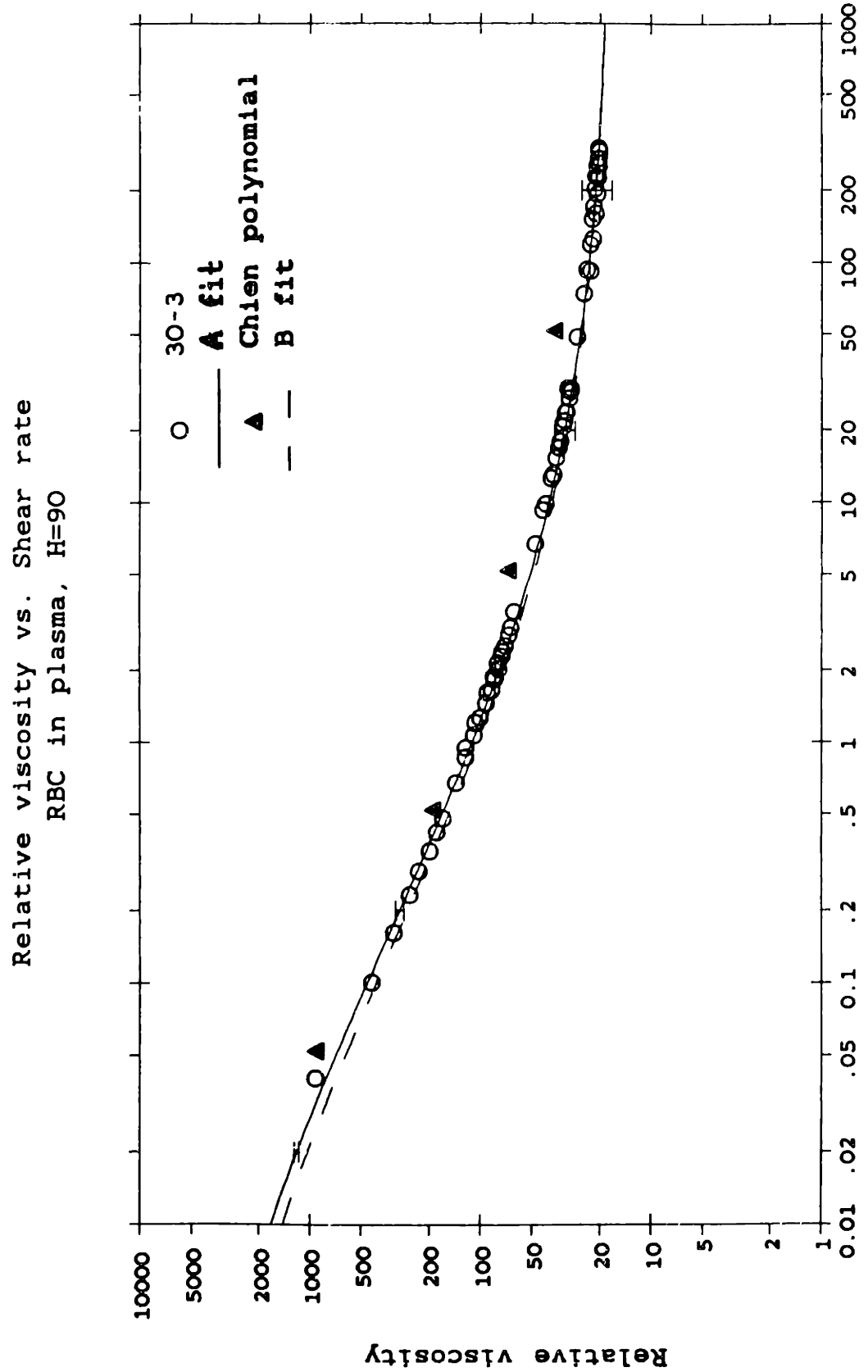

Figure 4-36: Plasma data, H=90.

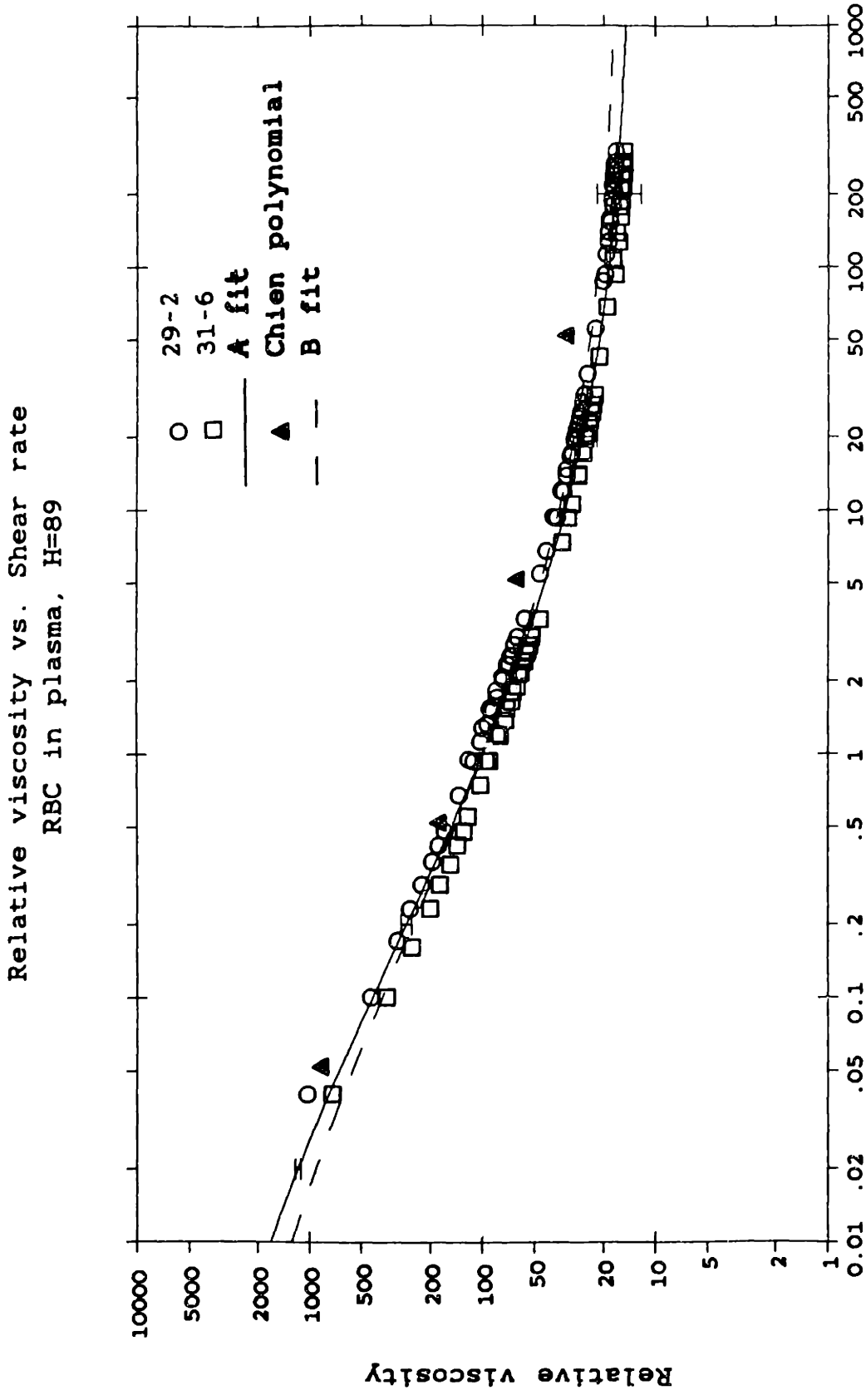

$\eta_{f,29}$=1.05 cP $\eta_{f,31}$=1.21 cP

Figure 4-37: Plasma data, H=89.

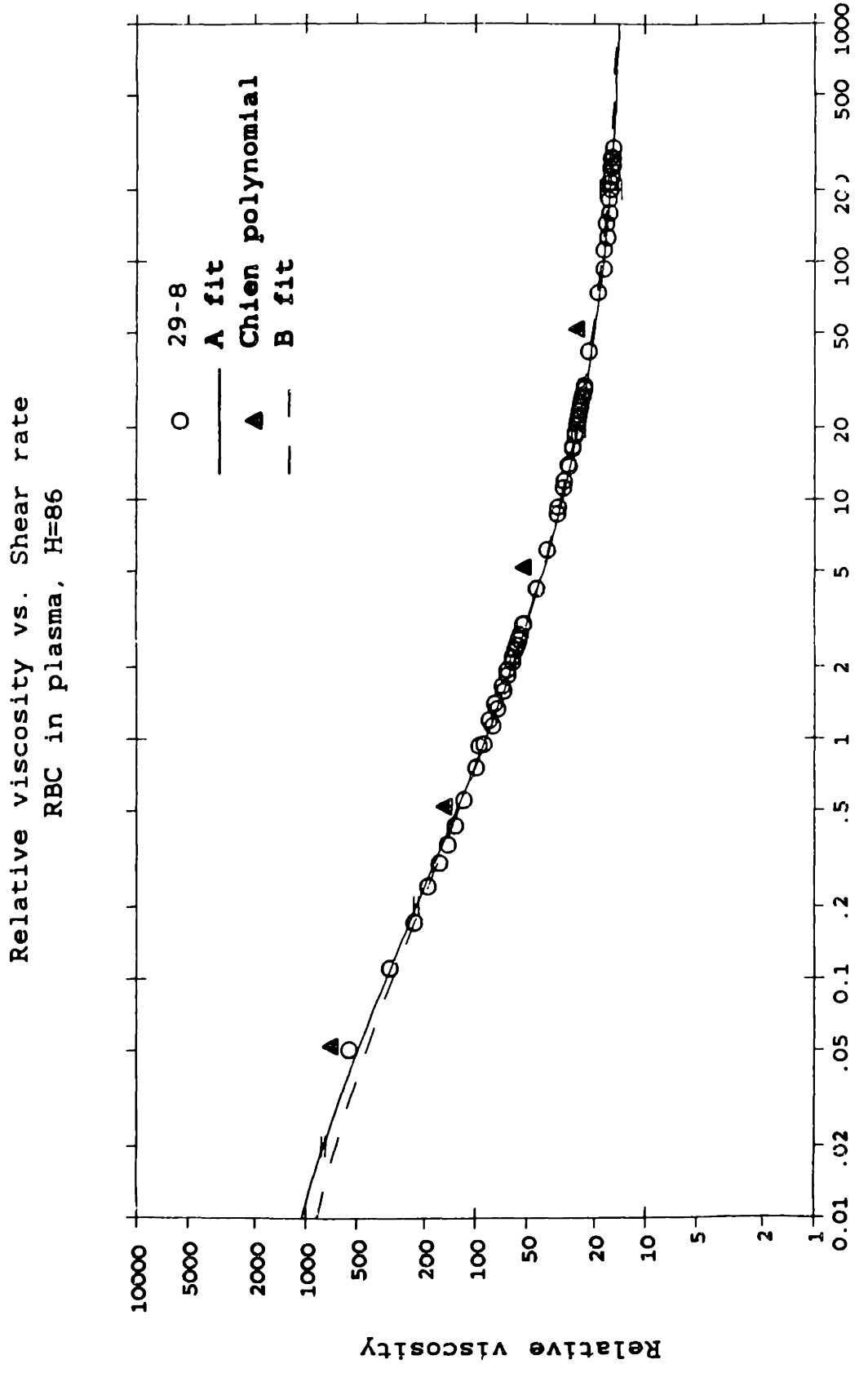

$\eta_{r,29}$=1.05 cP

Figure 4-38: Plasma data, H=86.

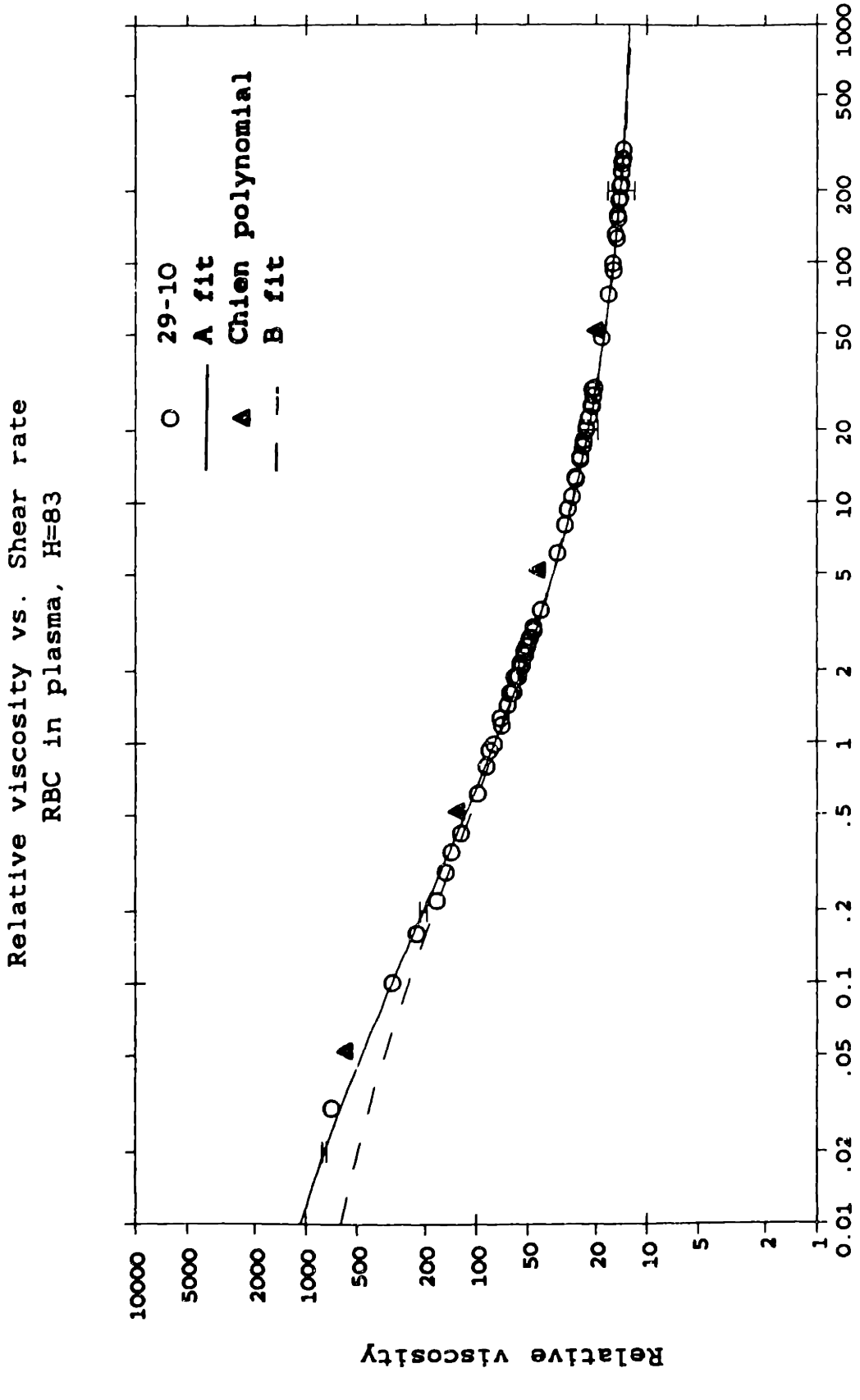

$\eta_{r,29}$=1.05 cP

Figure 4-30: Plasma data, H=83.

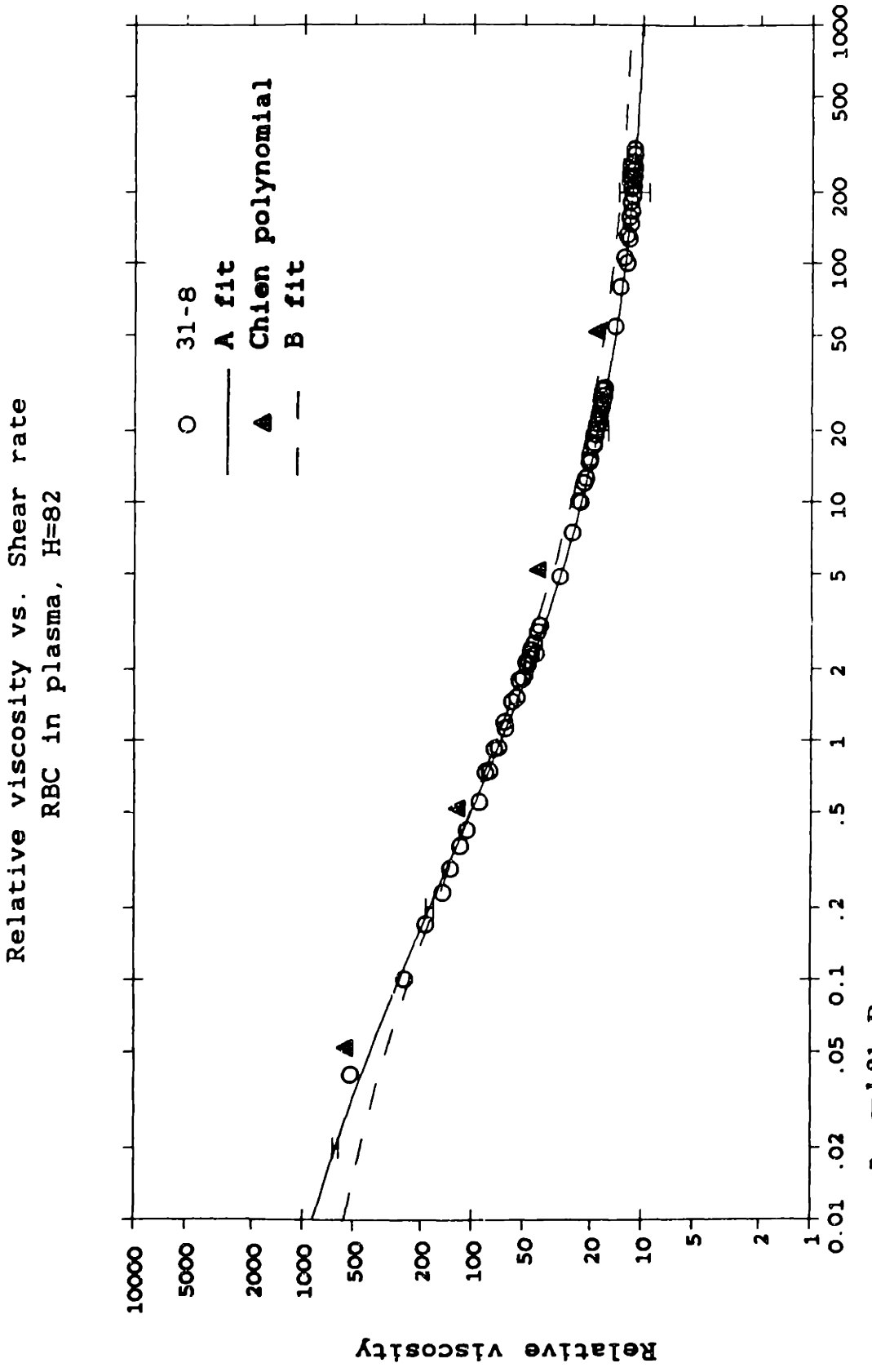

Figure 4-40: Plasma data, H=82.

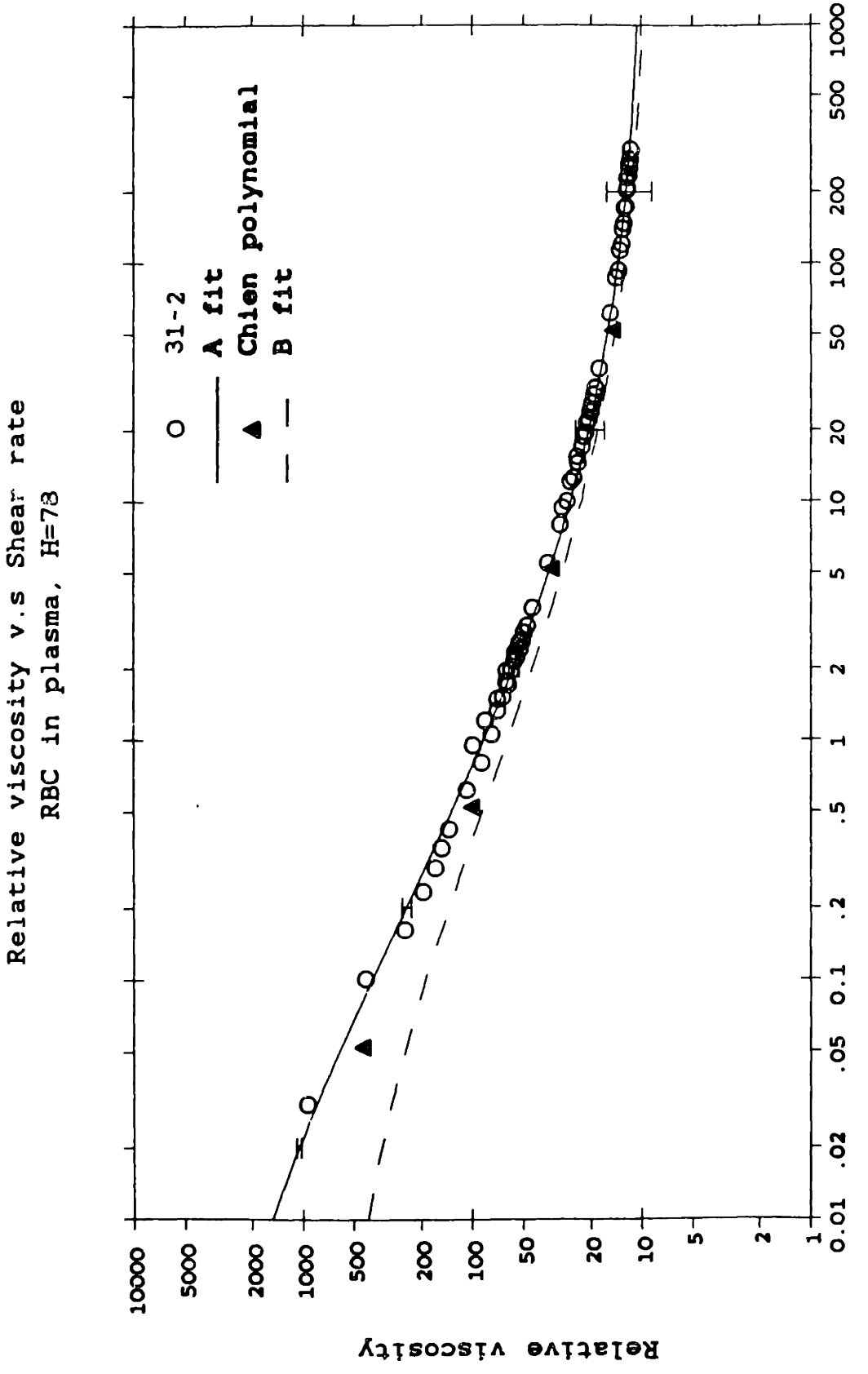

$\eta_{f,31}$=1.21 cP

Figure 4-41: Plasma data, H=78.

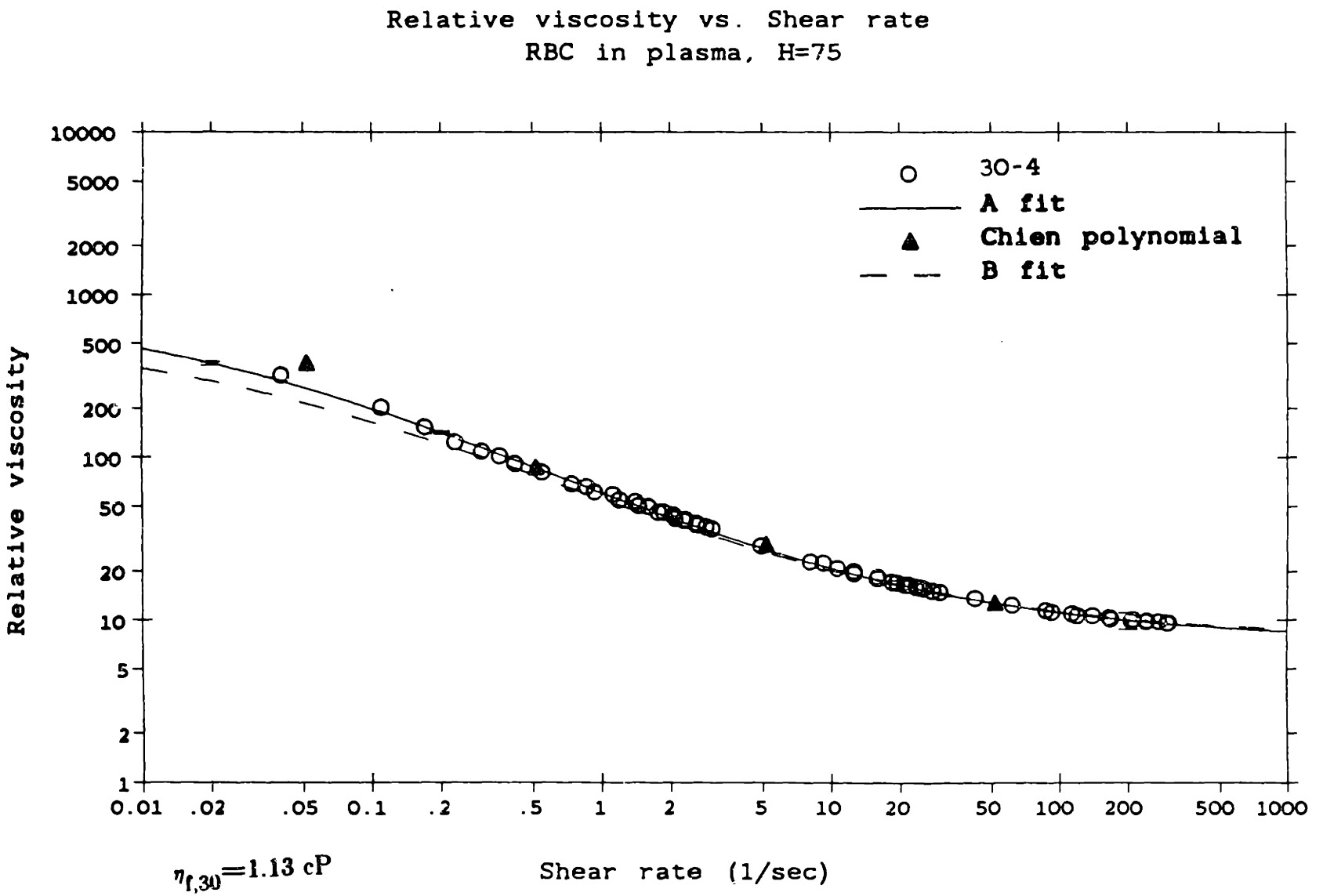

Figure 4-42: Plasma data, H=75.

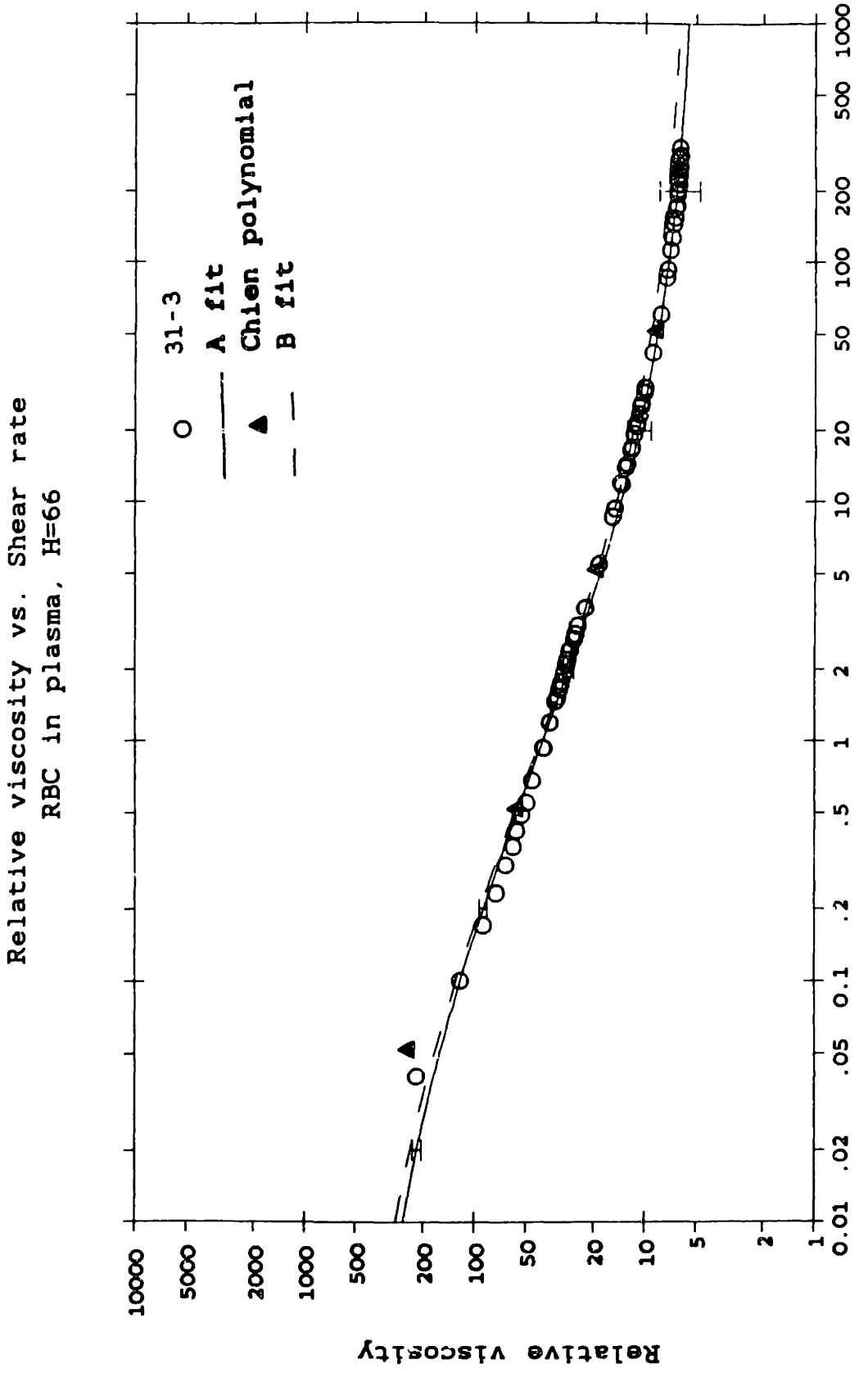

Figure 4-43: Plasma data, H=66.

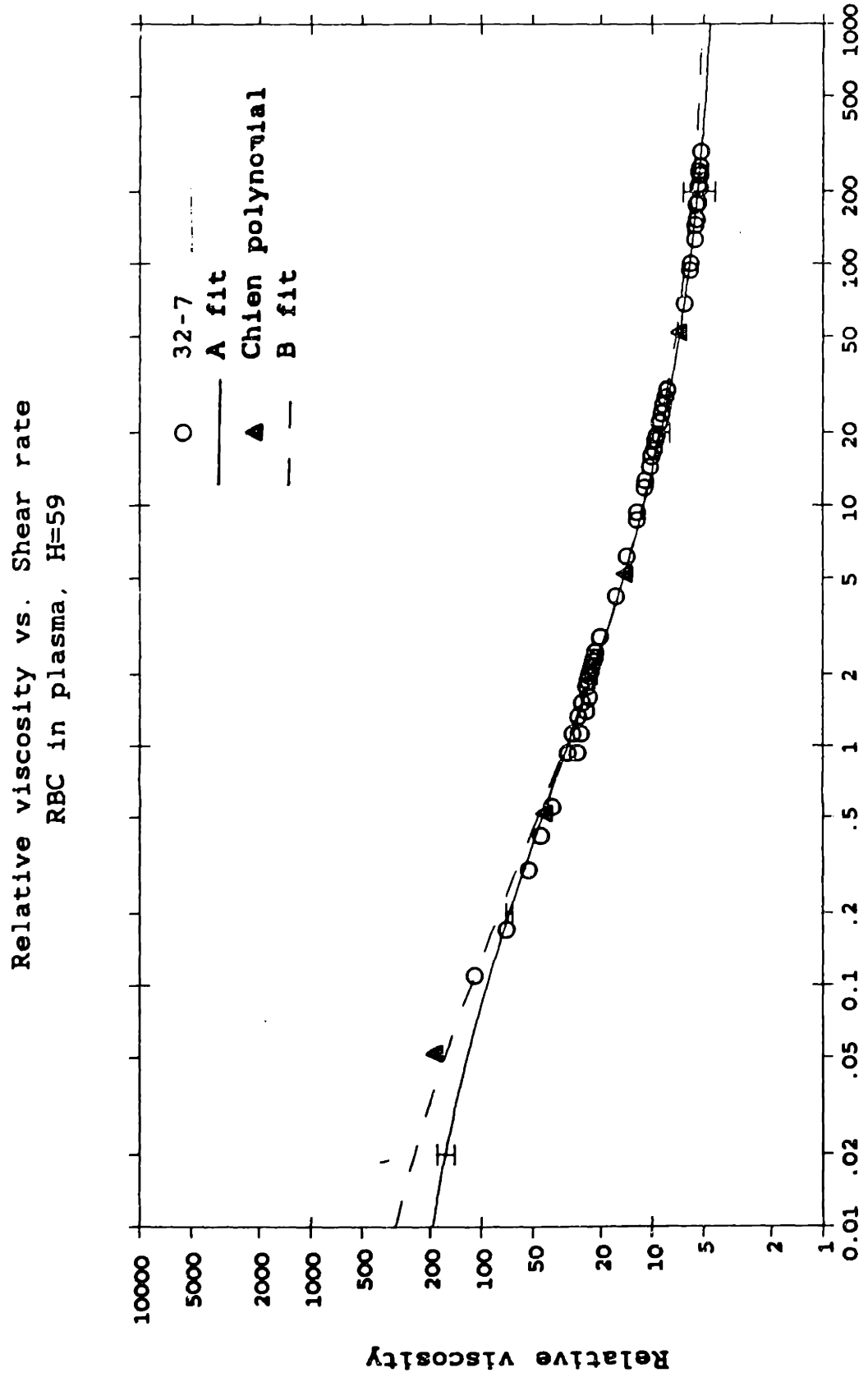

$\eta_{f,32}$=1.06 cP

Figure 4-44: Plasma data, H=59.

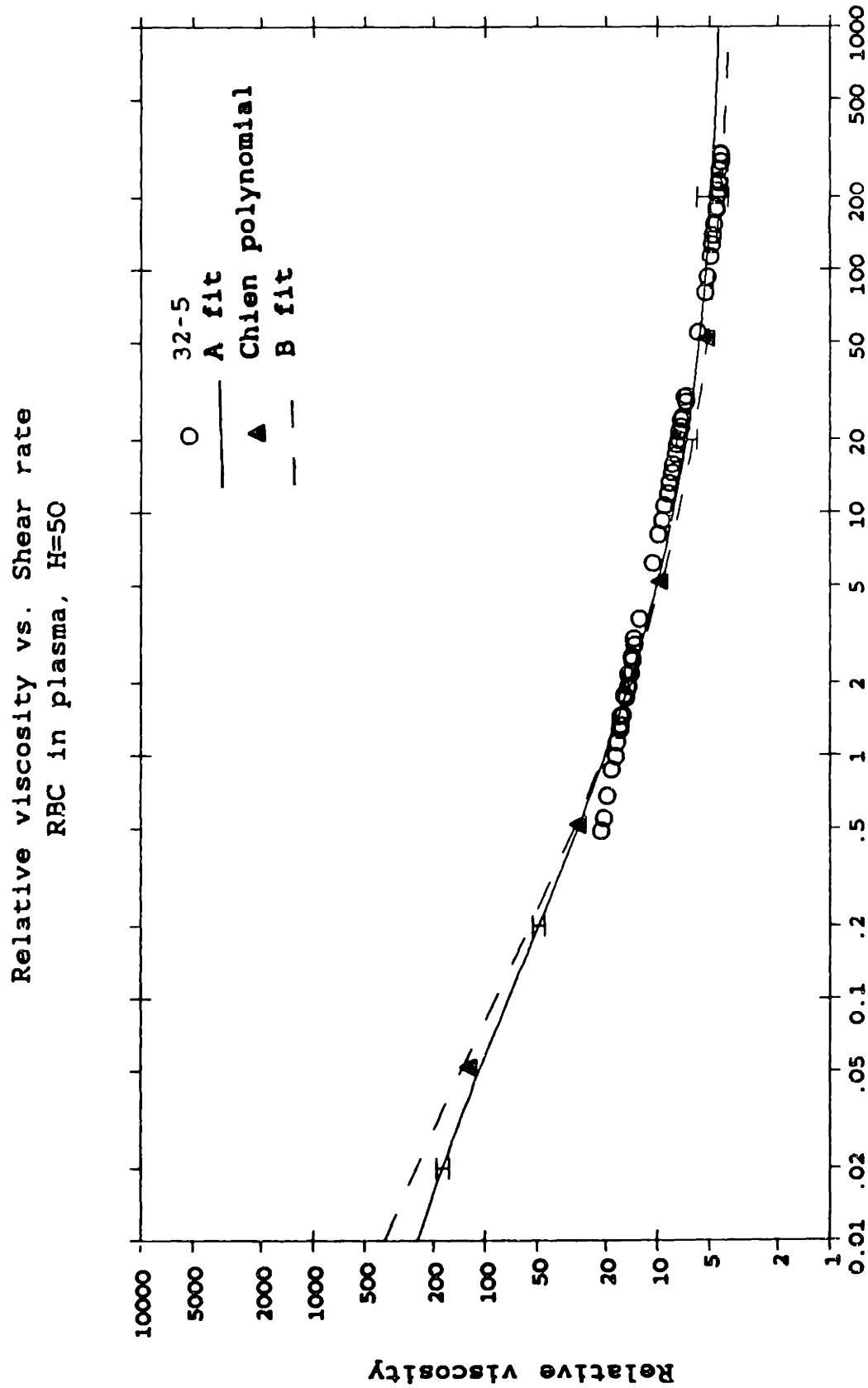

$\eta_{f,32}$=1.06 cP

Figure 4-45: Plasma data, H=50.

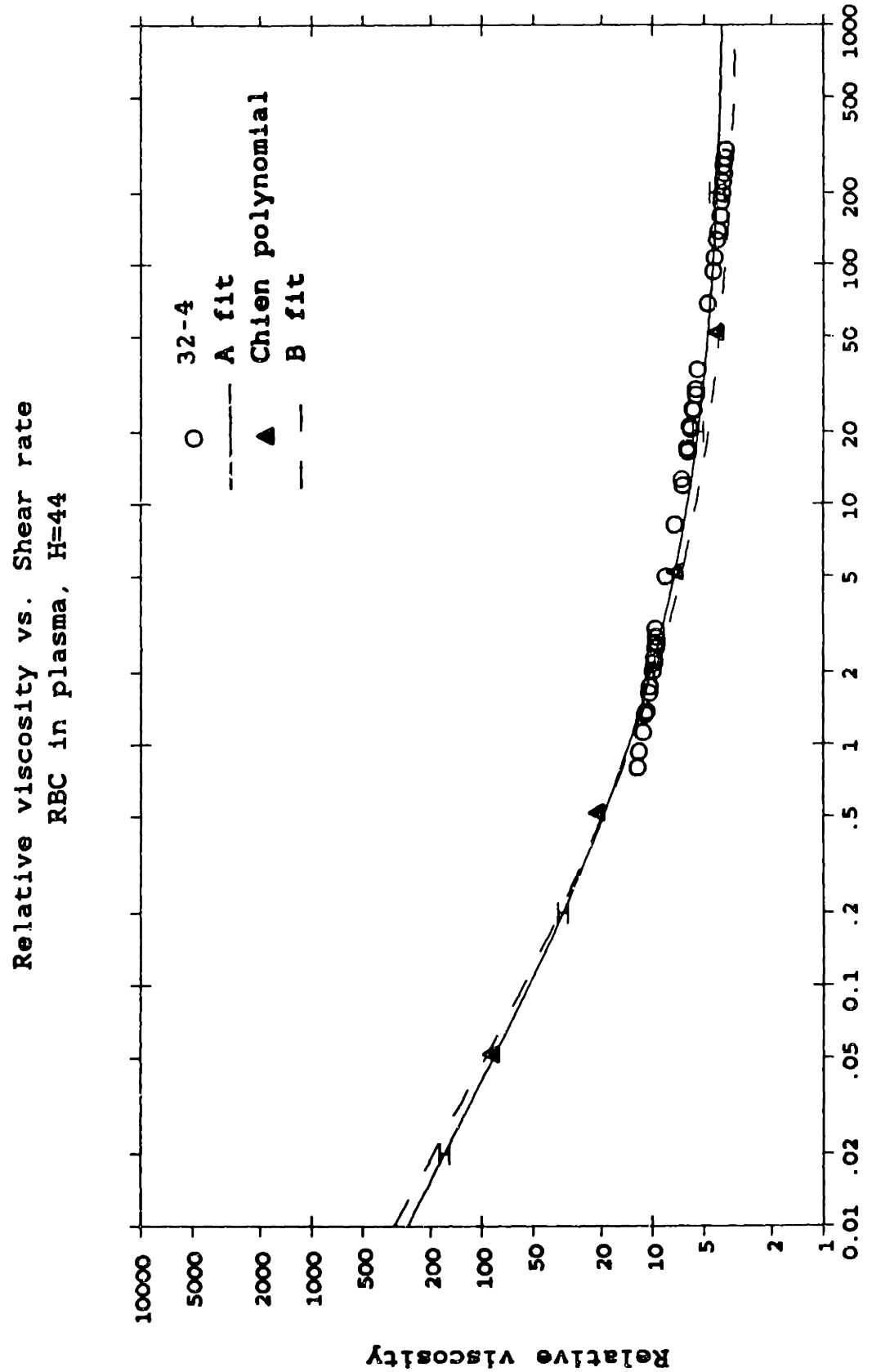

$\eta_{f,32}$=1.06 cP

Figure 4-46: Plasma data, H=44.

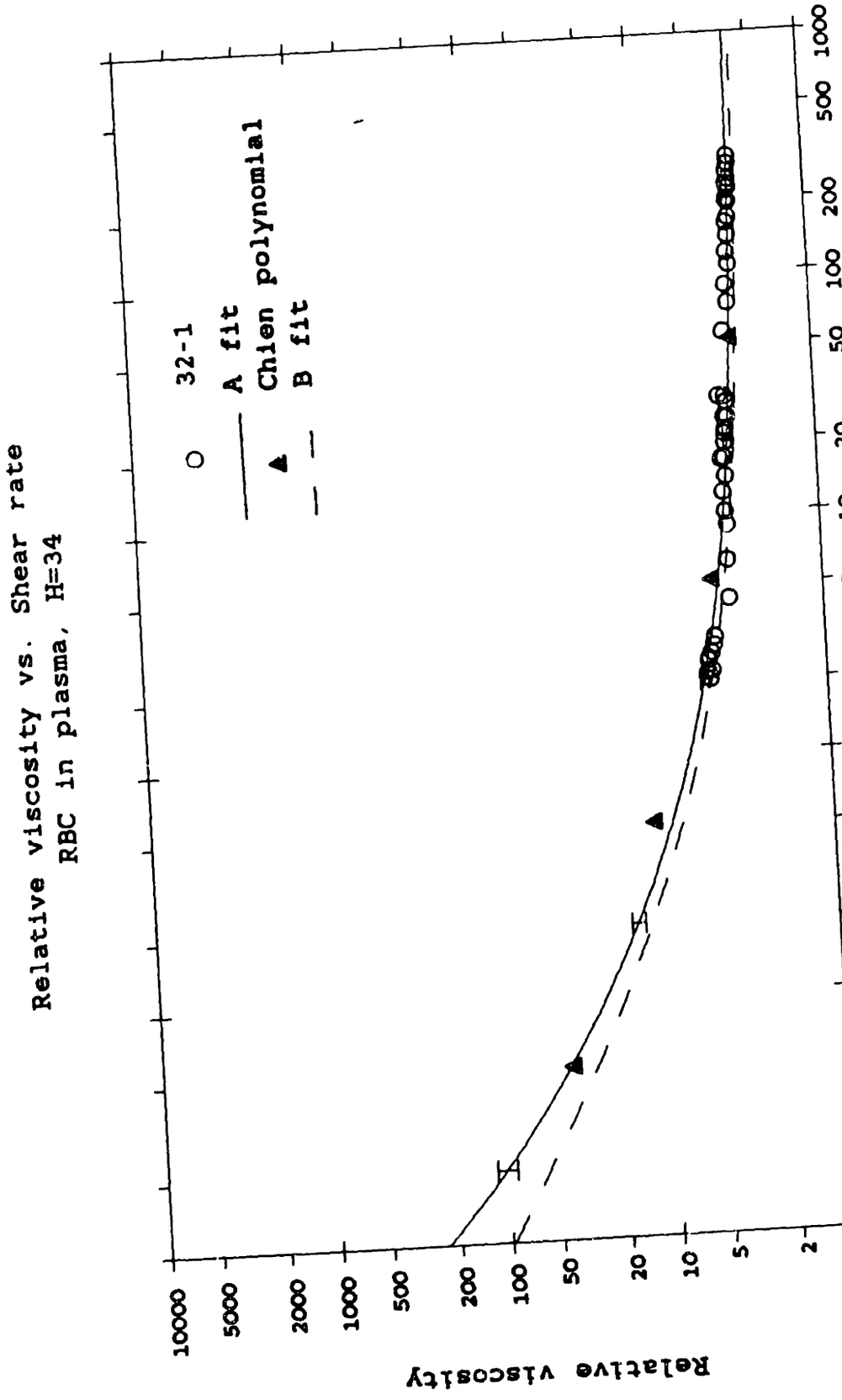

Figure 4-47: Plasma data, H=34.

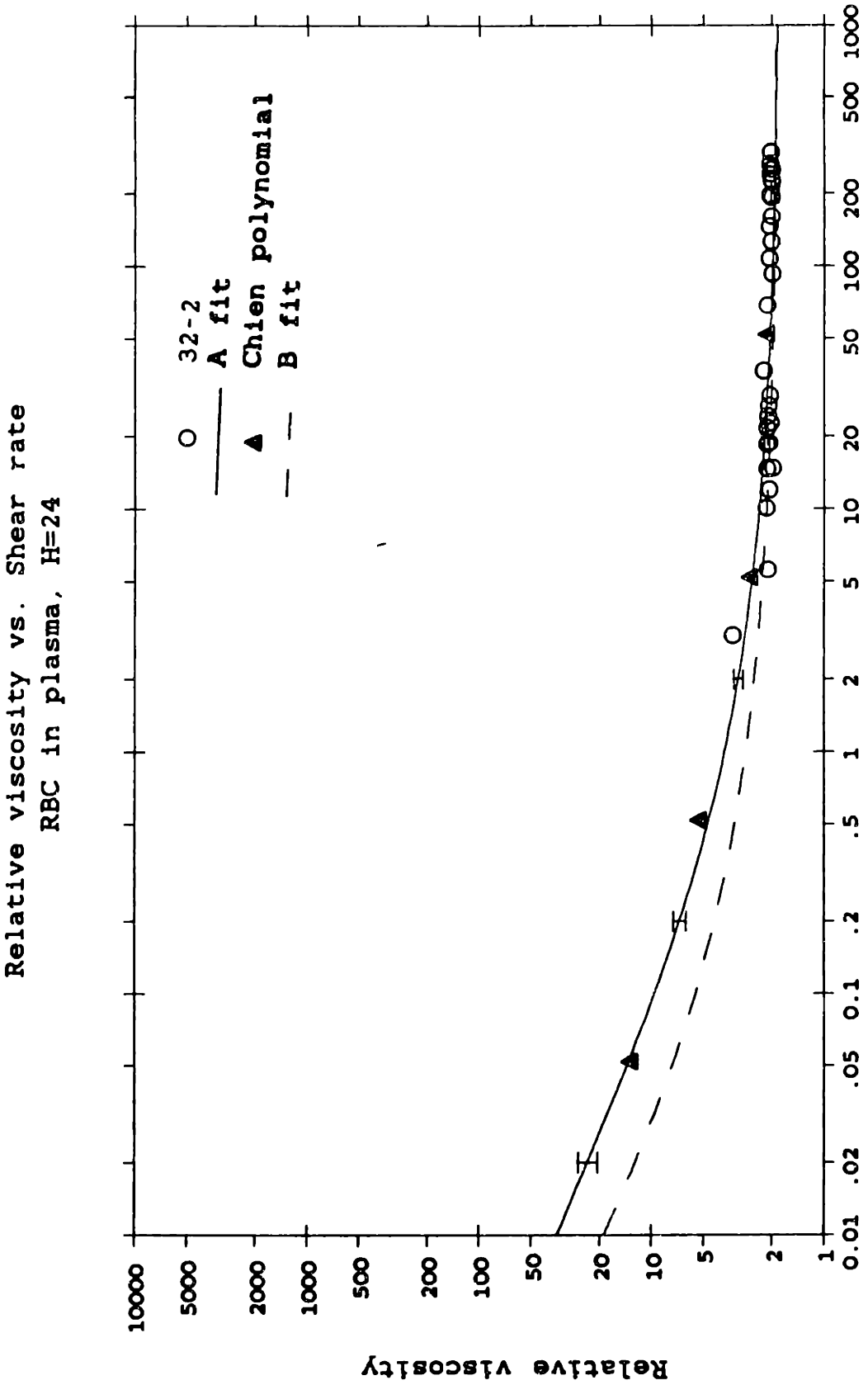

Figure 4-48: Plasma data, H=24.

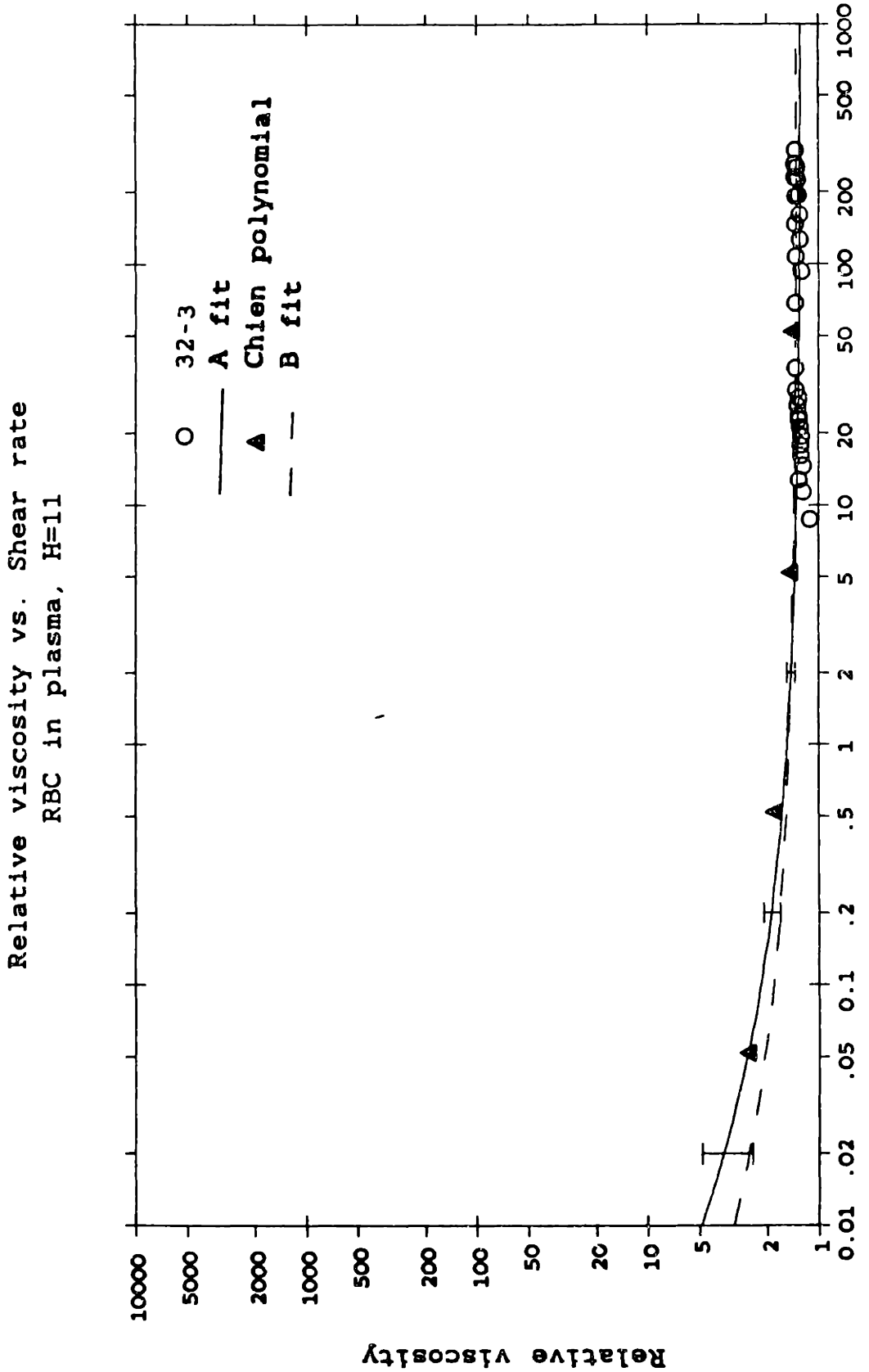

Figure 4-40: Plasma data, H=11.

three groups along the x-axis. This is an artifact resulting solely from the choice of the ranges of operation used and the selection of data points.

The data follows the trends for blood viscosity reported in the literature and reviewed in Chapter 2. Shear-thinning behavior is observed in all cases. At low shear rates, the viscosity seems to approach infinity at hematocrits above 90 and seems to level to an asymptote at hematocrits below 60, but there is not sufficient data to make a judgement as to the existence of a yield stress. Asymptotic values for viscosity are approached at the highest obtainable shear rate (300 sec^{-1}) for all plots, but only in the most concentrated suspensions (H>94) do they actually appear to be reached. The sensitivity of the viscometer limits the minimum shear rate at which data can be obtained: Above H=70, this minimum $\dot{\gamma}$ is on the order of 0.1 sec^{-1} or less; above H=50, it is between 0.1 and 1 sec^{-1}; below 40, the minimum is around 1 sec^{-1}.

A general pattern of increasing viscosity with increasing hematocrit is observed, with $\frac{d\eta}{dH}$ greatest at the highest concentrations. For example, at $\dot{\gamma} = 100$ sec^{-1}, an increase in hematocrit from 89 to 97 (a 6.7% increase) increases viscosity by over 70%; while increasing hematocrit from 42 to 48 (a 14% increase) increases viscosity by only about 15%. Even at hematocrits above 98, however, blood is very fluid.

4.3 Viscosity of RBC suspended in plasma

The data for RBC suspended in plasma solutions are shown in Figures 4-26 to 4-49 (pages 93 to 116). The range of hematocrits is from 98.1 to 11. Relative viscosities were calculated from the individual plasma viscosities for each sample, which are tabulated in Appendix F. The symbol conventions are the same as for the saline suspensions. For the data of Chien *et al.*, η_f was calculated as 1.18 cP in a

manner analagous to that used for Ringer's saline. The descriptive comments applied to Eagle's solution suspensions in the previous section qualitatively apply to plasma suspensions. Because the plasma samples are for the most part more viscous than their corresponsing saline samples, data could be obtained at somewhat lower shear rates but again, below hematocrits of about 40 it was not possible to get data over a broad spectrum of shear rates.

4.4 Comparison of saline and plasma data

Data from the two types of RBC suspensions are plotted together as η_r vs. H in Figure 4-50 and as η vs. H in Figure 4-51. Values are shown at shear rates of 200, 20, 2, and 0.2 sec^{-1}. In order to express values for all hematocrits at precisely each of these shear rates, the points shown are not actual data but are values from the Quemada equation fits (Fit A on the individual data plots) for each hematocrit. These fits are close enough to the actual data values that there would be no discernible difference on Figures 4-50 and 4-51. For the absolute viscosity, plasma suspension η_r was multiplied by a value of 1.1 cP for average plasma viscosity. Points are shown only where data was actually taken, thus there is no representation in this figure of the low hematocrit, low shear rate regions.

There is a greater amount of scatter from a monotonic relationship with hematocrit at low shear rates, where the data is less reliable, and a greater scatter in the saline suspensions versus the plasma suspensions. The relative values for Eagle's suspensions are consistently higher than those for plasma, although on an absolute basis, the plasma suspension viscosities are higher. For example, at H=96, the ratio of the relative viscosity in saline to that in plasma is between 1.29 and 1.49 at the shear rates given. For H=94 the range is 1.87 to 1.56; for H=90, 1.38 to 1.40; H=86, 1.06 to 1.40. There is no clear trend of the ratios increasing or

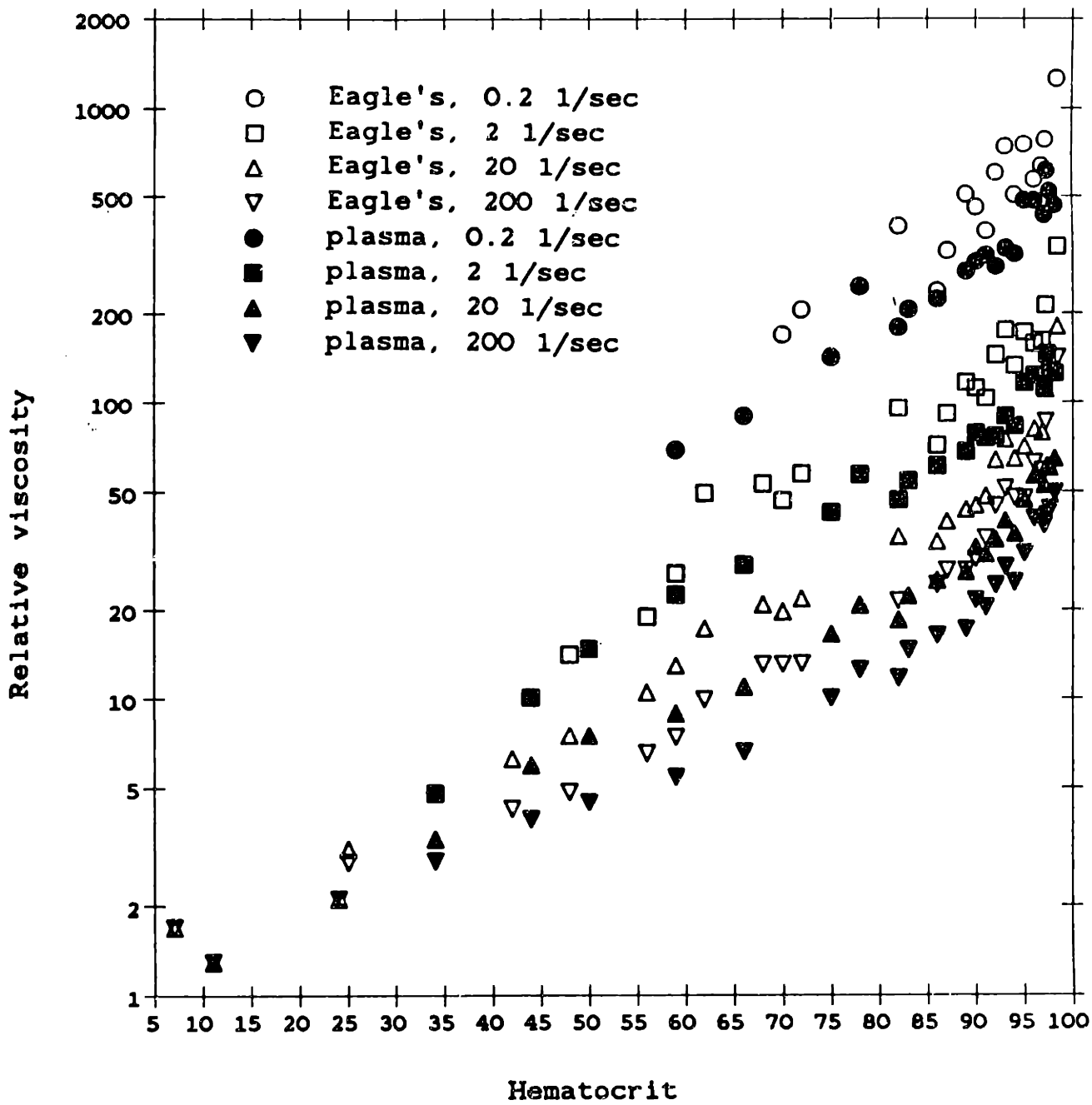

Figure 4-50: Relative viscosity vs. Hematocrit for Eagle's and plasma suspensions

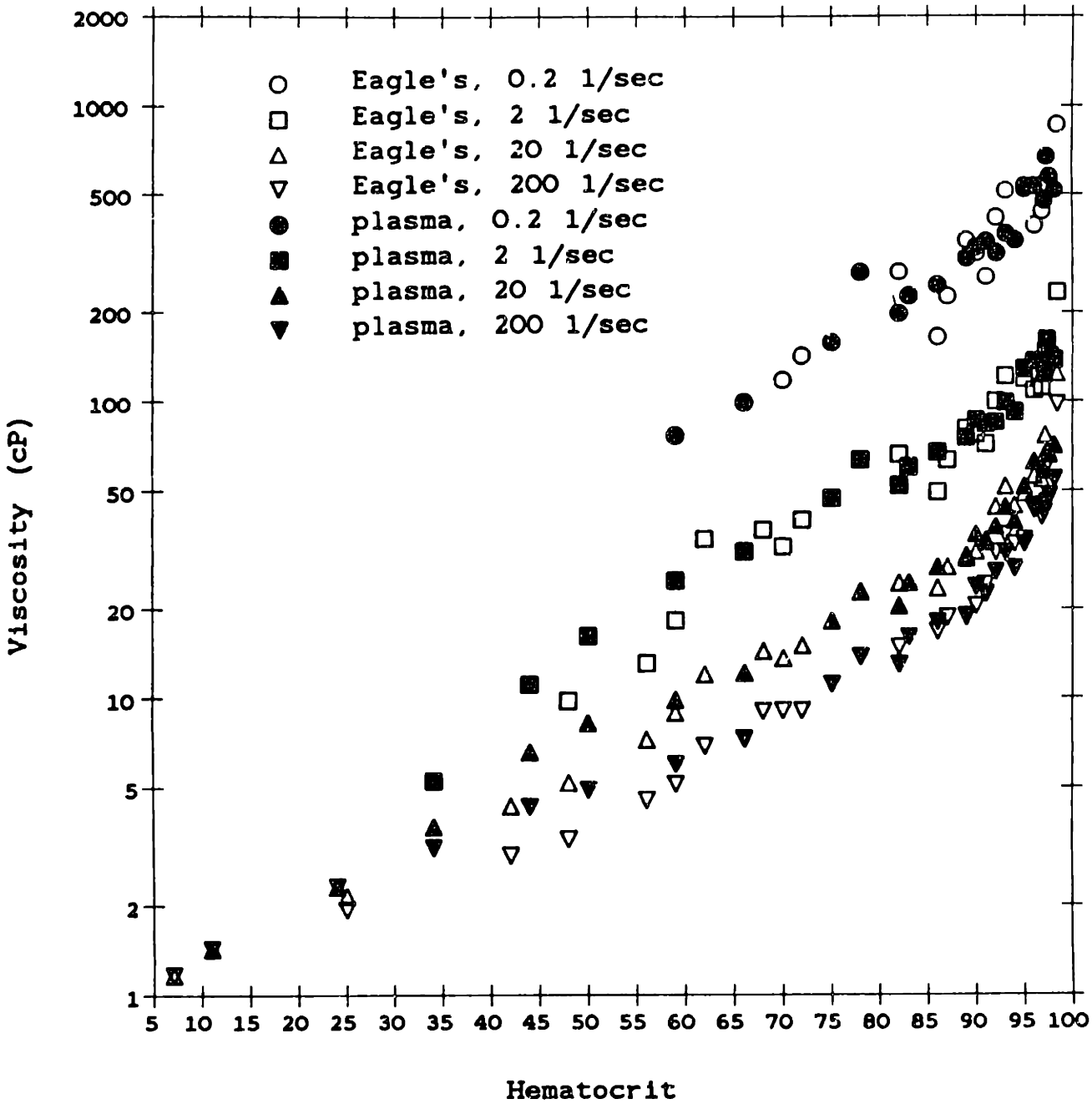

Figure 4-51: Absolute viscosity vs. Hematocrit for Eagle's and plasma suspensions

decreasing with shear rate. On a scale of absolute viscosities, the ratios just given would be decreased by a factor of about 0.6.

Figure 4-51 demonstrates how, on an absolute scale, the differences between saline and plasma suspensions decrease in the limit of high cell concentration. Above H=80, the data cannot be clearly distinguished between suspensions, particularly at high shear rates, and it appears at this point that an inversion phenomenon has taken place, with the cells behaving physically as the continuous phase. By an analysis of the behavior of the parameters for equation (2.11), Quemada [1981] has also suggested the importance of inversion, as will be discussed further in Chapter 5.

From Figures 4-50 and 4-51, it can be seen that, while the absolute viscosities become equal, the differences in relative viscosity are significant at high hematocrits. Viscosity becomes independent of η_f as the amount of suspending fluid becomes small, and the implication is that relative viscosity becomes a meaningless parameter in the limit of high hematocrits.

The decrease in relative viscosity with increasing viscosity of the continuous phase is a well-known aspect of the emulsion behavior of blood as described in Chapter 2. Dintenfass [1968b] suggests a modified form of the Taylor equation for emulsions, equation (2.5), to calculate the internal viscosity of the red cell:

$$\eta_r = \frac{1}{(1-c\cdot T)^{2.5}} \tag{4.1}$$

where $T(\eta_i, \eta_f)$ is the Taylor parameter described for equation (2.5) on page 22 and c is the cell volume fraction. The shear rate dependence of equation (4.1) comes from the internal viscosity of the red cell, which represents not only the cytoplasmic viscosity but also includes the effects of the red cell membrane. As discussed previously in Section 2.4, this equation has limited applicability in that it is only valid when the shear rate is high enough to prevent rouleau formation. Fits of the

data at γ=52 sec^{-1} yield values for η_i around 2 cP, which is comparable to values found in the literature [Dintenfass, 1971]. The Dintenfass equation is used in the next section to provide an evaluation of how viscosity is related to changes in the red cell properties.

4.5 Effect of erythrocyte age and anticoagulant

It has been known for some time that the viscosity of blood increases with age [Erslev and Atwater, 1963; Usami *et al.*, 1971]. Erythrocytes have been shown to have increased hemoglobin concentration as they get older, and this along with possible loss of membrane deformability may increase the intrinsic viscosity of the cell.

The blood units obtained from the Red Cross were stored in a refrigerator at a temperature of about 40 °F. There was a noticeable increase in the viscosity of the samples with longer storage times. This effect was largest at low shear rates. For example, the plot of H=92 in Eagle's solution, Figure 4-9, page 76, shows data for three samples from three units: Two (16-5 and 20-8) had their viscosities measured 10 days before the expiration date (11 and 15 days after collection, respectively) and one (18-4) was measured 2 days before expiration (19 days after collection). At 300 sec^{-1} the oldest sample has the highest viscosity, but its value is almost identical to that of one of the fresher samples and is 1.3 times that of the other. As shear rate decreases, the difference in viscosity increases substantially. At γ = 0.3 sec^{-1} the oldest sample has a viscosity 1.75 times that of the other two. This is not attributable to storage in the laboratory refrigerator because both samples 16-5 and 18-4 were measured two days after being obtained from the Red Cross.

Relevent samples which illustrate the effect of storage time are described in

sample	suspending fluid	anti-coagulant	H	d.s.c.	d.b.e.	v.s.f. (cP)
16-5	Eagle's	CPD	92	11	10	0.69
20-8	Eagle's	CPD-A1	92	14	10	0.69
18-4	Eagle's	CPD	92	25	2	0.69
19-10	Eagle's	CPD-A1	91	22	13	0.69
20-9	Eagle's	CPD-A1	91	25	10	0.69
16-3	Eagle's	CPD	90	11	10	0.69
18-9	Eagle's	CPD	90	19	2	0.69
16-9	Eagle's	CPD	87	11	10	0.69
20-10	Eagle's	CPD-A1	87	25	10	0.69
16-8	Eagle's	CPD	70	11	10	0.69
24-2	Eagle's	CPD-A1	70	35	0	0.69
29-9	plasma	AS-1	96	9	33	1.05
31-1	plasma	AS-1	96	11	31	1.21
30-1	plasma	AS-1	91	10	32	1.13
31-4	plasma	AS-1	91	11	31	1.21
29-2	plasma	AS-1	89	9	33	1.05
31-6	plasma	AS-1	89	11	31	1.21

d.s.c.--days since collection
d.b.e.--days before expiration
v.s.f.--viscosity of suspending fluid

Table 4-I: Description of samples which illustrate effect of erythrocyte age.

sample	visc. (cP) @ 0.3 1/sec	rel. visc.	visc. (cP) @ 3 1/sec	rel. visc.	visc. (cP) @ 30 1/sec	rel. visc.
16-5	208	301.4	69.3	100.4	38.7	56.1
20-8	223	323.2	66.0	95.7	32.5	47.1
18-4	392	568.1	99.3	143.9	43.2	62.6
19-10	184	266.7	59.0	85.5	29.6	42.9
20-9	206	298.6	63.0	91.3	31.0	44.9
16-3	175	253.6	53.0	76.8	27.5	39.9
18-9	260	376.8	89.0	129.0	27.7	40.1
16-9	170	246.4	56.0	81.2	27.0	39.1
20-10	161	233.3	51.0	73.9	23.6	34.2
16-8	58	84.1	23.0	33.3	10.2	14.8
24-2	95	137.7	32.0	46.4	14.0	20.3
29-9	382	363.8	114.0	108.6	59.2	56.4
31-1	438	362.0	126.0	104.1	54.0	44.6
30-1	233	206.2	62.0	54.9	34.0	30.1
31-4	293	242.1	80.0	66.1	33.6	27.8
29-2	232	221.0	65.0	61.9	26.6	25.3
31-6	210	173.6	61.5	50.8	26.7	22.1

sample	visc. (cP) @ 300 1/sec	rel. visc.	int. visc. (cP) @ 30 1/sec	int. visc. (cP) @ 300 1/sec
16-5	31.2	45.2	2.49	2.08
20-8	24.7	35.8	2.15	1.70
18-4	32.5	47.1	2.74	2.15
19-10	22.5	32.6	2.16	1.69
20-9	23.5	34.1	2.25	1.76
16-3	20.4	29.6	2.20	1.67
18-9	19.0	27.5	2.21	1.56
16-9	18.0	26.1	2.89	1.86
20-10	16.7	24.2	2.49	1.72
16-8	7.0	10.1	6.47	2.33
24-2	9.1	13.2	can't calculate	4.45
29-9	45.0	42.9	2.74	2.27
31-1	40.0	33.1	2.69	2.16
30-1	20.0	17.7	2.58	1.59
31-4	22.6	18.7	2.58	1.79
29-2	17.6	16.8	2.36	1.58
31-6	18.0	14.9	2.38	1.61

Table 4-II: Viscosities of samples from Table 4-I.

Table 4-I and their viscosities at selected shear rates are given in Table 4-II. A complete catalog of all sample ages and anticoagulants is given in Appendix F.

Similar age effects are observed in the Eagle's suspensions with H=91, 90 and 70. The samples for H=91 were obtained from the same unit, one measured 22 days after collection, the other 25 days after collection. For H=90, the difference is 11 days versus 19 days. At H=70, a sample 11 days after collection is compared to one measured on its date of expiration, 35 days after collection. In all of these cases the older blood had higher viscosity. These results are summarized graphically in Figure 4-52. The increases in viscosity at 0.3 sec^{-1} suggest an increase in the aggregation of the red cells, since this is the major determinant of suspension viscosity at low shear rate. The data for H=92 and H=87, which show decrease in viscosity with age, are probably related to the type of anticoagulant-preservative solution, as CPD-A_1-preserved suspensions consistently have lower viscosities than CPD-preserved suspensions.

There are analagous increases in viscosity with age for plasma suspensions (see Figure 4-53), and these are compounded by the fact that the plasma iself grows more viscous wih time. The plasma data at H=96, 91, and 89 all come from the same Red Cross unit and were measured over the course of three days, during which time the plasma viscosity increased from 1.05 to 1.13 to 1.21 cp. These samples were preserved in AS_1, which has a storage time of 42 days.

The Dintenfass equation, (4.1), was used to calculate the internal viscosity for the samples listed above for which age comparisons were made. These values are shown in Table 4-II. For saline suspensions they provide no additional information since η_f is a constant for all saline samples, but for plasma suspensions they provide an indication of the relative changes in the cell fluidity versus those in the plasma. The values for η_i in Table 4-II indicate either slight increases or no change in the

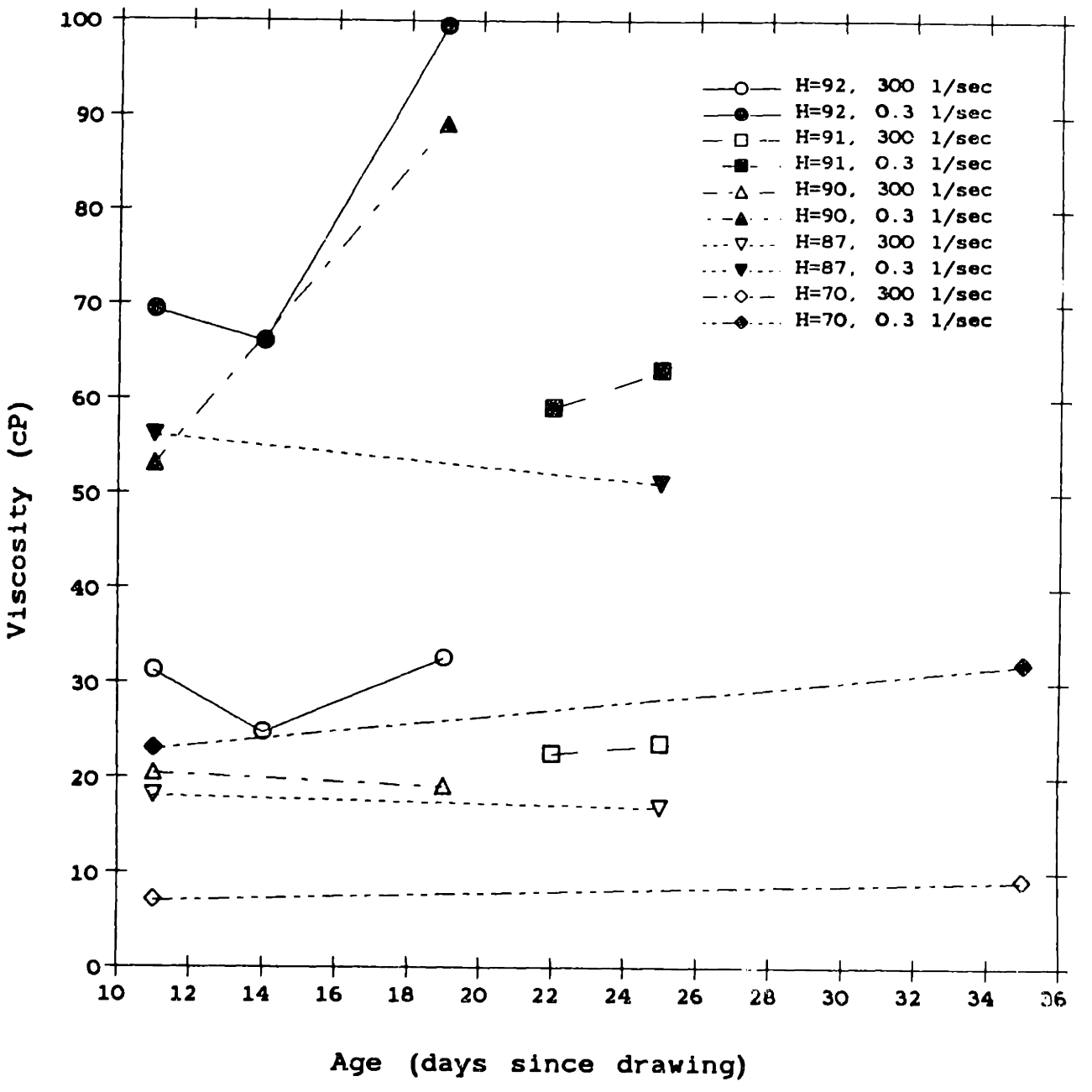

Figure 4-52: Effect of sample age on viscosity of Eagle's solution suspensions.

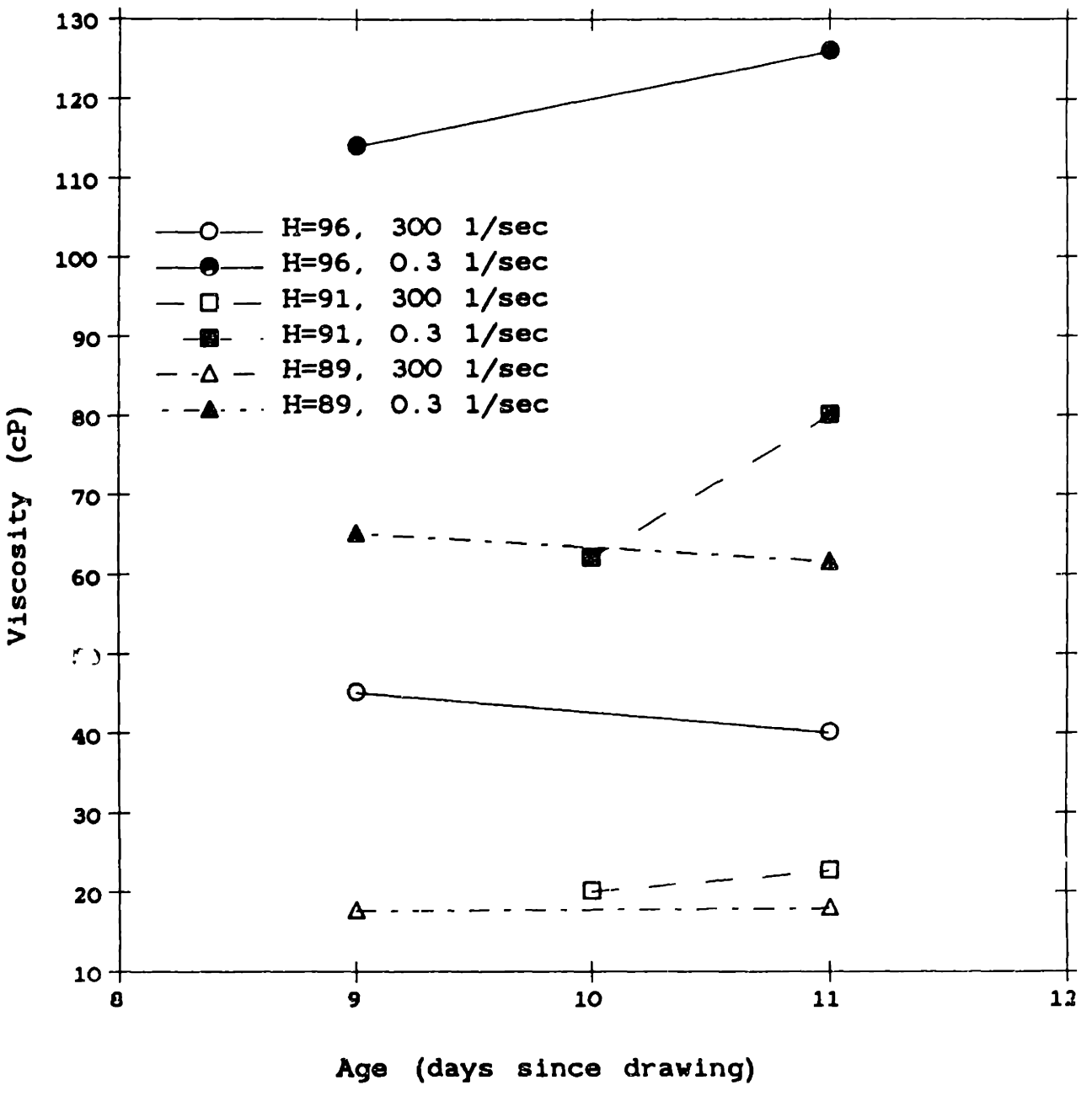

Figure 4-53: Effect of sample age on viscosity of plasma suspensions.

internal viscosity with time, but the Dintenfass equation is not applicable at low shear rates, where the age effects would be most noticeable.

To summarize, with all other things being equal, there is a rise in the viscosity of saline suspensions with erythrocyte age that is a reflection solely of the internal viscosity of the cell and which are more striking at low shear rates. Longer-lasting anticoagulant-preservative solutions appear to retard the age effects, to the extent that they are relatively insignificant. For plasma suspensions, the internal viscosity may rise slightly with storage in AS_1, and the plasma viscosity increases steadily with age.

4.6 Comparison to data of Chien *et al.*, 1966.

The data from Figure 4-51 is replotted versus curves from the equations of Chien *et al.* [1966] in Figures 4-54 and 4-55. Since Chien *et al.* reports only absolute viscosities, the values for plasma suspensions in this study have been adjusted by multiplying them by a value of 1.1 cP for average plasma viscosity, which is an almost undetectable difference in these plots. The general trends of the two sets of datas are similar. It must be remembered that the data points in these figures which represent the work of this paper are actually derived values from the curve fits, and therefore in the case of the lower hematocrits (less than 59 for plasma, less than 70 for saline) at low shear rates (0.052 sec^{-1} and 0.52 sec^{-1}) are only extrapolations of data. Filled symbols are used on Figures 4-54 and 4-55 to represent these extrapolations. The data for saline are comparable to each other at high hematocrits; below 85, the Chien data are consistently lower by factors of 2 or more. On Figures 4-20 to 4-23, the Chien values display a difference curvature with regards to shear rate dependence than the data of this work. The Chien points can be described as exhibiting a concavity, while the data shows convexity. More recent

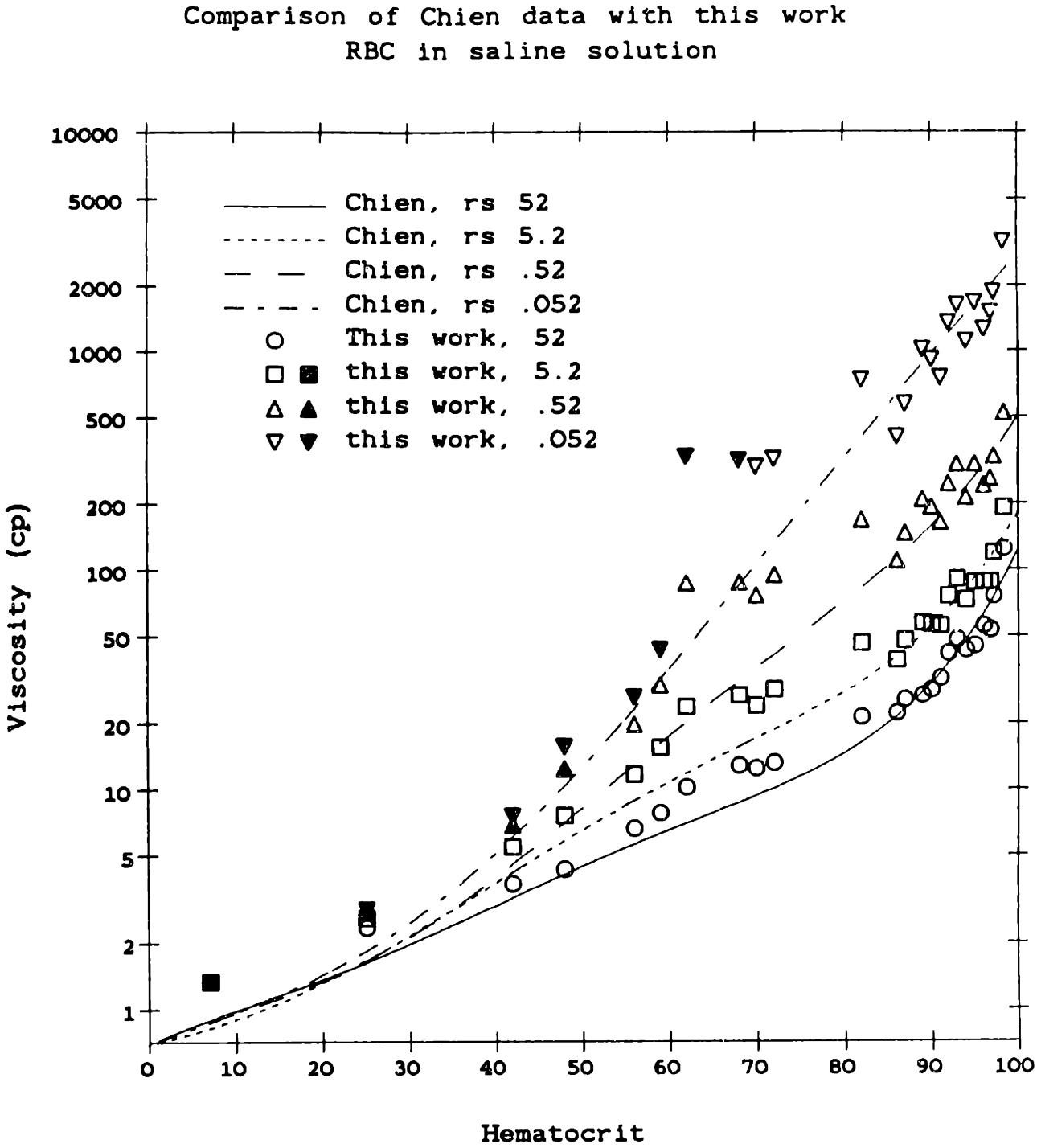

Figure 4-54: Comparison of data of this work to equations of Chien *et al.*, 1966 for saline suspensions.

"rs"--Ringer's Solution

Numbers in legend represent shear rate in sec^{-1}.

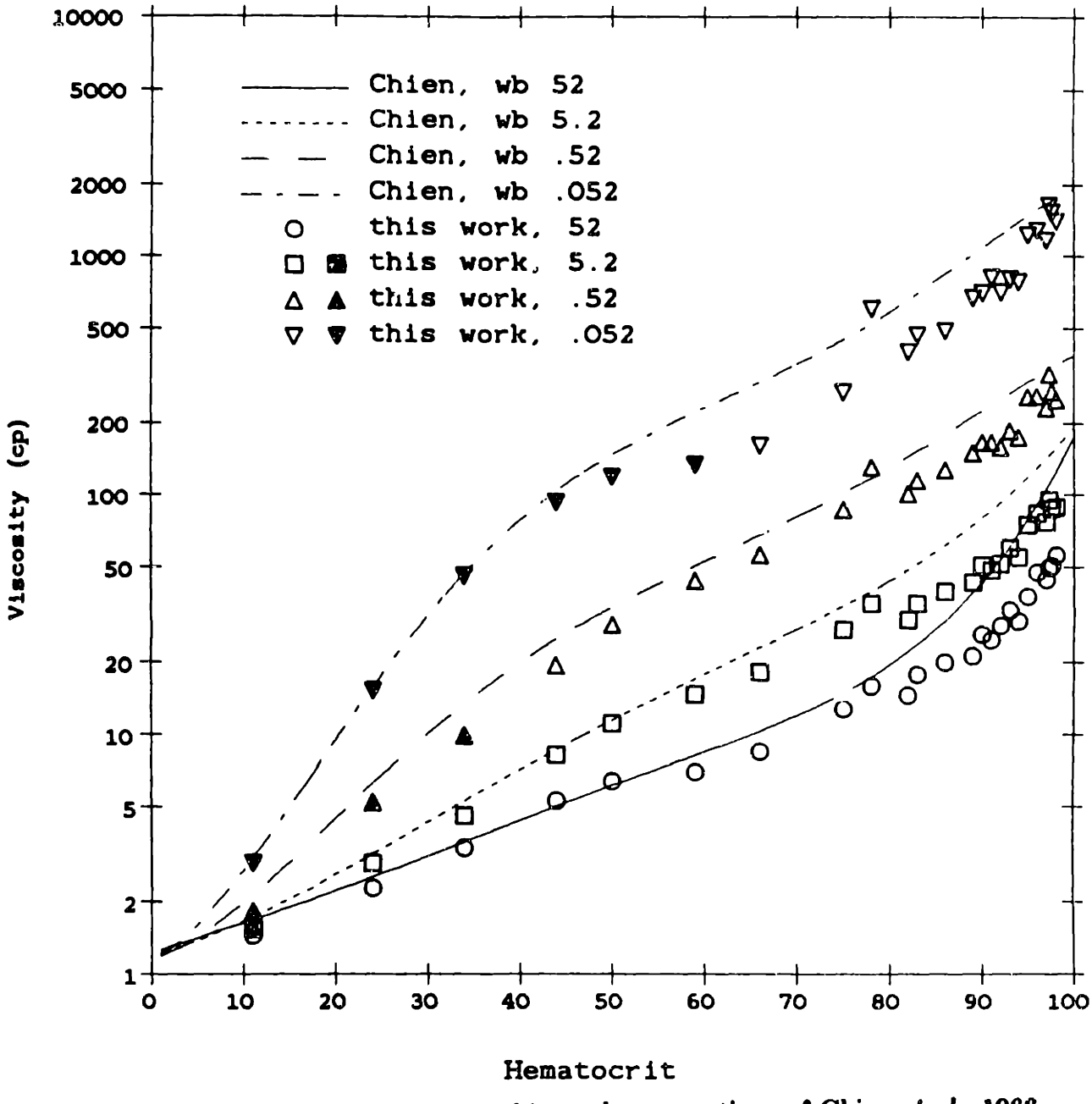

Figure 4-55: Comparison of data of this work to equations of Chien *et al.*, 1966 for plasma suspensions.

"wb"--whole blood

Numbers in legend represent shear rate in sec^{-1}.

data by Chien [1970], shown in Figure 2-3, also has a convex curvature. As will be discussed in Chapter 5, the convexity is the more physically reasonable behavior from the Quemada model. Perhaps by nature of their form, the Chien *et al.* [1966] equations, which model the hematocrit dependence by fifth-order polynomials, introduce a concavity artifact when plotted versus shear rate.

For plasma suspensions, the data of this work is lower than the Chien *et al.* values at the combination of high hematocrits and high shear rates. The magnitude of this difference ranges from 10-30% to factors of 2 or greater. This could be a reflection of the difference between the freshly drawn blood used by Chien *et al.* and the stored units used in this work, although the stored units would be expected to have a higher viscosity. Alternatively, dilution of plasma proteins by the anticoagulant-preservative could lower the viscosity, but this would have its largest impact at low shear rates. At hematocrits less than 80, the two sets of data are quite compatable with one another.

4.7 Global refitting of Chien *et al.* polynomials

It was desirable to examine whether the constants given in Table 2-I for equation (2.8) could be fitted to functions of shear rate, and thus the utility of the Chien polynomials expanded to a wider range. The values for saline suspensions oscillate greatly with shear rate (see Figure 4-56(a-f)) and can be best approximated by polynomials of $\ln(\dot{\gamma})$ of the form:

$$a_i = \sum_{j=0}^{3} \alpha_{ij} [\ln(\dot{\gamma})]^j \qquad (4.2)$$

The constants α_{ij} for these equation are given in Table 4-III. When such equations are plotted versus shear rate at a single hematocrit, they are seen to provide a good fit of data at high hematocrits (see Figure 4-57). As hematocrit decreases, the curve

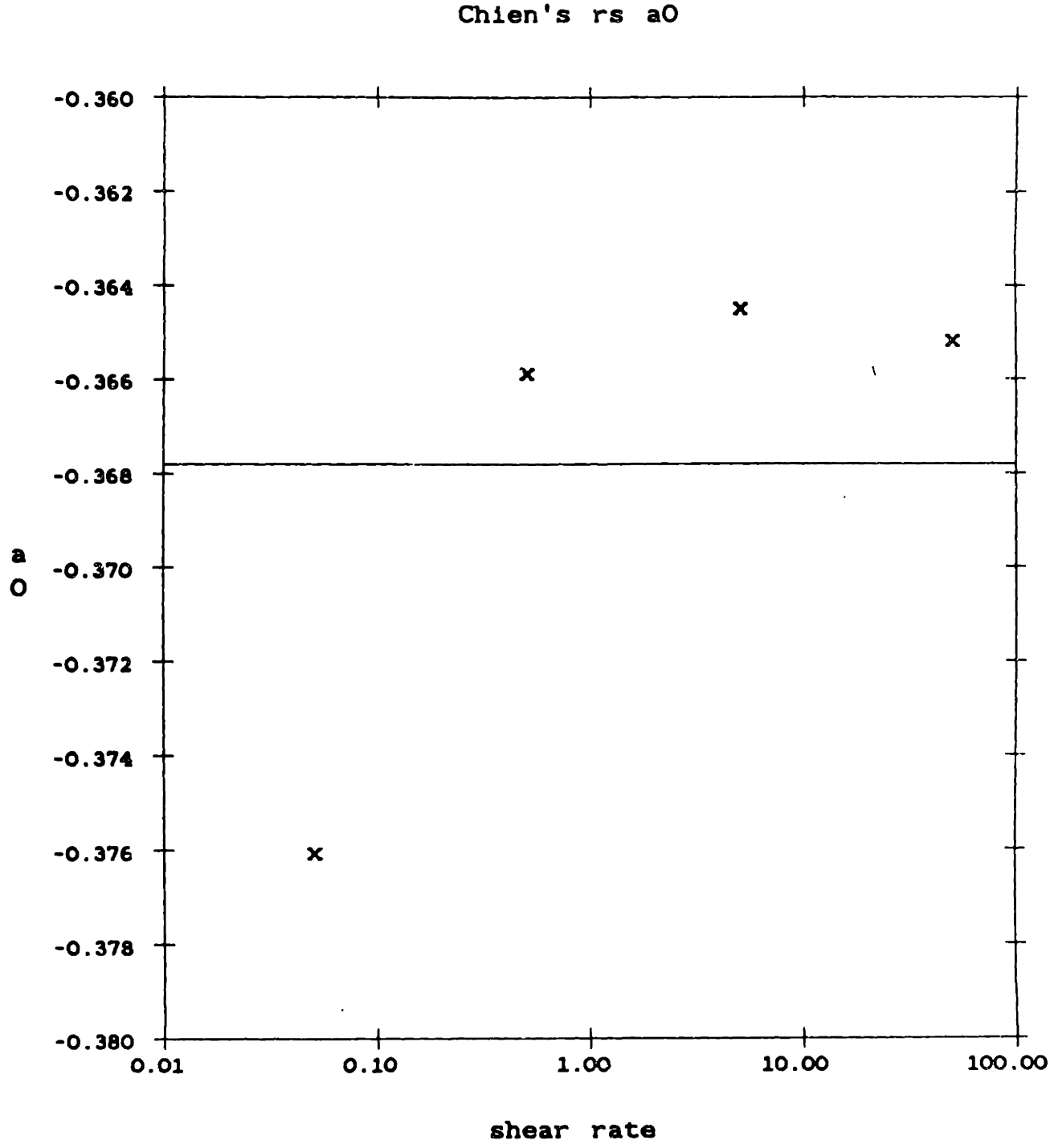

Figure 4-56: Plots of constants for Chien polynomial for saline versus shear rate.

(a) Plot for a_0 in Ringer's solution.

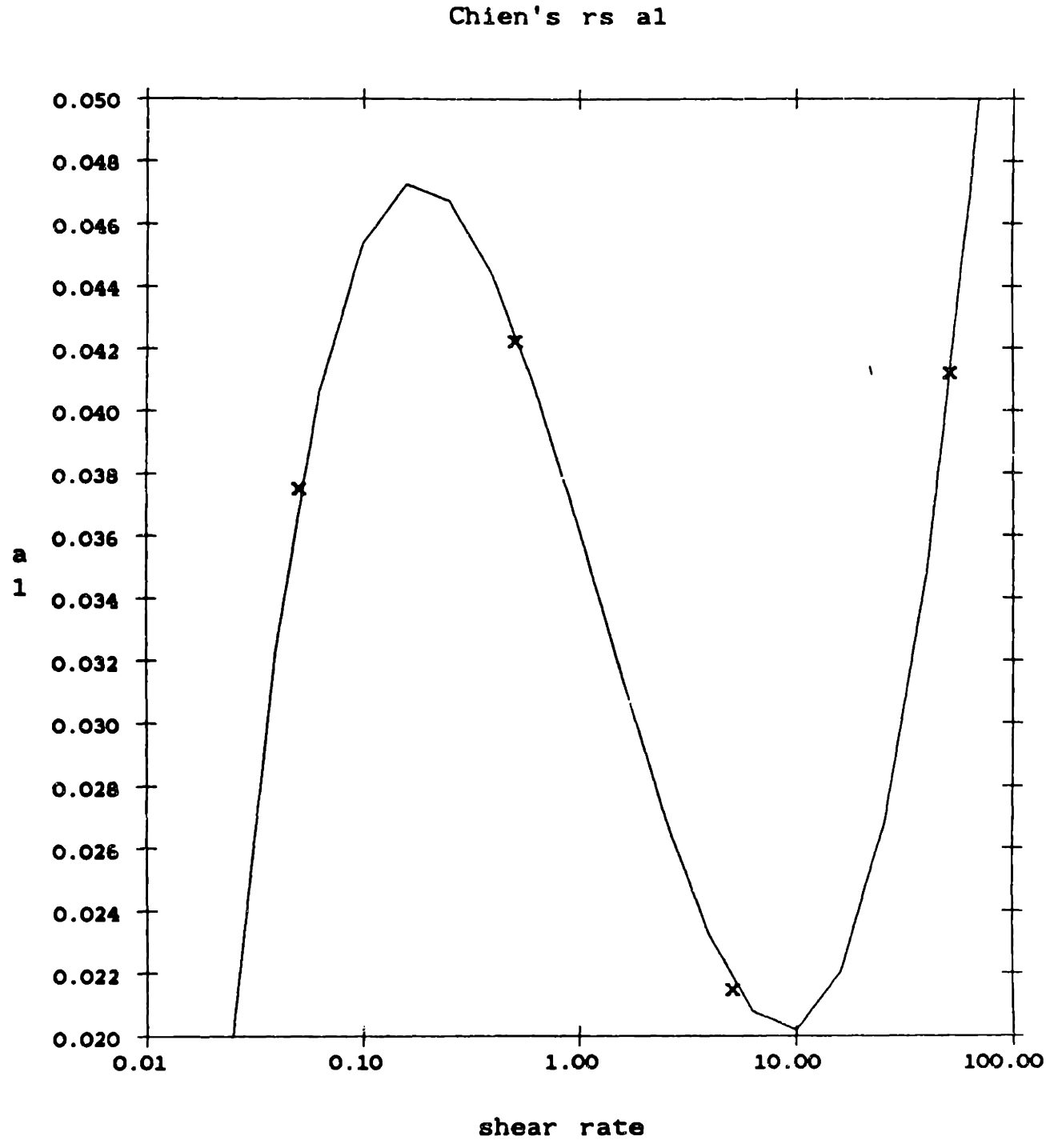

Figure 4-56(b) Plot for a_1 in Ringer's solution.

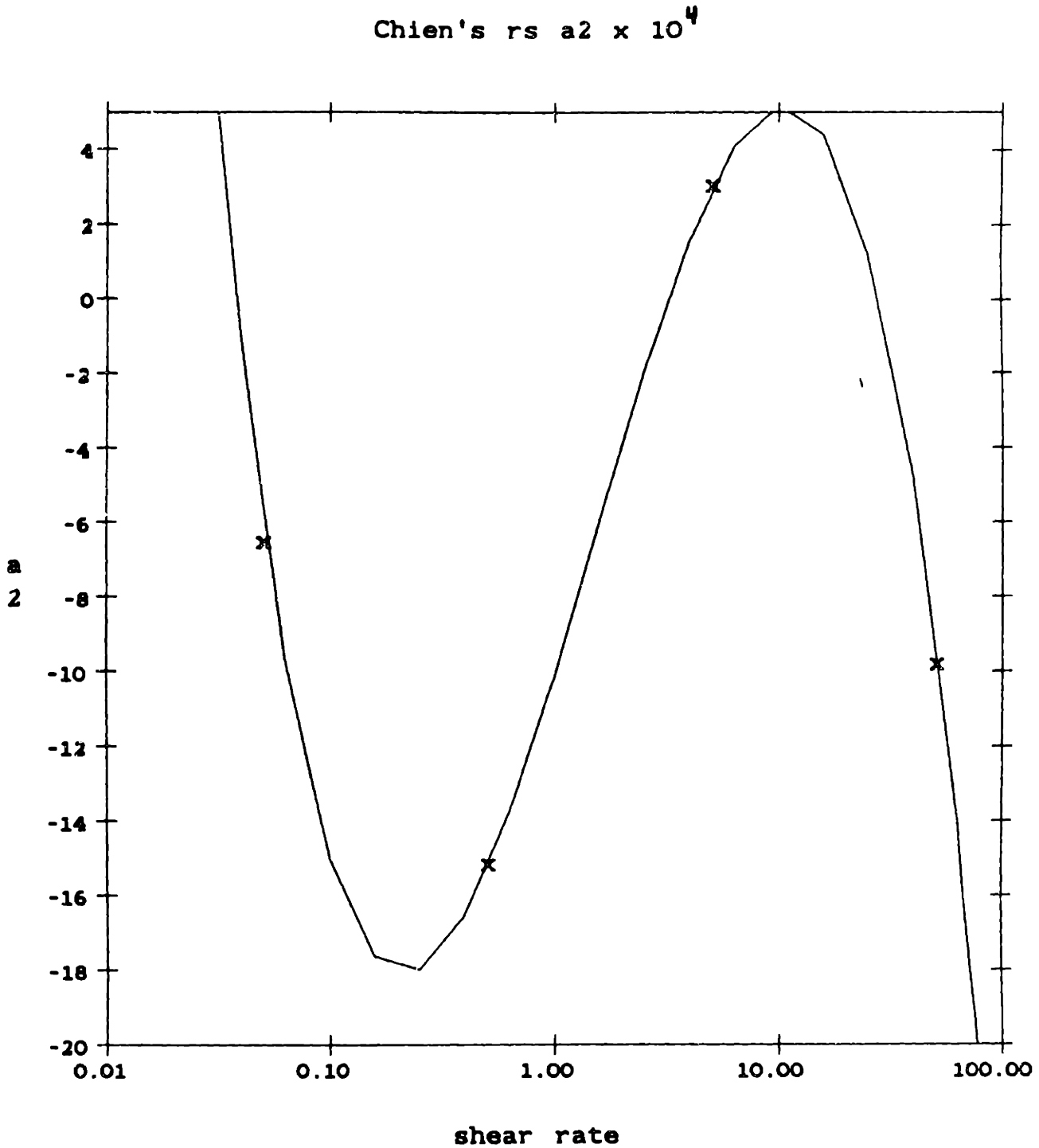

Figure 4-56(c): Plot for a_2 in Ringer's solution.

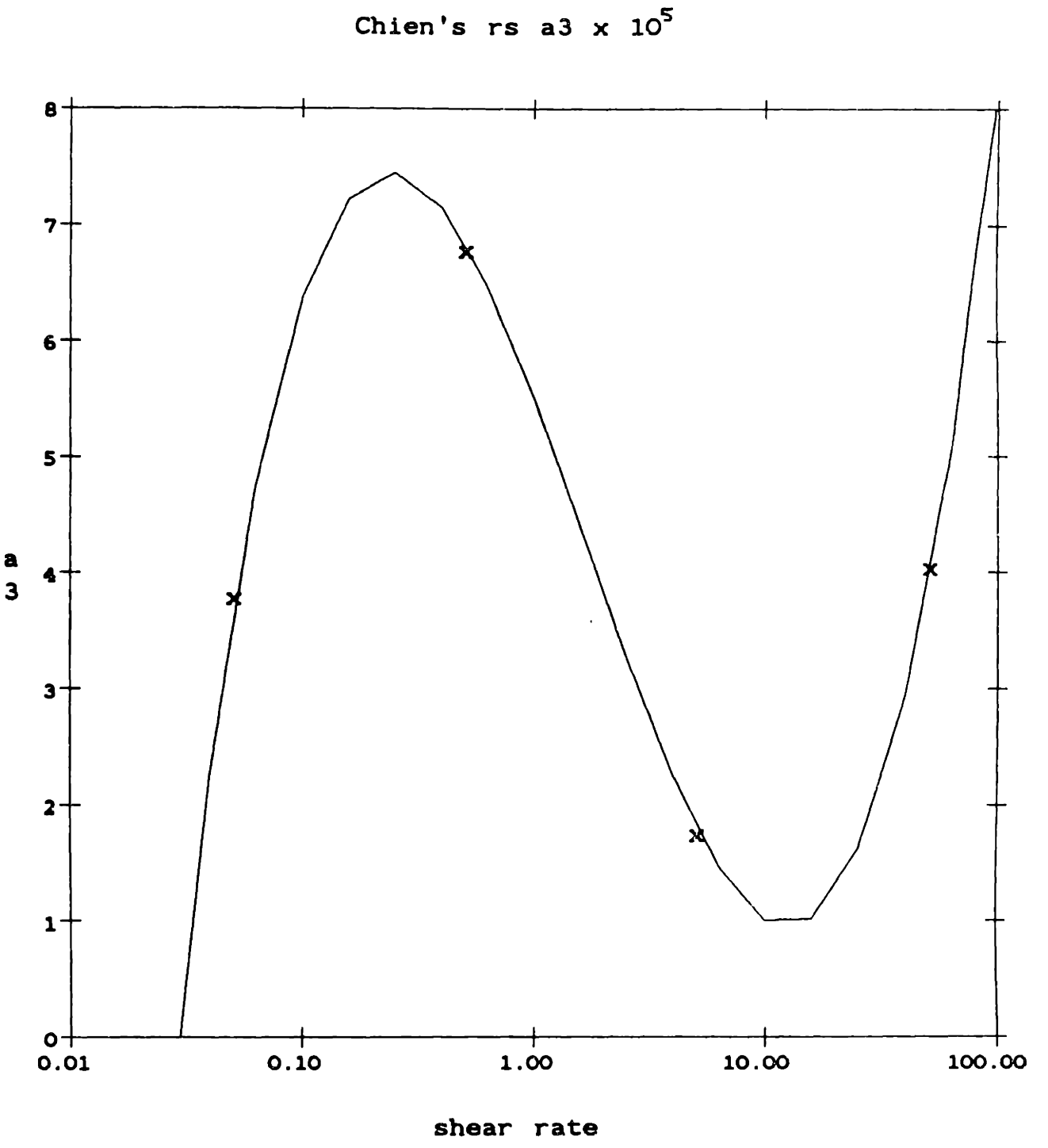

Figure 4-56(d): Plot for a_3 in Ringer's solution.

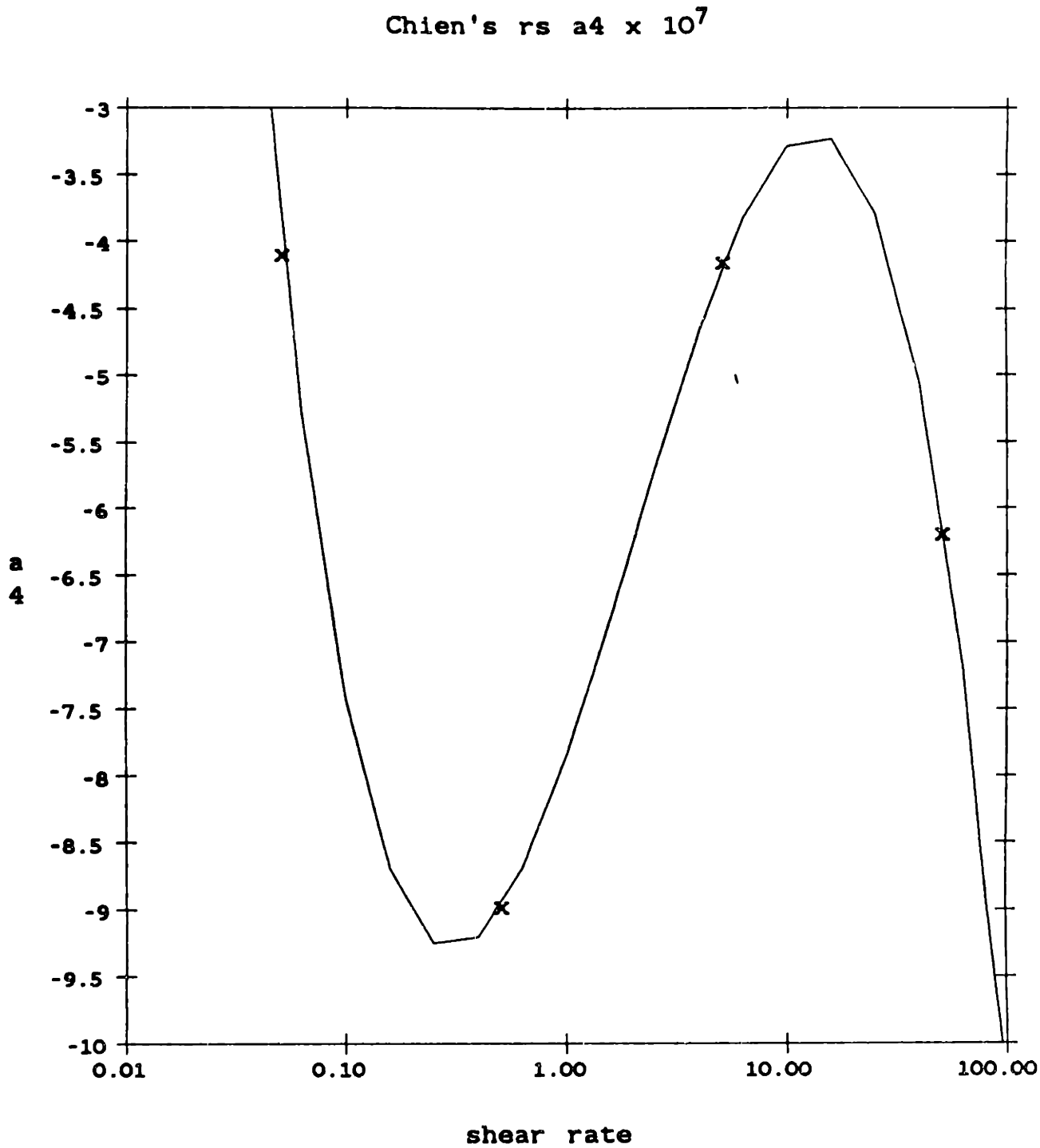

Figure 4-56(e): Plot for a_4 in Ringer's solution.

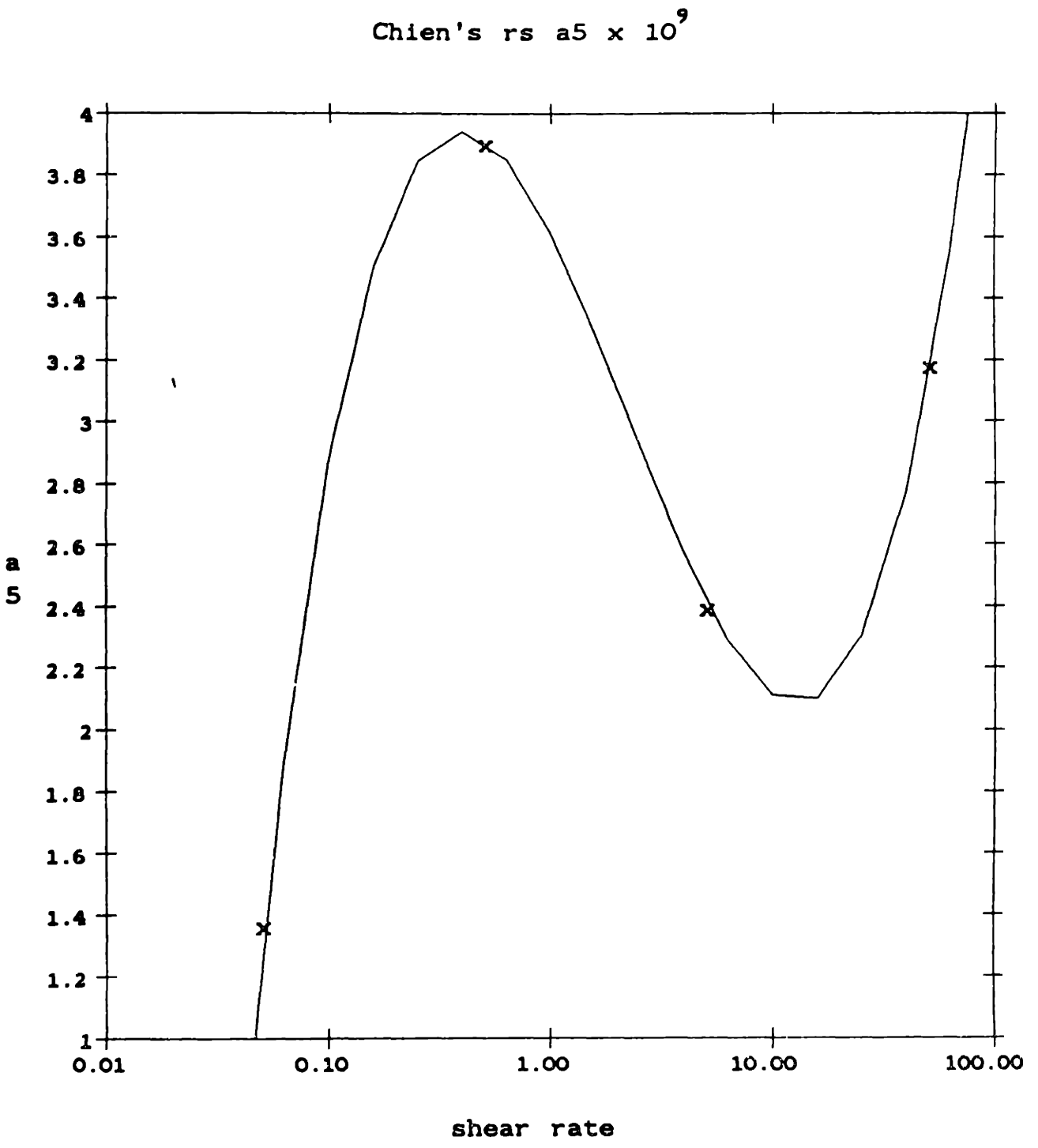

Figure 4-56(f): Plot for a_5 in Ringer's solution.

	j=0	j=1	j=2	j=3
i=0	-3.678e-01			
i=1	3.619e-02	-1.025e-02	-6.384e-04	9.009e-04
i=2	-1.012e-03	8.572e-04	9.811e-05	-7.906e-05
i=3	5.514e-05	-2.275e-05	-3.457e-06	2.097e-06
i=4	-7.856e-07	2.095e-07	4.721e-08	-2.264e-08
i=5	3.614e-09	-6.247e-10	2.119e-10	8.669e-11

Table 4-III: Constants for refit saline Chien equation (4.2).

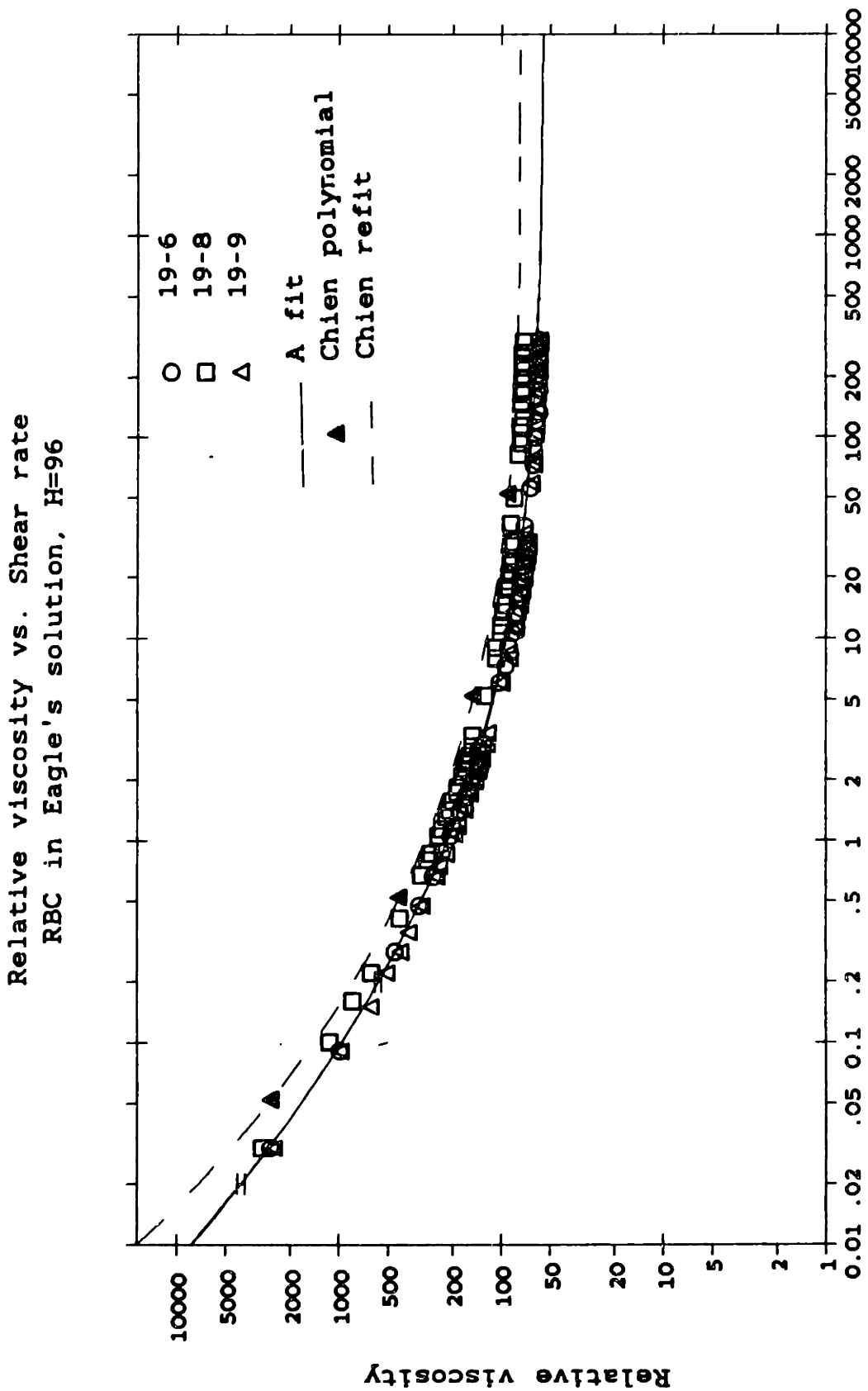

Figure 4-57: Plot of refit saline Chien equation versus shear rate at H=96.

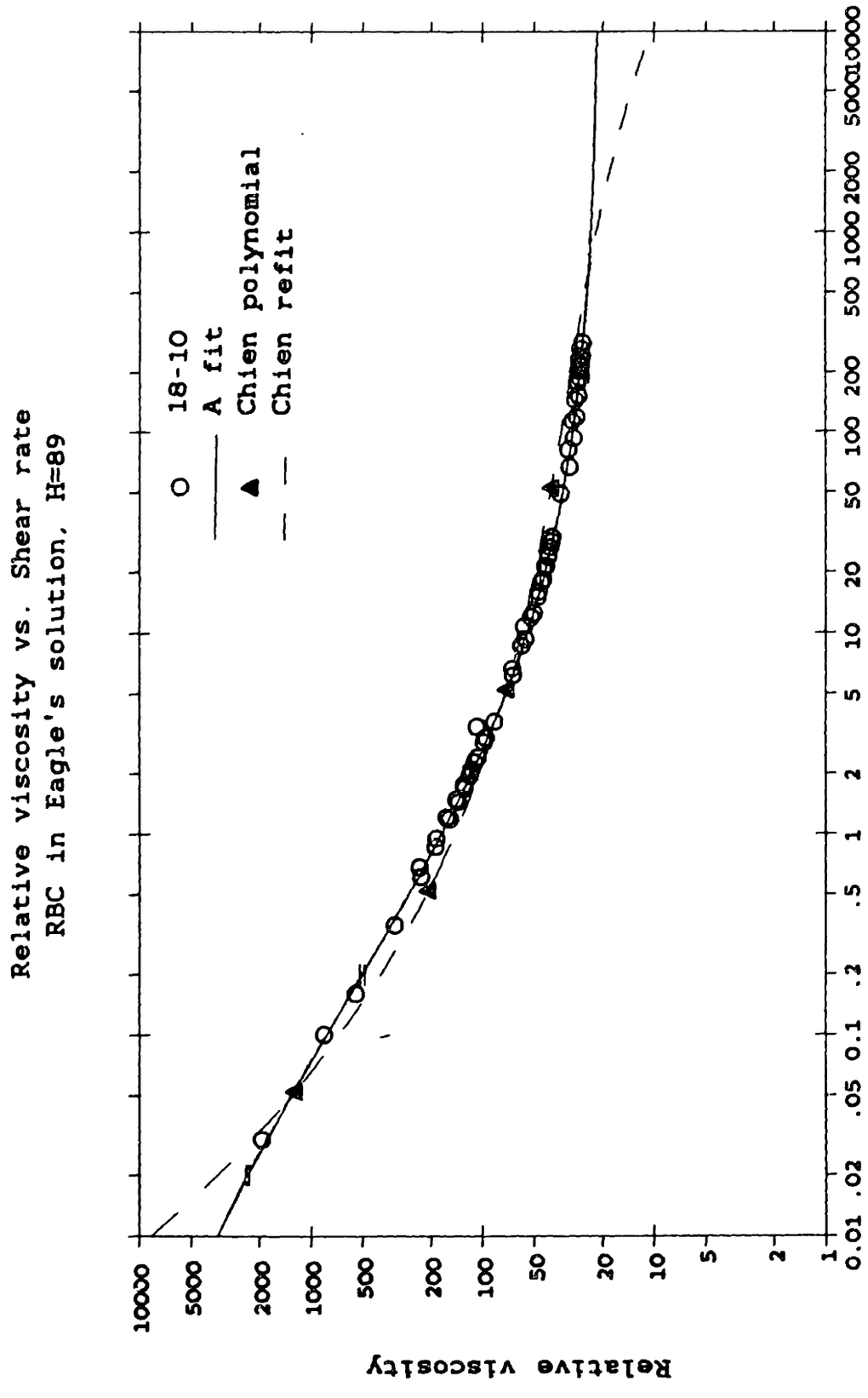

Figure 4-58: Plot of refit saline Chien equation versus shear rate at H=89.

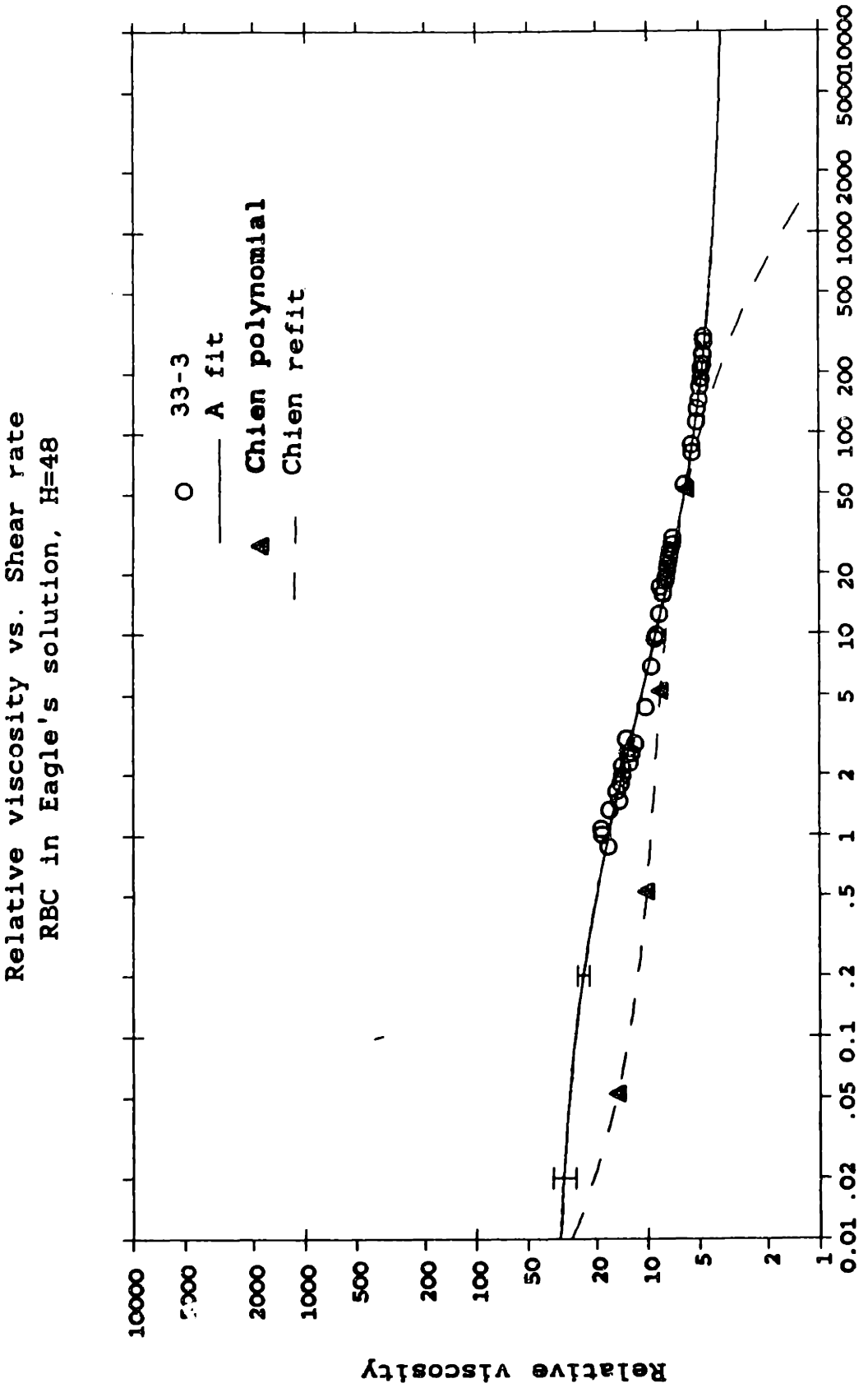

Figure 4-59: Plot of refit saline Chien equation versus shear rate at H=48.

becomes less adequate, veering downward at high shear rates (see Figures 4-58 and 4-59). The constants for plasma suspensions actually suggest asymptotic values at high shear rates (see Figure 4-60(a-f)). The following equations are plotted in Figure 4-60(a-f) as providing a reasonable representation of the functional dependence of the constants:

$$a_0 = 0.1672 \tag{4.3}$$

$$a_1 = \frac{8.513 \times 10^{-4}}{\dot{\gamma}} + 0.02595 \tag{4.4}$$

$$a_2 = \frac{-6.243 \times 10^{-3}\dot{\gamma}}{(0.8106+\dot{\gamma})} + 6.153 \times 10^{-3} \tag{4.5}$$

$$a_3 = 1.732 \times 10^{-4} \exp\left(\frac{-0.4886}{\dot{\gamma}}\right) - 1.639 \times 10^{-4} \tag{4.6}$$

$$a_4 = \frac{1.238 \times 10^{-5}}{\ln (1000 \cdot \dot{\gamma})} - 1.326 \times 10^{-6} \tag{4.7}$$

$$a_5 = 7.539 \times 10^{-9} \exp\left(\frac{-0.5584}{\dot{\gamma}}\right) - 6.009 \times 10^{-9} \tag{4.8}$$

These equations do not prove satisfactory, however, as it is not possible even to retrieve the original plots from them except at low hematocrits (see Figure 4-61). Once again the need is emphasized for a better representation of the data, in a more general form.

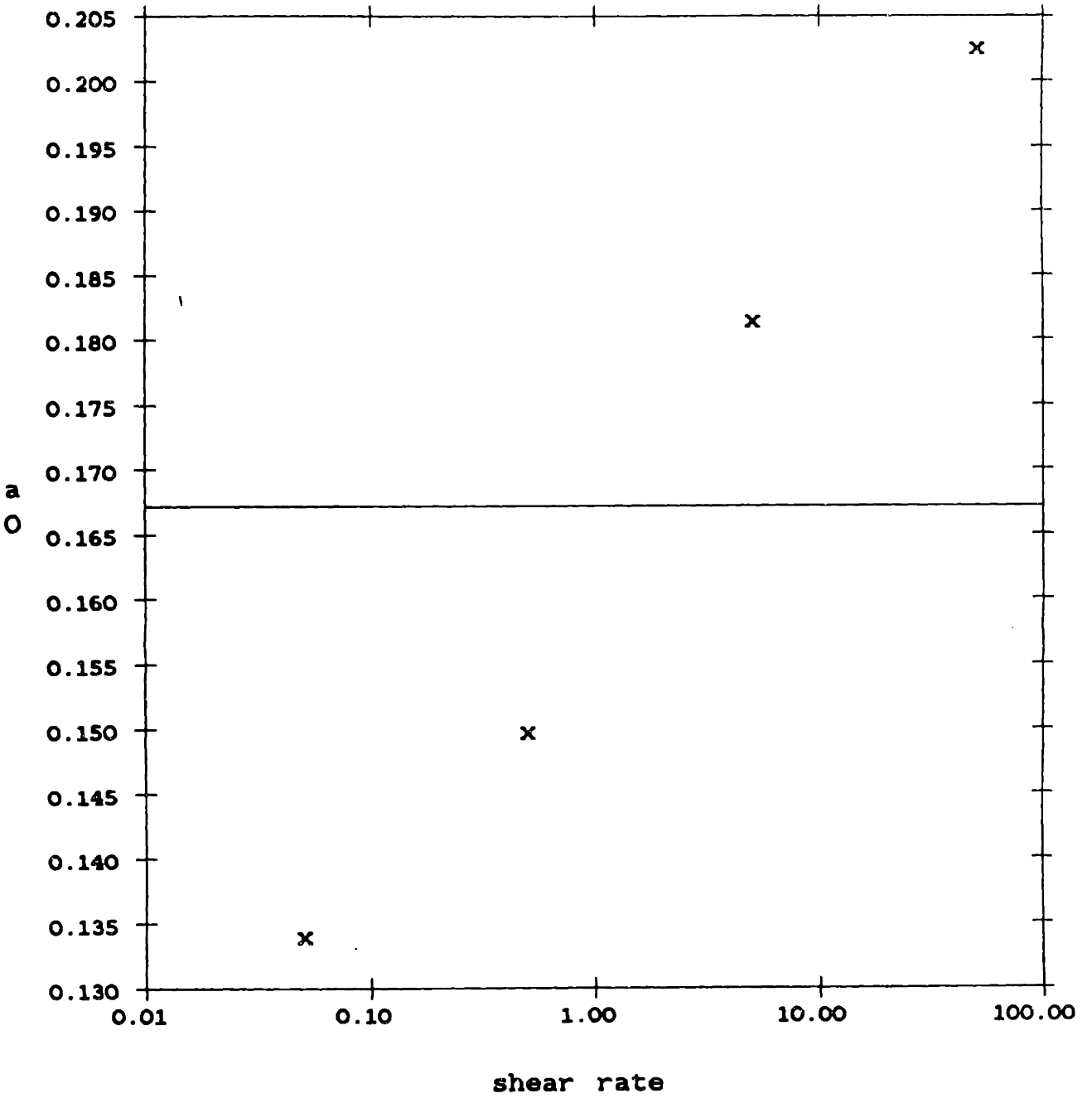

Figure 4-60: Plots of constants for Chien polynomial for plasma versus shear rate.

(a) Plot for a_0 in plasma.

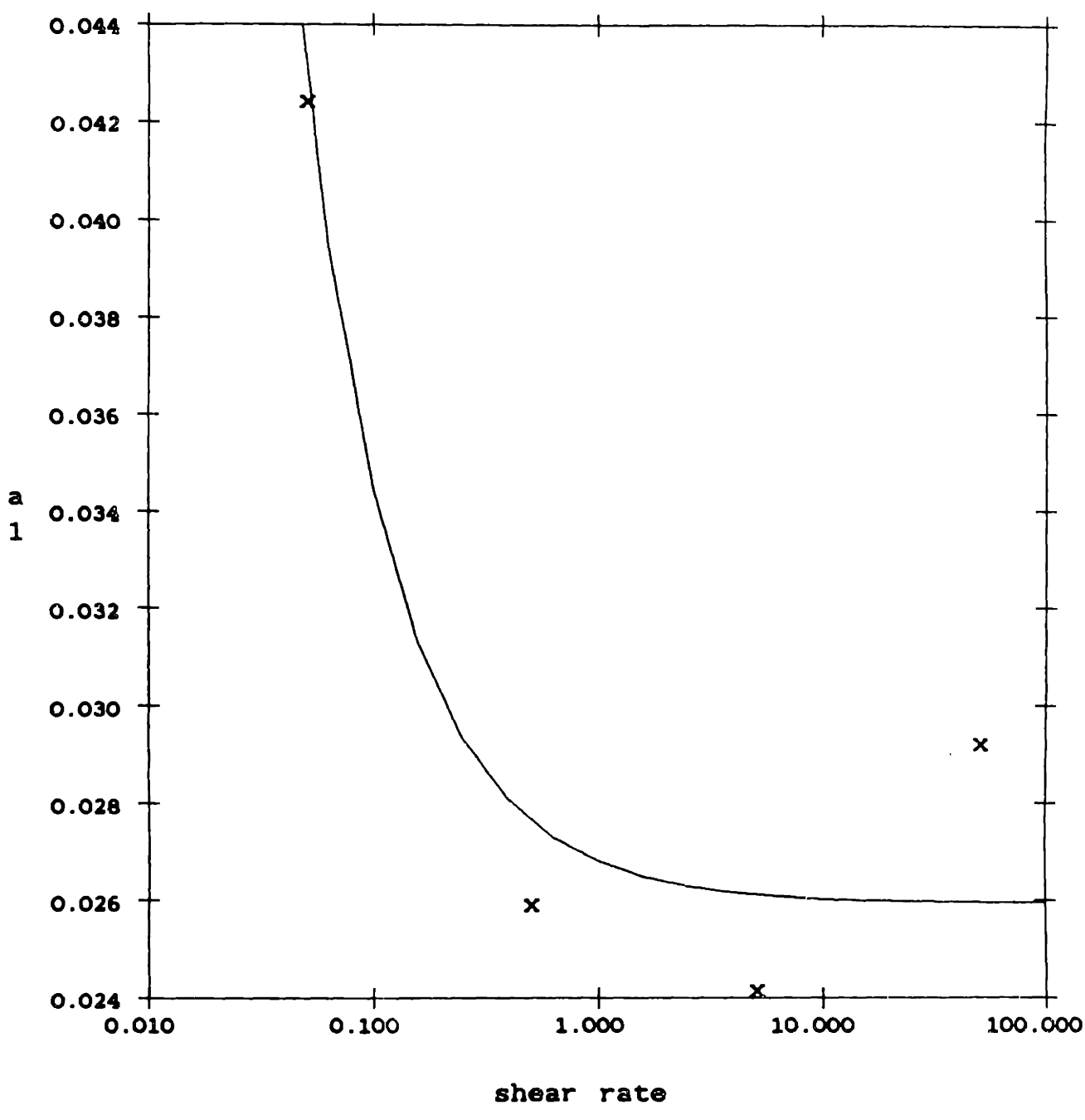

Figure 4-60(b): Plot for a_1 in plasma.

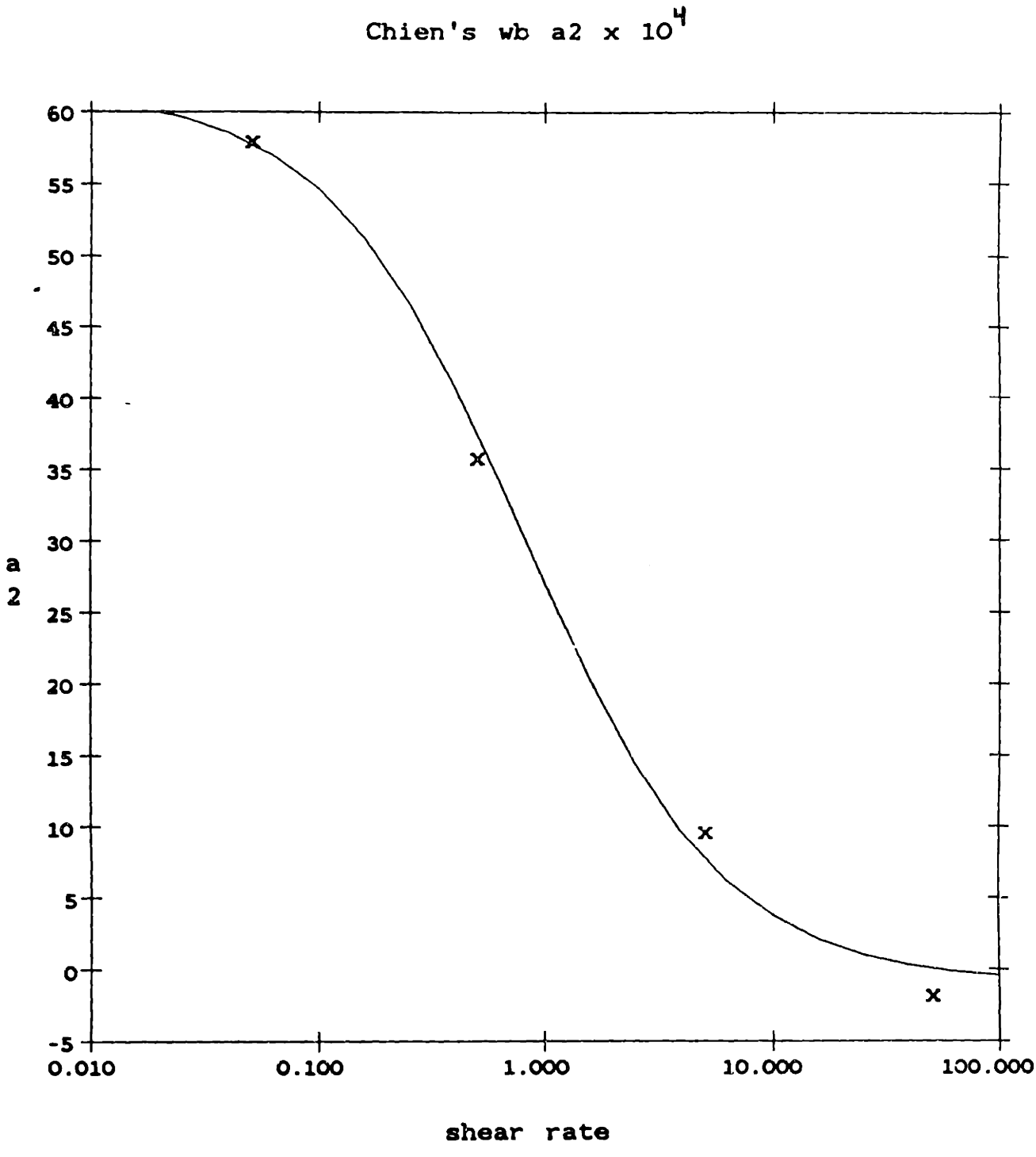

Figure 4-60(c): Plot for a_2 in plasma.

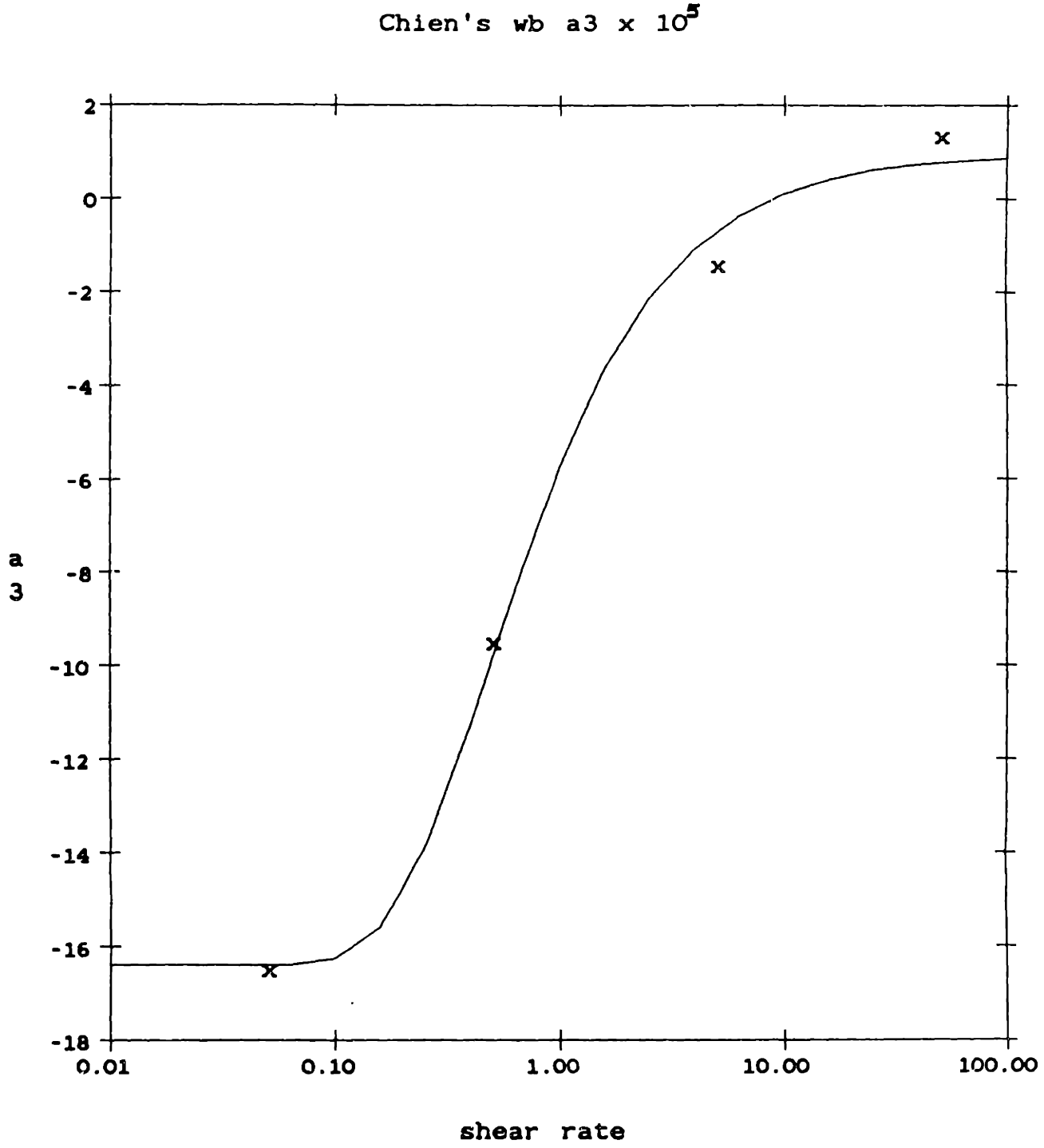

Figure 4-60(d): Plot for a_3 in plasma.

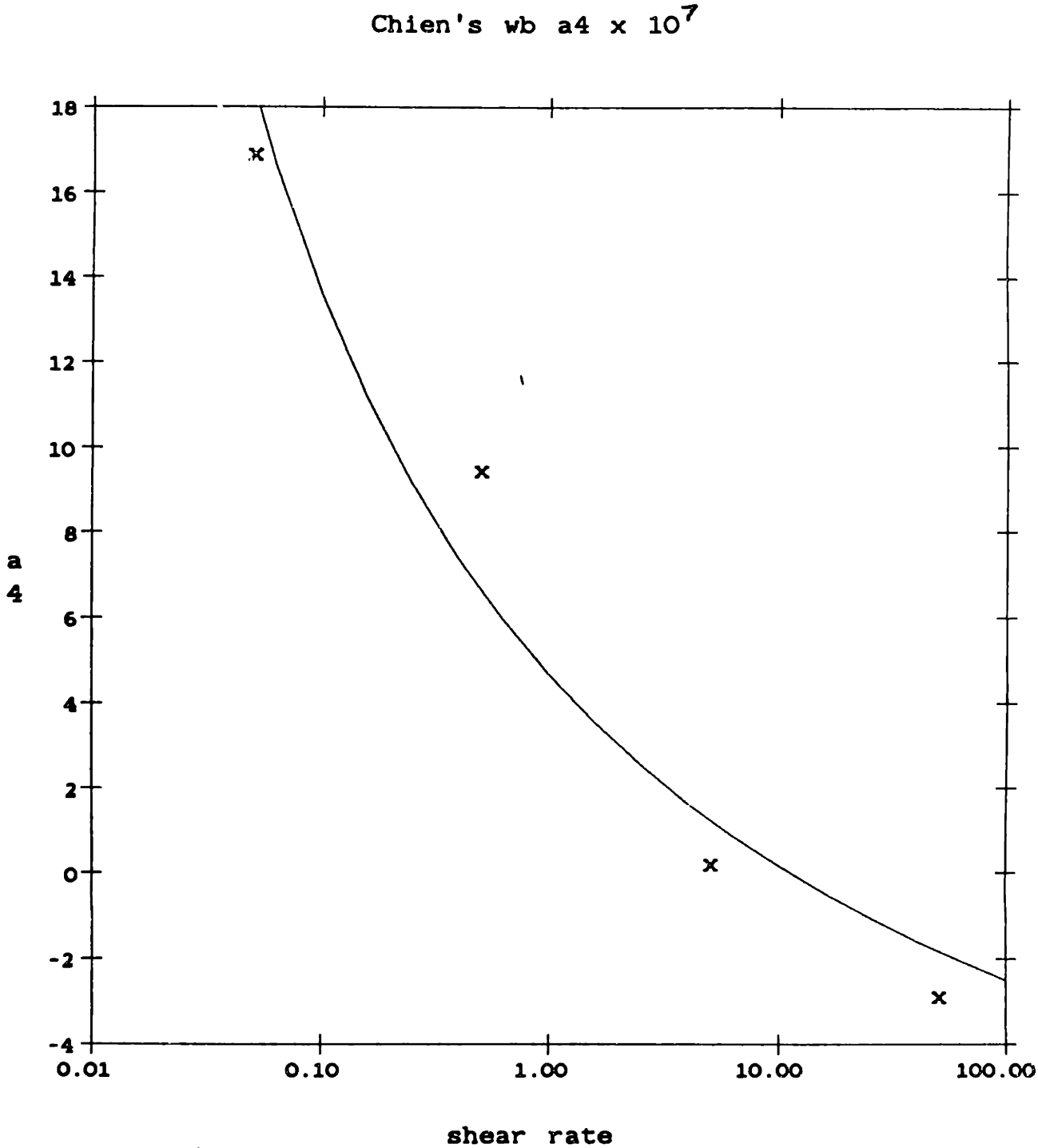

Figure 4-60(e): Plot for a_4 in plasma.

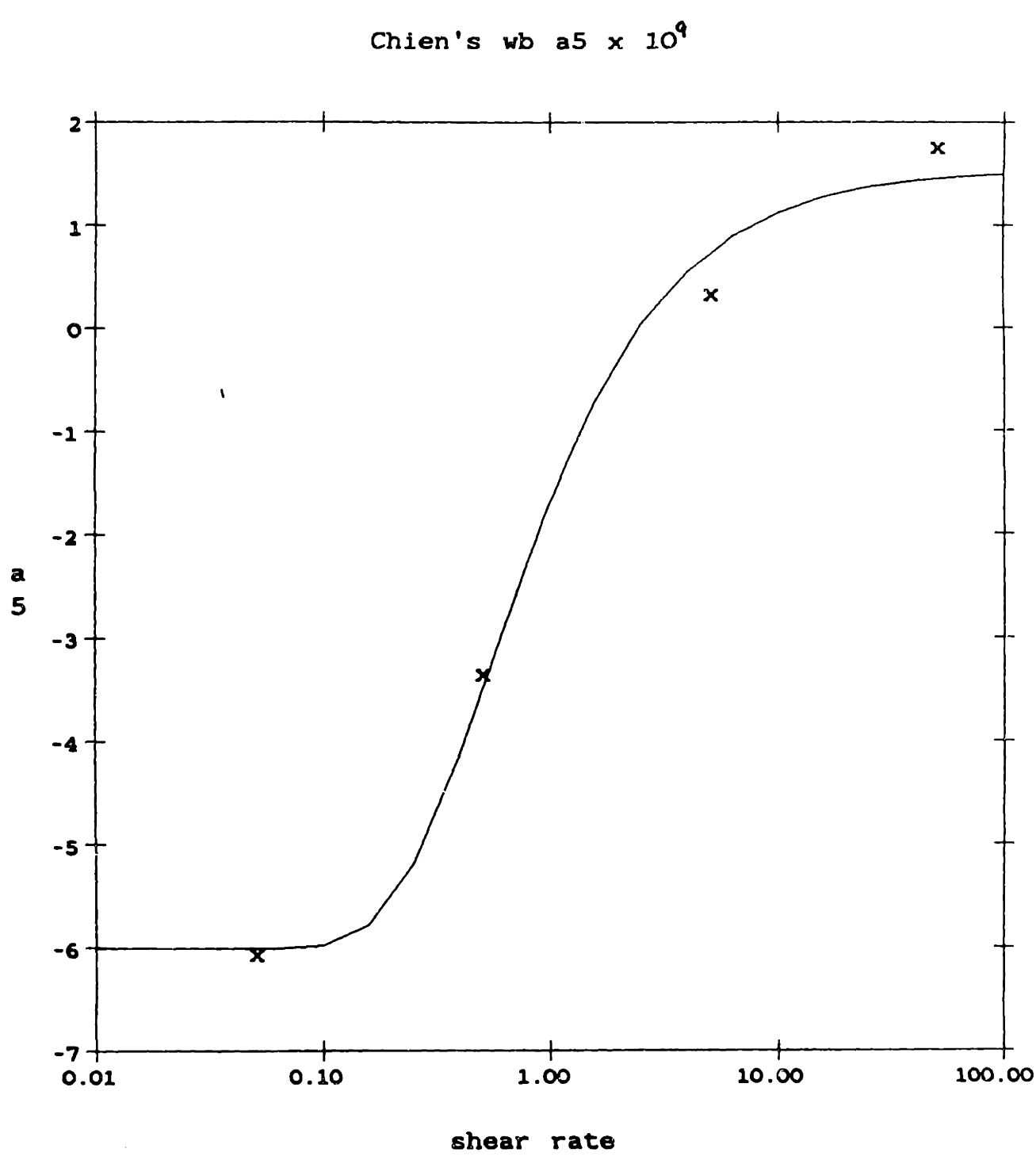

Figure 4-60(f): Plot for a_5 in plasma.

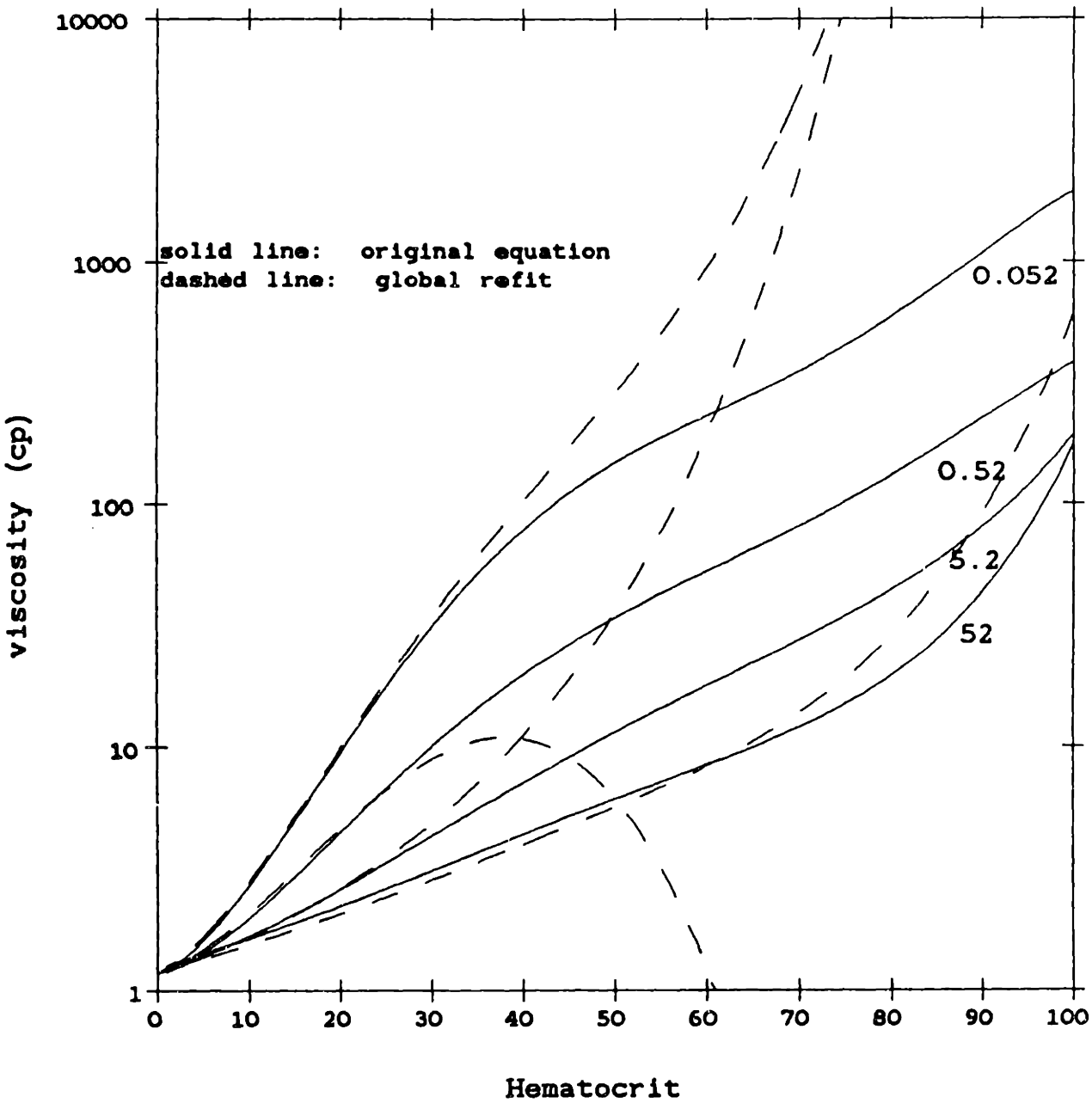

Figure 4-61: Plot of refit equations (4.3) to (4.8) for plasma suspensions. Numbers represent shear rates in sec^{-1}.

Chapter 5

DISCUSSION

5.1 Curve fits to data

The data from the previous chapter was fitted to the three-parameter Quemada expression, equation (2.11), using the method and computer program given in Section 3.4 and Appendix D. Equation (2.11) was rearranged to the following form for ease in calculation:

$$\eta_r = [1 - \frac{c}{2}(k_\infty + \frac{k_0 - k_\infty}{1+\sqrt{\gamma/\gamma_c}})]^{-2} \qquad (5.1)$$

This form of the equation minimizes the frequency of appearance of the shear rate term, whose fit, as will be seen, has the highest degree of uncertainty. It will be recalled that the term in parentheses is a general intrinsic viscosity $k(c,\gamma)$. The squared residuals were weighted by y_i^{-2}, where y_i is the predicted value of η_r from the equation, in order to assign equal relative weight to each point regardless of the magnitude of η_r. (When the term *relative weighting* is used henceforth, it will refer to a fit by this method. If there is additional weighting used, it will be so specified in each case.) In all cases the expression was able to provide a good representation of the data, and in almost every case the sum of squared weighted residuals using this equation was smaller than for any of several empirical equations attempted, the best of which were a fourth-order polynomial fit of $\ln(\eta)$ to $\ln(\gamma)$ and a fit of $\ln(\eta)$ to the form $b_1 + \frac{b_2}{\gamma^{b_3}}$ where b_1, b_2 and b_3 are constants.

The Quemada equation, when fitted to the low hematocrit plasma data from this work, often did not provide reasonable extrapolations to low shear rates where

data was unavailable. In order to provide a better behavior in the low hematocrit--low shear rate regime, the data points from the Chien *et al.*, [1966] equations were added to the plasma data where there was good agreement between the two sets. Therefore, for plasma suspension at H=50, 44, 34, 24, and 11 the fits are to this work plus the four points of Chien *et al.* at each hematocrit. In the case for Eagle's solution at H=7, the data was fit to a constant from which a value of k_∞ was calculated.

Statistical parameters for the goodness-of-fit of the equations are given in Table 5-I. The standard weighted error of regression is defined as $\sqrt{\frac{E}{N-P}}$, where E is the sum of squared weighted residuals as defined by equation (3.17), N is the number of data points and P is the number of parameters. It will be noted that the absolute magnitude of the correlation coefficients involving the critical shear rate are all very close to 1, suggesting a relative insensitivity of the fit to the value of γ_c. As will be recalled from the analytical discussion of the Quemada equation in Chapter 2, γ_c does not change the overall shape of the Quemada curve but instead acts as a scaling factor for the x-axis. Thus, for data that is relatively constant or that expresses asymptotic behavior at only one end, it will be more difficult to pinpoint the value of γ_c, as seen by the ρ_{23} values for plasma at low and high hematocrits (ρ_{13} values are practically constant for all cases because asymptotic approach to k_∞ is always seen). This uncertainty in γ_c will be expressed in relatively higher standard deviations for the value of its fit.

The high magnitudes of the correlation coefficients might also suggest an overspecification of the problem for any one curve. It is quite possible that a data at one hematocrit may be effectively represented by a two parameter equation, but three parameters are needed to model behavior over a large range of hematocrits.

The rheological parameters k_∞, k_0, and γ_c generated by the fits are given

Hematocrit	number of data points	std. wghtd. regress. err.	corr. coeff. 12	corr. coef. 13	corr. coeff. 23
98.4	60	7.651e-02	0.7437	-0.9413	-0.9225
97.2	55	3.342e-02	0.6890	-0.9251	-0.9075
96.8	60	2.879e-02	0.7147	-0.9379	-0.9069
96.0	170	1.013e-01	0.6957	-0.9301	-0.9065
95.0	129	4.210e-02	0.7297	-0.9573	-0.8901
94.0	112	3.153e-02	0.6876	-0.9382	-0.8893
93.0	181	2.096e-01	0.7366	-0.9544	-0.8986
92.0	161	1.757e-01	0.7166	-0.9506	-0.8905
91.0	122	4.011e-02	0.6809	-0.9410	-0.8776
90.0	118	1.212e-01	0.7102	-0.9610	-0.8678
89.0	54	3.829e-02	0.7056	-0.9721	-0.8443
87.0	120	7.184e-02	0.6203	-0.9541	-0.8067
86.0	57	5.163e-02	0.6543	-0.9385	-0.8587
82.0	47	5.303e-02	0.6715	-0.9692	-0.8235
72.0	46	5.949e-02	0.6517	-0.9658	-0.8091
70.0	107	1.789e-01	0.6385	-0.9513	-0.8261
68.0	48	9.703e-02	0.6850	-0.9142	-0.9127
62.0	53	1.638e-01	0.7176	-0.9397	-0.9046
59.0	57	3.020e-02	0.6533	-0.9307	-0.8642
56.0	54	2.435e-02	0.7450	-0.9321	-0.9233
48.0	46	4.270e-02	0.7650	-0.9269	-0.9406
42.0	30	1.689e-02	0.7872	-0.9131	-0.9644
25.0	32	6.469e-02	0.9061	-0.9740	-0.9745
7.0	14	4.355e-03			

Hematocrit	number of data points	std. wghtd. regress. err.	corr. coeff. 12	corr. coef. 13	corr. coeff. 23
98.1	65	2.584e-02	0.6980	-0.9283	-0.9085
97.6	63	6.425e-02	0.6985	-0.9423	-0.8919
97.3	59	4.792e-02	0.7018	-0.9659	-0.8550
97.0	60	1.471e-02	0.7015	-0.9463	-0.8859
96.0	122	9.660e-02	0.6694	-0.9489	-0.8604
95.0	63	2.514e-02	0.7077	-0.9673	-0.8541
94.0	62	2.112e-02	0.6850	-0.9572	-0.8545
93.0	62	2.943e-02	0.6732	-0.9492	-0.8590
92.0	122	3.445e-02	0.6610	-0.9590	-0.8322
91.0	124	8.631e-02	0.7064	-0.9699	-0.8479
90.0	62	3.614e-02	0.6788	-0.9642	-0.8361
89.0	124	1.004e-01	0.6931	-0.9694	-0.8378
86.0	65	3.351e-02	0.6708	-0.9573	-0.8418
83.0	65	3.515e-02	0.6661	-0.9638	-0.8251
82.0	68	3.697e-02	0.6518	-0.9631	-0.8161
78.0	64	5.593e-02	0.6997	-0.9781	-0.8225
75.0	59	2.728e-02	0.6263	-0.9662	-0.7844
66.0	65	5.593e-02	0.5921	-0.9614	-0.7654
59.0	54	5.786e-02	0.6677	-0.9543	-0.8420
50.0	59	1.437e-02	0.7276	-0.9382	-0.9028
44.0	45	1.193e-02	0.7828	-0.9162	-0.9608
34.0	44	4.518e-02	0.7449	-0.8327	-0.9880
24.0	31	6.291e-02	0.6682	-0.7513	-0.9886
11.0	31	3.329e-03	0.6812	-0.7019	-0.9982

Table 5-I: Standard weighted error of regression and correlation coefficients for Quemada fits to data.

Top, values for saline suspensions. *Bottom*, values for plasma suspensions.

For correlation coefficients: $1=k_\infty$, $2=k_0$, $3=\gamma_c$

Hematocrit	k-inf. A fit	st. dev. k-inf.	k-0 A fit	st. dev. k-0	gam.-crit. A fit	st. dev. gam. crit.
98.4	1.849	1.081e-02	2.039	2.085e-03	0.7572	1.873e-01
97.2	1.819	7.028e-03	2.063	1.582e-03	0.8711	1.123e-01
96.8	1.774	3.090e-03	2.069	6.329e-04	1.2130	5.526e-02
96.0	1.800	7.707e-03	2.087	1.346e-03	0.9387	1.064e-01
95.0	1.764	8.821e-03	2.100	8.093e-04	2.6770	2.519e-01
94.0	1.794	8.269e-03	2.126	1.321e-03	1.3300	1.337e-01
93.0	1.817	1.881e-02	2.146	2.033e-03	2.3230	4.980e-01
92.0	1.815	3.395e-02	2.171	4.001e-03	1.9850	7.161e-01
91.0	1.790	8.140e-03	2.184	1.148e-03	1.7760	1.442e-01
90.0	1.761	6.705e-02	2.206	5.263e-03	3.3170	1.715e+00
89.0	1.752	1.739e-02	2.231	7.749e-04	4.4220	4.876e-01
87.0	1.806	2.802e-02	2.268	1.940e-03	2.8530	5.700e-01
86.0	1.807	3.368e-02	2.289	4.791e-03	2.0640	5.662e-01
82.0	1.829	6.995e-02	2.412	3.550e-03	5.1660	1.898e+00
72.0	1.884	9.638e-02	2.709	5.382e-03	6.1900	2.276e+00
70.0	1.969	8.117e-02	2.802	8.218e-03	3.3140	1.146e+00
68.0	2.005	5.583e-02	2.874	2.499e-02	4.9410	1.767e+00
62.0	2.014	1.505e-01	3.155	4.397e-02	7.5150	4.714e+00
59.0	1.853	3.547e-02	2.983	7.337e-03	23.4500	3.234e+00
56.0	1.896	2.604e-02	3.004	9.297e-03	22.0800	2.836e+00
48.0	1.947	7.059e-02	3.476	3.734e-02	13.7800	4.065e+00
42.0	2.099	2.987e-02	3.730	5.228e-02	14.5500	2.937e+00
25.0	2.906	4.546e-01	3.787	4.281e-01	52.8800	2.248e+02
7.0	6.605	1.489e-01				

Hematocrit	k-inf. A fit	st. dev. k-inf.	k-0 A fit	st. dev. k-0	gam.-crit. A fit	st. dev. gam. crit.
98.1	1.728	3.730e-03	2.045	8.178e-04	0.91790	4.823e-02
97.6	1.711	9.668e-03	2.050	1.387e-03	1.48300	1.663e-01
97.3	1.700	8.846e-03	2.048	5.806e-04	2.56200	2.110e-01
97.0	1.698	3.011e-03	2.056	4.183e-04	1.59300	5.226e-02
96.0	1.724	1.395e-02	2.076	1.456e-03	1.80500	2.566e-01
95.0	1.678	1.495e-02	2.091	1.084e-03	3.26600	3.905e-01
94.0	1.651	7.985e-03	2.108	7.744e-04	2.55200	1.575e-01
93.0	1.699	1.909e-02	2.130	2.149e-03	2.33000	3.797e-01
92.0	1.684	1.435e-02	2.154	1.012e-03	2.21600	2.241e-01
91.0	1.649	4.420e-02	2.181	2.759e-03	3.11400	8.285e-01
90.0	1.682	3.542e-02	2.195	2.781e-03	3.29200	7.587e-01
89.0	1.630	5.729e-02	2.221	3.682e-03	3.88700	1.208e+00
86.0	1.674	2.977e-02	2.284	2.885e-03	3.75000	6.440e-01
83.0	1.696	4.127e-02	2.370	2.621e-03	3.57000	7.088e-01
82.0	1.625	5.459e-02	2.391	3.734e-03	4.38000	1.013e+00
78.0	1.722	8.138e-02	2.532	3.026e-03	5.30400	1.556e+00
75.0	1.688	3.757e-02	2.577	2.343e-03	6.30400	8.458e-01
66.0	1.653	1.266e-01	2.888	8.337e-03	6.99900	2.291e+00
59.0	1.695	1.245e-01	3.202	1.589e-02	6.80300	2.108e+00
50.0	2.018	1.275e-01	3.865	2.414e-02	2.07700	6.568e-01
44.0	2.181	7.282e-02	4.484	2.987e-02	0.95380	1.924e-01
34.0	2.219	7.624e-02	6.092	1.265e-01	0.30890	8.253e-02
24.0	2.150	9.283e-02	7.913	2.719e-01	0.23780	7.731e-02
11.0	2.023	1.434e-01	17.410	1.087e+01	0.01124	2.345e-02

Table 5-II: Quemada parameters for data of present study.

Top, values for saline suspensions. *Bottom*, values for plasma suspensions.

along with their standard deviations in Table 5-II for Eagle's solution and plasma suspensions. The curves generated by these parameters are plotted as solid lines designated as "Fit A" in the results graphs of Chapter 4. The hematocrit dependence of the parameters, to be discussed in the sections to follow, are used to generate the dashed lines designated as "Fit B" in Chapter 4. For comparison, fits were also made of the Quemada equation to the polynomials of Chien *et al.* for both saline and plasma at intervals of five hematocrit units. The values obtained from these fits are shown in Table 5-III.

As discussed in Chapter 2, the potential for singular points of infinite viscosity exists as the cell volume fraction approaches unity, dependent on the magnitude of $\frac{c}{2} \cdot k_0$. Some of the fits obtained had singular shear rates, and these are documented in Table 5-IV, although in all of these cases they occur well out of the limits of the data.

The standard deviations in Tables 5-II and 5-III are notable in that those for the critical shear rate are large relative to the value itself. At low hematocrits, the standard deviation may be several times the parameter value for γ_c and it is also larger for k_0. These observations underscore the fact that data at very low shear rates is needed to accurately fit these two constants.

5.2 Dependence of k_∞ on hematocrit and plasma proteins

The A fit values for k_∞ range from 1.752 to 6.605 for saline and 1.625 to 2.219 for plasma. On the whole, these values are compatible with the values around 1.8 fit by Quemada to other data (see Table 2-II, page 42), but lower because the data from this work extended to higher shear rates. The saline values for the A fit are plotted versus hematocrit along with the values obtained from the Ringer solution Chien polynomials in Figure 5-1. Since the data of Chien *et al.* does not

Hematocrit	k-infinity	st. dev. k-infinity	k-0	st. dev. k-0	gamma. crit.	st. dev. gamma. crit.
100	1.829	3.85e-03	2.005	2.74e-03	0.763400	1.37e-01
95	1.834	3.38e-03	2.112	1.84e-03	1.049000	9.23e-02
90	1.836	1.33e-02	2.227	6.17e-03	1.321000	3.05e-01
85	1.847	2.50e-02	2.348	1.07e-02	1.534000	5.01e-01
80	1.872	3.77e-02	2.474	1.62e-02	1.672000	6.83e-01
75	1.915	5.15e-02	2.604	2.34e-02	1.742000	8.68e-01
70	1.975	6.72e-02	2.736	3.34e-02	1.770000	1.08e+00
65	2.098	8.61e-02	2.865	4.75e-02	1.779000	1.35e+00
60	2.131	1.09e-01	2.985	6.74e-02	1.785000	1.72e+00
55	2.219	1.38e-01	3.091	9.48e-02	1.786000	2.23e+00
50	2.313	1.71e-01	3.175	1.31e-01	1.745000	2.87e+00
45	2.413	2.02e-01	3.234	1.80e-01	1.545000	3.40e+00
40	2.525	2.11e-01	3.280	2.57e-01	0.972800	2.90e+00
35	2.653	1.69e-01	3.389	5.33e-01	0.219800	9.26e-01
30	2.750	1.10e-01	5.054	1.82e+01	0.002042	4.21e-02
25	2.876	7.05e-02				
20	2.867	6.61e-02				
15	2.884	9.72e-02				
10	2.963	1.71e-01				
5	3.162	2.90e-01				

Hematocrit	k-infinity	st. dev. k-infinity	k-0	st. dev. k-0	gamma. crit.	st. dev. gamma. crit.
100	1.822	8.00e-03	2.054	4.00e-02	0.079000	6.70e-02
95	1.818	1.00e-03	2.110	1.00e-03	0.656100	2.44e-02
90	1.794	1.60e-02	2.210	7.00e-03	1.725000	4.36e-01
85	1.764	3.70e-02	2.328	1.00e-02	2.897000	1.05e+00
80	1.741	5.80e-02	2.463	1.40e-02	3.745000	1.59e+00
75	1.735	7.70e-02	2.618	1.80e-02	4.086000	1.85e+00
70	1.747	9.00e-02	2.798	2.00e-02	3.993000	1.76e+00
65	1.775	9.30e-02	3.009	2.30e-02	3.647000	1.46e+00
60	1.813	8.70e-02	3.257	2.30e-02	3.203000	1.05e+00
55	1.856	7.10e-02	3.551	2.10e-02	2.746000	6.53e-01
50	1.898	4.60e-02	3.902	1.50e-02	2.307000	3.12e-01
45	1.938	1.10e-02	4.324	4.00e-03	1.891000	5.70e-02
40	1.974	3.00e-02	4.835	1.40e-02	1.494000	1.06e-01
35	2.010	7.50e-02	5.458	4.50e-02	1.122000	1.85e-01
30	2.052	1.21e-01	6.222	9.78e-02	0.790000	1.99e-01
25	2.111	1.63e-01	7.156	1.94e-01	0.508900	1.73e-01
20	2.205	1.99e-01	8.286	3.89e-01	0.289600	1.30e-01
15	2.365	2.28e-01	9.676	8.81e-01	0.013150	8.47e-02
10	2.645	2.51e-01	12.304	3.64e+00	0.028990	3.92e-02
5	2.982	4.89e-01	31.373	3.01e+02	0.000528	1.39e-02

Table 5-III: Quemada parameters for data of Chien *et al.*, [1966].

Top, values for saline suspensions. *Bottom*, values for plasma suspensions.

Fit	Suspension	H	$\gamma(sec^{-1})$
A	saline	98.4	1.25×10^{-3}
A	saline	97.2	5.70×10^{-4}
A	saline	96.8	9.75×10^{-5}
A	saline	96	1.67×10^{-4}
A	plasma	98.1	3.73×10^{-4}
A	plasma	97.6	8.71×10^{-6}
B	saline	98.4	2.68×10^{-3}
B	saline	97.2	5.17×10^{-4}
B	saline	96.8	2.33×10^{-4}
B	saline	96	7.88×10^{-6}

Table 5-IV: Singular shear rates of curve fits.

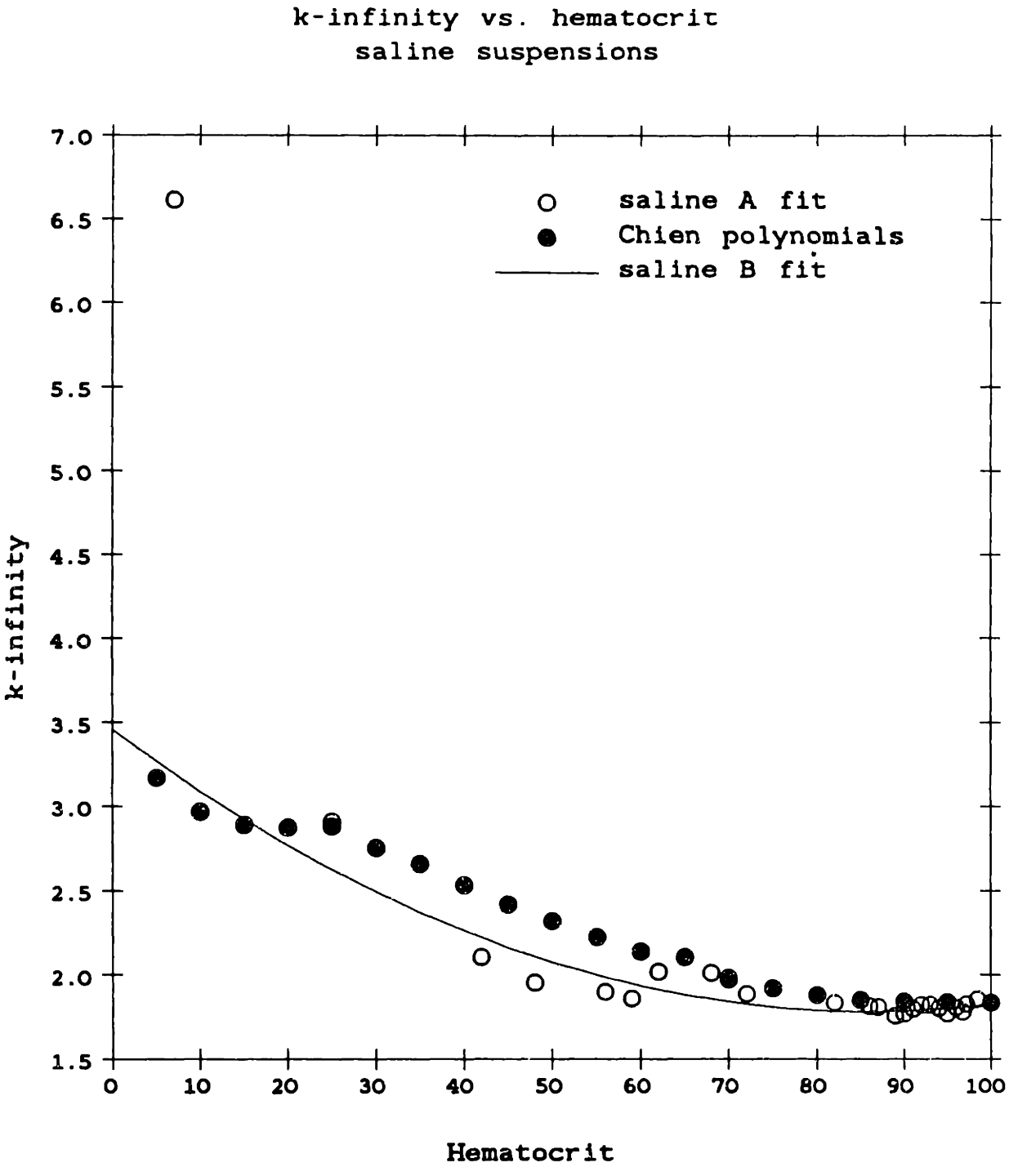

Figure 5-1: Plot of k_∞ versus hematocrit for saline suspensions.

extend to high shear rates, it is to be expected that the derived k_∞ values from that work will be of higher magnitude than those from the A fit. Similar behavior is shown by the k_∞ values for plasma suspensions in Figure 5-2.

The B fits in Figures 5-1 and 5-2 represent fits of the open symbols to function of cell concentration. For both saline and plasma suspensions the fits are to second-order polynomials:

$$k_\infty = \sum_{i=1}^{3} k_{\infty i} \cdot c^{(i-1)} \tag{5.2}$$

where $k_{\infty i}$ are constants and c is the volume concentration of cells. The values for the best fits of equation (5.2) and their standard deviations are, for saline,

$$k_{\infty 1} = 3.458 \pm 0.251$$
$$k_{\infty 2} = -3.894 \pm 0.730$$
$$k_{\infty 3} = 2.260 \pm 0.500$$

and for plasma,

$$k_{\infty 1} = 2.688 \pm 0.117$$
$$k_{\infty 2} = -2.300 \pm 0.433$$
$$k_{\infty 3} = 1.314 \pm 0.353.$$

Both fits were relatively weighted, and the values at hematocrits of 95 and above were triple weighted to provide better correlation at high hematocrit. For the same reason, the saline k_∞ value at H=7 was not included in the fit. The importance of accuracy at high hematocrit is seen by the sensitivity of the asymptotic relative viscosity at high shear rates, where $k=k_\infty$. The sensitivity is much greater at higher cell volume fractions because the magnitude of k_∞ does not change a great deal with H. For example, at c=0.95, $k_\infty \approx 1.7$, and $\frac{\partial \eta_r}{\partial k} = \frac{c}{(1-k \cdot c/2)^3} = 133$. At c=0.45, $k_\infty \approx 2.0$, and $\frac{\partial \eta_r}{\partial k} = 2.7$.

The saline and plasma fits are plotted together on Figure 5-3. Plasma values are consistently lower than those for saline. This is not due to cell-protein

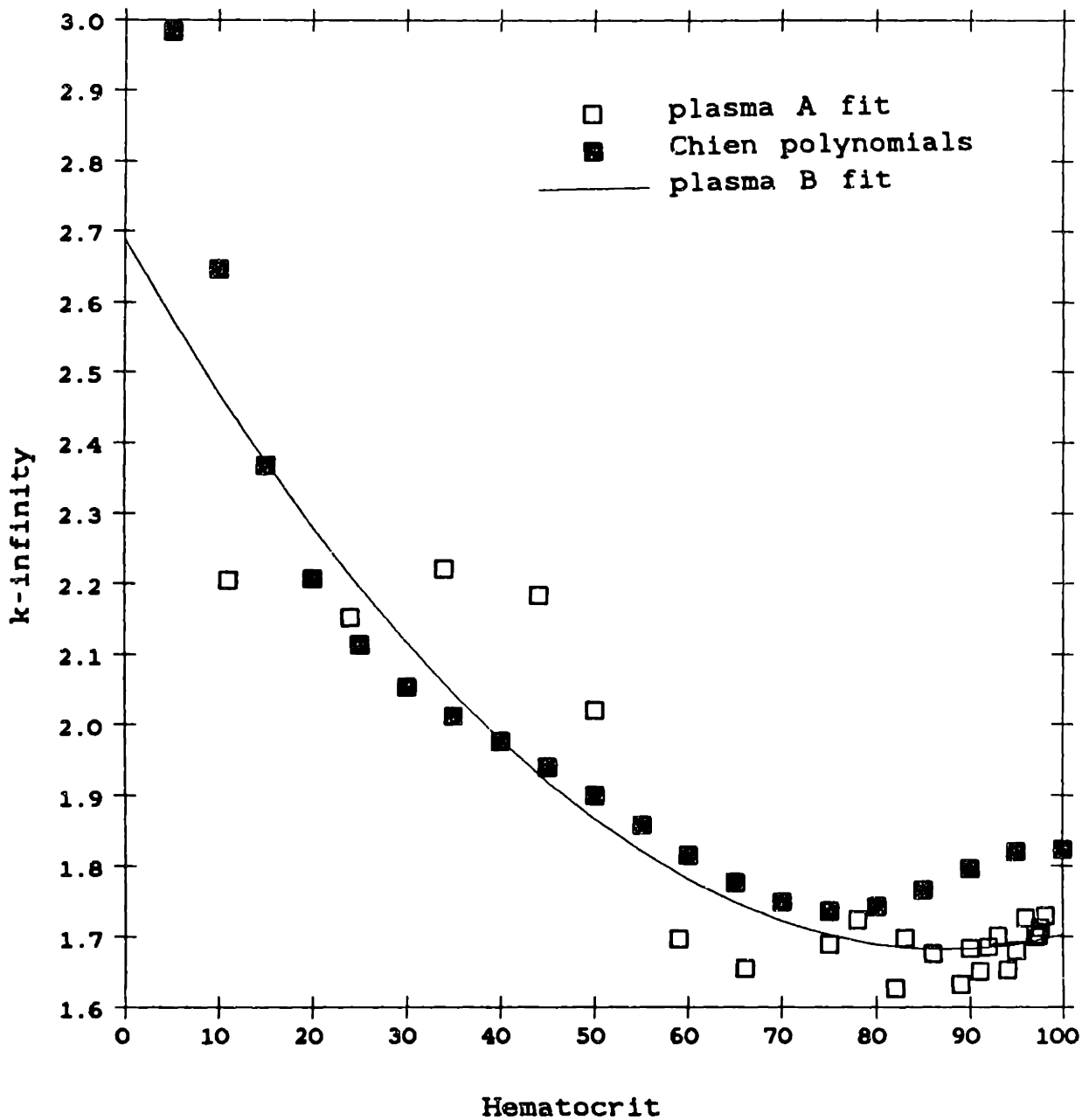

Figure 5-2: Plot of k_∞ versus hematocrit for plasma suspensions.

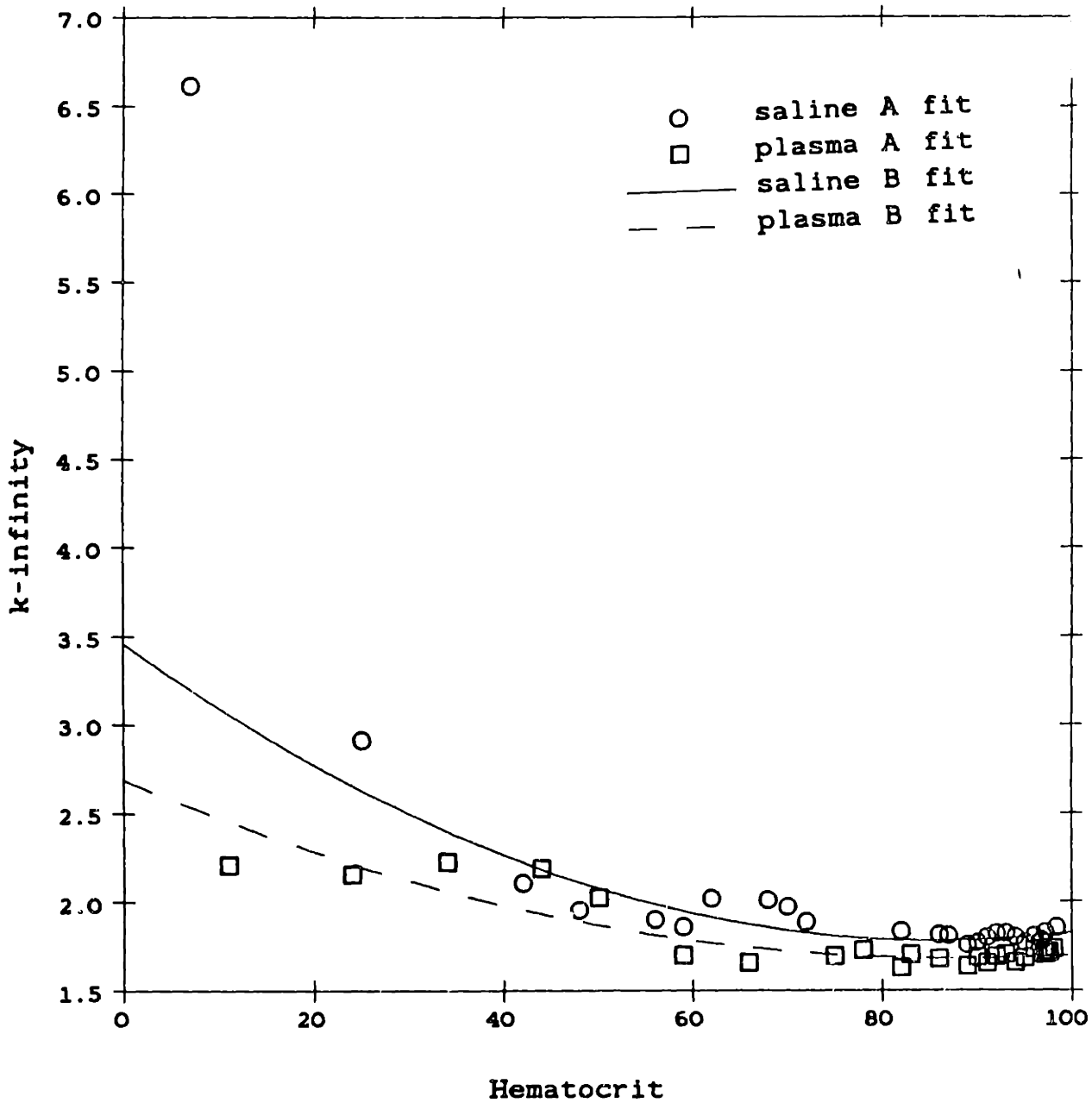

Figure 5-3: Comparison of k_∞ values for saline and plasma suspensions.

interactions, because at high shear rates aggregation effects are not important, but results directly from the differences in η_f and the emulsive properties of the erythrocytes. For rigid particles, k_∞ is independent of η_f; but for emulsions, the intrinsic viscosity will clearly have a functional dependence on the internal viscosity, and if η_i is lowered in more viscous media, then k_∞ will also be lowered. Quemada [1978b] obtained no difference in k_∞ from data [Chien, 1970] for erythrocytes in plasma and Ringer's albumin solution (see Figure 2-3 and Table 2-II), but these solutions all had the same η_f, which is not the case here.

As noted in Chapter 4, as $c \rightarrow 1$, the absolute viscosities of plasma and saline solutions become equal, and, barring the apparently negligible differences in cell properties from saline washing, the definition of the relative viscosity leads to contrived distinctions. These distinctions are manifested in the difference in k_∞ values at high hematocrits, as they are in the values for k_0 at high hematocrits. Thus $k_{\infty,\,saline}$ and $k_{\infty,\,plasma}$ can be related as a function of η_f. Since $\eta_{saline}=\eta_{plasma}$ at high H:

$$\frac{\eta_{f,\,plasma}}{\eta_{f,\,saline}} = \frac{(1-\frac{c}{2}k_{\infty,\,plasma})^2}{(1-\frac{c}{2}k_{\infty,\,saline})^2} \tag{5.3}$$

This reduces to

$$k_{\infty,\,plasma} = k_{\infty,\,saline}\cdot(\frac{\eta_{f,\,plasma}}{\eta_{f,\,saline}})^{0.5} - \frac{2}{c}\cdot((\frac{\eta_{f,\,plasma}}{\eta_{f,\,saline}})^{0.5} - 1) \tag{5.4}$$

The values at high hematocrit comply with this relationship.

Quemada [1981], in fitting the plasma data of Chien *et al.* [1966], noted that k_∞ reached a minimum at about H=75 and proposed that this represented the point of inversion of the emulsion, where the erythrocytes begin to behave physically as a continuous phase. Using the first-order approximation that the intrinsic viscosity scales as effective particle volume (see Appendix C), a physical

picture may be constructed in which the effective particle volume at low concentration and high shear rate is the hydrodynamic volume of a single red cell. The effective volume is reduced by crowding as hematocrit increases, and eventually a point is reached where the effective particle is no longer a single cell, but a volume of sterically interacting cells. At this point inversion takes place. With further crowding, the volume of this effective particle no longer changes, but the number of cells it contains increases, leading to increases in intrinsic viscosity. There is not clear-cut evidence of a minimum k_∞ in the results (Fit A) of this work, but there is a trend at hematocrits above 90 of k_∞ increasing with H. The polynomial curve fits to the data (Fit B) reach minimums at about H=86-87.

The Quemada equation demonstrates a better approach to an asymptotic value at high shear rate than any of the empirical fits attempted, but the curves continue to descend after 300 sec^{-1}. Comparison of data values at 300 sec^{-1} versus the limiting high shear rate asymptote for the Quemada equation, $(1-\frac{c}{2}\cdot k_\infty)^{-2}$, are shown in Table 5-V for both the A and B fits. The average difference between data and equation values is on the order of 15-20%, although in some cases can be greater than 40%. These results are shown graphically in Figures 5-4 and 5-5. From these figures it can be seen that the difference between the Chien *et al.* values at 52 sec^{-1} and the data at 300 sec^{-1} is large enough to bring into question any use of the Chien values as the limiting viscosity. For saline, ratio of the Chien value to the data at 300 sec^{-1} is about 1.1 to 1.2 over most of the hematocrits. For plasma, the ratio is greater than 2 for the most concentrated suspensions and about 1.1 at physiologic hematocrit.

Hematocrit	Rel. viscosity at 300 1/sec	A fit asymptote	% change from data	B fit asymptote	% change from data
98.4	151.3	122.7	-18.9	87.0	-42.5
97.2	86.7	74.4	-14.2	68.1	-21.5
96.8	59.3	50.0	-15.6	63.2	6.6
96.0	57.3	54.1	-5.6	55.1	-3.9
95.0	47.6	38.1	-20.0	47.1	-1.2
94.0	47.1	40.7	-13.7	40.8	-13.4
93.0	47.2	41.6	-11.9	35.8	-24.1
92.0	43.6	36.7	-15.9	31.8	-27.1
91.0	33.4	29.0	-13.0	28.5	-14.7
90.0	27.5	23.2	-15.6	25.7	-6.5
89.0	25.8	20.6	-20.2	23.4	-9.4
87.0	25.3	21.8	-14.0	19.7	-22.2
86.0	22.3	20.1	-9.8	18.2	-18.3
82.0	19.8	16.0	-19.3	13.9	-29.9
72.0	12.1	9.7	-20.2	8.5	-29.6
70.0	11.2	10.3	-7.6	7.9	-29.6
68.0	12.1	9.9	-18.4	7.3	-39.4
62.0	9.8	7.1	-27.7	6.0	-38.4
59.0	7.1	4.9	-31.5	5.5	-22.2
56.0	6.4	4.5	-29.0	5.1	-20.7
48.0	4.6	3.5	-23.4	4.1	-10.8
42.0	4.1	3.2	-22.0	3.5	-14.3
25.0	2.8	2.5	-11.9	2.2	-20.9
7.0	1.7	1.7	-0.5	1.3	-25.4

Hematocrit	Rel. viscosity at 300 1/sec	A fit asymptote	% change from data	B fit asymptote	% change from data
98.1	49.8	43.0	-13.6	35.4	-28.8
97.6	44.6	36.7	-17.7	33.5	-25.0
97.3	41.8	33.4	-20.0	32.3	-22.6
97.0	36.8	32.1	-12.7	31.3	-14.9
96.0	39.6	33.6	-15.1	28.2	-28.8
95.0	29.5	24.3	-17.7	25.6	-13.3
94.0	23.2	19.9	-14.1	23.3	0.5
93.0	26.5	22.7	-14.4	21.4	-19.3
92.0	21.3	19.7	-7.6	19.7	-7.5
91.0	18.2	16.0	-11.9	18.2	0.2
90.0	20.0	16.9	-15.4	16.9	-15.3
89.0	15.9	13.3	-16.6	15.8	-0.6
86.0	15.3	12.7	-16.7	13.1	-14.7
83.0	13.6	11.4	-16.2	11.0	-18.9
82.0	11.1	9.0	-19.1	10.5	-5.6
78.0	11.5	9.3	-19.4	8.7	-24.6
75.0	9.5	7.4	-21.8	7.6	-19.5
66.0	6.2	4.8	-21.9	5.5	-10.7
59.0	5.1	4.0	-21.6	4.5	-12.1
50.0	4.2	4.1	-3.0	3.5	-16.3
44.0	3.7	3.7	-0.1	3.0	-18.3
34.0	2.7	2.6	-4.5	2.4	-12.4
24.0	2.0	1.8	-9.2	1.9	-7.3
11.0	1.3	1.3	-2.6	1.3	2.8

Table 5-V: High shear rate asymptotes.

Top, saline suspensions. *Bottom*, plasma suspensions.

Average change from data for saline=$-16.7\%\pm7.3$ (A fit)

$=-20.0\%\pm12.2$ (B fit)

Average change from data for plasma=$-13.9\%\pm6.3$ (A fit)

$=-13.9\%\pm9.1$ (B fit)

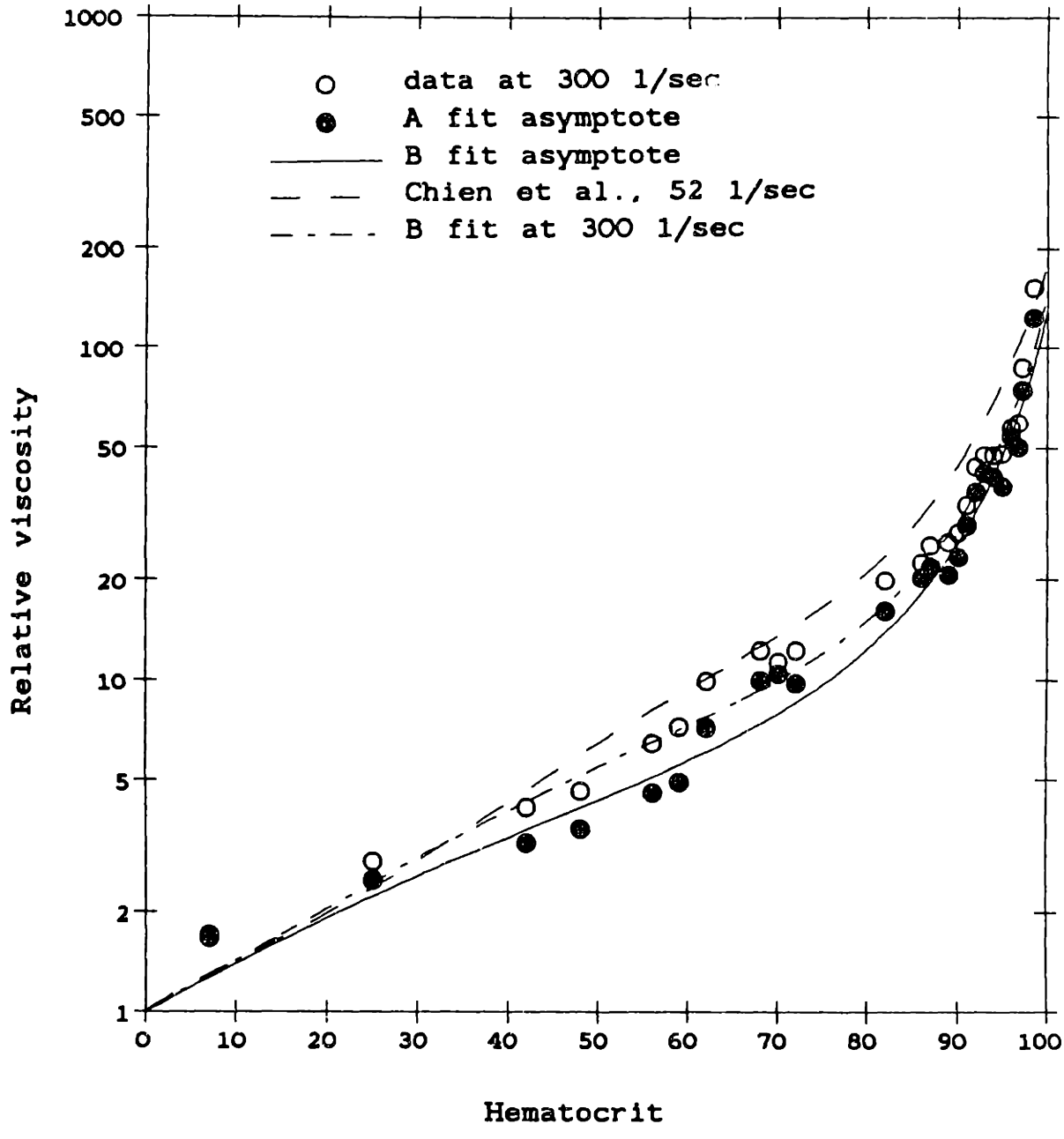

Figure 5-4: High shear rate asymptotes for saline fits.

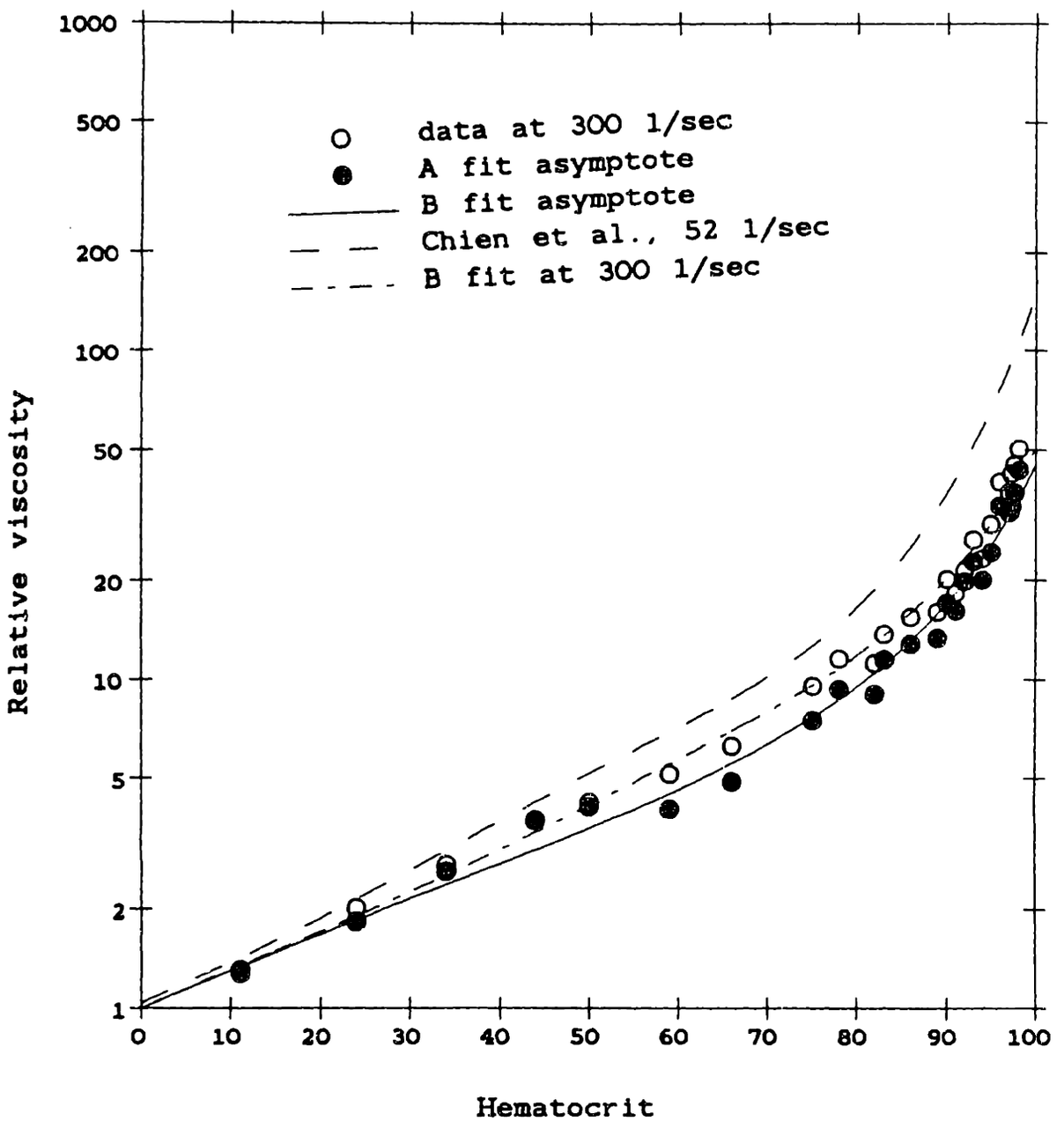

Figure 5-5: High shear rate asymptotes for plasma fits.

5.3 Dependence of k_0 on hematocrit and plasma proteins

The values for k_0 of 4.48 in plasma at H=44, 2.22 in plasma at H=89, and 3.48 in saline at H=48 were comparable to values previously fit by Quemada (see Table 2-II. The A fit values for k_0 are plotted versus hematocrit in Figure 5-6 for saline and in Figure 5-7 for plasma. Again, included in both plots are values from fits of the Quemada equation to the Chien polynomials. There is very close agreement between the A fit k_0 and the Chien k_0, particularly at high hematocrits, and this follows from the comparable viscosity values obtained at low shear rate and high hematocrits.

The B fits in Figure 5-6 represents a relatively weighted fit of the open symbol to a third-order polynomial, to which an exponential term has been added for plasma:

$$k_0 = \sum_{i=1}^{4} k_{0i} \cdot c^{(i-1)} + k_{05} \cdot exp(k_{06} \cdot c) \qquad (5.5)$$

The best-fit values and standard deviations for saline are

$k_{01} = 3.503 \pm 0.413$
$k_{02} = 3.467 \pm 2.140$
$k_{03} = -9.976 \pm 3.470$
$k_{04} = 5.026 \pm 2.841.$
$k_{05} = 0$
$k_{06} = 0.$

At $c<20$, the data is fit to a constant $k_0=3.838$. The polynomial reaches a maximum at about c=0.2, and there is no physical reason to expect k_0 to do this. It seems physically reasonable to expect k_0 to approach a constant at low hematocrits in saline, as will be explained shortly. Attempts were made to fit to equations which level off to a constant as c approaches zero, such as equations of the form k_{01} tanh $(k_{02}c+k_{03})$, but these did not prove satisfactory.

For the plasma fit, the exponential term is required to model the dependence

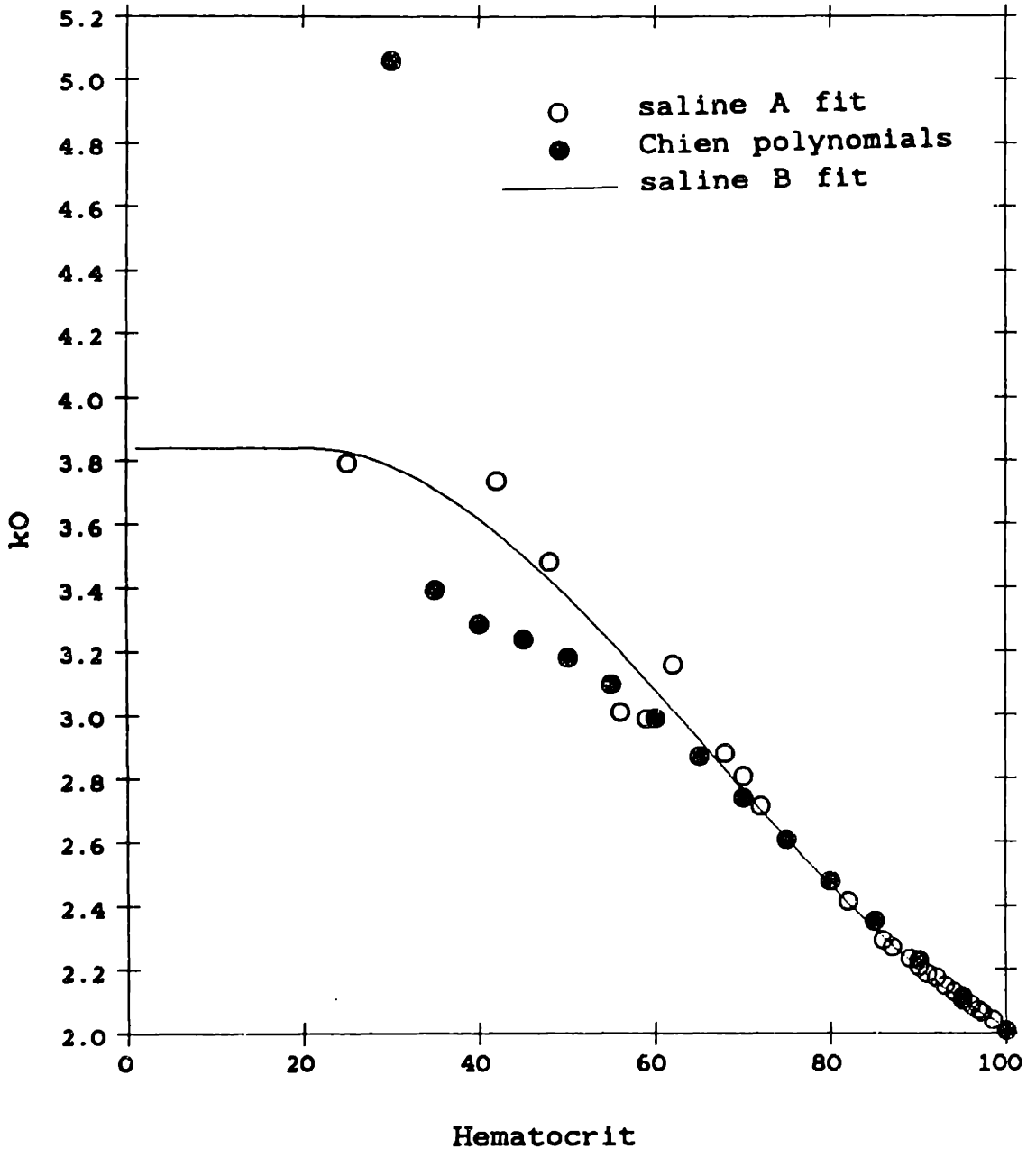

Figure 5-6: Plot of k_0 versus hematocrit for saline suspensions.

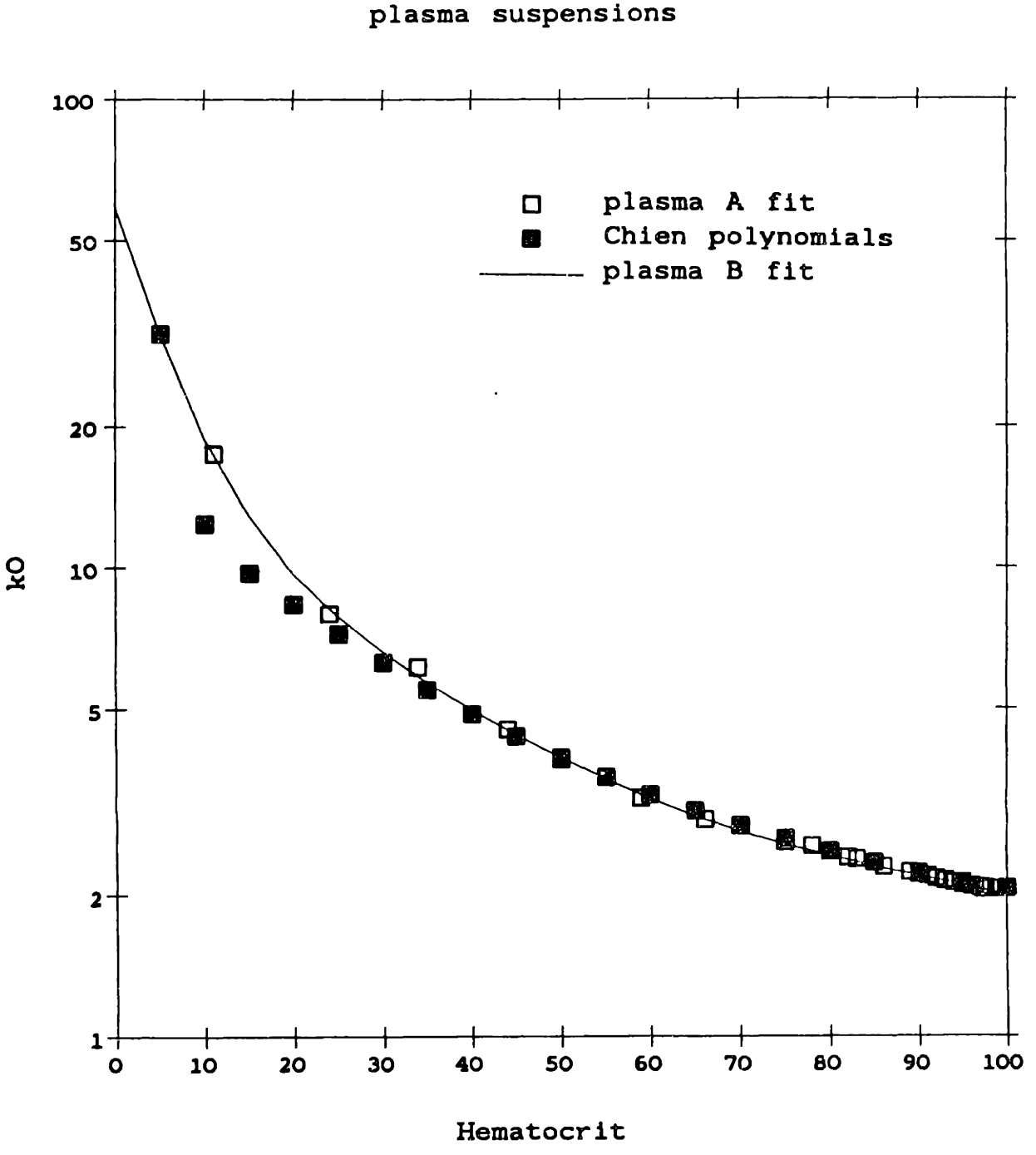

Figure 5-7: Plot of k_0 versus hematocrit for plasma suspensions.

at low hematocrits. The best-fit values for plasma are

$k_{01} = 13.28 \pm 0.60$
$k_{02} = -31.93 \pm 2.67$
$k_{03} = 32.13 \pm 3.74$
$k_{04} = -11.49 \pm 0.02$
$k_{05} = 45.46 \pm 1.06$
$k_{06} = -16.78 \pm 0.65.$

The plasma B fit is a relatively weigted fit to the open squares in Figure 5-7 plus the single filled square at H=5. The Chien polynomial value was included because these values closely followed the data at low hematocrit and because this is a critical region for fitting the exponential term. Values at hematocrits of 90 and above were additionally weighted by a factor of 10 to insure agreement at high H. This additional weighting is needed to avoid the appearance of singular points, where $\frac{c}{2}k_0 > 1$, in the B fits.

The sensitivity of the asymptotic zero-shear-rate viscosity to the value of k_0 is an expression for $\frac{\partial \eta_r}{\partial k}$ equivalent to that shown for k_∞ in the last section, with k now equal to k_0. For saline suspensions, this sensitivity is highest at high hematocrits. For plasma suspensions, the sensitivity is highest at low hematocrits because of the large values for k_0 at low hematocrits. For example, for both suspensions, at c=0.95, $k_0 \approx 2$ and $\frac{\partial \eta_r}{\partial k} = 760$. For saline at c=0.45, $k_0 \approx 3.2$ and $\frac{\partial \eta_r}{\partial k} = 20.5$. For plasma at c=0.45, $k_0 \approx 4.4$ and $\frac{\partial \eta_r}{\partial k} = 450{,}000$. Insurance must also be taken to avoid singular points in the refit Quemada equation where $\frac{c}{2}k_0 - 1 > 0$.

Saline and plasma values are plotted together on Figure 5-8. The values are almost identical at high hematocrits, down to about H=65. With further decrease in hematocrit, the saline values appear to level off, while the plasma values show a large increase. At zero shear rate, the emulsive and shear deformation effects are

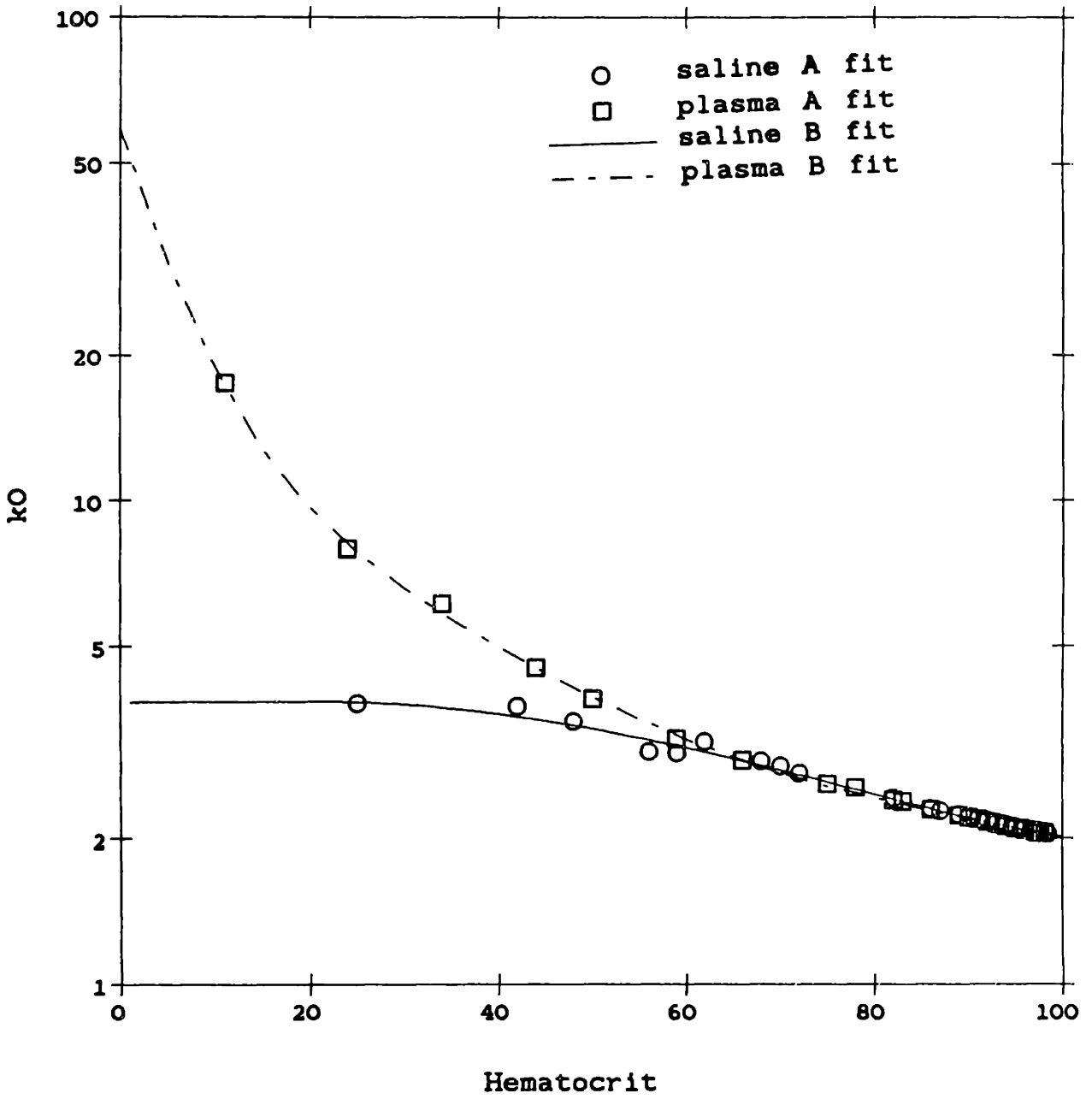

Figure 5-8: Comparison of k_0 values for saline and plasma suspensions.

minimized, and thus k_0 should principally be an indicator of cell-cell interactions, either protein-mediated (aggregation) or steric (crowding). At low hematocrits, crowding is not seen, and the difference between saline and plasma k_0 is caused by rouleaux formation. Where plasma and saline values are equal, at high hematocrits, should be where crowding effects predominate over aggregation. An analysis by Chien *et al.* [1966] suggested that at a hematocrit of 60, crowding interactions begin to influency viscosity relative to aggregation and that at H=80, they begin to be the dominant influence. This is also probably related to the inversion phenomenon. The merging of the B fit lines in Figure 5-8 around H=65 would seem to lend some credence to this hypothesis.

At low shear rate, and at hematocrits low enough so that crowding is not a factor, normal cells in saline solution should approximate the behavior of hardened cells in saline. The maximum packing concentration c_p for hardened erythrocytes in saline has been determined experimentally to be about 0.6 [Chien *et al.*, 1971]. Using the relationship derived in Appendix C for rigid particles, $k_0=2/c_p=3.33$, which compares reasonably well with the asymptotic value of 3.838 from the B fit.

The A and B fit values for viscosity at zero shear rate are plotted in Figures 5-9 and 5-10 for saline and plasma suspensions, respectively. Unlike for high shear rates, a smooth limiting envelope can not be generated from the k_0 values. The $\gamma=0$ curve for saline is not well-behaved at high hematocrits, and the $\gamma=0$ curve for plasma is obviously meaningless. The message behind these figures is that, except for low hematocrit saline suspensions, the Quemada equation is extremely sensitive to k_0 in the limit of low shear rate. If one wishes to use the Quemada equation at low shear rates, k_0 values must be derived from fits to data that clearly reach an asymptote at low γ. Values for k_0 which have been extrapolated from data at higher shear rates, such as those in this work, will do a satisfactory job of

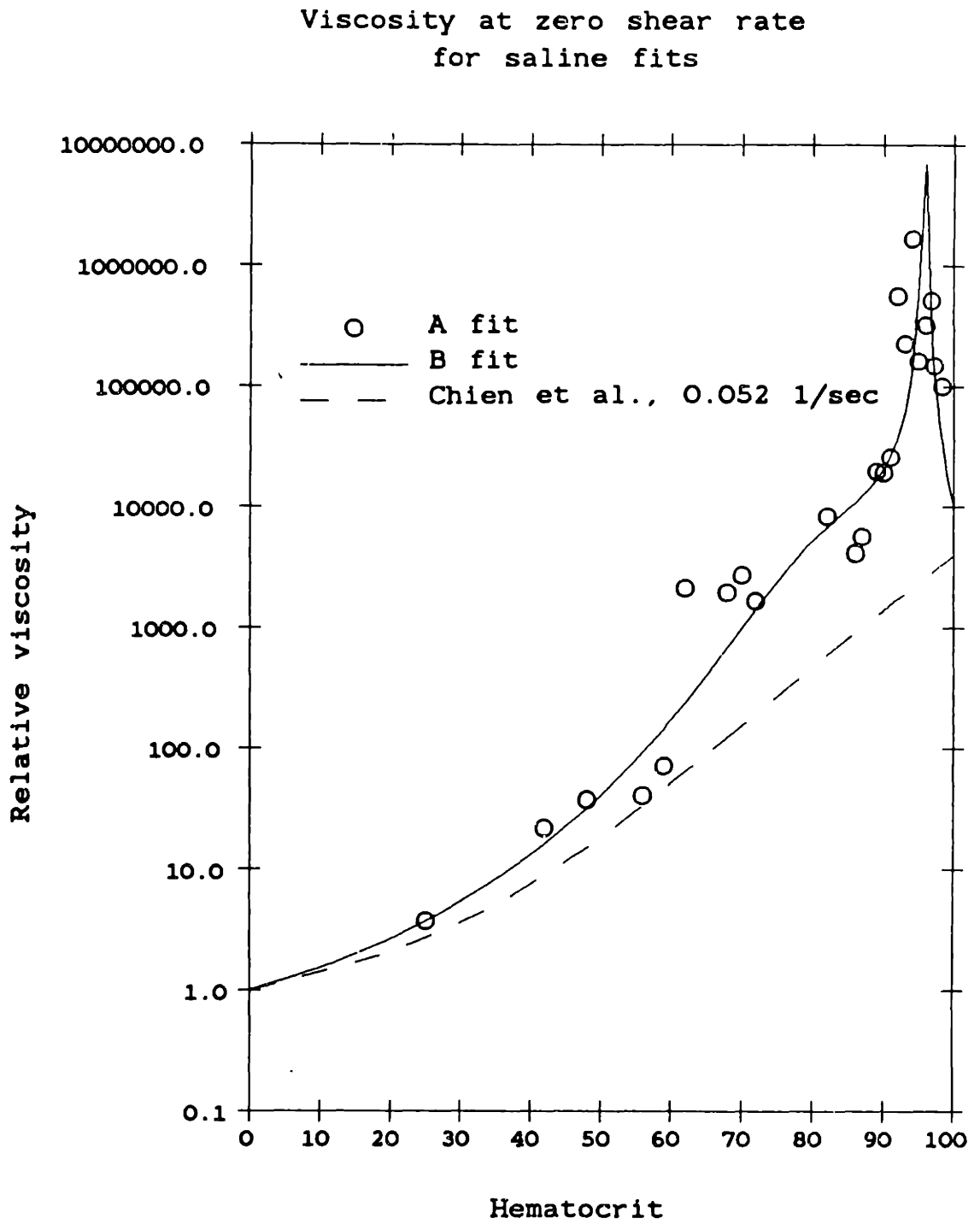

Figure 5-9: Zero shear rate asymptotes for saline fits.

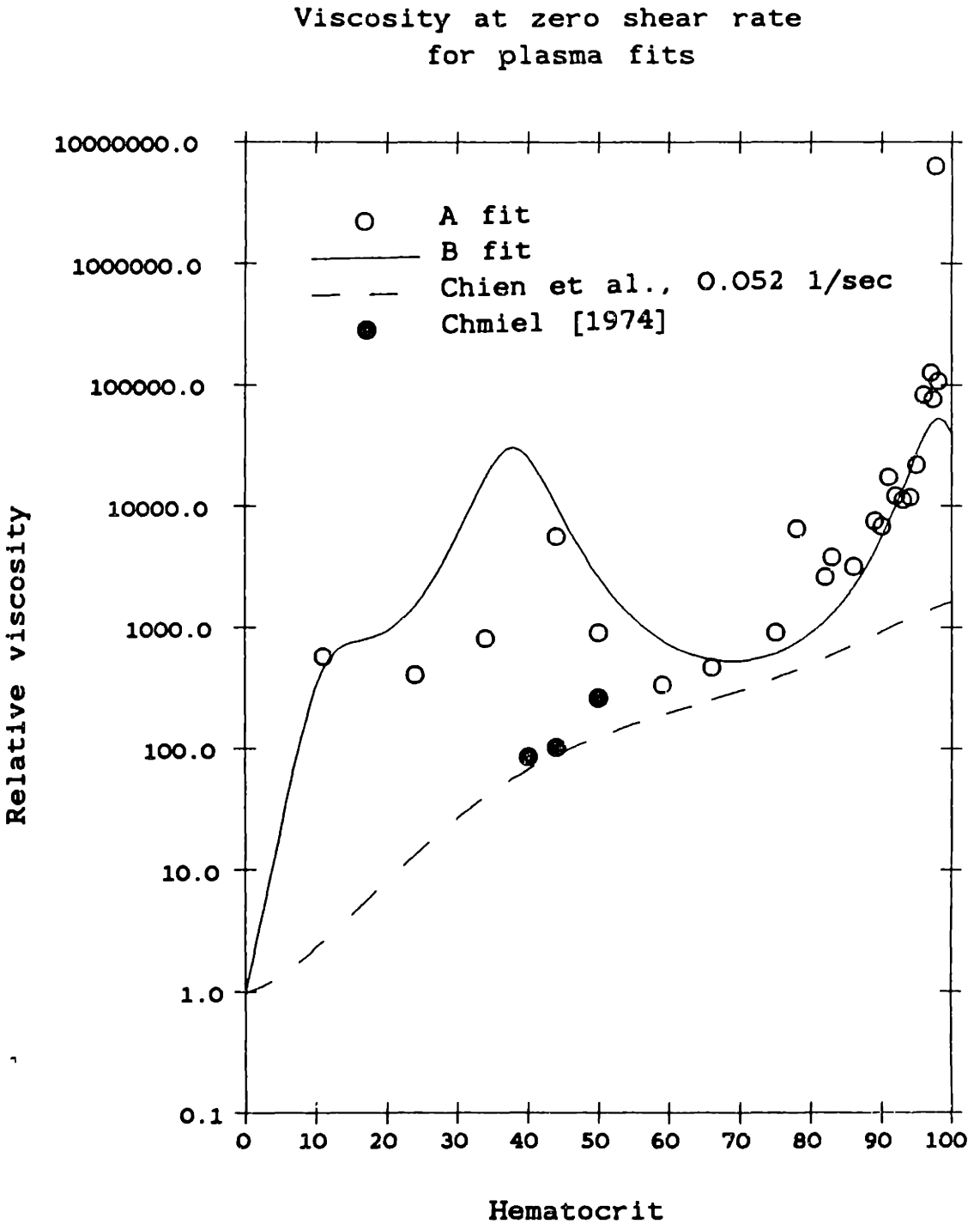

Figure 5-10: Zero shear rate asymptotes for plasma fits.

modeling overall behavior, but they will not be accurate enough for predicting viscosity at low shear rates.

At very high hematocrits, the difference between saline and plasma k_0 can probably also be related by equation (5.4), replacing k_∞ with k_0. An attempt was made to use this equation to derive new plasma k_0 values from the Fit A saline values, in hopes that the new values would provide a more realistic $\dot{\gamma} = 0$ curve. The highest hematocrit at which a singular point does not result from the saline A fit is 95. Using the saline value 2.1 at H=95, equation (5.4) gives a plasma k_0 of 2.099, and $\eta_r = 10^5$. Similarly, at H=94, the saline value of 2.126 results in a plasma value of 2.126 and $\eta_r = 10^6$. This indicates that at high hematocrits, the saline A fit values are inaccurate also, at least on the scale of determining low shear rate viscosity.

As an example of just how accurately k_0 must be determined, Chmiel [1974] collected data for whole blood at shear rates of 0.1 to 0.005 sec^{-1} in a wide-gap Couette system, in which an asymptotic approach to a constant viscosity at low shear rate was demonstrated. Assuming a η_f, which is not explicitly given in the paper, of 1.2 cP, relative viscosities at H=50, 44, and 40 correspond to k_0 values of 3.75, 4.09 and 4.45, respectively. The parameter values from this study of 3.87 at H=50 and 4.48 at H=44 are both comparable, within 3 and 10 per cent of the Chmiel values, respectively, and yet the calculated viscosities at $\dot{\gamma}=0$ are an order of magnitude or more higher. For comparison, Chmiel's data is shown on Figure 5-10 as filled circles.

From an analytical standpoint, the difficulty stems from the fact that for plasma, $\frac{c}{2}k_0$ is always approximately equal to 0.99. Thus a smooth plot of $(1-\frac{c}{2}\cdot k_0)^{-2}$ depends on accurately representing small deviations from zero.

5.4 Dependence of γ_c on hematocrit and plasma proteins

The values for the A fits of γ_c for saline are plotted versus hematocrit in Figure 5-11. Also plotted are values derived from fits of the Quemada equation to the Chien *et al.* polynomials. There is a good deal of scatter in the A fit values, but the trend seems to be for γ becoming large as hematocrit decreses. The values from the Chien polynomials decay toward zero as hematocrit decreases. The result of these opposing trends is seen in the different curvatures of the two sets of data along the γ axis (see Figures 4-20 to 4-23). The data from this work and the A fits are convex, while the Chien points indicate a concave curvature.

From a strictly analytical viewpoint, it can be seen how γ_c affects this curvature. It will be recalled from the discussion in Section 2.4 that the Quemada equation results in a sigmoidal curve along the x-axis (γ axis). As γ_c increases, the curve is shifted to the right, and the curvature at a fixed shear rate becomes more convex. As γ_c decreases, the reverse happens.

The question exists whether the high γ_c values are artifacts resulting from secondary flows in the viscometer at higher shear rates and low hematocrits. Jerrard [1950] has developed charts for assessing the onset of instability in rotating-cylinder viscometers in which the outer cylinder rotates, such as the Haake viscometer used in this work. Based on the geometry of the Haake viscometer, the critical shear rate in sec^{-1} for secondary flow is $3.5 \times 10^5 \nu$, where ν is the kinematic viscosity of the fluid in stokes. For water, plasma, and red cells in saline at H=42, the calculated values are 2300, 4100, and 10,000 sec^{-1}, respectively. It would seem that secondary flow is not a consideration, and yet shear-thickening behavior was noted in the measurement of both saline and plasma viscosities, which is normally an indication of some instability.

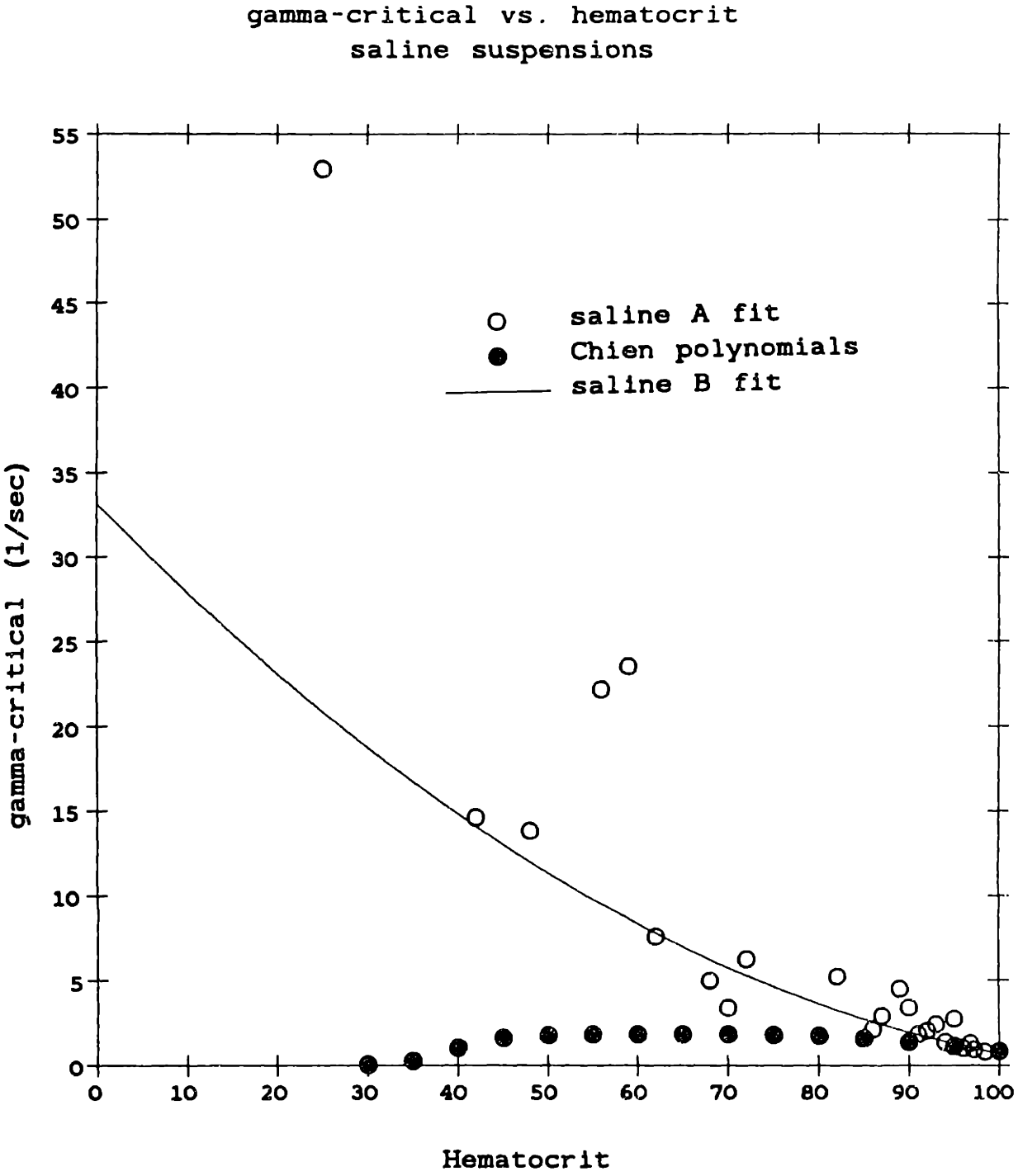

Figure 5-11: Plot of γversus hematocrit for saline suspensions.

It is possible that the concavity of the Chien *et al.* values is forced from the nature of the fifth-order polynomials used to calculate them, and that the actual data of Chien [et al.] would correspond to the data of this work. Later data by Chien [1970] shows convex curvature similar to the A fits (see Figures 2-3 and 2-11). Quemada [1978b] fit a γ_c value of 25 sec^{-1} to this later data of Chien, which agrees with the values shown in Figure 5-11.

Plasma values for γ_c are plotted in Figure 5-12. Both the Chien polynomials and the A fits indicate $\gamma_c \approx 0$ at H=0, then an increase to a maximum at about H=70-75, and subsequent decrease with incresing H. Correspondingly, the A fits are concave at both high and low hematocrits, but around H=70 (see Figures 4-42 to 4-44) a more sigmoidal curve is seen.

The B fit in Figure 5-11 represents a relatively weighted fit of the saline A fit values to the form

$$\gamma_c = \sum_{i=1}^{3} \gamma_{ci} \cdot c^{(i-1)} \tag{5.6}$$

where the best-fit values are

$\gamma_{c1} = 33.16 \pm 11.95$

$\gamma_{c2} = -54.79 \pm 28.57$

$\gamma_{c3} = 22.33 \pm 16.93.$

A second-order polynomial was fit to the Chien values in Figure 5-11. This fit, when substituted for the saline B fit curve from this study, resulted in a shifting of the curve to the left and predicted relative viscosities up to an order of magnitude lower than the data at low shear rates. For plasma, the B fit is of the form

$$\gamma_c = \gamma_{c1} \cdot \exp(-(\gamma_{c2} c + \gamma_{c3})^2) \tag{5.7}$$

where by a relatively weighted fit, the values are

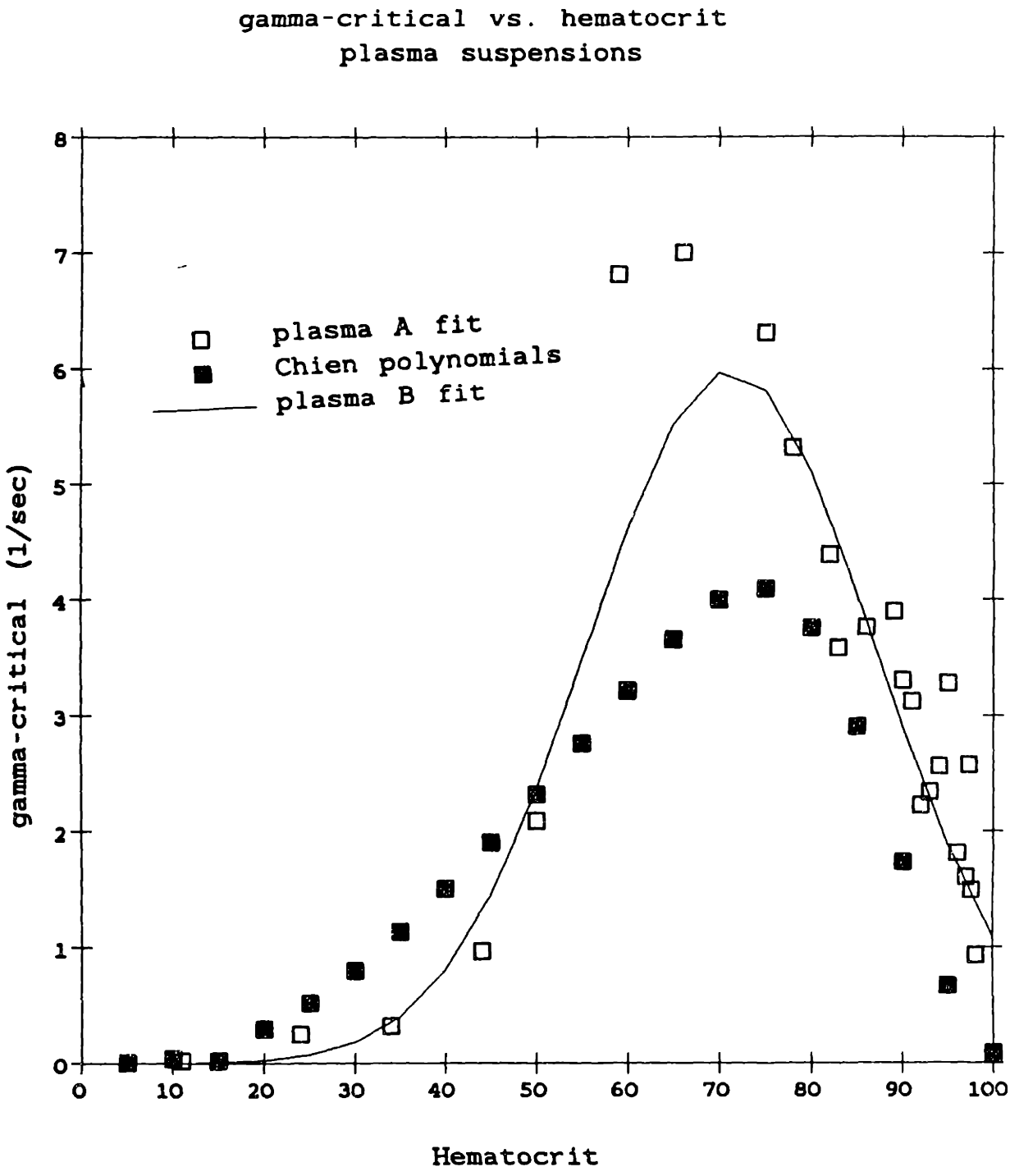

Figure 5-12: Plot of γ_c versus hematocrit for plasma suspensions.

$\gamma_{c1} = 5.979 \pm 0.580$

$\gamma_{c2} = -4.536 \pm 0.162$

$\gamma_{c3} = 3.232 \pm 0.098.$

The saline and plasma values are plotted together on Figure 5-13. The values from the two suspensions converge with increasing hematocrit at about H=70 and are comparable at high concentrations, with the saline values somewhat higher.

From a physical interpretation, γ_c is analagous to a rotational diffusion constant, with a dependence $\gamma_c \sim a^{-3}$, where a is the particle radius (see Appendix C). Thus effects which increase effective particle size will decrease γ_c. The two such mechanisms for increasing effective particle size are aggregation and crowding. In saline, the cells do not aggregate, and so there is a simple trend of γ_c decreasing with hematocrit. In plasma suspensions, one could imagine that initially as concentration increases, crowding acts to diminish rouleau and aggregate size, and γ_c increases. When γ_c reaches a maximum that roughly corresponds to inversion, crowding acts to pack cells together and γ_c decreases.

5.5 Limiting behavior of parameters

A major concern in globally refitting the Quemada expression over all hematocrits is the limiting behavior of the equation, and specifically the intrinsic viscosity $k=k_\infty + \frac{k_0-k_\infty}{1+\sqrt{\gamma_r}}$ as the cell volume concentration goes to zero. Since the equation was derived for concentrated dispersions, it may be appropriate to say that it is not valid in the limit $c \to 0$. Nevertheless, the equation can be fit successfully to low concentration data, and the parameters do appear to approach asymptotic values at low hematocrits.

Newtonian behavior should be recovered where k is not a function of shear

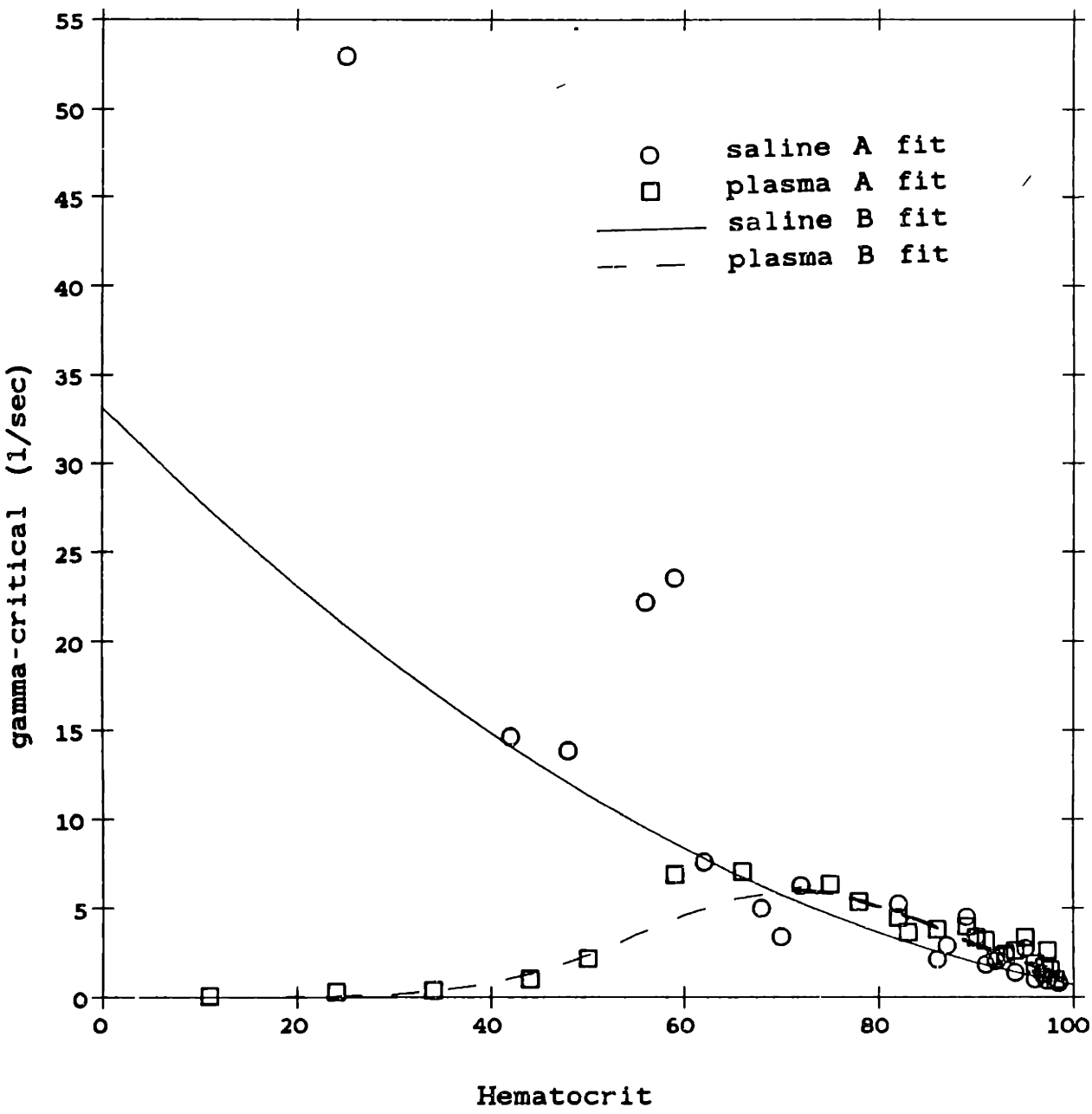

Figure 5-13: Comparison of γ_c for saline and plasma suspensions.

rate. There are three possible mathematical ways by which k can become independent of shear rate, and these will be considered in turn, first from a purely analytical standpoint, and then by how the analysis relates to data and to physical interpretation:

- $k_\infty = k_0$. Quemada [1981] proposed that at the Newtonian thresholds H=30 for saline suspensions and H=5 for plasma suspensions, k_∞ and k_0 become equal at some intermediate value. The data does not support this, as the difference between the two parameters is greatest at low hematocrits for both plasma and saline suspensions. Additionally, from a conceptual standpoint, it would seem that even in the absence of aggregation and cell-cell crowding, orientation and deformation would lead to a finite distinction between intrinsic viscosities at low and high shear rates.
- $\dot{\gamma}_c \rightarrow \infty$, $k \rightarrow k_0$. This behavior is demonstrated by the Eagle's solution data of this work and appears to correlate with the analysis of $\dot{\gamma}_c$ as inversely proportional to particle radius, although if this were strictly true, some asymptotic finite value would be expected. Also, the limit of $k \rightarrow k_0$ is troublesome, because it indicates that as long as $\dot{\gamma}_c$ is finite, the viscosity will decrease at large enough $\dot{\gamma}$. A more realistic stating of this limit that would satisfy these concerns is to combine this criterion with the first case, so that $\dot{\gamma}_c$ approaches a large, but finite, value and $k_\infty \rightarrow k_0$.
- $\dot{\gamma}_c \rightarrow 0$, $k \rightarrow k_\infty$. This behavior is demonstrated by both sets of Chien data and by the plasma data of this work after incorportation of the Chien data, and it is also coupled with a large increase in k_0, which causes the curves to increase sharply at low H. It appears to be

incompatible with the idea of γ_c as a rotational diffusion constant dependent solely on effective particle radius, although it seems logical that as concentration decreases, non-Newtonian behavior will be expressed at increasingly lower shear rates. A possible explanation is that there is an initial increase in the frequency of particle collisions as cell concentration increases, with a resulting enhancement of aggregate formation, followed by a decrease when steric effects limit mobility. It is interesting to note that the maximum in γ_c in all cases occurs around H=70-75, which again corresponds with the analysis of Chien *et al.* [1966] as the advent of prominent effects from cell crowding.

5.6 Comparison of global fit equations to data

The B fit values for the rheological parameters are shown in Table 5-VI. These values are obtained from the equations discussed in the previous three sections, and are used to plot the dashed curves in Figures 4-2 to 4-49. As shown in Figures 5-14 to 5-17, the B fits provide a reasonable representation of the data, whether plotted as a function of hematocrit or of shear rate. The fits are best at shear rates greater than 0.5 sec^{-1}. The plasma curves provide better fits to data at shear rates down to 0.05 sec^{-1}, despite the crossing over of the plasma curves of Figure 5-17 and the relatively smooth behavior of the saline curves in Figure 5-15. Even in the absence of data, the saline curves probably adequately model viscosity at low hematocrits and low shear rates, since the behavior is Newtonian. At hematocrits greater than 98, both the saline and plasma fits tend to underestimate the data. When plotted against the Chien polynomials (see Figures 5-18 and 5-19) the same comments can be made as for the comparison of the polynomials to the data of this work (see Figures 4-54 and 4-55).

Hematocrit	k-inf. B fit	k-0 B fit	gam.-crit. B fit
98.4	1.815	2.044	0.868
97.2	1.808	2.063	1.001
96.8	1.806	2.070	1.047
96.0	1.803	2.084	1.141
95.0	1.798	2.102	1.262
94.0	1.795	2.122	1.388
93.0	1.791	2.142	1.519
92.0	1.788	2.163	1.653
91.0	1.786	2.184	1.793
90.0	1.784	2.207	1.936
89.0	1.782	2.230	2.084
87.0	1.781	2.278	2.394
86.0	1.781	2.303	2.556
82.0	1.785	2.409	3.247
72.0	1.826	2.704	5.287
70.0	1.840	2.766	5.749
68.0	1.855	2.828	6.228
62.0	1.912	3.016	7.774
59.0	1.947	3.108	8.607
56.0	1.986	3.199	9.480
48.0	2.110	3.425	12.006
42.0	2.221	3.572	14.087
25.0	2.626	3.825	20.858
7.0	3.838	3.699	29.434

Hematocrit	k-inf. B fit	k-0 B fit	gam.-crit. B fit
98.1	1.696	2.030	1.357
97.6	1.695	2.040	1.433
97.3	1.694	2.046	1.480
97.0	1.693	2.052	1.528
96.0	1.691	2.073	1.696
95.0	1.689	2.093	1.874
94.0	1.687	2.112	2.062
93.0	1.685	2.132	2.259
92.0	1.684	2.152	2.466
91.0	1.683	2.172	2.680
90.0	1.682	2.192	2.901
89.0	1.682	2.212	3.127
86.0	1.682	2.275	3.822
83.0	1.684	2.343	4.501
82.0	1.686	2.366	4.714
78.0	1.693	2.470	5.444
75.0	1.702	2.558	5.809
66.0	1.742	2.899	5.649
59.0	1.788	3.268	4.390
50.0	1.867	3.922	2.361
44.0	1.930	4.501	1.297
34.0	2.058	5.838	0.344
24.0	2.212	8.119	0.060
11.0	2.451	17.319	0.003

Table 5-VI: B fit values of Quemada parameters for Eagle's solution and plasma. *Top*, values for Eagle's solution. *Bottom*, values for plasma.

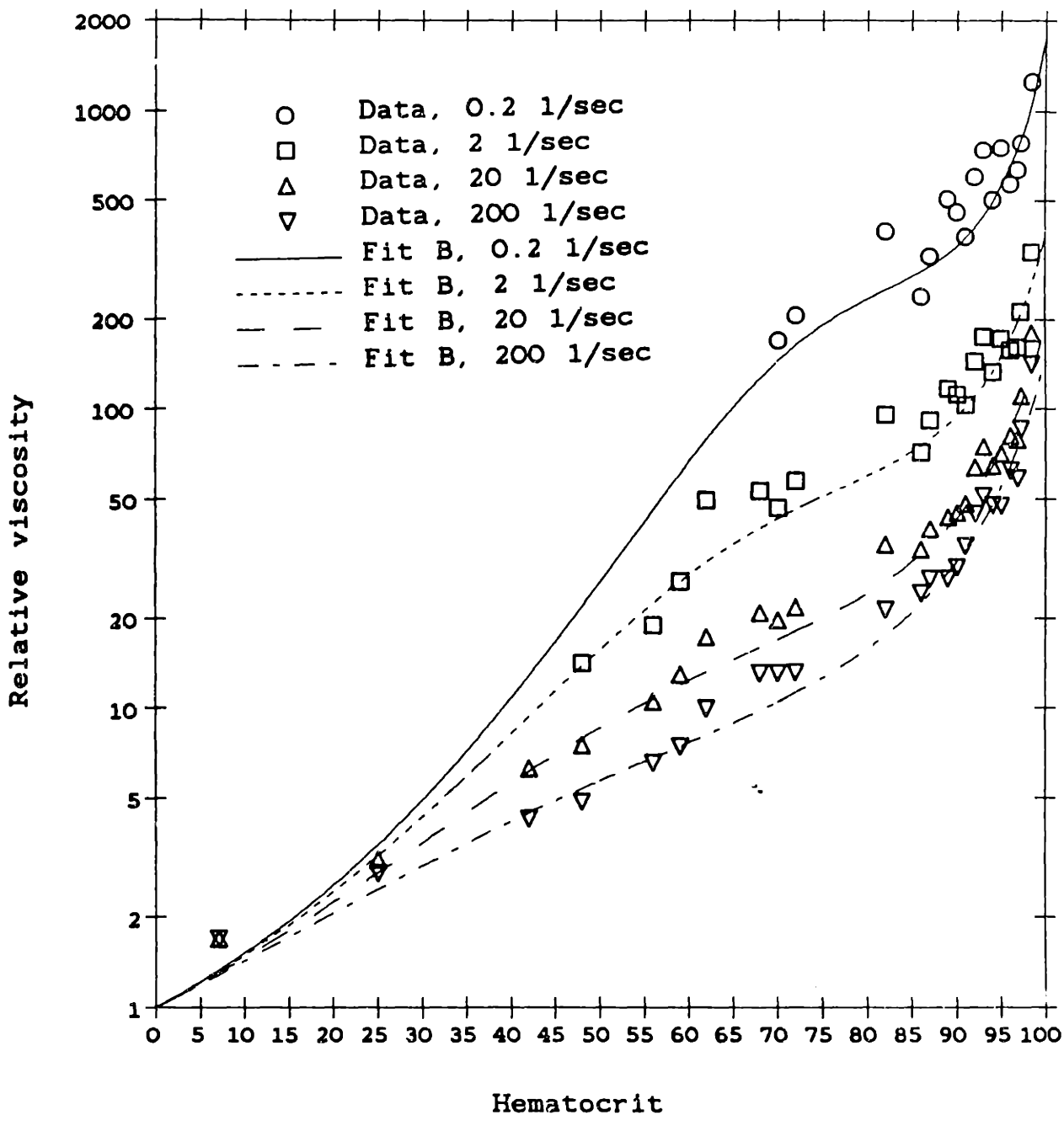

Figure 5-14: Comparison of saline global fit to data as a function of hematocrit.

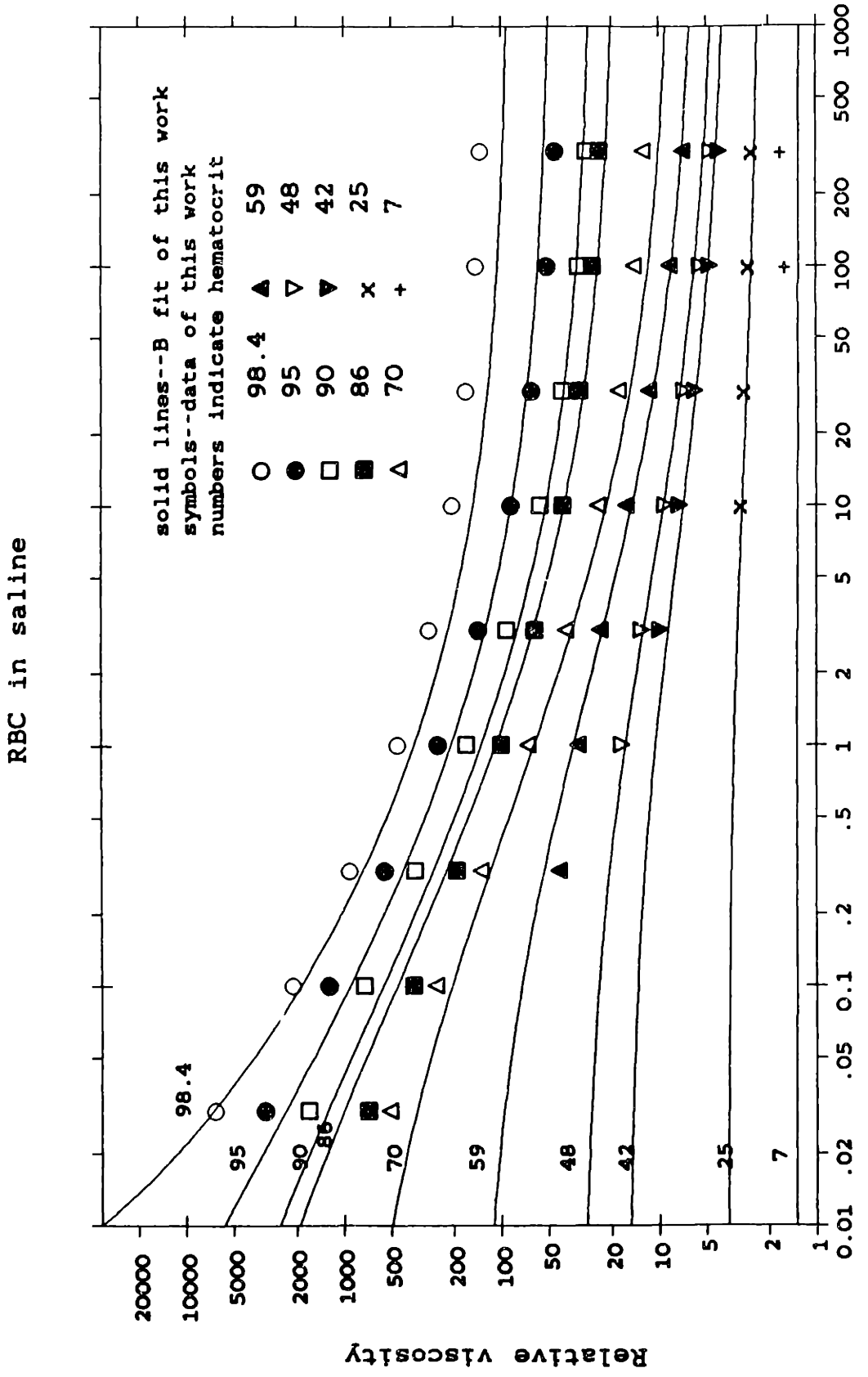

Figure 5-15: Comparison of saline global fit to data as a function of shear rate.

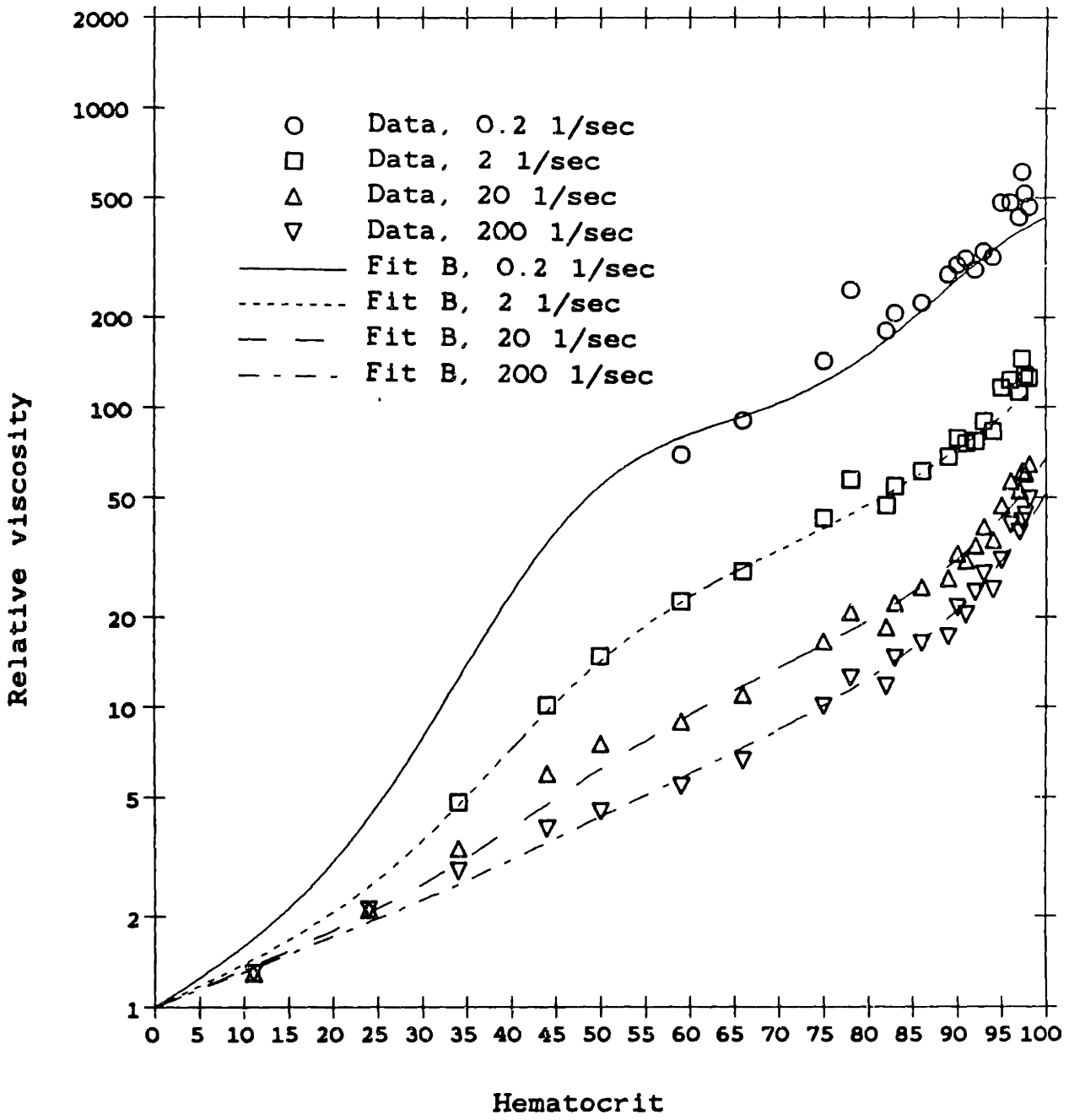

Figure 5-16: Comparison of plasma global fit to data as a function of hematocrit.

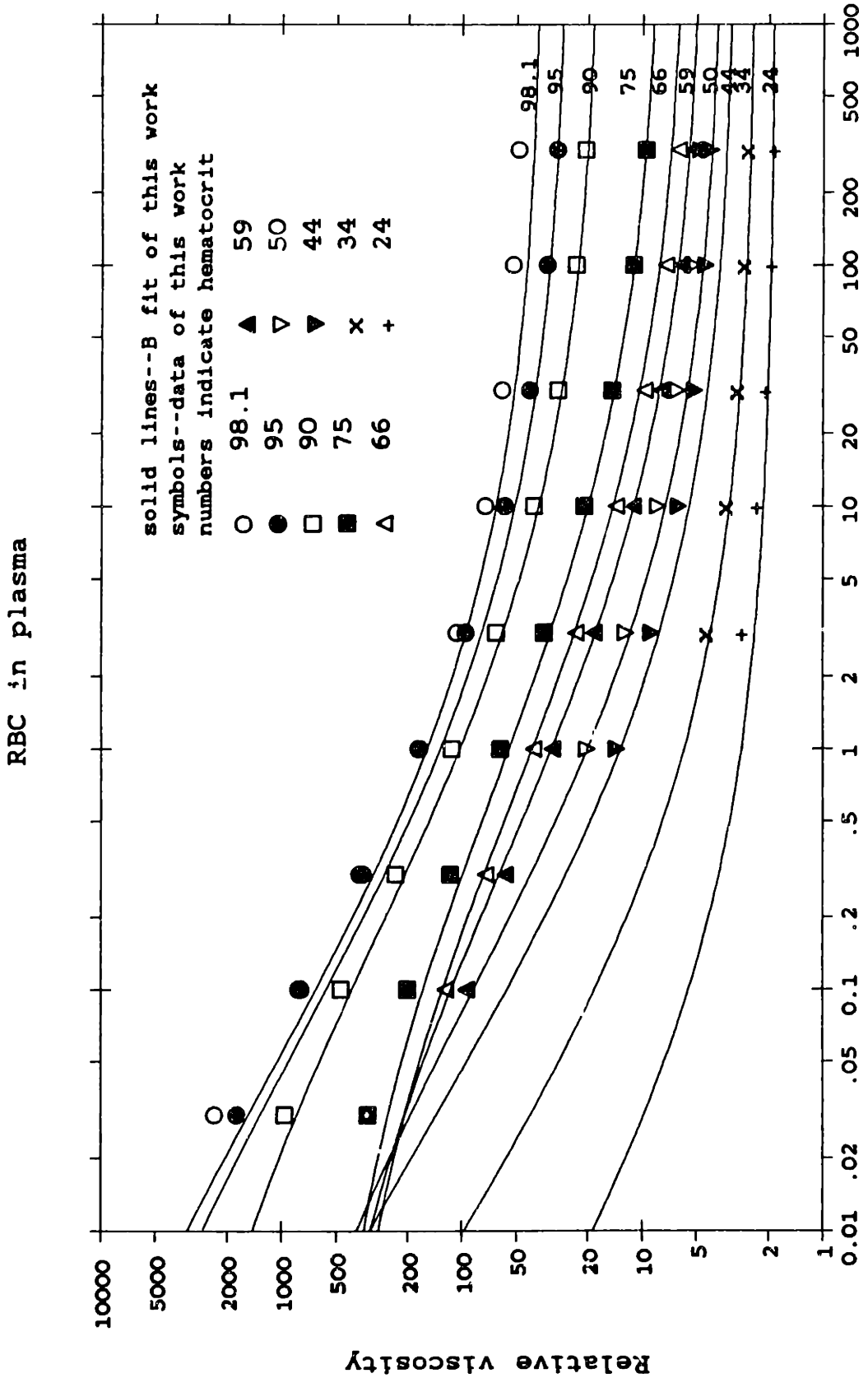

Figure 5-17: Comparison of plasma global fit to data as a function of shear rate.

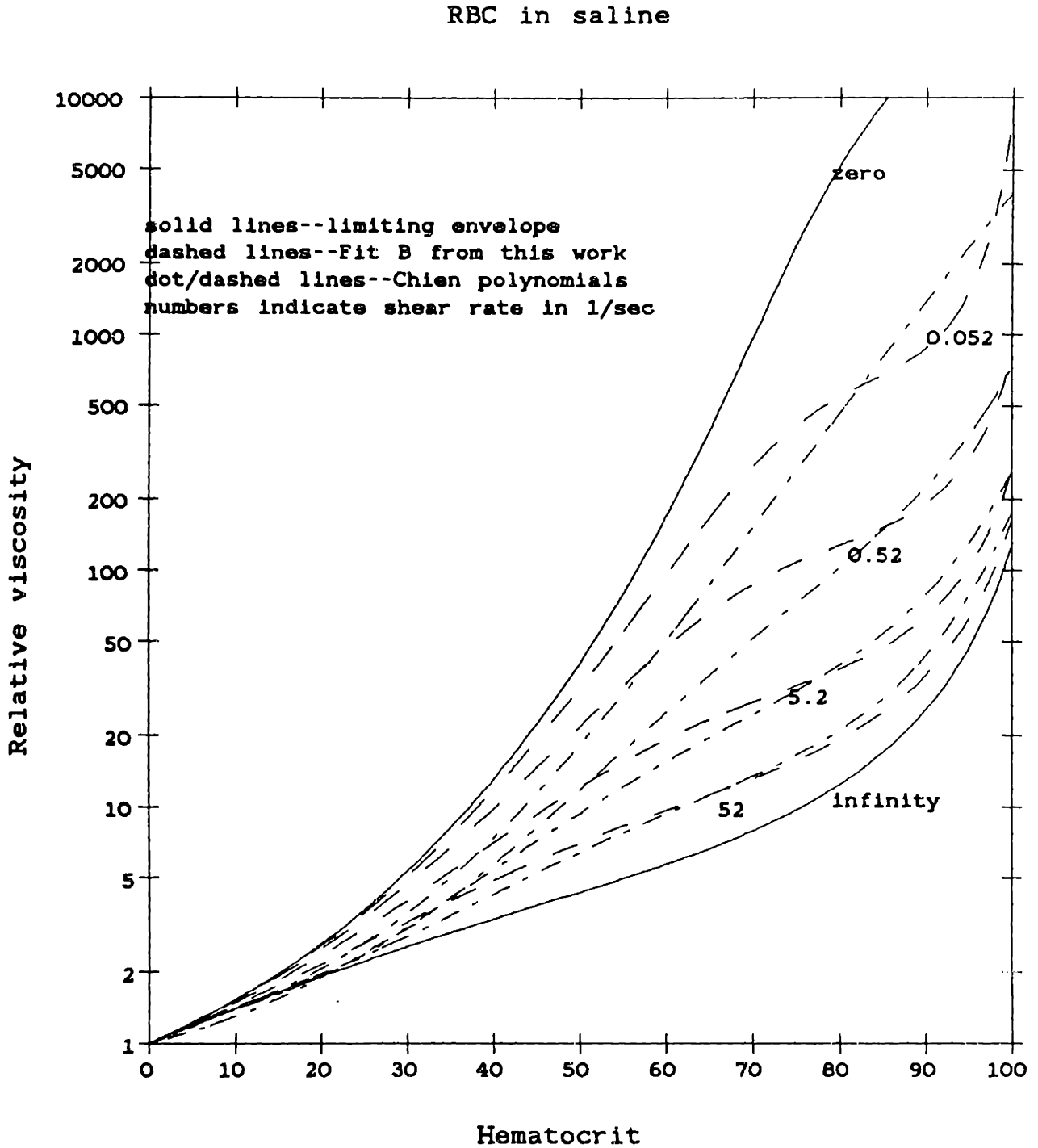

Figure 5-18: Comparison of saline global fit to Chien polynomials.

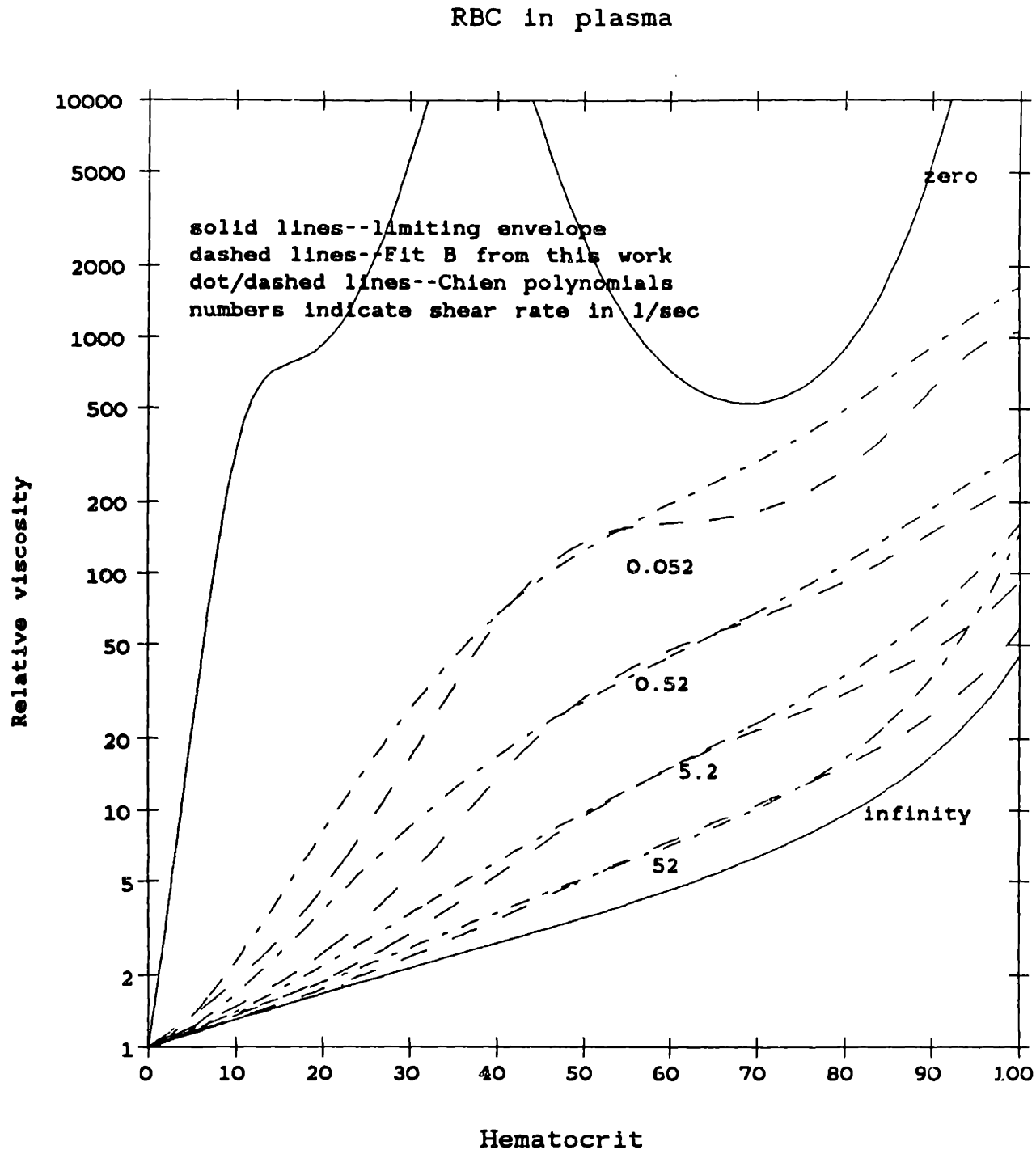

Figure 5-19: Comparison of plasma global fit to Chien polynomials.

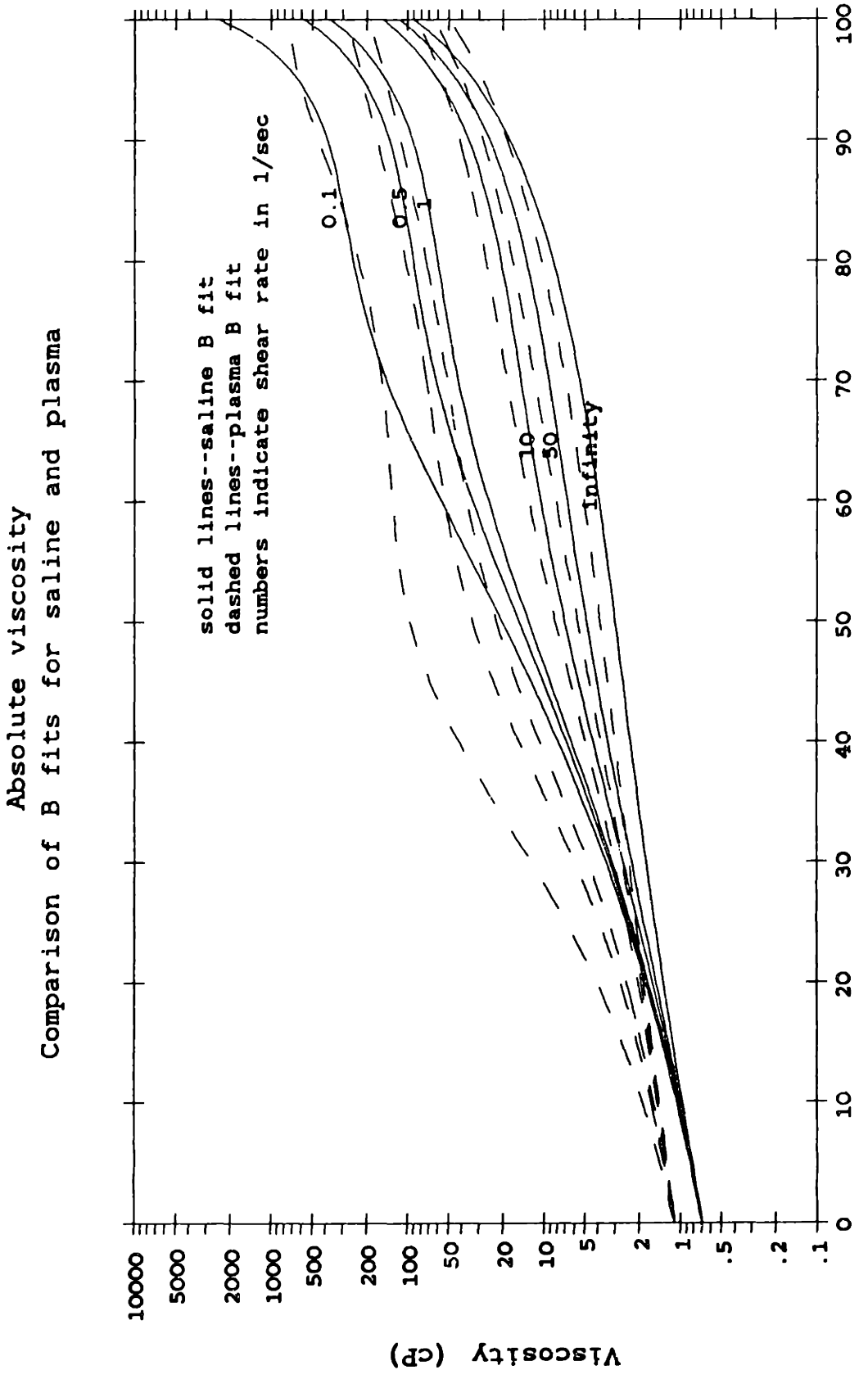

Figure 5-20: Comparison of B fit curves for plasma and saline.

The B fit curves for plasma and saline are compared at various shear rates in Figure 5-20. In the limit of high hematocrit, the B fit curves begin to approach each other in a manner similar to the data (see Figure 5-21). Plasma suspensions maintain slightly higher viscosities until about H=92-95 when the curves cross. This crossing is primarily due to the saline data at H=98.4, where the viscosity was much higher than for any other sample.

The final global fits (B fits) are summarized in Table 5-VII. The equations are plotted alone as functions of hematocrit and shear rate in Figures 5-22 and 5-23 for saline and in Figures 5-24 and 5-25 for plasma.

5.7 Summary, conclusions, and recommendations

Data collected at hematocrits above 90 shows the still-fluid nature of packed cells, emphasizing that blood is more like an emulsion than a suspension of rigid particles. At high hematocrits, the difference in viscosity between cells in plasma and cells in saline solution is small, but it increases at lower hematocrits and lower shear rates, indicating the effects of the plasma proteins on aggregation.

The complex interactions of blood cells and plasma, summarized in Section 2.4, constitute the challenge of developing theoretical expressions for blood rheology. To date, theory can only be taken so far, and then at some point one must incoporate empirical fits into the theory.

The three-parameter Quemada equation has been fit individually to data at each hematocrit and has proven to be an effective model on this basis. The parameters were empirically fitted to functions of hematocrit, and in this way a set of equations has been derived which can be used with the Quemada expression to represent blood viscosity over a wide range of hematocrits and shear rates,

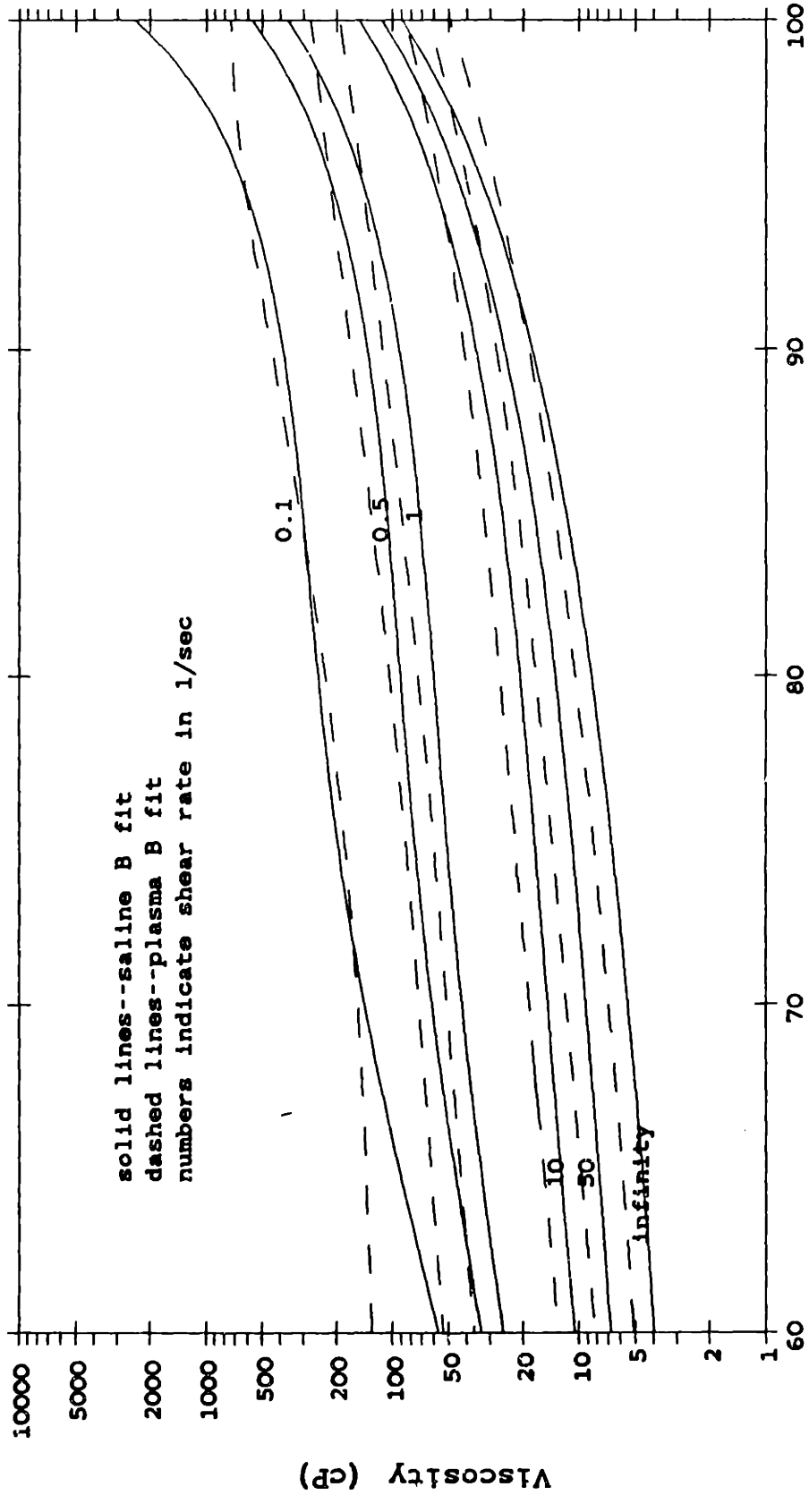

Figure 5-21: High hematocrit viscosities from the B fit for saline and plasma.

QUEMADA EQUATION

$$\eta_r = [1 - \frac{c}{2}(k_\infty + \frac{k_0 - k_\infty}{1+\sqrt{\gamma/\gamma_c}})]^{-2}$$

Parameter Equation	Constants	
	saline	plasma
$k_\infty = \sum_{i=1}^{3} k_{\infty i} \cdot c^{(i-1)}$	$k_{\infty 1}$=3.458 $k_{\infty 2}$=−3.804 $k_{\infty 3}$=2.260	$k_{\infty 1}$=2.688 $k_{\infty 2}$=−2.300 $k_{\infty 3}$=1.314
$k_0 = \sum_{i=1}^{4} k_{0i} \cdot c^{(i-1)} + k_{05} \exp(k_{06} \cdot c)$ (*Note*: for saline and c<20, k_0=3.838)	k_{01}=3.503 k_{02}=3.467 k_{03}=−9.976 k_{04}=5.026 k_{05}=0 k_{06}=0	k_{01}=13.28 k_{02}=−31.93 k_{03}=32.13 k_{04}=−11.49 k_{05}=45.46 k_{06}=−16.78
saline $\gamma_c = \sum_{i=1}^{3} \gamma_{ci} \cdot c^{(i-1)}$ plasma $\gamma_c = \gamma_{c1} \exp(-(\gamma_{c2} c + \gamma_{c3}))^2)$	γ_{c1}=33.16 γ_{c2}=−54.79 γ_{c3}=22.33 γ_{c1}=5.979 γ_{c2}=−4.536 γ_{c3}=3.232	

Table 5-VII: Summary of global fits for saline and plasma suspensions.

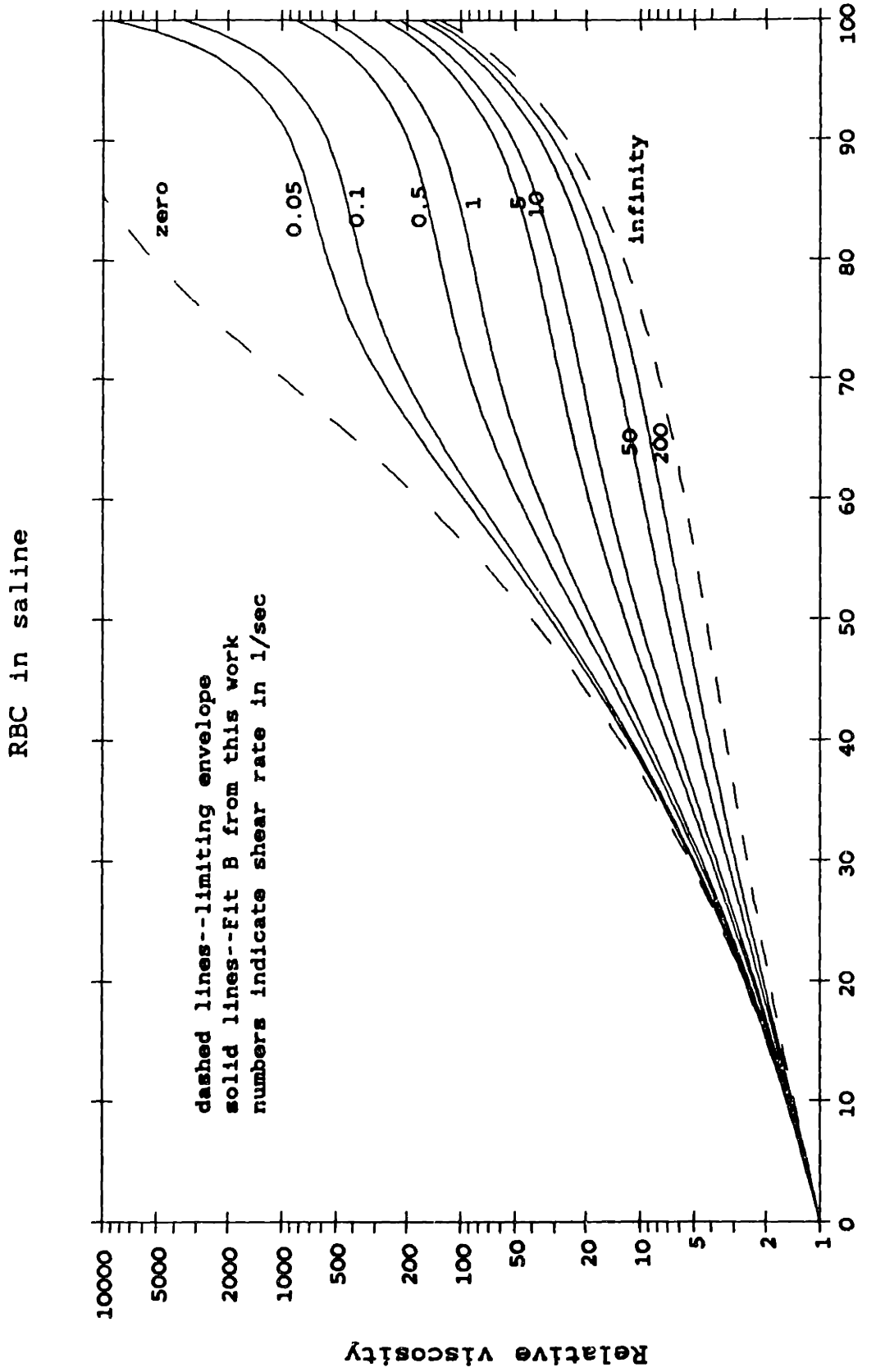

Figure 5-22: Plot of saline global equations versus hematocrit.

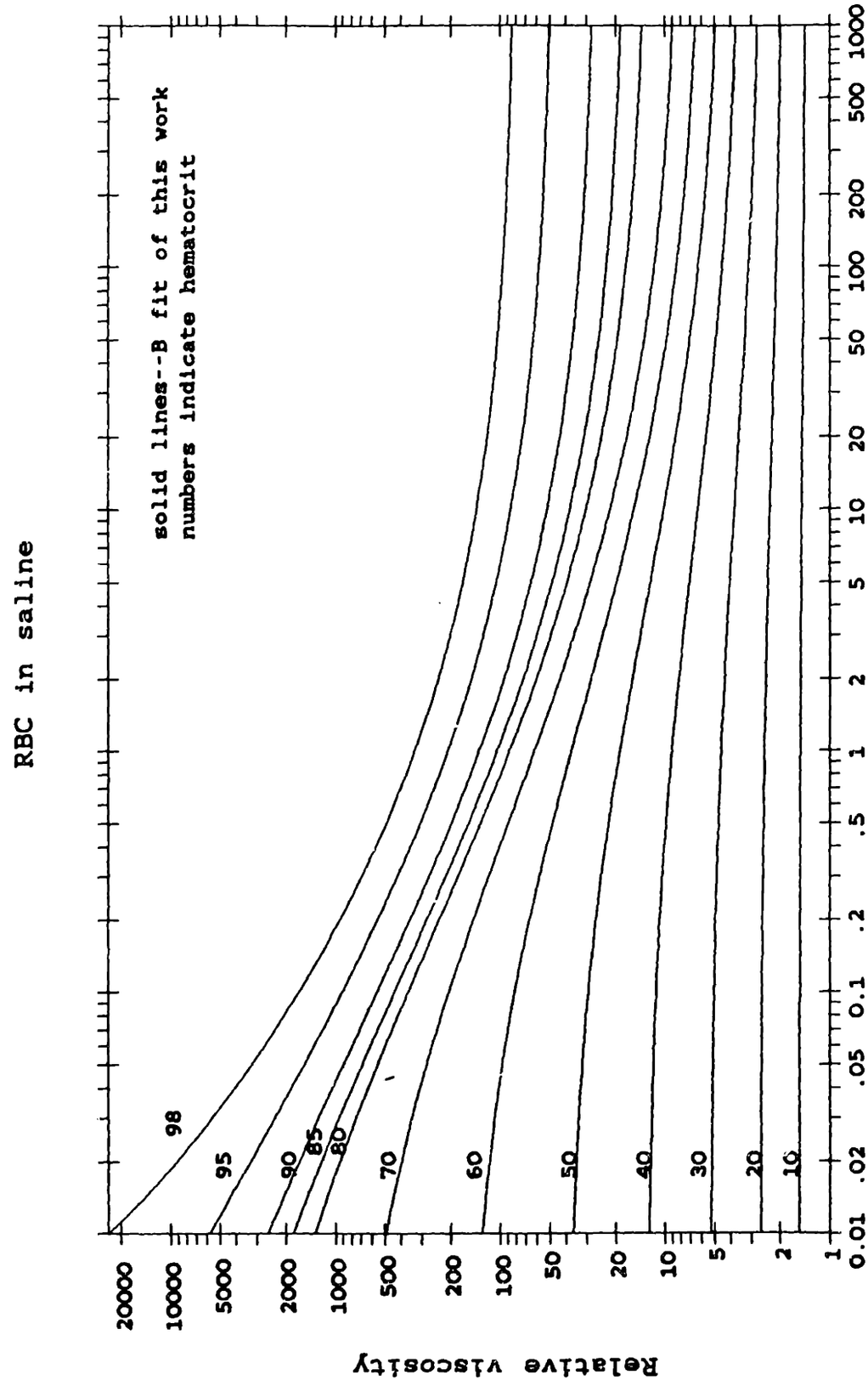

Figure 5-23: Plot of saline global equations versus shear rate.

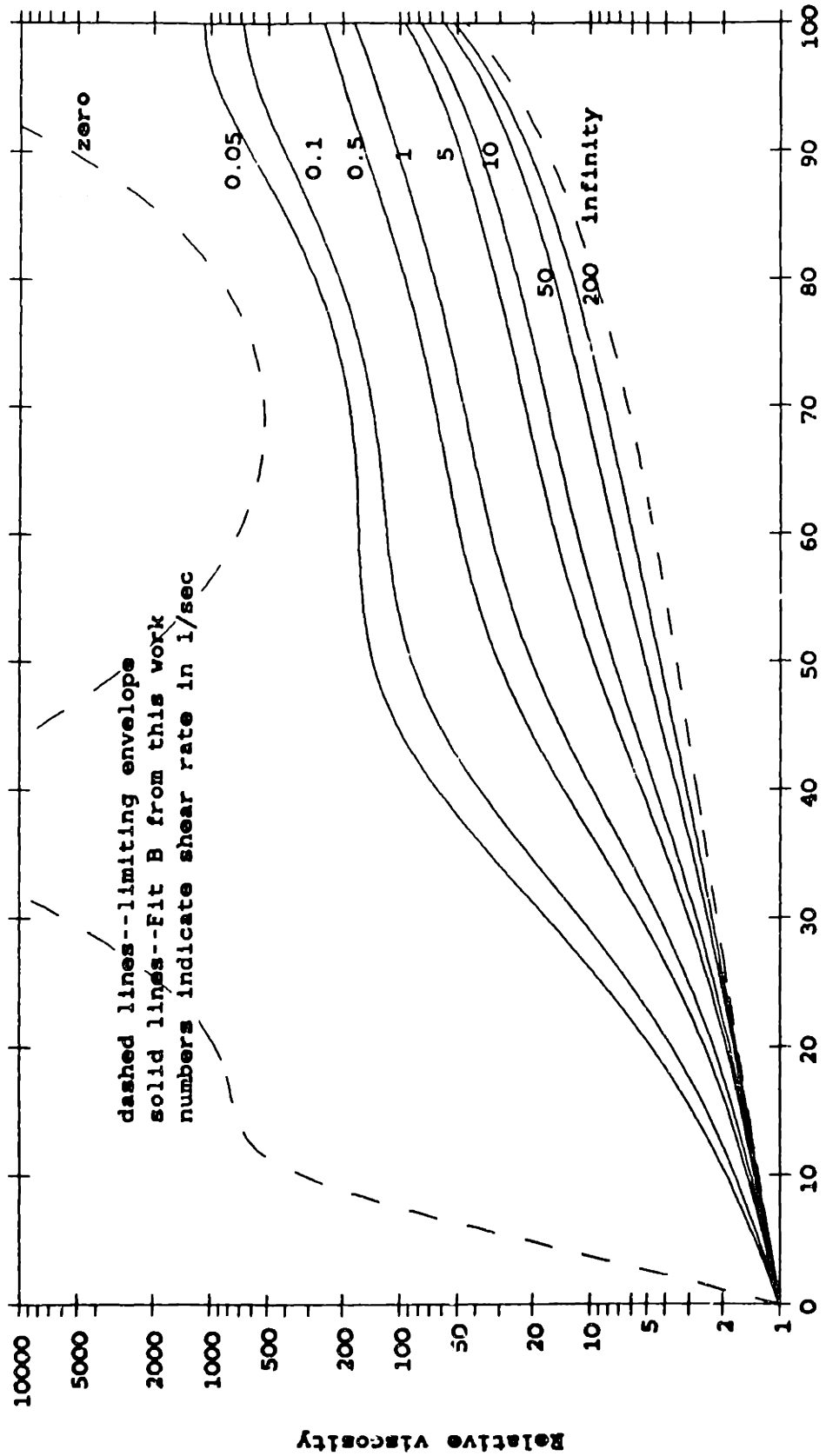

Figure 5-24: Plot of plasma global equations versus hematocrit.

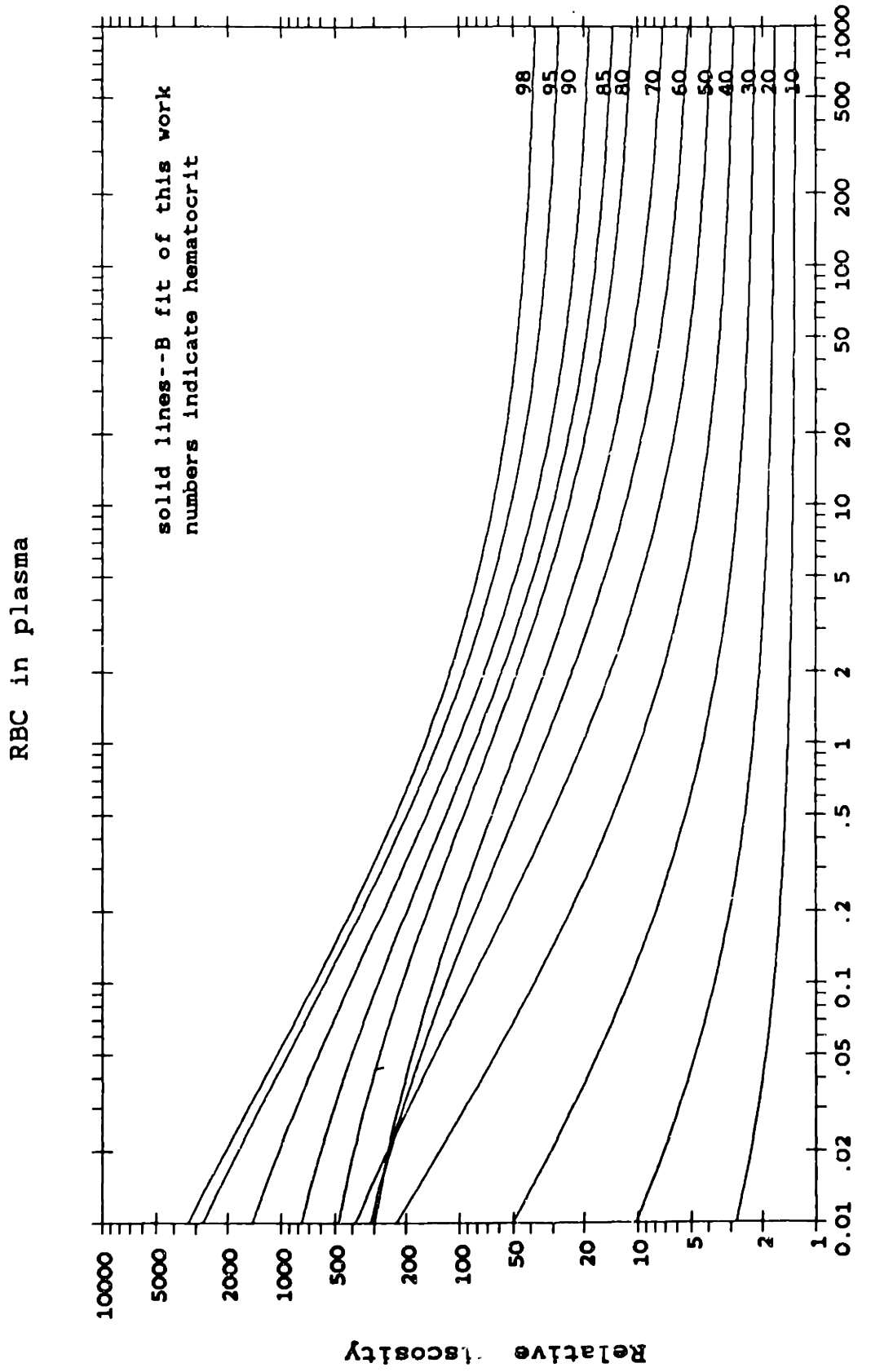

Figure 5-25: Plot of plasma global equations versus shear rate.

particularly those of interest for cross-flow membrane plasmapheresis phenomena. The data of this work did not extend to low enough shear rates for plasma suspensions to reasonably model viscosity dependence at $\dot{\gamma} < 0.1$ sec^{-1} globally.

The difficulties in extending the Quemada equation to all hematocrit lies in the extreme sensitivity of the equation to the value of k_0 at low shear rates. Ideally, determination of the parameters requires data at only three shear rates: $\dot{\gamma} = 0, \infty$, and $\dot{\gamma}_c$, which is defined as the point where $k = \frac{k_\infty + k_0}{2}$. It would be interesting to see if a fit to only three shear rates could actually model behavior everywhere. Data from a device such as a wide-gap Couette viscometer should be obtained to extend the low shear rate utility of the equations.

In extending the Quemada equation to all hematocrits and shear rates, the present development uses ten constants for saline solution and twelve constants for plasma suspensions. The complexity of this fits seems reasonable when one considers that Chien *et al.* required six constants to model viscosity behavior over all hematocrits at a single shear rate. Interpretation of the meaning of the parameter dependence suffers from the fact that they are conceptual properties than physically measureable quantities.

The Quemada expression does an overall satisfactory job of describing blood viscosity and is probably the most promising way to develop a set of global equations for every hematocrit and every shear rate. A major drawback is that it does not flatten to its limiting high shear rate value as quickly as one would like. One adjustment that could be made is in the power dependence of the square root term, which was obtained from an empirical representation $\theta = \dot{\gamma}_r^p$ where p=0.5 (see Appendix C). Perhaps a larger value could be assigned to p, or p could be allowed to vary with hematocrit.

The hematocrit dependence of the two limiting viscosities shows an added variation due to the suspending fluid viscosity. A possible modification to the equation is to include the emulsive properties of erythrocytes into the idea of the intrinsic viscosity and thus make the rheological parameters independent of η_f. This can be done by incorporating some sort of Taylor coefficient, with a simplifying assumption of constant internal viscosity.

Most formulations for representing viscosity are for η_r, and thus there is an implicit dependence of η on η_f at all hematocrits. Ideally, η should become independent of η_f at high hematocrits, and a truly general expression for viscosity should provide for this. With regards to this, the Quemada model seems to indicate that cell crowding effects and inversion becomes important at hematocrits of 65 to 80 and above, as this seems to be the region where all three rheological parameters become similar for saline and plasma suspensions.

Appendix A

Physical Properties of Human Blood and the Red Blood Cell

Properties of whole blood

Whole blood	
specific gravity(25/4 °C)	1.056
Plasma	
specific gravity(25/4 °C)	1.0239
viscosity (37 °C)	1.2 cP
Plasma proteins	
albumin	m.w. 69,000 4.5 g/100 ml plasma
globulins	m.w. 35,000-1,000,000 2.5 g/100ml plasma
fibrinogen	m.w. 330,000 0.3 g/100ml plasma
Erythrocytes	
concentration	
male	5.2×10^6/mm^3 whole blood 42 volume %
female	4.7×10^6/mm^3 whole blood 38 volume %
Leukocytes	
concentration	7.0×10^3/mm^3 whole blood 0.1 to 0.5 volume %
Platelets	
concentration	3.0×10^5/mm^3 whole blood 0.1 to 0.6 volume %

Properties of Red Blood Cell

Red blood cell	
specific gravity	1.098
mean corpusular volume	85-100 μm^3
surface area	140 μm^2
diameter	8.4 μm
center thickness	1 μm
peripheral thickness	2.4 μm
mean corpuscular hemoglobin concentration	31-35 g/100 ml packed red cells

Sources: Beck [1981] and Guyton [1981].

Appendix B
Modified Eagle's Solution Recipe

In one liter of distilled water, dissolve

NaCl	6.2 gm
KCl	0.36 gm
$NaH_3PO_4 \cdot H_2O$ (sodium phosphate monobasic)	0.13 gm
$NaHCO_3$	2.0 gm
$CaCl_2$	0.18 gm
$MgCl_2 \cdot 6H_2O$	0.15 gm
dextrose	0.9 gm

Adapted from Eagle [1959].

Appendix C
Derivation of Quemada Equation

Quemada [1977, 1978a, 1978b] examined the steady-state viscometric flow of concentrated disperse systems. He noted that in such flows the concentration of the dispersed phase is not uniform but that an approximation to two-phase flow is developed: an axial region of high concentration and a region near the wall of low concentration, which in a sense provides a region of lubricant flow. What follows here describes his application of the principle of minimum energy dissipation, which states that with fixed system properties (concentration, temperature, flow conditions, fluid characteristics), the steady-state solution is that which minimizes the rate of energy dissipation (or, more generally, the rate of entropy production). The development assumes many features which are strictly valid only for suspensions of uniform, non-deformable rigid spheres but, as seen in the text (Section 2.4), with appropriate modifications the final result correlates well with experimental data for blood suspensions.

Consider simple viscometric flow in direction x between two plates separated by a distance 2Y along axis y, where $v_y=v_z=0$, $v_x=v_x(y)$ and no-slip conditions at the walls. The concentration profile in the channel is c=c(y). The viscous dissipation rate term in the conservation of momentum equation is [Bird *et al.*, 1960]

$$\frac{DU}{Dt}\Big|_{\text{viscous}} = \underline{\tau}:\nabla\mathbf{v} = \frac{1}{2}\eta\sum_i\sum_j\left[\left(\frac{\partial v_i}{\partial x_j}+\frac{\partial v_j}{\partial x_i}\right)-\frac{2}{3}(\nabla\cdot\mathbf{v})\delta_{ij}\right]^2 \qquad (C.1)$$

where U is the internal energy, $\frac{D}{Dt}$ is the substantial time derivative, $\underline{\tau}$ is the stress tensor, and δ_{ij} is the Kronecker delta function. For viscometric flow with an incompressible fluid, $(\nabla\cdot\mathbf{v})=0$, and this reduces to

$$\underline{\tau}:\nabla \mathbf{v} = \frac{1}{2}\eta\left(\frac{\partial v_x}{\partial y}\right)^2 \qquad (C.2)$$

Generalizing this to include dissipation from mass fluxes and integrating over the surface element s_x normal to the x-direction gives

$$\left.\frac{DU}{Dt}\right|_{\text{viscous}} = \int_{s_x}\left[\frac{1}{2}\eta\left(\frac{\partial v_x}{\partial y}\right)^2 + \frac{1}{2}D\left(\frac{\partial c}{\partial y}\right)^2\right] ds_x \qquad (C.3)$$

where D is the diffusivity of the dispersed particles.

Equation (C.3) is to be minimized subject to the following constraints:

1. Flow rate contraints

   Fluid flow constraints $Q_f = \int_{s_x}(1-c)\cdot v\cdot ds_x$

   Particle flow constraints $Q_p = \int_{s_x} c\cdot v\cdot ds_x$

2. Mean particle concentration

$$\bar{c} = \frac{\int_{s_x} c\cdot ds_x}{s_x}$$

3. Upper and lower limits of concentration, $c_w \leq c \leq c_b$. Using a method of optimum control theory, this constraint can be written as

   $\psi^2 = (c_b - c)(c - c_w)$

   so that ψ has an imaginary solution when c lies outside of the limits.

Equation (C.3) is minimized by the use of Lagrange multipliers [Wylie, 1975]. The auxiliary function to be solved is

$$F = \int_{s_x}\left\{\frac{1}{2}\eta v_x'^2 + \frac{1}{2}Dc'^2 + \lambda_1(1-c)v_x + \lambda_2 c v_x + \right. \qquad (C.4)$$
$$\left. \lambda_3 c + \Lambda(x)[\psi^2 - (c-c_b)(c-c_w)]\right\} ds_x$$

where λ_1, λ_2, λ_3, and $\Lambda(x)$ are the multipliers, and the "prime" symbol denotes

partial differentiation with respect to x. Solution of F for extrema satisfies the set of equations:

$$\frac{\partial}{\partial x}\left(\frac{\partial F}{\partial f'}\right) - \frac{\partial F}{\partial f} = 0 \qquad (C.5)$$

where f = v_x, c, and ψ.

At this point Newtonian behavior in the viscometer is assumed and the equations obtained are

$$(\eta v_x')' = \lambda_1(1-c) + \lambda_2 c \qquad (C.6)$$

$$(Dc')' = \frac{1}{2} v_x'^2 \frac{\partial \eta}{\partial c} + (\lambda_2 - \lambda_1) v_x + \lambda_3 + \Lambda(2c - c_b - c_w) \qquad (C.7)$$

$$0 = \Lambda\psi \qquad (C.8)$$

Quemada [1977] notes that other works using the principle of minimum energy dissipation have yielded similar sets of equations. Equation (C.6) can be considered as a generalization of the momentum transport equation, since it reduces to the Navier-Stokes equations for the case of a homogeneous (c=0) incompressible fluid, with λ_1 equal to the pressure gradient. Equation (C.7) is a generalized mass transport equation, and equation (C.8) provides the boundaries of the admissible domain.

Further solution is based on the observation that the transition between the concentration in the bulk and the concentration near the wall is relatively sharp. Also, for particles with radius $\geq$ 1 μm, Brownian diffusion is negligible compared to viscous drag.

Equations (C.6) and (C.7) are now decoupled by setting the left hand side of equation (C.7) to zero and using an empirical "rectangular" concentration profile similar to the one used by Vand [1948] to describe the viscometric flow of a suspended solution of rigid spheres:

$$c = \begin{cases} c_b & \text{for } 0 \leq y \leq \beta Y \\ c_w & \text{for } \beta Y \leq y \leq Y \end{cases}$$

where $\beta<1$.

Satisfaction of extrema at the break point $y_b=\beta Y$ is accounted for by Erdmann-Weierstrass corner conditions [Tolle, 1975]:

$$\frac{\partial F}{\partial f_i'}\Big|_{y_{b+}} = \frac{\partial F}{\partial f_i'}\Big|_{y_{b-}}$$

$$F - \sum_i \frac{\partial F}{\partial f_i'} f_i'\Big|_{y_{b+}} = F - \sum_i \frac{\partial F}{\partial f_i'} f_i'\Big|_{y_{b-}}.$$

Additionally, the velocity must be continuous at y_b. Defining $\Delta f = f|_{y_{b+}} - f|_{y_{b-}}$, these conditions become

$$\Delta v_x = 0 \tag{C.9}$$

$$\Delta(\eta v_x') = 0 \tag{C.10}$$

$$\Delta(Dc') = 0 \tag{C.11}$$

$$\Delta\frac{\partial F}{\partial \psi'} = 0 \tag{C.12}$$

$$\Delta(\frac{1}{2}\eta v_x'^2 - (\lambda_1(1-c)v_x + \lambda_2 c v_x + \lambda_3 c)) = 0 \tag{C.13}$$

These equations can now be used to solve for the velocity profile. Assuming two-phase flow with c_b, v_b in the core and c_w, v_w near the wall and applying equations (C.6), (C.9), and (C.10), the result is the same as that derived for any two-phase Newtonian flow:

$$v_w(y) = \frac{Y^2\Delta p}{4L\eta_w}(1 - \frac{y^2}{Y^2}) \tag{C.14}$$

$$v_b(y) = \frac{Y^2\Delta p}{4L\eta_w}(1 - \beta^2) + \frac{Y^2\Delta p}{4L\eta_b}(\beta^2 - \frac{y^2}{Y^2}) \tag{C.15}$$

Solving equations (C.7) and (C.13) for the concentration relationship gives

$$(\frac{d\phi}{dc})_b + (\frac{d\phi}{dc})_w = \frac{2}{c_b - c_w}(\phi_b - \phi_w) \tag{C.16}$$

where ϕ is a relative viscosity based on the pure fluid viscosity, $\phi \equiv \eta_f/\eta \equiv 1/\eta_r$. In the limiting case where $c_w \to 0$,

$$\frac{d\phi}{dc} - k(c,\gamma) = \frac{2}{c}(\phi - 1) \qquad (C.17)$$

where $k \equiv -(\frac{d\phi}{dc})_{c \to 0} = (\frac{d\eta_r}{dc})_{c \to 0}$ is the intrinsic viscosity.

The intrinsic viscosity is a commonly used empirical parameter in polymer rheology. Deviations from the Einstein value k=2.5 from equation (2.9) are used for determination of dispersion characteristics such as polydispersity, solvation, particle ellipticity, and molecular weight (see, for example, Hiemenz [1977], Chapter 2).

Equation (C.17) is integrated using the condition that in the limit as c approaches its packing concentration c_p, $\eta \to \infty$, $\frac{d\eta}{dc} \to \infty$ and the result is

$$\eta_r = \frac{1}{\phi} = (1 - \frac{1}{2}kc)^{-2} \qquad (C.18)$$

This expression is rigorously valid only for Newtonian viscosities, and the boundary condition as $c \to c_p$ is true only for rigid particles. Quemada argues, however, that in highly concentrated systems the two-phase flow model is still valid and that with appropriate modifications this equation is applicable to blood suspensions. The form of equation (C.18) is very similar to that of other equations modified from the Einstein equation, (2.9).

The non-Newtonian aspects of blood are related to changes in the particle morphology (from aggregation, plasma trapping, deformation, crowding, *etc.*) at changing concentration and shear rate. Equation (C.18) can be empirically modified to incorporate these effects in one of two ways:

First, k is defined as before, but c is now the volume concentration of *effective* particles, where an effective particle is defined as a statistically-averaged "typical" aggregation of individual units, including any trapped fluid. If cells aggregated without deforming or trapping fluid, then c would be constant no matter

the degree of aggregation. With fluid trapping, aggregation would lead to effective particles with a larger volume than the individual cells, and c would increase by a factor of $(1-\epsilon)^{-1}$, where ϵ is the porosity of the effective particle.

The alternative and more convenient method is to define c as before, equal to the volume percent of solids, but to now empirically incorporate the effective volume changes into k. To visualize this, two samples of suspensions of rigid, attracting particles can be imagined, each at identical concentration c, one at shear rate γ_1 and the other at $\gamma_2 > \gamma_1$.

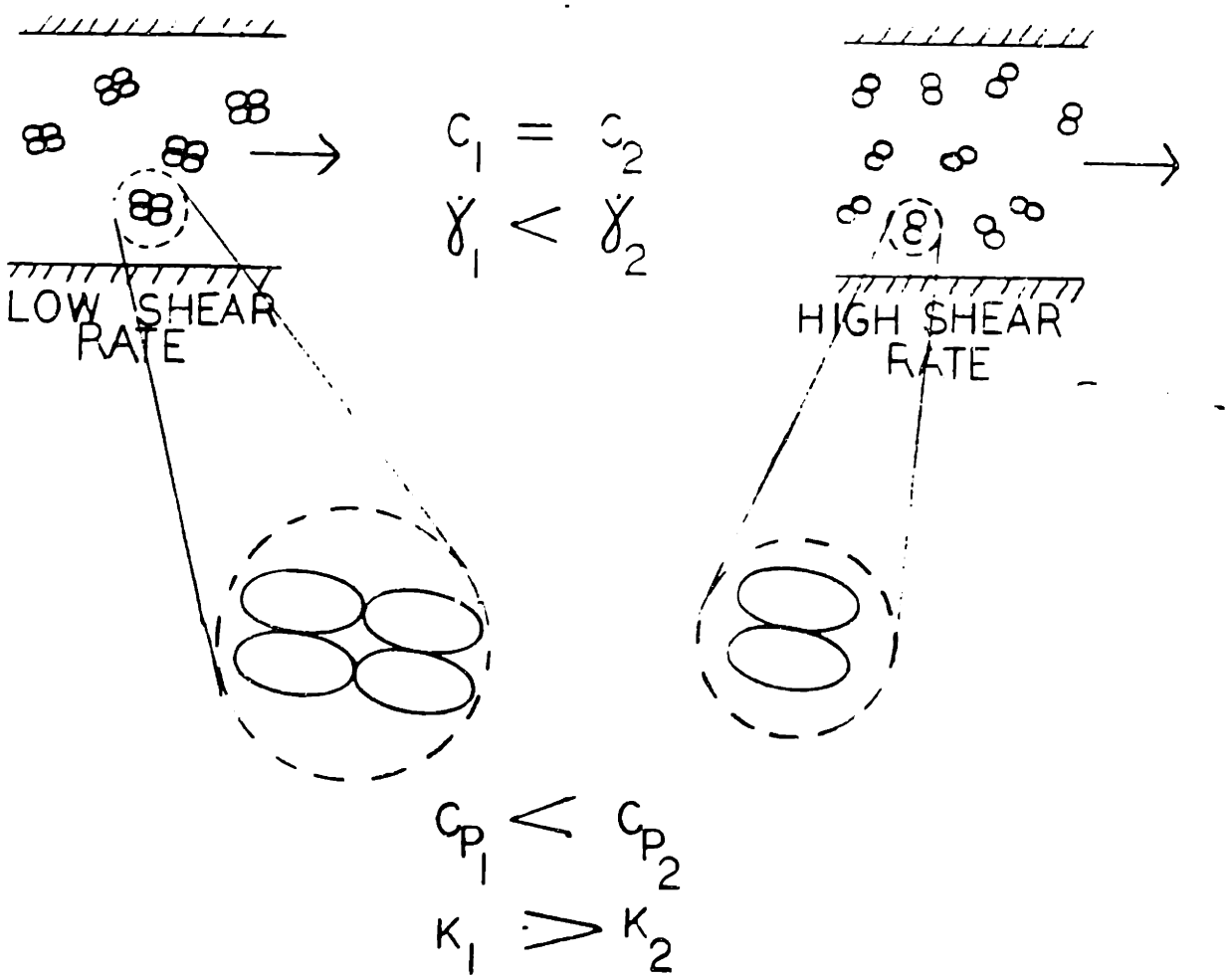

Figure C-1: Hypothetical comparison of two samples with identical solid concentrations at different shear rates.

As shown in Figure C-1, at γ_1, the average effective particle consists of four

units, and at γ_2, the average effective particle is two units. Because of the extra fluid trapping, the particles at γ_1 can not be packed as tightly as those at γ_2. If the packing concentration c_p is defined as the maximum volume concentration of solids achievable by packing the effective particles as closely as possible, then $c_{p1} < c_{p2}$. Also, as $c \rightarrow c_p$, $\eta \rightarrow \infty$ and from equation (C.18),

$$c_p = \frac{2}{k(c,\gamma)} \qquad (C.19)$$

Since in the above example $c_1=c_2$, the effect of increasing γ at constant c is to lower k, consistent with shear-thinning behavior. If the individual units could deform elastically and orient themselves along fluid streamlines, these effects would result in a further reduction of k with shear rate.

Thus, for relatively rigid particles, the intrinsic viscosity is proportional to the volume occupied by a single effective particle. For fluid particles such as red blood cells, equation (C.18) and especially equation (C.19) are true only in a qualitative sense, as the boundary condition of infinite viscosity at high concentration is obviously not justifiable. Nevertheless, Quemada [1981] has used this model to estimate the size and structure of red cell aggregates as a function of hematocrit and shear rate.

Continuing with the development for rigid spheres, it is at this point necessary to address the concentration and shear rate dependence of the intrinsic viscosity k. Simplifying to the case of constant concentration, Quemada proposes an expression for k based on a two limit relaxation model. Defining $k_0 = k(\gamma=0)$ and $k_\infty = k(\gamma$ large, but not high enough to disrupt individual units), the model assumes aggregate formation dependent on collision frequency and aggregate disruption by shear. At a constant concentration,

$$\text{for aggregation,} \quad \left(\frac{dk}{dt}\right)_A = \frac{1}{\tau_A}(k_0 - k) \tag{C.20}$$

$$\text{for disaggregation,} \quad \left(\frac{dk}{dt}\right)_D = \frac{1}{\tau_D}(k - k_\infty) \tag{C.21}$$

$$\frac{dk}{dt} = \frac{1}{\tau_A}(k_0 - k) - \frac{1}{\tau_D}(k - k_\infty). \tag{C.22}$$

where τ_A and τ_D represent the time constants for aggregation and disaggregation. At steady-state,

$$k = \frac{k_0 + \theta k_\infty}{1 + \theta} \tag{C.23}$$

where $\theta = \tau_A / \tau_D$.

For dilute suspensions of rigid spheres, the time constant for aggregation, τ_A, is assumed to be the inverse of the Brownian collision frequency as derived by Smoluchowski [1917]:

$$\tau_A = \frac{\pi \eta_f a^3}{2c\kappa T} \tag{C.24}$$

where a is the sphere radius, κ is Boltzmann's constant, and T is absolute temperature. This expression is comparable to both the time constant for translation of the particle over a distance equal to its radius and to the time constant for rotation of a sphere through π radians.

The time constant for disaggregation due to shear, τ_D, is assumed to be the inverse of the shear-induced collision frequency developed by Goldsmith and Mason [1967]:

$$\tau_D = \frac{\pi \gamma}{8c} \tag{C.25}$$

Combining equations (C.24) and (C.25),

$$\theta = \gamma_r \tag{C.26}$$

where the relative shear rate $\gamma_r = \gamma / \gamma_c$ and the critical shear rate γ_c is $\frac{\kappa T}{4\eta_f a^3}$. For

dilute suspenions of rigid spheres γ_c is roughly equivalent to the rotational diffusion coefficient. Equivalent ratios to θ appear frequently in the literature of polymer rheology. Batchelor [1976] described this ratio as a Peclet number $\frac{\gamma a^2}{D}$ which represents the time constant for diffusional rotation divided by the time constant for shear-induced motion.

For non-rigid paticles such as blood, the relaxation model must also incorporate time constants for changes in particle shape. Assuming that a basic functional relationship $\theta(\gamma_r)$ exists as it does for rigid particles, it then becomes necessary to formulate an expression for γ_c for deformable bodies. Using the Maxwell relaxation time, Quemada suggests

$$\gamma_c = \frac{E_i}{\eta_i} \qquad (C.27)$$

where E_i is the elastic modulus and η_i is the internal viscosity of the particle. Since $E_i \sim a^{-3}$, the variance with particle size is the same as for spheres.

Using equation (C.26) as a starting point, Quemada derived a semi-empirical relationship for concentrated suspensions:

$$\theta = \gamma_r^p \qquad (C.28)$$
$$\text{for} \quad 0 \le p \le 1$$

where for blood p≈0.5. Substituting equations (C.23) and (C.28) into equation (C.18) and rearranging leads to the final form of the equation:

$$\eta = \left(1 - \frac{c}{2} \cdot \frac{k_0 + k_\infty \sqrt{\gamma_r}}{1 + \sqrt{\gamma_r}}\right)^{-2} \qquad (C.29)$$

where k_0 and k_∞ are functions of concentration and γ_r is a function of concentration and directly proportional to the shear rate. In this work, the concentration dependences of the three rheological parameters k_∞, k_0, and γ_c are found from empirical fits to data.

To summarize, the Quemada equation is derived from a model of a concentrated suspension of rigid, attracting spheres in which two-phase viscometric flow is observed. Deviation of particle behavior from this model, such as deformability and fluidity, are incorporated empirically into the parameters.

The Quemada expression does not predict a yield shear stress *per se*, but in the limit of high concentration, $c \rightarrow c_p$, equation (C.29) can be shown to yield the Casson relation, equation (2.7) [Quemada, 1981]. In the limit of low shear, $\dot{\gamma} \ll \dot{\gamma}_c$, no yield shear stress is obtained and Newtonian behavior is recovered from the equation. Quemada argues that, while it is possible that blood may indeed have a yield shear stress, it is of almost negligible magnitude due to the smallness of the cohesive forces between cells. In the limit of high shear, $\dot{\gamma} \gg \dot{\gamma}_c$, a pseudo-yield stress can be extrapolated to zero shear rate.

Appendix D
Computer Program for Data Fitting

This is the FORTRAN computer program described in Section 3.4 for regression of data to non-linear functions. It is adapted from Zydney [1985].

```
      program datafit

      double precision b(5), bl(5), bo(5), f(5), fl(5), a(5,5),
      1 ainv(5,5), yl(200), dy(200,5), y(200), ee, el, ss,
      1 xtx(5,5), c(5,5), gamma(200), eta(200), delz(5),
      1 zval, zvalnew
      character*5 type, hct


c ASSIGN DIFFERENTIAL MUTIPLIERS AND CONVERGENCE REQUIREMENTS
      d1=0.999
      d2=.99
      c1=.001
      c2=.001

c READ IN DATA FROM DATAFILE
      print *, 'enter sample type and hematocrit'
      read *, type, hct
      open (unit=4,
     1   file=type(:len(type))//'dat'//hct(:len(hct))//'.dat',
     1   status='old')
      do 10 i=1,200
            read (4,501) gamma(i), eta(i)
501         format(2(f10.3))
            if (gamma(i) .eq. -100. .and. eta(i) .eq. -100.) goto 20
10    continue
20    n=i-1

c INPUT INITIAL GUESSES
      print *, 'cell volume fraction and number of unknowns'
      read *, h, ir
      do 30 i=1,ir
            print *, 'initial guess for unknown #',i,'?'
            read *, b(i)
30    continue

c LOOP TO EVALUATE RESIDUALS AND JACOBIAN
35     do 130 ii=1, ir+1
            do 80 jj=1, ir+1
c     CALCULATE SUM OF SQUARED RESIDUALS (SS)
c         AND SUM OF WEIGHTED SQUARED RESIDUALS (EE)
                  ee=0.
                  ss=0.
                  do 40 i=1,n
                        call predictval(gamma(i),y(i),b,h)
                        ee=ee+((y(i)-eta(i))/y(i))**2.
                        if (ii .eq. 1 .and. jj .eq. 1)
                              ss=ss+(y(i)-eta(i))**2.
                        endif
40                      continue
c     PRINT VALUE OF SUM OF SQUARES BEFORE DERIVATIVES ARE EVALUATED
```

```
                        if (ii .eq. 1 .and. jj .eq. 1) then
                                print *,'sum of weighted sqd residuals=',ee
                        endif
c       IF THIS IS THE FIRST PASS, THEN SET LAST VALUES (BL) EQUAL TO
c       CURRENT GUESSES (B) AND DO NOT EVALUATE DERIVATIVE
                        if (jj .eq. 1) then
                                el=ee
                                do 50 i=1,ir
                                        bl(i)=b(i)
50                              continue
                                goto 70
c       OTHERWISE, DETERMINE THE DERIVATIVE VALUE (F) FOR THIS B
                        else
                                f(jj-1)=(ee-el)/(b(jj-1)-bl(jj-1))
c       RESET B VALUES
                                do 60 i=1,ir
                                        b(i)=bl(i)
60                              continue
                        endif
c       MAKE SMALL CHANGE IN THE NEXT B AND START LOOP TO EVALUATE
c       NEXT F
70                      b(jj)=d1*b(jj)
80              continue
c       BEGIN DETERMINATION OF JACOBIAN (A)
c       ON FIRST PASS, MAKE OLD VALUES EQUAL TO CURRENT VALUES
                if (ii .eq. 1) then
                        do 90 i=1,ir
                                bo(i)=bl(i)
                                fl(i)=f(i)
90                      continue
                        goto 110
c       OTHERWISE, EVALUATE JACOBIAN FOR THIS F AND B
                        else
                                do 100 i= 1, ir
                                  a(i,ii-1)=f((i)-fl(i))/(bl(ii-1)-bo(ii-1))
100                             continue
                        endif
c       RESET B VALUES
110             do 120 i=1,ir
                        b(i)=bo(i)
120             continue
c       MAKE DIFFERENTIAL CHANGE IN NEXT B
                b(ii)=d2*b(ii)
130     continue
c END OF LOOP TO CALCULATE RESIDUALS AND JACOBIAN

c INVERT JACOBIAN AND RESET B VALUES
        call invert(ir,a,ainv)
        do 140 i=1,ir
                b(i)=bo(i)
140     continue
```

```
c MAKE NEXT GUESSES FOR B
        do 160 j=1,ir
                do 150 i=1,ir
                        b(j)=b(j)-f1(i)*ainv(j,i)
150             continue
160     continue

c CHECK FOR CONVERGENCE
        do 170 i=1,ir
                if (abs(1-b(i)/bo(i)) .gt. c1) goto 180
                if (abs(f(i)) .gt. c2) goto 180
170     continue

c ON CONVERGENCE, GO TO FINAL OUTPUT STAGE
        goto 200
c IF NOT CONVERGED, OUTPUT NEXT GUESS
180     do 190 i=1,ir
                print *, 'next guess for b(',i,')=',b(i)
190     continue
        goto35

c FINAL OUTPUT
200     do 260 jj=1, ir+1
                do 210 i=1,n
                        call predictval(gamma(i),y(i),b,h)
210             continue
c EVALUATE STANDARD DEVIATIONS FOR B VALUES
c       EVALUATE COMPONENTS OF X MATRIX (DY)
                if (jj .gt. 1) then
                        do 220 i=1,n
                                dy(i,jj-1)=(y(i)-yl(i))/(b(jj-1)-bl(jj-1))
220                     continue
                else
                        do 230 i=1,n
                                yl(i)=y(i)
230                     continue
                        do 240 i=1,ir
                                bl(i)=b(i)
240                     continue
                endif
                do 250 i=1,ir
                        b(i)=bl(i)
250             continue
                b(jj)=d1*b(jj)
260     continue
C       EVALUATE COVARIANCE MATRIX (C)
        do 290 i=1,ir
                do 280 j=1,ir
                        s=0.
                        do 270 k=1,n
                                s=s+dy(k,i)*dy(k,j)
```

```
270                     continue
                        xtx(i,j)=s
280             continue
290     continue
        call invert(ir,xtx,c)
        do 300 i=1,ir
                print *, 'standard deviation of b(',i,)=',sqrt(c(i,i)*ss/(n-ir))
300     continue

c CALCULATION OF CORRELATION COEFFICIENTS
        do 307 i=1,ir
                do 305 j=1,ir
                        corcoef=c(i,j)/sqrt(c(i,i)*c(j,j))
                        print *,'coeff.',i,'-',j,'=',corcoef
305             continue
307     continue

c CALCULATION OF 95% CONFIDENCE LIMITS EVALUATED AT GAMMA=.02,.2,2,20,200
c       GET STUDENT T VALUE AND ESTABLISH VALUES AT WHICH TO CALCULATE
        print *,'input student t value'
        read*, tval
        do 360 ij=-2,2
                gam=2.*10.**ij
c       CALCULATE DERIVATIVES
                call predictval(gam,zval,b,h)
                do 310 i=1, ir
                        bo(i)=b(i)
310             continue
                do 330 ii=1,ir
                        b(ii)=d2*b(ii)
                        call predictval(gam,zvalnew,b,h)
                        delz(ii)=(zval-zvalnew)/(bo(ii)-b(ii))
                        do 320 jj=1,ir
                                b(jj)=bo(jj)
320                     continue
330             continue

c       CALCULATE VARIANCE IN EQUATION AT THIS VALUE
                v=0.
                do 350 i=1,ir
                        do 340 j=1,ir
                                v=v+delz(i)*delz(j)*ss/(n-ir)*c(i,j)
340                     continue
350             continue
c       OUTPUT CONFIDENCE LIMITS
                print *, '95% conf. int. at shear rate',gam,'=',tval*sqrt(v)
360     continue
        end


c SUBROUTINE TO CALCULATE PREDICTED VALUES BASED ON THEORY
```

```
      subroutine predictval(xx,yy,b,h)
      double precision b(5), xx, yy
      yy=1./(1.-(b(1)+(b(2)-b(1))/(1+sqrt(xx/b(3))))*h/2.)**2.
      return
      end

c SUBROUTINE TO INVERT MATRIX
      subroutine invert(ir,rorigmatx,rinvmatx)
      double precision rorigmatx(5,5), rinvmatx(5,5)
      do 3 i=1,ir
            do 2 j=1,ir
                  rinvmatx(i,j)=0.
                  if (i .eq. j) rinvmatx(i,j)=1.
2           continue
3     continue
      do 60 j=1,ir
            i=j-1
10          i=i+1
            if (i .gt. ir) then
                  print *, 'singular matrix'
                  stop 100
            endif
            if (rorigmatx(i,j) .eq. 0) goto 10
            do 20 k=1,ir
                  q=rorigmatx(j,k)
                  qq=rorigmatx(i,k)
                  rorigmatx(j,k)=qq
                  rorigmatx(i,k)=q
                  q=rinvmatx(j,k)
                  qq=rinvmatx(i,k)
                  rinvmatx(j,k)=qq
                  rinvmatx(i,k)=q
20          continue
            t=1/rorigmatx(j,j)
            do 30 k=1,ir
                  rorigmatx(j,k)=t*rorigmatx(j,k)
                  rinvmatx(j,k)=t*rinvmatx(j,k)
30          continue
            do 50 l=1,ir
                  if (l .eq. j) goto 50
                  t=-rorigmatx(l,j)
                  do 40 k=1, ir
                      rorigmatx(l,k)=rorigmatx(l,k)+t*rorigmatx(j,k)
                      rinvmatx(l,k)=rinvmatx(l,k)+t*rinvmatx(j,k)
40                  continue
50          continue
60    continue
      return
      end
```

Appendix E
Notation

The dimensions given are in terms of mass (M), length (L), time (t), and temperature (T). When no dimensions are listed, the units are dimensionless, or they may vary.

a	radius of particle or rouleau, L.
A_c	contact area between cells in rouleau, L^2.
A_{ij}	component of jacobian matrix$=\frac{\partial F_i}{\partial b_j}$.
a_i	constants for Chien polynomials.
b_i	parameter of function Y to be fit to data.
c	cell volume fraction=H/100.
c_b	volume fraction of particles in bulk region.
c_p	packing concentration=2/k.
$c_{protein}$	protein concentration, ML^{-3}.
c_w	volume fraction of particles in wall layer.
D	dissipated energy of rouleau formation, ML^2t^{-2}.
$\mathcal{D}$	translational diffusivity, L^2t^{-1}.
E	elastic stored energy in rouleau, ML^2t^{-2}. sum of squared residuals.
E_i	elastic modulus, $ML^{-1}t^{-2}$.
F	auxiliary equation from method of Lagrange multipliers.
F_i	component of the matrix which represents the gradient of E$=\frac{\partial E}{\partial b_i}$.
f_i	independent variables of F.
H	hematocrit=100·c.
h	length of capillary, L.
K	kinetic energy of rouleau, ML^2t^{-2}. fitted parameter for centrifugation equation (3.2), $M^{-1}Lt^2$.
k	intrinsic viscosity.

k_0 intrinsic viscosity at zero shear rate.

k_{0i} parameter to fit k_0 as a function of c.

k_∞ intrinsic viscosity at high shear rate.

$k_{\infty i}$ parameter to fit k_∞ as a function of c.

L length of capillary or channel, L.

M torque exerted on inner cylinder of viscometer, ML.

N number of data points to fit to equation Y.

P number of parameters for equation Y.

p pressure, $ML^{-1}t^{-2}$.

Q volumetric flow rate, L^3t^{-1}.

Q_f volumetric flow rate of fluid, L^3t^{-1}.

Q_p volumetric flow rate of particles, L^3t^{-1}.

R radius of capillary, L.

R_i radius of inner cylinder of viscometer, L.

R_o radius of outer cylinder of viscometer, L.

S total entropy of fluid volume, $ML^2t^{-2}T^{-1}$.

s_x integrated surface area normal to x-direction, L^2.

T absolute temperature, T.

t time, t.

T_0 reference temperature, T.

U total internal energy of fluid volume, ML^2t^{-2}.

V total volume of fluid element, L^3.

v velocity, Lt^{-1}.

W work done by external surface and body forces on rouleau, ML^2t^{-2}.

x rectangular coordinate, L.

x_i rectangular coordinate, L.

X_{ij} component of matrix with elements $\frac{\partial Y_i}{\partial b_j}$.

Y function to be fit to data.

y rectangular coordinate, L.

y_i calculated values from function Y corresponding to experimental

value $y_{i,exp}$.

$y_{i,exp}$ experimental value corresponding to calculated value y_i.

Greek symbols

α shape factor for Einstein equation (2.9).

γ surface energy of cell membrane, Mt^{-2}.

$\dot{\gamma}$ shear rate, t^{-1}.

$\dot{\gamma}_c$ critical shear rate for Quemada equation (2.11), t^{-1}.

$\dot{\gamma}_{ci}$ parameter to fit $\dot{\gamma}_c$ as a function of c.

$\dot{\gamma}_r$ relative shear rate $=\dot{\gamma}/\dot{\gamma}_c$.

δ_{ij} Kronecker delta function.

ϵ local porosity=1-c.

$\bar{\epsilon}$ average porosity in a cell column.

ϵ_0 local porosity at zero compressive pressure.

η non-Newtonian viscosity, $ML^{-1}t^{-1}$.

η_b viscosity of suspension in bulk region, $ML^{-1}t^{-1}$.

η_f viscosity of suspending fluid phase, $ML^{-1}t^{-1}$.

η_r relative viscosity$= \eta/\eta_f$.

η_w viscosity of suspension in wall layer, $ML^{-1}t^{-1}$.

θ ratio τ_A/τ_D.

κ Boltzmann's constant, $ML^2t^{-2}T^{-1}$.

Λ Lagrange multiplier.

λ_i Lagrange multiplier.

μ Newtonian viscosity, $ML^{-1}t^{-1}$.

μ_N Casson Newtonian viscosity, $ML^{-1}t^{-1}$.

μ_p plasma viscosity, $ML^{-1}t^{-1}$.

μ_w water viscosity, $ML^{-1}t^{-1}$.

ν kinematic viscosity$=\eta/\rho$, L^2t^{-1}.

π 3.14159 . . . .

compressive pressure, $ML^{-1}t^{-2}$.

ρ_c density of erythrocyte, ML^{-3}.

ρ_f density of suspending fluid, ML^{-3}.

σ_y	standard deviation of function Y.
T	Taylor coefficient for equation (2.5).
τ	shear stress, $ML^{-1}t^{-2}$.
$\underline{\tau}$	stress tensor.
τ_A	time constant for rouleau aggregation, t.
τ_D	time constant for rouleau disaggregation, t.
τ_y	yield shear stress, $ML^{-1}t^{-2}$.
ϕ	relative viscosity$=1/\eta_r$.
ψ	control theory constraint, $\psi^2=(c_b-c)(c-c_w)$.
ω	angular velocity, radians/t.

Appendix F
Data From Viscosity Measurements

Listed in this appendix are the tables of data used in Chapter 4. Data is listed by hematocrit, and the beginning of different samples within a hematocrit is noted in the left-hand column. The beginning of data for a new hematocrit is delineated by a new set of column headings. A description of the units of blood and the various batches and samples obtained from the units is given in Table F-I. The Eagle's solution data begins on page 225, the plasma data begins on page 237.

Unit expiration date	anti-coagulant	Batch	suspending fluid	suspending fluid viscosity (cP)	days since drawing	days before expiration
27-AUG-84	CPD	16	Eagle's	0.69	11	10
11-SEP-84	CPD	18	Eagle's	0.69	25	2
27-SEP-84	CPD-A1	19	Eagle's	0.69	22	13
		20	Eagle's	0.69	25	10
21-DEC-84	CPD-A1	24	Eagle's	0.69	35	0
06-JUN-85	AS-1	29	plasma	1.05	9	33
		30	plasma	1.13	10	32
		31	plasma	1.21	11	31
06-AUG-85	AS-1	32	plasma	1.06	10	32
		33	Eagle's	0.69	12	30

Table F-I: Catalog of units and batches used in this work.

Table F-II: Data tables for Eagle's solution suspensions.

0 sample and hematocrit	1 shear rate (1/sec)	2 viscosity (cP)	3 relative viscosity
1 20-5	0 03	4066 671	5892 887
2 H=98 4	0 10	1609 959	2333 240
3	0 16	1126 194	1646 658
4	0 22	888 269	1287 491
5	0 29	731 250	1059 783
6	0 35	634 872	920 104
7	0 42	564 668	818 359
8	0 48	515 038	746 432
9	0 61	437 024	633 368
10	0 80	369 e37	535 735
11	0 87	346 768	502 562
12	0 99	322 404	467 252
13	1 13	294 675	427 0e5
14	1 18	293 125	424 819
15	1 40	263 096	381 299
16	1 43	262 084	379 835
17	1 66	240 920	348 590
18	1 69	242 420	351 333
19	1 93	224 486	325 342
20	1 94	226 007	327 54e
21	2 19	210 956	305 700
22	2 20	212 410	307 841
23	2 39	202 811	293 929
24	2 45	202 481	293 451
25	2 59	196 779	285 187
26	2 79	190 366	275 893
27	3 00	186 040	269 623
28	3 43	182 386	264 328
29	5 98	148 946	215 864
30	8 01	133 720	193 797
31	8 93	134 528	195 035
32	10 66	125 098	181 301
33	13 32	119 865	173 717
34	13 e4	121 914	176 687
35	15 98	116 576	168 951
36	16 19	118 452	171 670
37	18 73	116 117	168 286
38	19 29	115 e37	166 891
39	21 29	114 402	165 960
10	22 60	111 993	162 164
41	25 11	112 958	163 128
42	25 27	110 668	160 388
43	28 59	109 798	159 128
44	36 39	115 829	167 868
45	61 74	110 593	160 290
46	66 03	101 227	146 706
47	93 57	108 240	156 870
48	98 88	101 760	147 478
49	119 10	107 154	155 276
50	138 15	106 754	154 716
51	163 65	106 324	154 093
52	165 09	102 471	148 509
53	198 18	102. 664	148. 788
54	201 75	105 978	153 591
55	231 09	102 934	149. 180
56	239 88	103 e53	149 120
57	250 92	103 109	149 433
58	265 44	105 515	152. 920
59	277 38	103 374	149 817
60	299. 76	104 353	151. 236

0 sample and hematocrit	1 shear rate (1/sec)	2 viscosity (cP)	3 relative viscosity
1 20-3	0. 04	1920 301	2783 045
2 H=97. 2	0 10	908 883	1317 222
3	0 17	651 079	943 595
4	0 23	505. 837	732. 097
5	0 29	434 286	629. 400
6	0 42	339 943	492. 671
7	0 61	268 692	389 409
8	0 87	218. 062	316 032
9	0 93	211 825	306 993
10	1 0e	194 783	282. 294
11	1 38	169 747	246. 010
12	1 40	168 679	244 462
13	1 63	156. 552	226 897
14	1 73	152 379	220 839
15	1 89	146 224	211 919
16	2. 06	140 298	203 330
17	2 14	137 544	199 339
18	2 40	131 414	190 455
19	2 45	129 911	188 277
20	2 92	120 592	174 771
21	3 45	118 914	172 339
22	6 20	97 244	140 933
23	8 60	87 749	127 172
24	8 75	87 697	127 097
25	11. 29	82. 094	118 977
26	11 91	80 730	117 000
27	13 84	78 578	113 891
28	15 21	76 612	111 032
29	17 04	75 436	109 328
30	17 86	74 227	107 575
31	20 21	73 352	106 307
32	20 49	72 918	105 049
33	23 39	71 800	104 058
34	23 79	70 623	102 642
35	25 78	70 045	101 514
36	25 95	70 737	102 517
37	28 44	69 202	100 293
38	29 96	69 168	100 243
39	36 72	69 771	101 117
40	55 80	66 129	95 839
41	84 22	60 021	86 987
42	87 54	63 849	92 529
43	106 68	62 711	90 886
44	125 85	59 666	86 472
45	138 42	62 007	89 865
46	163 95	61 337	88 184
47	165 54	59 514	86 252
48	195 78	61 140	88 609
49	205 20	59 415	86 109
50	221 10	60 868	88 214
51	238 20	59 395	86 080
52	252 96	60 614	87 846
53	257 97	59 367	86 039
54	277 80	59 406	86 096
55	299 79	59 812	86 684

0 sample and hematocrit	1 shear rate (1/sec)	2 viscosity (cP)	3 relative viscosity
1 20-4	0 09	1357 419	1967 274
2 H=96 8	0 11	668 180	968 290
3	0 17	485 913	704 225
4	0 24	390 164	565 455
5	0 30	329 681	477 799
6	0 49	239 438	347 012
7	0 60	225 874	327 354
8	0 68	196 047	284 126
9	0 80	186 612	270 452
10	0 94	164 499	238 404
11	1 00	161 025	233 384
12	1 19	146 117	211 764
13	1 26	139 020	201 478
14	1 39	133 793	193 903
15	1 51	126 540	183 391
16	1 59	124 745	180 790
17	1 77	117 233	169 903
18	1 92	113 719	164 810
19	2 02	110 450	160 072
20	2 21	105 905	153 486
21	2 25	105 182	152 438
22	2 45	101 310	146 826
23	2 47	101 034	146 426
24	2 91	93 670	135 754
25	4 06	84 072	121 843
26	5 32	75 540	109 470
27	6 61	70 318	101 910
28	7 98	65 103	94 352
29	9 14	63 404	91 890
30	11 06	60 369	87 491
31	11 28	59 224	85 832
32	12 97	57 885	83 891
33	14 58	55 669	80 680
34	14 89	56 119	81 332
35	17 24	53 676	77 791
36	17 44	54 331	78 741
37	19 22	52 449	76 013
38	19 34	53 101	76 958
39	21 27	52 067	75 459
40	22 94	51 007	73 923
41	23 17	51 275	74 312
42	25 09	50 588	73 316
43	25 20	49 931	72 364
44	29 87	48 604	70 441
45	35 67	50 664	73 426
46	48 45	47 889	69 404
47	66 18	43 028	62 359
48	67 59	45 699	66 220
49	99 12	42 058	60 954
50	99 39	43 882	63 597
51	124 89	43 137	62 517
52	138 81	41 470	60 101
53	156 78	42 527	61 648
54	165 24	41 253	59 797
55	168 64	42 118	61 041
56	198 33	41 050	59. 493
57	226 77	41 815	60 601
58	231 30	40 934	59 325
59	291 33	40 778	59 099
60	299 76	41 103	59 570

0 sample and hematocrit	1 shear rate (1/sec)	2 viscosity (cP)	3 relative viscosity
1 19-6	0 03	1007 609	2619 723
2 H=96	0 09	673 443	97e 004
3	0 28	307 006	444 936
4	0 47	219 480	318 087
5	0 66	178 826	259 168
6	0 87	157 898	228 838
7	1 05	140 092	203 032
8	1 14	134 747	195 286
9	1 37	122 744	177 890
10	1 40	121. 600	176 232
11	1 62	112 673	163 294
12	1 73	109. 296	158 545

13		1 94	104 454	[illegible] 383	112	19-9	0 03	171[illegible] 111	2479 571
14		2 00	102 387	[illegible] 952	113	H=96	0 09	[illegible] [illegible]	963 864
15		2 19	98 756	[illegible] 125	114		0 15	434 [illegible]	630 379
16		2 20	98 197	[illegible] 314	115		0 22	345 [illegible]	521 149
17		2 43	94 234	[illegible] 600	116		0 28	285 [illegible]	413 539
18		2 46	93 415	135 284	117		0 35	252 [illegible]	365 842
19		2 79	88 957	128 933	118		0 47	209 [illegible]	303 759
20		2 84	93 397	135 358	119		0 66	171 [illegible]	246 400
21		3 00	86 931	125 987	120		0 74	162 864	237 494
22		6 02	69 412	100 597	121		0 85	149 [illegible]	216 042
23		7 30	63 798	92 461	122		1 07	132 104	191 455
24		9 20	61 115	88 572	123		1 17	126 368	183 142
25		10 61	57 522	83 365	124		1 40	115 025	166 [illegible]
26		13 02	55 976	81 125	125		1 43	114 466	165 893
27		13 26	54 569	79 086	126		1 69	106 391	154 170
28		15 98	53 715	77 848	127		1 73	104 897	152 [illegible]
29		16 55	52 103	75 512	128		1 94	99 567	144 [illegible]
30		18 76	51 711	74 943	129		2 00	98 214	142 309
31		19 88	50 267	72 851	130		2 20	94 656	137 103
32		21 32	50 448	73 113	131		2 26	93 189	135 [illegible]
33		22 53	49 199	71 303	132		2 39	91 675	132 862
34		24 52	49 164	71 252	133		2 53	88 881	128 813
35		25 20	48 284	69 977	134		2 99	83 138	120 490
36		27 08	48 379	70 114	135		3 41	82 364	119 368
37		28 53	47 350	68 623	136		5 97	67 290	97 522
38		29 98	47 330	68 594	137		8 00	59 978	86 925
39		34 30	48 760	70 667	138		8 50	60 561	87 770
40		55 50	45 297	65 648	139		11 05	56 578	81 997
41		72 57	43 034	62 366	140		11 30	54 944	79 629
42		87 18	43 014	62 339	141		13 59	53 740	77 884
43		98 91	42 220	61 188	142		14 60	51 907	75 228
44		118 98	41 634	60 340	143		16 77	51 354	74 426
45		132 06	39 800	57 681	144		17 25	50 221	72 784
46		156 48	41 123	59 599	145		19 89	48 920	70 903
47		171 69	39 560	57 333	146		19 96	49 785	72 152
48		189 15	40 508	58 707	147		23 15	48 292	69 980
49		204 75	39 370	57 058	148		23 87	47 344	68 614
50		220 95	40 231	58 306	149		25 86	46 804	67 832
51		237 78	39 213	56 830	150		26 35	47 298	68 544
52		246 42	40 078	58 084	151		28 56	45 899	66 551
53		271 74	39 965	57 920	152		29 98	45 134	65 [illegible]
54		277 35	[illegible] 232	56 858	153		33 30	43 956	70 805
55		299 76	39 518	57 272	154		59 01	44 291	64 190
56	19-8	0 03	2028 571	2939 958	155		73 17	42 530	61 638
57	H=96	0 10	779 310	1129 435	156		78 18	42 801	62 030
58		0 15	563 089	816 071	157		103 77	41 564	60 238
59		0 22	430 108	623 245	158		113 01	41 480	60 116
60		0 41	287 001	415 943	159		135 81	40 713	59 004
61		0 67	212 124	307 426	160		139 65	40 904	59 281
62		0 80	194 159	281 390	161		165 99	40 636	58 893
63		0 86	184 008	266 [illegible]	162		167 61	40 302	58 409
64		1 08	165 930	235 [illegible]	163		192 75	[illegible] 268	[illegible] 355
65		1 13	159 059	228 [illegible]	164		193 26	39 [illegible]	57 958
66		1 30	149 35[illegible]	215 [illegible]	165		218 79	39 782	57 655
67		1 40	142 053	205 874	166		219 63	39 [illegible]	57 771
68		1 56	136 077	197 213	167		246 12	39 621	57 422
69		1 70	127 510	184 797	168		250 71	39 [illegible]	57 448
70		1 82	126 095	182 746	169		292 83	38 [illegible]	56 820
71		2 06	118 222	171 336	170		299 76	39 168	56 765
72		2 07	116 585	171 062					
73		2 26	113 457	164 430					
74		2 39	111 471	161 552					
75		2 52	108 238	156 857					
76		2 64	106 900	154 929					
77		2 92	102 201	148 117					
78		3 28	102 697	148 836					
79		5 20	86 005	124 645					
80		8 00	73 070	105 899					
81		9 01	72 099	105 941					
82		10 66	68 207	98 851					
83		11 58	68 458	99 214					
84		13 48	65 977	95 619					
85		14 62	63 666	92 270					
86		16 04	63 717	92 343					
87		17 93	61 185	88 674					
88		17 96	62 286	90 270					
89		20 53	60 791	88 103					
90		21 28	59 499	86 230					
91		23 09	59 585	86 355					
92		23 96	58 316	84 516					
93		25 01	58 993	85 497					
94		28 63	56 629	82 [illegible]					
95		29 97	56 988	82 591					
96		37 11	59 418	86 113					
97		49 95	56 517	81 909					
98		81 63	53 510	77 591					
99		92 28	50 715	73 500					
100		113 52	51 462	75 336					
101		125 29	49 940	72 377					
102		145 35	51 290	74 333					
103		164 85	49 718	72 055					
104		170 73	50 [illegible]	73 [illegible]					
105		196 23	50 466	73 139					
106		197 97	49 432	71 641					
107		221 67	50 332	72 945					
108		231 03	49 266	71 [illegible]					
109		257 43	49 143	71 252					
110		299 95	50 075	72 572					
111		297 00	49 061	71 103					

0 sample and hematocrit	1 shear rate (1/sec)	2 viscosity (cP)	3 relative (viscosity)
1 18-5	0 04	1632 432	2365 840
2 H=95	0 11	817 318	1184 519
3	0 30	394 378	571 562
4	0 47	327 810	475 087
5	0 67	251 598	364 635
6	0 68	229 088	332 012
7	0 93	200 646	290 791
8	0 94	184 926	268 009
9	1 19	169 490	245 638
10	1 19	161 131	233 523
11	1 44	144 484	209 397
12	1 46	148 735	215 558
13	1 65	135 572	196 481
14	1 70	131 838	191 070
15	1 79	131 054	189 933
16	1 95	121 917	176 691
17	2 05	121 625	176 268
18	2 14	116 580	168 957
19	2 32	113 860	165 014
20	2 40	110 244	159 774
21	2 58	107 190	155 348
22	2 59	106 314	154 078
23	2 91	100 649	145 868
24	3 00	98 099	142 [illegible]
25	4 20	82 976	120 255
26	5 99	72 823	105 541
27	6 11	70 147	101 662
28	8 64	62 813	91 033
29	8 66	61 309	88 854
30	11 28	56 742	82 205
31	11 85	55 101	79 857
32	14 40	52 167	75 604
33	15 25	51 504	74 667
34	16 94	49 685	72 297
35	17 34	53 720	77 855
36	17 80	48 296	71 443
37	19 48	43 214	69 875

38			19 88	47 781		10		0 87	147 649		
39			21 41	47 162		11		0 87	141 426		
40			22 93	46 389		12		1 18	120 492		
41			23 20	46 280		13		1 27	116 947		
42			24 91	45 422		14		1 57	103 980		
43			25 85	45 065		15		1 66	100 231		
44			27 51	44 095		16		1 85	94 690		
45			29 48	43 555		17		2 06	90 052		
46			29 98	43 652		18		2 32	87 937		
47			46 81	42 156		19		2 46	85 320		
48			57 98	37 627		20		2 52	84 888		
49			58 37	38 570		21		2 85	80 015		
50			58 58	35 658		22		3 00	79 065		
51			82 66	35 319		23		4 91	66 209		
52			105 91	34 519		24		7 36	56 913		
53			119 19	35 668		25		8 09	55 640		
54			125 93	33 994		26		10 65	50 831		
55			144 69	34 916		27		11 90	49 899		
56			152 07	33 537		28		13 95	47 916		
57			176 49	34 277		29		15 72	46 431		
58			178 53	33 146		30		17 26	45 150		
59			211 47	32 934		31		19 54	44 372		
60			214 68	33 241		32		19 90	43 669		
61			237 87	33 755		33		22 09	43 222		
62			253 14	33 341		34		23 19	42 200		
63			270 99	32 647		35		24 63	42 187		
64			269 73	33 800		36		25 84	41 403		
65			299 79	32 803		37		27 16	41 552		
66			0 04	1773 984		38		28 49	40 584		
67	18-8		0 10	771 171		39		29 98	40 489		
68	H=95		0 29	361 983		40		30 60	44 216		
69			0 41	327 658		41		62 31	38 373		
70			0 55	239 284		42		66 33	37 122		
71			0 67	226 839		43		81 48	36 782		
72			0 74	198 450		44		100 59	35 789		
73			0 99	184 545		45		105 69	35 409		
74			1 07	164 356		46		138 81	34 709		
75			1 31	141 541		47		139 02	34 463		
76			1 33	140 999		48		170 73	34 124		
77			1 56	126 913		49		172 08	34 100		
78			1 60	130 002		50		202 44	33 632		
79			1 89	127 906		51		205 05	33 753		
80			1 82	117 189		52		231 36	33 536		
81			1 93	116 487		53		224 30	33 470		
82			2 07	109 593		54		277 53	33 228		
83			2 26	106 264		55		294 79	33 594		
84			2 33	103 351		56	19-5	0 04	1106 818		
85			2 52	100 464		57	H=24	0 10	520 809		
86			2 52	99 769		58		0 17	374 667		
87			2 71	96 888		59		0 23	303 121		
88			2 79	95 598		60		0 42	206 762		
89			3 00	92 653							
90			3 60	85 917							
91			5 33	73 746		61		0 61	164 328		
92			5 51	70 811		62		0 87	135 724		
93			7 42	62 859		63		0 94	133 429		
94			7 96	62 208		64		1 31	108 943		
95			9 97	56 758		65		1 40	107 574		
96			10 60	56 027		66		1 57	100 575		
97			12 52	52 708		67		1 80	95 447		
98			13 91	51 240		68		1 68	92 978		
99			15 08	50 030		69		2 06	89 419		
100			16 80	53 462		70		2 20	86 223		
101			17 63	47 484		71		2 39	83 730		
102			17 88	47 676		72		2 52	81 564		
103			19 55	46 777		73		2 59	81 039		
104			19 66	46 412		74		2 71	79 221		
105			22 11	45 436		75		2 86	77 547		
106			22 49	44 988		76		3 00	76 329		
107			24 65	44 342		77		3 03	78 168		
108			25 14	43 866		78		5 57	61 712		
109			27 19	43 436		79		7 48	55 598		
110			28 45	42 649		80		7 95	53 678		
111			29 97	42 599		81		9 39	52 204		
112			48 69	40 234		82		11 26	48 521		
113			60 30	35 970		83		11 92	48 616		
114			74 10	37 247		84		14 56	45 498		
115			79 98	34 771		85		15 11	45 880		
116			105 93	35 316		86		17 21	43 822		
117			106 56	33 742		87		17 66	44 336		
118			137 88	34 258		88		20 20	43 065		
119			139 50	33 000		89		20 91	42 297		
120			169 77	33 539		90		22 76	42 103		
121			172 59	32 513		91		23 14	41 353		
122			199 05	32 231		92		25 31	41 206		
123			201 51	33 065		93		25 79	40 429		
124			225 39	32 044		94		29 10	39 578		
125			233 28	32 697		95		29 94	43 086		
126			231 85	31 924		96		29 98	39 678		
127			288 81	32 474		97		61 74	37 026		
128			478 28	31 819		98		79 62	33 421		
129			499 73	31 944		99		99 83	34 584		
						100		112 47	32 222		
						101		125 40	33 684		
						102		145 59	31 733		
						103		157 52	33 047		
						104		179 68	31 420		
						105		182 76	32 649		
						106		208 26	32 347		
						107		211 74	31 269		
						108		241 00	32 068		
						109		244 68	31 192		
						110		265 41	31 943		
						111		277 44	31 185		
						112		299 79	31 432		

sample and hematocrit	shear rate (1/sec)	viscosity (cP)	relative viscosity
1 19-4	0 04	1284 252	1861 235
2 H=96	0 10	584 751	847 465
3	0 17	403 085	584 181
4	0 23	312 402	452 757
5	0 29	271 650	393 990
6	0 36	239 163	345 164
7	0 42	217 190	314 768
8	0 42	217 190	314 768
9	0 61	172 901	250 581

0 sample and hematocrit	1 shear rate (1/sec)	2 viscosity (cP)	3 relative viscosity
1 18-3	0 04	2052. 857	2975 155
2 H=93	0 17	671. 174	972 716
3	0 36	406. 339	588 897
4	0 61	289 932	420. 191
5	0 73	281. 421	407. 357
6	0 87	231. 372	335 612
7	1. 00	225 930	327 435
8	1 06	204 925	296 993
9	1 26	192. 593	279 120
10	1 32	180 370	261 646
11	1 57	164 364	238 499
12	1 66	162 638	235 707
13	1 82	152. 491	221 001
14	2 04	145 473	210 800
15	2. 14	139 519	202 201
16	2. 40	132. 957	192. 112
17	2. 45	131 956	191 241
18	2. 71	124 320	180 174
19	2 72	123. 271	178 654
20	2. 72	125. 146	181 371
21	2. 98	119 119	172 636
22	3. 00	119 468	173 113
23	4 63	96 766	140 241
24	4 68	98 673	143 004
25	7 32	82 297	119 271
26	9. 74	73 988	107 229
27	9 95	73 778	106 925
28	12. 60	68 866	99 806
29	12 91	68 162	98 786
30	15 46	64 882	94 032
31	15 92	65 401	94 784
32	16 44	71 390	103 406
33	18 02	62 649	90 796
34	19 25	61 643	89 336
35	20 59	60 945	88 32[illegible]
36	21 91	59 725	86 55[illegible]
37	23. 78	59 309	85 9[illegible]
38	24 58	58 510	84 7[illegible]
39	26 35	58 071	84 161
40	27. 23	57 207	82 909
41	29 98	56 637	82 083
42	42 03	55. 889	80 999
43	60 21	49 452	71 670
44	67 47	51. 645	74 84[illegible]
45	79 80	48 195	69 84[illegible]
46	92 73	49 563	71 8[illegible]
47	118 32	48 165	69. 80[illegible]
48	119 28	46 730	67. 7[illegible]
49	143 91	47 405	68 703
50	145 83	46 184	66. 9[illegible]
51	175 74	46 654	67 614
52	178 95	45 e24	66. 1[illegible]
53	201 24	46 266	67 052
54	218 e1	45. 238	65 562
55	239 37	45 858	66. 461
56	251 61	45 006	65. 226
57	264 84	45 635	66 138
58	278. 07	44 877	65 039
59	299. 76	45 086	65 342
60 18-6	0 04	1532 857	2221 532
61 H=93	0 17	514 795	746 080
62	0. 36	307 756	446 023
63	0 45	292 053	423. 265
64	0. 61	217. 294	314 919
65	0. 67	223. 792	324. 306
66	0 93	180 032	260 916
67	0 93	169 102	245. 075
68	1. 19	146 613	212. 483
69	1. 20	152. 643	221. 222
70	1. 51	129 041	187. 016
71	1 53	131 739	190 926
72	1 73	122. 506	177 545
73	1. 82	116 428	168. 736
74	2. 08	108 225	156 848
75	2. 13	109 401	158. 552
76	2 39	100. 914	146 252
77	2. 46	101 466	147 052
78	2. 65	96 151	139. 349
79	2. 79	94. 399	136. 810
80	3 00	90 909	131 752
81	3 00	91 393	132 454
82	5. 54	68 211	98. 857
83	6 65	65 005	94. 210
84	8 08	58 076	84. 168
85	9 29	56. 294	81. 586
86	10 64	52 525	76 123
87	11. 94	51. 319	74 375
88	14 45	47 509	68 854
89	15 25	47 128	68 301
90	17 40	49 483	71 714
91	17. 65	44 795	64. 862
92	18 55	44 307	64. 213
93	20 83	42. 648	61. 809
94	21 86	42 128	61 055
95	23 84	41 140	59 623
96	24 01	41 241	59 770
97	27 80	39 563	57 338
98	29 97	38 955	56 457
99	29 97	39 026	56. 559
100	42 81	37 631	54 538
101	60 09	33 125	48 007
102	68 25	34 044	49 339
103	79 86	31 649	45 868
104	87 39	32 e12	47 264
105	99 69	30 635	44 399
106	119 16	30 979	44 897
107	132 81	29 614	42 919
108	151 05	30 079	43 991
109	152 55	29 213	42 338
110	182 85	29 377	42 575
111	185 61	28 641	41 509
112	208 47	28 980	42 004
113	212 07	28 377	41 126
114	240 00	28 613	41 468
115	245 10	28 060	40 667
116	265 59	28 386	41 139
117	278 16	27 836	40 342
118	299 79	27 920	40 464
119 18-7	0 05	1243 790	1802 536
120 H=93	0 11	631 016	914 516
121	0 24	366 165	530 674
122	0 43	243 017	352 199
123	0 60	213 675	309 674
124	0 62	192 668	279 229
125	0 75	171 303	248 265
126	0 79	176 511	255 813
127	0 94	140 579	219 332
128	1 06	144 759	209 796
129	1 26	124 424	180 339
130	1 32	125 714	182 194
131	1 51	113 175	164 022
132	1 65	110 e27	160 329
133	1 75	105 394	152 745
134	1 77	103 872	150 539
135	1 92	101 595	147 239
136	2 02	96 749	140 216
137	2 18	93 911	136 103
138	2 34	89 254	129 354
139	2 45	88 657	128 488
140	2 53	86 141	124 842
141	2 58	86 336	125 134
142	2 71	84 228	122 070
143	2 72	83 414	120 890
144	2 98	79 996	115 976
145	3 66	71 575	103 752
146	6 21	56 042	81 220
147	7 29	54 039	78 312
148	9 25	48 979	70 984
149	9 39	47 684	69 107
150	11 91	44 647	64 706
151	11 94	44 006	63 777
152	14 50	41 463	60 094
153	15 21	41 185	59 e26
154	17 05	39 565	57 341
155	17 34	42 388	61 432
156	18. 51	38 793	56 222
157	20 23	37 763	54 729
158	21 83	37 033	53 671
159	22 14	36 933	53 526
160	24 69	35 962	52 119
161	25 13	35 e24	51. 629
162	27 23	35 237	51 060
163	27 74	34 812	50 452
164	29 98	34 391	49 842
165	42 78	32 819	47 564
166	59 61	28 636	41. 501
167	74 67	29 450	42. 681
168	100 02	28 044	40. 643
169	105 93	26 423	38 294
170	125 52	27 187	39 401
171	138 90	25 724	37. 281
172	157 35	26 482	38 380
173	176 37	26 144	37 890
174	178 56	25 193	36. 512
175	208 29	25 731	37. 291
176	211 56	24 950	36 159
177	238 08	24. 773	35 903
178	240 03	25 391	36 799
179	265 59	25 189	36 506
180	277 65	24 657	35 735
181	299 76	24 740	35 855

0 sample and hematocrit	1 shear rate (1/sec)	2 viscosity (cP)	3 relative viscosity
1 16-5	0 18	257 264	372 846
2 H=92	0 50	154 573	224 019
3	0 60	136 8ee	198 357
4	0 81	119 049	172 505
5	0 86	115 457	167 329
6	1 13	102 704	148. 846
7	1. 19	98 208	142 330
8	1 39	93 143	134 990
9	1 41	100 851	146 161
10	1. 52	89 143	129 193
11	1 71	85 707	124 213
12	1 85	82 936	120 197
13	1 96	81 160	117 623
14	2 18	77 212	111 901

15			2 28	76 529	113 915	109		231 63	32 463	47 048	
16			2 44	74 420	107 855	110		258 06	32 368	46 939	
17			2 60	73 534	106 571	111		285 62	33 104	47 977	
18			2 77	70 979	102 889	112		291 18	32 315	46 833	
19			2 80	69 943	100 787	113		298 79	32 578	47 214	
20			3 97	65 129	94 390	114	20-8	0 04	950 000	1376 812	
21			6 30	53 930	78 159	115	H=92	0 11	439 395	636 790	
22			7 78	52 641	76 291	116		0 17	324 961	470 378	
23			9 99	49 608	70 446	117		0 30	223 317	323 646	
24			10 94	48 177	69 822	118		0 42	205 143	297 309	
25			11 31	53 846	78 038	119		0 60	154 287	223 604	
26			12 88	45 398	65 794	120		0 82	144 252	209 104	
27			14 14	45 395	65 790	121		1 00	111 699	161 752	
28			15 53	43 540	63 101	122		1 06	110 175	159 674	
29			16 69	43 705	63 384	123		1 32	46 059	134 216	
30			18 84	41 965	60 817	124		1 93	91 498	132 606	
31			19 88	42 176	61 125	125		1 68	87 701	127 103	
32			21 14	40 764	59 078	126		1 70	85 955	123 997	
33			22 43	41 267	59 807	127		1 92	81 298	117 800	
34			24 79	39 671	57 784	128		2 02	78 771	114 141	
35			25 62	40 212	58 278	129		2 25	75 962	110 090	
36			26 76	39 420	57 130	130		2 33	74 361	107 770	
37			28 15	39 436	57 443	131		2 52	71 897	104 199	
38			29 41	38 706	56 086	132		2 59	70 915	102 775	
39			29 97	38 879	56 346	133		2 98	64 744	96 730	
40			30 39	40 967	59 372	134		4 87	54 418	78 867	
41			35 89	36 608	53 055	135		6 64	48 300	70 000	
42			39 94	34 134	49 470	136		7 42	46 748	67 751	
43			43 99	34 193	49 497	137		10 98	41 623	60 323	
44			88 42	32 770	47 493	138		11 24	41 249	59 781	
45			125 85	33 159	48 057	139		14 54	38 177	55 329	
46			139 05	32 039	46 433	140		15 69	37 630	54 536	
47			164 07	32 492	47 090	141		18 91	35 960	52 145	
48			172 17	31 713	45 961	142		19 92	35 764	51 832	
49			189 57	32 173	46 628	143		21 82	34 578	50 113	
50			205 11	31 490	45 638	144		23 34	34 407	49 865	
51			221 37	31 901	46 233	145		24 46	33 759	48 926	
52			231 27	31 268	45 315	146		25 88	33 032	48 742	
53			246 84	31 745	46 007	147		29 09	32 537	47 155	
54			257 67	31 191	45 204	148		41 55	31 810	46 101	
55			280 76	31 037	44 980	149		60 27	27 959	40 528	
56	18-4		0 04	1695 530	2457 812	150		79 74	[illegible] 349	41 084	
57	H=92		0 11	825 896	1196 664	151		99 [illegible]	[illegible] 127	38 300	
58			0 23	466 837	676 575	152		119 [illegible]	26 824	38 875	
59			0 43	304 232	440 962	153		139 [illegible]	25 422	36 843	
60			0 68	228 018	330 461	154		159 [illegible]	25 675	37 190	
61			0 73	236 459	342 955	155		180 [illegible]	25 630	37 145	
62			0 95	189 790	275 043	156		199 [illegible]	24 974	36 194	
63			1 00	190 181	275 625	157		219 99	25 365	36 761	
64			1 06	171 725	248 891	158		233 05	24 809	35 959	
65			1 26	162 892	236 075	159		264 45	25 105	36 384	
66						160		298 32	24 568	35 606	
67			1 38	147 460	213 717						
68			1 59	140 535	203 674						
69			1 70	130 663	189 367						
70			1 86	128 096	185 643						
71			2 02	119 459	173 104						
72			2 12	119 372	173 003						
73			2 27	113 071	163 871						
74			2 36	112 165	162 556						
75			2 58	106 818	154 800						
76			2 65	104 284	151 126						
77			2 85	101 517	147 120						
78			2 87	99 843	144 700						
79			3 00	99 029	143 520						
80			4 77	77 487	112 340						
81			6 71	69 150	100 217						
82			7 96	62 985	91 283						
83			10 51	57 165	82 848						
84			10 67	57 677	83 590						
85			10 92	63 324	91 774						
86			13 68	52 610	76 246						
87			13 97	52 652	76 307						
88			16 87	49 618	71 910						
89			17 28	49 392	71 583						
90			20 07	47 466	68 791						
91			20 59	47 174	68 368						
92			23 22	45 743	66 294						
93			24 53	45 336	65 704						
94			25 87	44 927	64 532						
95			27 06	44 414	64 368						
96			28 52	43 558	63 128						
97			29 98	43 270	62 710						
98			36 42	43 410	62 913						
99			61 92	38 978	56 490						
100			86 57	35 940	52 087						
101			93 60	36 602	53 048						
102			106 11	34 097	49 416						
103			119 13	35 470	51 406						
104			144 69	34 750	50 362						
105			159 60	33 075	47 935						
106			176 55	34 112	49 439						
107			195 57	33 624	49 020						
108			198 66	32 664	47 339						
109			227 37	33 441	48 465						

	Sample and Hematocrit	Shear rate (1/sec)	Viscosity (cP)	Relative Viscosity
1	19-10	0 04	805 691	1167 668
2	H=91	0 10	372 537	539 909
3		0 16	269 301	390 291
4		0 23	222 193	322 018
5		0 29	184 877	267 938
6		0 35	165 785	240 239
7		0 42	149 426	216 559
8		0 48	141 319	204 810
9		0 67	116 429	168 738
10		0 74	115 128	166 852
11		0 93	95 511	138 422
12		1 12	89 934	130 294
13		1 13	90 563	131 251
14		1 37	81 416	118 374
15		1 47	80 315	116 399
16		1 63	75 129	108 883
17		1 80	72 805	105 514
18		1 88	70 644	102 383
19		2 01	68 799	99 709
20		2 06	68 430	99 178
21		2 26	66 087	95 778
22		2 33	64 846	93 980
23		2 46	63 497	92 029
24		2 58	62 005	89 862
25		2 65	59 968	86 913
26		3 00	58 640	85 071
27		3 62	54 [illegible]	78 641
28		6 16	44 [illegible]	64 780
29		7 94	40 [illegible]	58 644
30		8 70	40 055	58 051
31		10 58	37 [illegible]	54 042
32		11 26	37 [illegible]	54 000
33		13 23	35 [illegible]	50 980
34		13 77	35 283	51 149
35		15 86	33 [illegible]	48 751
36		16 99	33 [illegible]	49 681
37		18 51	32 [illegible]	47 054
38		19 82	32 [illegible]	47 094
39		21 15	31 [illegible]	45 678
40		22 68	31 [illegible]	45 898
41		23 13	30 [illegible]	44 838
42		24 63	30 [illegible]	44 900
43		25 11	30 [illegible]	44 120
44		27 15	30 365	44 007
45		27 76	29 831	43 233
46		29 68	29 [illegible]	42 926
47		34 27	30 356	43 994
48		74 55	26 237	38 025

49		79.38	24.734	35.875
50		93.57	25.361	36.755
51		99.15	24.115	34.94[illegible]
52		118.77	23.693	34.33[illegible]
53		119.10	24.547	35.575
54		145.20	23.316	33.79[illegible]
55		150.93	23.942	34.699
56		178.32	22.905	33.196
57		189.12	23.441	33.972
58		217.95	22.698	32.896
59		233.55	22.987	33.314
60		237.78	22.597	32.749
61		250.98	22.532	32.655
62		265.56	22.831	33.088
63		284.13	22.411	32.460
64		299.76	22.538	32.664
65	20-9	0.04	814.179	1179.970
66	H=91	0.10	430.792	624.306
67		0.17	299.457	433.996
68		0.29	206.721	299.596
69		0.42	165.338	239.620
70		0.61	133.759	193.854
71		0.80	120.187	174.184
72		0.60	116.075	168.225
73		1.06	100.823	146.120
74		1.13	99.470	144.159
75		1.31	90.782	131.568
76		1.46	87.129	126.274
77		1.63	81.561	118.204
78		1.80	78.693	114.048
79		1.95	75.423	109.309
80		2.06	73.936	107.154
81		2.20	71.224	103.223
82		2.32	69.853	101.236
83		2.52	67.396	97.675
84		2.52	67.412	97.699
85		2.85	63.821	92.494
86		3.00	62.800	91.014
87		3.53	58.895	85.355
88		5.44	49.625	71.920
89		6.68	45.919	66.404
90		8.62	42.339	61.361
91		10.64	39.515	57.268
92		11.79	38.636	55.994
93		14.35	36.662	53.133
94		14.60	36.228	52.504
95		17.54	34.963	50.671
96		17.92	34.389	49.809
97		20.56	33.249	48.259
98		20.72	33.548	48.620
99		23.21	32.398	46.954
100		23.26	32.740	47.449
101		25.19	31.807	46.09[illegible]
102		25.79	32.020	46.406
103		29.15	30.865	44.732
104		30.63	32.566	47.197
105		56.10	29.556	41.386
106		75.09	27.167	39.372
107		92.40	25.584	37.078
108		94.26	26.273	38.077
109		113.40	25.608	37.113
110		132.00	24.648	35.722
111		138.90	25.043	36.294
112		164.94	24.218	35.099
113		170.79	24.548	35.577
114		198.06	23.909	34.651
115		202.59	24.226	35.110
116		224.52	23.697	34.343
117		228.03	24.023	34.816
118		244.29	23.600	34.207
119		253.53	23.861	34.581
120		272.40	23.789	34.477
121		284.01	23.413	33.932
122		299.76	23.536	34.110

	0 sample and hematocrit	1 shear rate (1/sec)	2 viscosity (cP)	3 relative viscosity
1	16-3	0.04	508.547	737.025
2	H=90	0.10	325.994	472.455
3		0.29	175.934	254.977
4		0.60	96.020	139.159
5		0.61	106.565	154.442
6		0.99	81.871	118.654
7		1.00	74.198	107.533
8		1.50	72.087	104.474
9		1.53	61.823	89.599
10		1.74	69.604	100.875
11		1.82	63.782	92.438
12		1.93	58.937	85.416
13		2.20	62.028	89.896
14		2.33	55.874	80.977
15		2.52	57.048	82.678
16		2.86	52.672	76.336
17		3.00	52.982	76.786
18		4.30	46.927	68.010
19		6.64	39.372	57.061
20		6.84	40.029	58.028
21		7.77	42.471	61.552
22		8.61	36.588	53.026
23		10.01	35.806	51.893
24		11.93	33.557	[illegible].028
25		13.21	33.352	[illegible].236
26		15.23	31.702	45.715
27		16.39	31.493	45.642
28		19.20	30.033	43.526
29		19.58	30.244	43.832
30		22.49	29.068	42.128
31		22.76	29.367	42.561
32		25.13	28.385	41.128
33		25.30	28.638	41.504
34		26.46	29.252	42.394
35		28.45	27.675	40.109
36		29.98	27.568	39.954
37		57.39	24.935	36.133
38		64.80	23.333	33.815
39		98.32	23.234	33.672
40		108.66	21.894	31.730
41		125.46	22.143	32.091
42		140.16	21.297	30.865
43		156.48	21.607	31.314
44		171.63	20.958	30.374
45		187.38	21.230	30.768
46		202.98	20.692	29.988
47		218.40	20.962	30.380
48		234.33	20.561	29.799
49		249.36	20.777	30.112
50		271.95	20.463	29.657
51		274.11	20.652	29.930
52		299.76	20.476	29.675
53	18-9	0.04	1106.294	1602.329
54	H=90	0.11	523.944	[illegible].339
55		0.23	312.580	453.014
56		0.30	263.101	[illegible]
57		0.42	207.431	300.625
58		0.43	222.[illegible]37	323.0[illegible]
59		0.55	174.533	253.091
60		0.66	169.683	[illegible]
61		0.68	154.574	224.0[illegible]
62		0.93	135.081	195.7[illegible]
63		1.00	122.219	17[illegible].126
64		1.19	115.369	167.9[illegible]6
65		1.25	107.180	155.333
66		1.45	101.731	147.455
67		1.51	96.837	140.343
68		1.71	89.942	130.205
69		1.72	92.352	133.843
70		1.76	88.515	128.283
71		1.99	84.978	123.157
72		2.02	82.724	119.890
73		2.25	79.899	115.796
74		2.54	75.196	[illegible]
75		2.34	76.813	111.323
76		2.51	75.046	108.765
77		2.53	73.885	107.[illegible]
78		2.78	71.069	102.[illegible]
79		2.98	68.636	[illegible].472
80		3.00	68.450	[illegible].214
81		4.89	52.221	75.683
82		7.31	45.267	65.604
83		8.05	42.013	60.888
84		9.95	39.771	57.639
85		11.87	36.291	52.596
86		12.59	36.283	52.564
87		14.43	34.022	49.307
88		15.29	33.829	49.028
89		16.65	36.126	52.357
90		16.98	32.353	46.888
91		17.69	32.076	46.487
92		19.52	31.020	44.957
93		20.53	30.712	44.510
94		21.44	30.221	43.799
95		23.17	29.636	42.951
96		23.99	29.348	42.533
97		25.81	28.640	41.5[illegible]7
98		26.55	28.597	41.445
99		28.46	27.929	40.477
100		29.98	27.719	40.172
101		42.15	26.540	38.475
102		66.48	22.676	32.864
103		73.98	23.297	33.764
104		92.79	21.403	31.019
105		105.84	21.[illegible]97	31.590
106		125.91	20.407	29.579
107		137.79	20.945	30.355
108		159.00	19.830	28.739
109		169.62	20.348	29.490
110		192.06	19.437	28.172
111		201.45	19.911	28.857
112		218.58	19.208	27.833
113		233.10	19.588	28.386
114		239.35	19.094	27.672
115		265.08	19.536	28.023
116		271.26	18.912	27.409
117		291.15	18.810	27.261
118		299.70	18.959	27.477

0 sample and hematocrit	1 shear rate (1/sec)	2 viscosity (cP)	3 relative viscosity
1 16-10	0.02	1315.741	1906.871
2 H=89	0.10	571.473	828.222
3	0.16	373.221	540.900
4	0.25	221.129	320.477
5	0.61	155.919	225.970
6	0.88	153.226	221.313
7	0.86	127.729	185.114
8	0.94	126.849	183.839
9	1.18	105.785	153.312
10	1.20	109.965	159.370
11	1.43	93.946	136.154
12	1.47	96.488	139.838
13	1.67	85.667	125.604
14	1.69	86.496	125.357
15	1.74	87.777	127.213
16	1.94	80.247	116.300
17	2.07	79.082	114.612
18	2.26	75.096	108.835
19	2.39	72.545	105.138
20	2.86	66.737	96.725
21	3.00	65.162	94.435
22	3.39	70.202	101.735
23	3.59	58.012	84.075
24	4.14	65.029	94.274
25	4.62	65.432	94.843
26	8.81	40.418	58.577
27	9.33	38.096	55.213
28	10.77	39.136	56.719
29	11.92	35.509	51.462
30	12.50	34.257	49.648
31	15.05	32.265	46.761
32	15.89	31.986	46.357
33	17.67	30.903	44.787
34	18.24	30.367	44.010
35	21.17	29.164	42.267
36	21.41	29.000	42.029
37	23.81	28.142	40.786
38	23.96	28.174	40.832
39	26.50	27.406	39.717
40	28.45	26.802	38.843
41	28.97	26.564	38.498
42	49.02	23.607	34.503
43	66.12	21.121	30.610
44	80.76	21.545	31.225
45	92.43	20.026	29.023
46	112.65	20.320	29.449
47	118.80	19.280	27.942
48	144.48	19.591	28.393
49	151.80	19.696	28.545
50	176.28	19.078	27.651
51	184.83	18.935	27.444
52	201.66	18.752	27.179
53	211.29	19.110	27.698
54	227.22	18.484	26.788
55	237.69	17.929	25.984
56	259.05	18.211	26.393
57	277.29	17.749	25.723

0 sample and hematocrit	1 shear rate (1/sec)	2 viscosity (cP)	3 relative viscosity
1 16-9	0.02	935.000	1355.072
2 H=87	0.09	381.053	552.251
3	0.10	184.511	267.407
4	0.15	267.689	387.955
5	0.33	164.163	237.917
6	0.58	116.624	169.020
7	0.71	109.996	159.414
8	0.77	102.078	147.939
9	0.96	93.886	136.067
10	1.01	87.819	127.274
11	1.27	80.819	117.129
12	1.32	79.515	115.239
13	1.59	73.187	106.068
14	1.63	72.584	105.194
15	1.90	67.245	97.457
16	2.00	66.013	95.671
17	2.22	63.634	92.223
18	2.31	64.013	92.772
19	2.31	61.850	89.638
20	2.47	61.029	88.448
21	2.62	58.883	85.338
22	2.72	58.931	85.407
23	2.97	56.829	82.361
24	3.13	43.061	62.407
25	7.29	39.284	56.930
26	9.95	35.747	51.807
27	10.57	35.823	51.917
28	13.25	32.716	47.414
29	13.77	33.059	47.912
30	16.56	30.853	44.714
31	16.97	31.146	45.139
32	19.88	29.443	42.671
33	20.15	29.763	43.135
34	22.70	28.791	41.726
35	22.83	29.763	43.135
36	23.18	28.241	40.929
37	25.83	27.996	39.994
38	25.63	27.876	40.420
39	28.49	26.897	38.971
40	29.97	26.766	38.781
41	48.30	24.242	35.130
42	66.48	23.674	34.312
43	80.10	23.674	34.312
44	96.19	20.884	30.267
45	105.60	20.574	29.817
46	112.88	20.056	29.067
47	127.28	19.753	28.629
48	145.65	19.427	28.155
49	179.62	19.120	27.710
50	178.83	18.936	27.444
51	207.54	18.794	27.238
52	211.83	18.609	26.970
53	235.23	18.391	26.654
54	239.19	18.565	26.905
55	253.09	18.266	26.472
56	264.75	18.439	26.723
57	284.67	18.116	26.255
58	299.73	18.184	26.354
59 20-10	0.04	610.204	884.354
60 H=87	0.11	321.008	465.229
61	0.17	233.919	339.013
62	0.30	161.647	234.271
63	0.36	147.103	213.193
64	0.43	131.783	190.990
65	0.49	122.454	177.470
66	0.67	107.824	156.267
67	0.74	96.491	139.842
68	1.00	86.565	125.487
69	1.06	80.[illegible]18	117.055
70	1.32	72.961	105.741
71	1.33	74.995	108.690
72	1.57	67.[illegible]59	97.480
73	1.66	67.240	97.459
74	1.83	63.103	91.469
75	1.92	62.412	90.452
76	2.08	59.138	85.707
77	2.19	59.103	85.657
78	2.24	56.539	81.941
79	2.58	54.590	79.123
80	2.59	54.213	78.576
81	2.89	52.349	75.868
82	3.00	51.291	74.335
83	3.56	48.430	70.190
84	5.47	39.221	56.842
85	7.37	35.079	50.839
86	9.25	32.481	47.074
87	9.92	31.897	46.228
88	12.56	29.463	42.700
89	13.11	29.279	42.433
90	15.22	27.830	40.333
91	16.31	27.317	39.590
92	17.86	26.664	38.643
93	18.86	26.487	38.387
94	19.86	25.907	37.546
95	21.42	25.651	37.175
96	22.49	25.101	36.378
97	23.96	24.944	36.151
98	24.48	24.581	35.625
99	26.50	24.400	35.367
100	28.45	23.765	34.442
101	29.58	24.726	35.849
102	29.97	23.636	34.252
103	54.96	21.337	30.923
104	79.41	18.870	27.346
105	80.40	19.806	28.708
106	93.12	19.340	28.029
107	112.17	18.767	27.199
108	119.10	17.909	25.955
109	137.70	18.209	26.390
110	152.22	17.462	25.308
111	156.96	17.907	25.952
112	185.19	17.107	24.793
113	188.82	17.545	25.428
114	218.28	16.876	24.458
115	220.59	17.271	25.030
116	244.74	16.743	24.265
117	246.12	17.106	24.791
118	265.26	17.002	24.641
119	277.68	16.646	24.125
120	299.79	16.731	24.248

0 sample and hematocrit	1 shear rate (1/sec)	2 viscosity (cP)	3 relative viscosity
1 16-4	0.04	476.056	689.936
2 H=86	0.10	210.888	305.635
3	0.17	171.174	248.078
4	0.23	137.227	198.880
5	0.30	111.618	161.765
6	0.42	99.436	144.107
7	0.49	92.563	134.149
8	0.74	75.040	108.754
9	0.80	76.695	111.094
10	0.93	68.037	98.604
11	1.19	61.708	89.432
12	1.20	63.236	91.646

13	1 44	56 959	32 549
14	1 53	57 261	32 987
15	1 64	53 715	31 846
16	1 93	51 958	29 722
17	1 99	51 236	29 255
18	2 26	48 038	27 420
19	2 27	47 642	27 046
20	2 92	46 026	26 704
21	2 99	45 376	25 762
22	3 85	43 771	25 430
23	3 97	40 957	23 356
24	6 12	33 675	19 804
25	7 31	30 701	17 494
26	9 30	29 409	16 622
27	11 28	27 072	15 215
28	12 90	26 953	15 062
29	14 58	25 321	14 497
30	15 68	25 427	14 851
31	17 90	23 962	14 728
32	18 24	24 493	15 467
33	20 79	23 672	14 307
34	21 22	23 191	13 610
35	23 33	22 907	13 196
36	23 86	22 531	12 654
37	26 94	23 280	13 290
38	29 15	21 545	12 225
39	37 29	21 440	12 072
40	56 43	19 537	10 814
41	79 29	17 386	9 197
42	89 17	18 050	9 159
43	105 66	16 794	8 309
44	120 00	17 138	8 838
45	151 89	16 640	8 116
46	151 95	16 160	8 420
47	177 42	15 317	8 038
48	191 61	15 860	8 986
49	202 83	15 092	8 302
50	217 89	15 675	8 717
51	234 57	15 864	8 020
52	250 99	15 545	8 529
53	260 04	15 759	8 859
54	290 52	15 397	8 314

0 sample and hematocrit	1 shear rate (1/sec)	2 viscosity (cP)	3 relative viscosity
1 24-1	0 04	362 590	525 490
2 H=72	0 11	194 286	281 574
3	0 17	131 194	190 136
4	0 30	94 248	136 591
5	0 49	74 338	107 736
6	0 73	63 562	92 119
7	0 80	52 230	75 688
8	1 12	49 720	72 058
9	1 26	49 758	72 171
10	1 51	44 924	65 107
11	1 59	44 327	64 242
12	1 83	41 136	59 617
13	1 92	40 630	58 884
14	2 25	37 542	54 409
15	2 37	37 500	54 348
16	2 45	36 369	52 709
17	2 66	35 525	51 486
18	2 85	33 902	49 133
19	3 41	25 912	37 554
20	7 32	22 434	32 513
21	8 61	21 192	30 713
22	11 28	19 059	27 622
23	12 44	18 331	26 567
24	15 26	16 965	24 587
25	15 62	16 908	24 504
26	18 57	15 808	22 914
27	19 45	15 496	22 748
28	22 56	14 809	21 462
29	23 63	14 638	21 649
30	25 82	14 367	20 881
31	29 53	10 729	15 545
32	45 18	12 102	17 539
33	68 28	10 207	14 794
34	77 34	10 444	15 136
35	101 70	9 462	13 713
36	109 47	9 695	14 051
37	128 76	9 110	13 203
38	135 03	9 331	13 523
39	167 40	9 005	13 051
40	169 80	8 701	12 610
41	199 65	8 824	12 788
42	210 30	8 492	12 307
43	231 57	8 660	12 551
44	243 96	8 344	12 093
45	284 49	8 233	11 932
46	297 99	8 369	12 129

0 sample and hematocrit	1 shear rate (1/sec)	2 viscosity (cP)	3 relative viscosity
1 24-3	0 04	839 680	1216 932
2 H=62	0 10	396 165	574 192
3	0 16	272 445	394 946
4	0 29	188 843	273 686
5	0 54	133 896	193 994
6	0 55	128 070	185 609
7	0 80	104 906	152 038
8	1 00	94 473	136 917
9	1 18	85 417	123 793
10	1 46	77 817	112 778
11	1 70	80 847	117 170
12	1 86	68 732	99 612
13	2 14	63 528	92 070
14	2 19	62 909	91 026
15	2 52	58 919	85 390
16	2 92	54 746	79 342
17	2 94	54 031	78 306
18	5 50	40 153	58 193
19	7 36	36 443	52 816
20	8 68	32 861	47 625
21	10 01	31 905	46 239
22	11 86	29 226	42 357
23	13 97	27 930	40 483
24	15 68	26 448	38 330
25	18 60	25 229	36 562
26	19 51	24 699	35 795
27	21 91	23 868	34 591
28	22 70	23 584	34 180
29	23 67	24 842	36 003
30	26 91	22 621	32 784
31	29 18	21 740	31 507
32	29 98	21 768	31 548
33	49 17	19 280	27 942
34	67 21	16 652	24 133
35	81 00	17 019	24 665
36	105 75	15 305	22 181
37	119 16	15 708	22 830
38	145 38	14 579	21 129
39	157 41	15 028	21 780
40	170 38	14 169	20 535
41	189 30	14 612	21 177
42	211 53	13 906	20 154
43	214 71	14 371	20 828
44	240 12	14 174	20 542
45	244 59	13 707	19 865
46	277 53	13 555	19 645
47	299 82	13 618	19 736

0 sample and hematocrit	1 shear rate (1/sec)	2 viscosity (cP)	3 relative viscosity
1 16-8	0 11	120 563	174 729
2 H=70	0 20	70 732	102 510
3	0 30	57 719	83 651
4	0 36	60 183	87 222
5	0 62	40 984	59 397
6	0 73	33 814	49 006
7	0 87	36 047	52 242
8	0 99	31 862	46 177
9	1 06	33 568	48 678
10	1 31	29 827	43 228
11	1 39	29 025	42 065
12	1 63	27 331	39 610
13	1 79	26 641	38 610
14	1 95	26 210	37 986
15	2 18	24 495	35 500
16	2 21	25 493	36 946
17	2 51	24 168	35 026
18	2 53	24 311	35 233
19	2 98	22 464	32 557
20	4 28	18 569	26 912
21	5 30	17 340	25 159
22	6 82	15 704	22 759
23	9 26	14 512	21 032
24	9 36	14 236	20 661
25	12 55	12 866	18 646
26	12 57	13 142	19 046
27	15 22	12 366	17 922
28	16 09	11 990	17 377
29	17 87	11 776	17 067
30	19 56	11 373	16 483
31	21 17	11 172	16 191
32	22 75	10 888	15 780
33	24 47	10 663	15 454
34	25 94	10 591	15 349
35	29 09	10 159	14 723
36	42 09	9 979	14 462
37	60 06	8 566	12 414
38	67 53	8 863	12 845
39	93 03	8 288	12 012
40	106 26	7 806	11 313
41	124 92	7 877	11 416
42	145 86	7 507	10 880
43	156 69	7 630	11 058
44	172 41	7 360	10 667
45	194 91	7 411	10 741
46	212 01	7 202	10 438
47	233 01	7 281	10 552
48	245 04	7 131	10 335

49		264 90	7 203	19 439
50		284 67	7 046	20 241
51		290 97	7 089	20 572
52		298 73	7 091	21 271
53	24-2	0 04	382 299	153 667
54	H=70	0 10	182 440	254 406
55		0 16	138 522	246 771
56		0 23	109 737	159 039
57		0 35	85 508	123 625
58		0 48	71 038	102 994
59		0 67	60 628	87 967
60		0 67	61 676	89 335
61		0 93	50 402	73 046
62		0 93	52 701	76 378
63		1 18	47 425	68 722
64		1 40	44 392	64 336
65		1 50	42 089	60 997
66		1 73	39 606	57 694
67		1 82	39 007	56 532
68		2 06	37 155	53 819
69		2 14	36 423	53 512
70		2 39	35 219	51 042
71		2 45	34 810	50 484
72		2 85	32 586	47 226
73		3 00	32 196	46 661
74		4 25	28 011	40 596
75		6 80	22 938	33 243
76		7 32	21 917	31 764
77		9 34	20 405	29 571
78		10 63	19 142	27 742
79		12 53	18 190	26 362
80		15 09	17 133	24 830
81		15 26	16 614	24 515
82		17 63	16 379	23 736
83		19 22	15 748	22 820
84		20 17	15 717	22 778
85		22 09	15 249	22 100
86		22 50	15 023	21 772
87		24 64	14 845	21 514
88		25 17	14 564	21 151
89		28 49	14 035	20 341
90		29 98	13 970	20 246
91		42 18	13 485	19 543
92		41 32	12 048	17 949
93		66 87	11 060	16 072
94		93 03	10 960	15 928
95		93 12	10 480	15 188
96		119 55	10 040	14 551
97		124 95	10 329	15 037
98		136 96	10 006	14 501
99		139 15	9 644	13 980
100		182 52	9 778	14 171
101		192 27	9 410	13 638
102		212 13	9 321	13 509
103		214 44	9 553	13 899
104		228 53	9 189	13 317
105		259 02	9 385	13 601
106		284 88	9 052	13 119
107		299 79	9 136	13 241

0 sample and Hematocrit	1 shear rate (1/sec)	2 viscosity (cP)	3 relative viscosity
1 24-7	0 40	84 771	122 857
2 H=68	0 59	71 596	103 762
3	0 87	67 903	98 410
4	0 91	64 226	93 098
5	1 23	49 976	72 429
6	1 33	33 574	48 659
7	1 49	34 342	49 771
8	1 79	40 298	58 403
9	1 81	32 863	47 628
10	2 13	43 278	62 722
11	2 19	25 356	36 749
12	2 38	37 765	54 732
13	2 53	28 360	41 142
14	2 64	30 296	43 907
15	2 73	33 447	48 474
16	2 93	25 349	36 738
17	4 12	28 871	41 842
18	7 30	20 386	29 545
19	7 35	18 171	26 335
20	11 13	17 811	25 813
21	12 00	16 754	24 281
22	14 33	15 987	23 170
23	15 98	14 685	21 282
24	15 88	14 692	21 293
25	15 96	15 356	22 255
26	20 06	14 219	20 607
27	20 25	13 153	19 062
28	20 28	13 243	19 193
29	26 45	13 286	19 255
30	28 59	12 020	17 420
31	29 97	12 727	18 445
32	35 10	13 222	19 162
33	66 93	10 081	14 610
34	87 05	10 762	15 641
35	86 04	10 711	15 523
36	98 85	10 349	14 999
37	110 07	9 249	13 404
38	117 99	10 003	14 497
39	143 58	9 609	13 926
40	152 79	8 659	12 549
41	175 44	9 236	13 386
42	169 91	8 594	12 455
43	207 33	8 909	12 906
44	225 57	8 332	12 075
45	232 74	8 733	12 657
46	264 57	8 992	13 032
47	285 09	8 232	11 930
48	299 82	8 367	12 126

0 sample and Hematocrit	1 shear rate (1/sec)	2 viscosity (cP)	3 relative viscosity
1 24-8	0 43	72 067	104 445
2 H=62	0 56	87 709	127 114
3	0 75	61 307	88 851
4	1 07	25 302	36 670
5	1 39	21 564	31 252
6	1 41	39 418	57 128
7	1 65	45 849	66 448
8	1 75	30 474	44 165
9	1 90	32 871	47 639
10	2 15	30 133	43 671
11	2 22	31 235	45 268
12	2 35	33 665	48 790
13	2 48	35 028	50 765
14	2 67	22 266	32 270
15	2 96	28 339	41 071
16	3 00	22 640	32 812
17	3 55	32 450	47 033
18	5 47	27 197	39 416
19	6 70	16 803	24 352
20	6 75	25 431	36 857
21	9 02	16 027	23 223
22	9 29	14 953	21 671
23	10 67	11 581	16 785
24	12 47	12 259	17 767
25	13 32	11 473	16 628
26	15 29	11 207	16 242
27	15 66	10 541	15 277
28	17 95	10 622	15 394
29	18 22	11 271	16 335
30	20 58	10 496	15 212
31	21 41	11 205	16 239
32	23 23	9 434	13 672
33	23 96	10 883	15 772
34	28 51	10 032	14 539
35	29 98	9 925	14 384
36	42 30	9 823	14 236
37	67 83	8 107	11 749
38	72 96	8 906	12 907
39	99 57	7 150	10 362
40	112 71	8 046	11 661
41	125 04	6 936	10 052
42	144 33	6 922	10 032
43	152 43	7 367	10 677
44	169 86	6 826	9 893
45	185 58	7 246	10 646
46	195 18	6 649	9 636
47	212 10	7 140	10 348
48	220 68	6 611	9 581
49	229 47	6 899	9 999
50	239 85	6 628	9 606
51	265 56	6 456	9 357
52	276 04	6 856	9 936
53	289 76	6 773	9 816

0 sample and Hematocrit	1 shear rate (1/sec)	2 viscosity (cP)	3 relative viscosity
1 16-11	0 33	30 832	44 684
2 H=59	0 39	29 094	42 165
3	0 58	25 052	36 307
4	0 71	22 420	32 493
5	0 83	21 478	31 417
6	1 07	21 133	30 628
7	1 09	21 231	30 770
8	1 26	20 162	29 220
9	1 46	19 725	28 587
10	1 51	18 496	26 806
11	1 84	17 950	26 014
12	1 88	18 288	26 449
13	2 15	17 517	25 387
14	2 25	17 804	25 803
15	2 40	17 109	24 839
16	2 56	16 881	24 465
17	2 72	16 560	24 000
18	2 91	16 478	23 881
19	2 87	16 586	24 038
20	3 00	16 665	24 152
21	3 56	15 143	21 946
22	6 65	12 155	17 616
23	6 79	12 586	18 241
24	9 29	10 970	15 898
25	9 30	11 025	15 977
26	11 85	10 415	15 094
27	11 94	10 352	15 003
28	14 40	9 958	14 432
29	15 26	9 628	13 955
30	17 59	9 294	13 472
31	17 90	9 179	13 305

32	20 53	8 854	12 632
33	21 40	8 855	12 903
34	23 64	8 507	12 329
35	24 59	8 513	12 328
36	26 46	8 129	11 701
37	28 97	8 055	11 674
38	30 09	7 398	10 722
39	31 62	6 475	9 384
40	33 26	5 793	8 338
41	36 97	5 985	8 674
42	38 72	5 475	7 935
43	112 50	5 667	8 213
44	119 43	5 325	7 717
45	128 06	5 443	7 888
46	145 77	5 186	7 516
47	163 65	5 316	7 704
48	165 57	5 110	7 406
49	182 91	5 240	7 594
50	192 03	5 015	7 268
51	208 44	5 145	7 457
52	211 77	4 979	7 216
53	230 67	5 058	7 330
54	238 29	4 935	7 152
55	259 17	5 012	7 264
56	277 92	4 884	7 078
57	299 70	4 905	7 109

0 sample and hematocrit	1 shear rate (1/sec)	2 viscosity (cP)	3 relative viscosity
1 1a-12	0 70	15 930	22 912
2 H=56	0 89	15 267	22.126
3	0 96	15 047	21 867
4	1 10	14 754	21 383
5	1 28	14 067	20 387
6	1 32	14 045	20 355
7	1 46	14 426	20 907
8	1 57	13 395	19 413
9	1 71	12 991	18 [illegible]
10	1 88	13 462	19 510
11	1 97	12 834	18 600
12	2 13	13 393	19 416
13	2 15	12 942	18 757
14	2 37	12 709	18 419
15	2 40	12 566	18 212
16	2 62	12 208	17 693
17	2 72	12 089	17 520
18	2 81	12 016	17 414
[illegible]	3 00	12 181	17 654
[illegible]	3 66	11 641	16 871
21	6 21	9 807	14 214
[illegible]	7 26	9 041	[illegible]
23	8 75	8 095	11 [illegible]
24	9 90	8 960	[illegible]
25	11 30	8 294	[illegible]
[illegible]	12 54	8 091	[illegible]
[illegible]	13 85	7 948	[illegible]
28	15 85	7 490	10.855
29	17 04	7 492	10 858
[illegible]	19 16	7 179	[illegible]
[illegible]	19 59	7 185	[illegible]
[illegible]	21 80	6 930	[illegible]
33	23 77	6 899	[illegible]
[illegible]	24 45	6 696	9 704
35	25 32	6 778	[illegible]
36	29 06	6 453	9 352
37	29 97	6 454	9 354
38	37 26	6 304	9 136
39	69 12	5 417	7 851
40	72 48	5 070	7 348
41	94 47	5 091	7 378
42	105 42	4 744	6 875
43	119 88	4 895	7 094
44	138 42	4 569	6 622
45	158 10	4 712	6.829
46	164 85	4 495	6.514
47	189 99	4 628	6 707
48	191 40	4 436	6.429
49	215 46	4 571	6 625
50	217 77	4 400	6 377
51	244 20	4 273	6.038
52	247 23	4 515	6 543
53	270 43	4 461	6 320
54	299 73	4 412	6 394

0 sample and hematocrit	1 shear rate (1/sec)	2 viscosity (cP)	3 relative viscosity
1 33-3	0 87	11 5050	16 674
2 H=48	1 00	12 5410	18 175
3	1 06	12 6630	18 352
4	1 32	11 3440	16 441
5	1 46	9 9990	14 346
6	1 64	10 3370	14 901
7	1 79	9 7970	14 199
8	1 95	9 5760	13.878
9	2 18	9 5400	13 826
10	2 27	8 6340	12 513
11	2 51	8 8680	12 852
12	2 93	8 4170	12.199
13	2 84	8 0500	11.679
14	3.00	9 0480	13.113
15	4 20	6 9850	10 [illegible]
16	6 66	6 4600	[illegible]
17	8 39	6 1250	[illegible]
18	8 91	6 0100	[illegible]
19	12 56	5 7890	[illegible]
20	12 98	5 7954	[illegible]
21	15 76	5 5540	8 049
22	15 87	5 5230	[illegible]
23	17 10	5 7620	[illegible]
24	18 32	5 3550	7 761
25	19 16	5 2860	7 661
26	20 89	5 1900	7 522
27	22 46	5 1140	[illegible]
28	23 42	5 0920	7 380
29	24 44	5 0330	7 294
30	25 97	4 9820	7 220
31	27 74	4 8770	7 068
32	29 97	4 8530	7 033
33	95 35	4 1540	6 020
34	79 77	3 7160	5 386
35	87 21	3 7560	5 443
36	112 77	3 5060	5 081
37	131 79	3 4790	5 042
38	145 80	3 3790	4 897
39	170 13	3 3570	4 865
40	185 46	3 2760	4 748
41	208 35	3 2760	4 748
42	218 55	3 2190	4 665
43	244 86	3 1850	4 616
44	246 57	3 2250	4 674
45	284 49	3 1550	4 572
46	299 73	3 1720	4 597

0 sample and hematocrit	1 shear rate (1/sec)	2 viscosity (cP)	3 relative viscosity
1 33-1	3 76	6 322	9 133
2 H=42	6 94	5 521	8 001
3	8 24	4 808	6 968
4	10 11	5 006	7 255
5	12 54	4 604	6 6 [illegible]
6	13 93	4 617	[illegible]
7	15 85	4 472	[illegible]
8	17 75	4 454	6 455
9	19 15	4 226	[illegible]
10	20 94	4 289	6 216
11	23 10	4 158	6 026
12	24 11	4 168	[illegible]
13	24 51	4 241	6 146
14	25 75	4 058	5 881
15	25 65	[illegible]	[illegible]
16	28 39	4 006	[illegible]
17	32 64	3 475	[illegible]
18	92 34	3 161	[illegible]
19	94 50	3 203	4 640
20	119 94	3 105	4 500
21	132 00	3 014	4 368
22	158 31	3 004	4 354
23	164 94	2 945	[illegible]
24	190 05	2 949	[illegible]
25	191 55	2 901	[illegible]
26	221 05	2 907	[illegible]
27	224 49	2 861	[illegible]
28	253 65	2 809	[illegible]
29	277 14	2 810	[illegible]
30	299 76	2 822	[illegible]

0 sample and hematocrit	1 shear rate (1/sec)	2 viscosity (cP)	3 relative viscosity
1 33-2	5 93	2 451	3 552
2 H=25	[illegible] 97	1 955	2 833
3	9 98	2 285	3 312
4	13 28	1 [illegible]	2 891
5	13 82	2.152	3 119
6	16 60	2 001	2 900
7	17 01	2 134	3 093
8	19 24	2 002	2 901
9	20 18	2 142	3.104
10	22 53	2 012	2 916
11	23 04	2 [illegible]	3 733
12	23 36	2 090	3 029
13	25.18	2 003	2 903
14	25 28	2 064	2 991
15	29 48	2 001	2 900
16	48 39	2 [illegible]	3 281
17	73 89	2 [illegible]	[illegible] 090
18	93 00	1 881	2 697
19	99 27	2 051	2 972
20	124 71	1 965	2 891
21	126 09	1 843	2.671
22	150 27	1 [illegible]	2 872
23	152 55	1 865	2 703
24	175 89	1 [illegible]	2 858
25	178 98	1 867	2.706
26	201 36	1 962	2 843
27	211 95	1 [illegible]	2.738
28	226 83	1 933	2 801
29	244 92	1 [illegible]	2 686
30	246 03	1 892	2 742
31	284 70	1 892	2 742
32	299 76	1 914	2 774

0 sample ant hematocrit	shear rate (1/sec)	2 viscosity (cP)	3 relative viscosity
1 33-5	24 21	1 341	1 940
2 Hm7	68 76	1 195	1 732
3	100 65	1 177	1 706
4	105 87	1 086	1 574
5	138 75	1 171	1 697
6	145 47	1 121	1 625
7	178 56	1 137	1 648
8	183 27	1 173	1 700
9	204 93	1 118	1 620
10	215 19	1 181	1 712
11	231 21	1 128	1 635
12	246 90	1 185	1 717
13	277 35	1 151	1 668
14	299 70	1 178	1 707

Table F-III: Data tables for plasma suspensions.

0 sample, hct, plasma visc	1 shear rate (1/sec)	2 viscosity (cP)	3 relative viscosity
1 31-7	0.04	2086.400	1724.298
2 H=98.1	0.10	926.471	765.679
3 1.21 cP	0.17	696.364	542.450
4	0.23	514.660	425.339
5	0.29	433.676	358.410
6	0.36	386.667	319.560
7	0.42	347.105	286.864
8	0.47	277.185	229.079
9	0.67	260.676	215.435
10	0.87	226.075	186.839
11	0.93	222.923	184.234
12	1.12	197.697	163.386
13	1.20	192.832	159.365
14	1.44	174.098	143.883
15	1.59	168.235	139.036
16	1.69	160.638	132.759
17	1.86	155.886	128.831
18	1.95	151.486	125.195
19	2.12	145.930	120.603
20	2.27	142.229	117.545
21	2.39	138.593	114.540
22	2.52	135.784	112.218
23	2.92	127.621	105.472
24	3.00	127.060	105.008
25	3.62	122.020	100.843
26	5.34	103.200	84.942
27	5.97	99.799	82.479
28	7.44	95.685	79.079
29	8.60	89.784	74.202
30	9.98	88.311	72.984
31	11.24	84.285	69.657
32	12.53	83.605	69.095
33	13.89	80.295	66.326
34	15.11	80.298	66.342
35	17.20	76.971	63.612
36	18.30	77.341	63.918
37	19.84	75.064	62.034
38	20.21	75.861	62.695
39	22.48	73.485	60.731
40	22.76	74.268	61.379
41	25.12	72.116	59.600
42	25.31	73.035	60.360
43	28.43	70.827	58.535
44	29.64	75.911	62.736
45	29.97	70.768	58.486
46	48.72	69.458	57.403
47	73.29	62.035	51.285
48	74.16	69.838	54.428
49	99.66	64.028	52.916
50	99.72	61.312	50.671
51	118.65	63.287	52.303
52	126.15	60.809	50.255
53	144.21	62.935	51.698
54	145.92	60.547	50.039
55	169.68	62.023	51.259
56	172.53	60.320	49.851
57	192.27	60.165	49.723
58	195.09	61.633	50.936
59	218.73	60.074	49.648
60	220.44	61.323	50.680
61	238.47	60.033	49.614
62	246.00	61.110	50.504
63	271.29	60.953	50.374
64	284.88	59.909	49.512
65	299.70	60.300	49.835

0 sample, hct, plasma visc	1 shear rate (1/sec)	2 viscosity (cP)	3 relative viscosity
1 29-4	0.04	1884.211	1794.487
2 H=97.6	0.10	888.630	846.314
3 1.05 cP	0.17	617.722	588.307
4	0.23	500.130	476.314
5	0.36	374.350	356.524
6	0.55	296.057	281.959
7	0.74	247.870	236.067
8	0.93	195.210	185.914
9	1.00	208.562	198.630
10	1.19	172.169	163.970
11	1.25	182.565	173.871
12	1.39	158.714	151.156
13	1.44	168.526	160.501
14	1.59	147.430	140.410
15	1.70	155.563	148.155
16	1.79	139.117	132.492
17	1.95	141.274	134.547
18	1.99	132.085	125.795
19	2.18	126.910	120.867
20	2.27	129.171	123.020
21	2.38	121.683	115.889
22	2.52	123.273	117.403
23	2.78	115.641	110.134
24	2.95	107.325	102.214
25	3.00	112.693	107.327
26	6.13	79.491	75.706
27	8.67	71.080	67.698
28	9.27	70.754	67.385
29	11.23	68.643	65.377
30	11.92	68.225	64.214
31	13.76	62.330	59.381
32	14.57	61.952	59.002
33	16.31	59.673	56.831
34	17.20	59.096	56.282
35	18.86	57.716	54.968
36	19.85	57.237	54.607
37	20.79	56.522	53.830
38	21.82	55.898	53.236
39	23.32	55.178	52.550
40	25.13	53.791	51.230
41	25.24	54.327	51.740
42	27.14	53.476	50.930
43	28.43	52.501	50.001
44	29.97	52.207	49.721
45	30.27	62.240	59.276
46	42.93	58.001	55.239
47	68.43	53.617	51.064
48	92.94	50.000	47.619
49	93.72	51.601	49.144
50	119.34	48.768	46.446
51	125.55	50.131	47.744
52	145.80	48.107	45.816
53	157.50	49.143	46.803
54	172.23	47.553	45.289
55	189.27	48.518	46.208
56	198.60	47.130	44.886
57	221.07	48.012	45.726
58	231.57	46.820	44.590
59	251.43	46.665	44.443
60	252.93	47.646	45.377
61	271.95	47.468	45.208
62	284.58	46.584	44.366
63	299.73	46.852	44.621

0 sample, hct, plasma visc	1 shear rate (1/sec)	2 viscosity (cP)	3 relative viscosity
1 29-1	0.03	2501.786	2382.653
2 H=97.3	0.10	1038.509	989.056
3 1.05 cP	0.16	712.406	678.482
4	0.22	555.674	529.213
5	0.29	473.069	450.542
6	0.35	428.400	408.000
7	0.48	347.712	331.154
8	0.67	292.253	278.336
9	0.86	249.948	238.046
10	0.94	236.474	225.213
11	1.05	222.273	211.689
12	1.27	199.306	189.891
13	1.31	197.704	188.290
14	1.60	173.117	164.778
15	1.63	177.716	169.253
16	1.93	160.006	152.387
17	1.94	161.925	154.214
18	2.26	146.750	139.762
19	2.26	147.826	140.787
20	2.46	141.171	134.449
21	2.92	141.486	134.749
22	2.72	136.586	130.082
23	2.99	131.693	125.422
24	4.31	96.446	91.853
25	6.85	80.061	76.249
26	9.93	72.724	69.261
27	10.61	71.622	68.211
28	12.58	66.531	63.363
29	13.91	65.703	62.574
30	15.77	63.197	60.188
31	17.22	62.154	59.194
32	18.97	60.446	57.569
33	20.52	59.225	56.405
34	20.88	59.124	56.309
35	23.15	57.678	54.931
36	23.41	57.701	54.953
37	25.14	56.761	54.058
38	25.96	56.725	54.024
39	27.78	55.464	52.823
40	29.98	55.834	53.179
41	29.98	54.964	52.347
42	36.66	54.583	51.984
43	55.83	50.779	48.361
44	81.15	48.503	46.193
45	92.19	46.241	44.039
46	106.65	47.314	45.061
47	131.76	44.968	42.827
48	138.54	46.405	44.179
49	164.76	44.538	42.417
50	176.79	45.647	43.473
51	191.31	44.293	42.146
52	208.65	45.248	43.093
53	217.65	44.025	41.929
54	240.39	44.890	42.752
55	244.08	43.879	41.790
56	265.89	44.691	42.563
57	270.48	43.800	41.714
58	290.31	43.005	41.719
59	299.76	44.105	42.005

0 sample, hct, plasma visc	1 shear rate (1/sec)	2 viscosity (cP)	3 relative viscosity
1 29-9	0.04	1484.507	1413.816
2 H=97	0.11	701.695	668.281
3 1.05 cP	0.17	485.816	462.682
4	0.23	392.031	373.363
5	0.30	337.033	320.984
6	0.36	298.671	284.449
7	0.55	229.614	218.680
8	0.74	196.769	187.399
9	0.93	175.531	167.172
10	0.93	171.842	163.659
11	1.12	154.109	146.770
12	1.20	152.484	145.223
13	1.31	144.011	137.153
14	1.50	133.425	127.071
15	1.57	131.307	125.054
16	1.79	123.397	117.711
17	1.82	121.296	115.520
18	2.02	115.617	110.111
19	2.06	115.862	110.345
20	2.27	110.462	105.208
21	2.32	109.792	104.564
22	2.52	105.481	100.458
23	2.52	105.372	100.354
24	2.78	101.089	96.275
25	3.00	98.489	93.799
26	3.69	93.328	88.884
27	5.60	79.336	75.558
28	8.15	69.613	66.298
29	9.25	67.521	64.304
30	10.06	65.453	62.334
31	12.56	61.667	58.730
32	13.87	59.939	57.085
33	15.66	57.889	55.132
34	17.06	56.997	54.283
35	19.18	54.975	52.357
36	19.61	55.156	52.530
37	22.15	53.602	51.050
38	22.47	53.104	50.575
39	24.69	52.205	49.719
40	25.12	51.702	49.240
41	26.60	51.488	49.036
42	27.76	50.735	48.319
43	29.91	53.360	50.819
44	29.97	50.035	47.652
45	61.71	45.843	43.660
46	92.97	42.046	40.044
47	93.54	43.008	40.960
48	125.28	41.475	39.500
49	125.97	40.532	38.602
50	150.81	40.820	38.876
51	152.52	39.910	38.010
52	178.83	39.389	37.513
53	188.88	40.025	38.119
54	205.23	39.029	37.170
55	220.71	39.568	37.684
56	238.08	38.710	36.867
57	252.48	39.259	37.390
58	271.62	39.110	37.248
59	284.34	38.500	36.667
60	299.73	38.565	36.724

0 sample, hct, plasma visc	1 shear rate (1/sec)	2 viscosity (cP)	3 relative viscosity
1 29-9	0.03	1869.565	1780.538
2 H=96	0.10	746.951	711.382
3 1.05 cP	0.16	564.750	537.857
4	0.23	440.691	419.706
5	0.29	382.158	363.960
6	0.42	300.793	286.470
7	0.61	240.967	229.492
8	0.73	226.137	215.369
9	0.80	206.243	196.422
10	1.00	189.210	180.200
11	1.05	178.164	169.680
12	1.26	167.476	159.501
13	1.37	157.071	149.591
14	1.59	150.691	143.477
15	1.63	147.060	140.057
16	1.86	140.055	133.386
17	1.95	135.615	129.157
18	2.12	131.231	124.982
19	2.20	128.673	122.546
20	2.38	124.651	118.715
21	2.46	122.658	116.817
22	2.91	114.906	109.434
23	3.01	115.269	109.780
24	5.94	92.262	87.869
25	7.97	81.212	77.345
26	8.09	81.751	77.858
27	10.64	75.853	72.241
28	11.27	73.763	70.250
29	13.18	71.471	68.068
30	13.93	69.917	66.207
31	15.72	68.479	65.218
32	16.55	66.848	63.665
33	17.64	66.859	63.675
34	19.87	64.231	61.172
35	20.17	64.622	61.735
36	22.49	62.647	59.664
37	22.73	62.944	59.947
38	24.64	61.907	58.959
39	25.14	61.093	58.184
40	26.55	61.017	58.111
41	27.80	59.914	57.061
42	29.97	59.249	56.428
43	30.06	62.874	59.880
44	49.11	56.284	53.599
45	68.13	53.192	50.659
46	86.07	48.310	46.010
47	87.27	51.289	48.847
48	106.32	49.887	47.511
49	119.16	46.579	44.742
50	131.82	48.612	46.297
51	145.47	46.278	44.074
52	157.29	47.797	45.521
53	172.05	45.789	43.609
54	182.82	47.145	44.900
55	204.96	45.389	43.228
56	208.29	46.695	44.471
57	231.36	45.124	42.975
58	252.75	46.065	43.871
59	264.48	44.896	42.758
60	271.65	45.864	43.680
61	277.31	46.417	44.207
62	290.85	44.796	42.663
63	299.70	45.135	42.986
64 31-1	0.04	2177.444	1799.540
65 H=96	0.10	951.163	786.085
66 1.21 cP	0.17	641.220	529.942
67	0.23	543.937	449.535
68	0.29	438.940	362.760
69	0.36	393.792	325.448
70	0.42	344.690	284.868
71	0.49	312.801	258.513
72	0.74	249.716	206.377
73	0.93	211.097	174.460
74	1.12	199.091	164.536
75	1.31	183.771	151.877
76	1.50	164.858	136.246
77	1.68	163.929	135.479
78	1.69	163.362	135.175
79	1.89	152.417	125.964
80	2.08	143.600	118.678
81	2.27	139.019	114.892
82	2.46	134.496	111.154
83	2.65	128.497	106.196
84	4.22	102.914	85.053
85	7.40	82.050	67.810
86	9.27	76.731	63.414
87	9.95	74.118	61.255
88	11.91	70.385	58.169
89	12.50	67.788	56.023
90	14.55	66.007	54.551
91	15.04	64.971	53.693
92	16.54	62.329	52.503
93	17.59	62.265	51.459
94	19.18	60.901	50.331
95	20.14	59.908	49.511
96	21.84	58.626	48.451
97	22.68	58.341	48.216
98	23.81	57.357	47.402
99	24.60	57.188	47.263
100	25.80	56.158	46.412
101	27.11	55.521	45.885
102	27.14	55.897	46.196
103	29.76	54.310	44.884
104	35.88	53.930	44.570
105	42.24	52.131	43.083
106	61.38	48.289	39.908
107	85.74	44.682	36.927
108	93.27	45.191	37.348
109	118.71	42.937	35.485
110	118.77	43.698	36.114
111	150.66	42.573	35.184
112	151.95	41.935	34.657
113	176.13	41.932	34.671
114	184.89	41.230	34.074
115	201.63	41.467	34.270
116	217.89	40.782	33.704
117	220.74	41.207	34.055
118	244.35	40.430	33.413
119	246.18	40.921	33.819
120	265.29	40.755	33.682
121	277.44	40.160	33.190
122	299.73	40.236	33.253

0 sample, hct, plasma visc	1 shear rate (1/sec)	2 viscosity (cP)	3 relative viscosity
1 30-2	0.040	1705.263	1509.082
2 H=95	0.100	807.580	714.673
3 1.13 cP	0.170	613.745	543.135
4	0.220	474.805	420.181
5	0.290	389.613	344.790
6	0.360	344.677	305.024
7	0.421	304.484	269.455
8	0.610	247.134	218.703
9	0.730	245.768	217.494
10	0.800	214.275	189.624
11	0.990	201.207	178.059

12	1.060	182.468	161 476
13	1.250	165.353	146 330
14	1.260	173 124	153 207
15	1.500	151.986	134 501
16	1.520	156.679	138.654
17	1.700	142.276	125 908
18	1.790	142.388	126 007
19	1.890	134.182	118 745
20	2.050	132.048	116 857
21	2.140	126.959	112.353
22	2.320	123 728	109 494
23	2.390	120.316	106 474
24	2.400	121.402	107 435
25	2.520	118 321	104 709
26	2.650	114 522	101 347
27	2.850	111.078	98 299
28	3 000	109.388	95 919
29	4.940	86.278	76 352
30	7 490	72.527	64 183
31	9.280	68.429	60 734
32	10.040	65.202	57.701
33	12.380	61.445	54 376
34	12.590	60.262	53 329
35	15.130	56.811	50 275
36	15.230	57.573	50 950
37	17.680	54.326	48 076
38	19.200	53.148	47.034
39	20 210	52.205	46 199
40	22.490	50.834	44 986
41	23.390	50.224	44 446
42	24 480	49 540	43 841
43	25.310	49 259	43 592
44	27.130	48.020	42.496
45	29.970	47 092	41.674
46	36 480	46 234	40 915
47	49 170	42 941	38 001
48	74 610	39 445	34 907
49	92.190	37 761	33 417
50	100 140	37.478	33.166
51	125.520	36.281	32.107
52	131.820	35 858	31 733
53	151.050	35.523	31 436
54	164.730	34 901	30.886
55	170 160	35 025	30 996
56	197.730	34 247	30 307
57	201.960	34 456	30 492
58	224 220	33 902	30 002
59	227.370	34 136	30 209
60	250 620	33 991	29 727
61	252.840	33 873	29 976
62	276 960	33 354	29 517
63	299.700	33 377	29 537

0 sample, hct, plasma visc	1 shear rate (1/sec)	2 viscosity (cP)	3 relative viscosity
1 31-5	0 04	1135.664	938 565
2 H=94	0.11	571.671	472 455
3 1.21 cP	0.17	413.121	341 422
4	0 23	339.332	280 440
5	0.30	281.048	232.271
6	0.36	252.702	208 845
7	0.42	229.341	189 538
8	0.49	209.231	172.918
9	0.68	174 536	144 245
10	0 87	151.381	125 108
11	0.93	154.323	127.540
12	1.06	134.840	111 438
13	1.19	132.312	109 349
14	1.31	120.648	99 709
15	1.53	115 746	95.656
16	1.57	111.120	91 835
17	1.83	103.205	85 293
18	1.86	104.882	86 679
19	2.06	100.088	82 717
20	2.08	97.173	80 308
21	2.25	95.550	78 967
22	2.33	92.934	76 821
23	2.45	91.554	75 664
24	2.59	88.522	73.160
25	2.78	86.022	71 093
26	3.00	83.832	69.283
27	3.56	77.173	63 779
28	6.09	62.660	51 785
29	8.64	55.938	45 899
30	9.32	54.472	45 018
31	11.82	50 216	41 501
32	11.96	50.163	41.457
33	15.01	47.062	38 894
34	15 28	46 692	38 588
35	17.56	45.072	37 250
36	18.58	44 091	36 439
37	20.09	43.520	35.967
38	21.23	42.622	35 225
39	22.01	42.930	35 149
40	23.87	41.403	34 217
41	24.94	41.372	34 192
42	28 49	39 587	32.717
43	29.97	39 473	32.622
44	36.00	39 725	32.831
45	35.17	35 971	29 728
46	74 22	33 868	27 990
47	93 36	31 199	25 784
48	99 69	32.146	26 567

49	125 16	31 057	25 667
50	133 11	29.707	24 551
51	150 69	30.338	25 073
52	166 05	29.075	24 029
53	175 98	29.714	24 557
54	192.60	28.687	23 707
55	201 40	29.299	24 214
56	219 09	28.381	23 455
57	226.95	28.972	23 944
58	238 83	28 234	23 334
59	246 18	28.781	23 786
60	271 44	28 555	23 599
61	278 25	28.023	23 160
62	299 64	28.132	23 250

0 sample, hct, plasma visc	1 shear rate (1/sec)	2 viscosity (cP)	3 relative viscosity
1 29-7	0.04	1077.778	1026 455
2 H=93	0 10	513 043	488 612
3 1.05 cP	0 17	375 090	357 229
4	0.23	298 960	284 724
5	0.30	268.293	255 517
6	0.36	220.903	210 384
7	0.42	222.636	212 033
8	0.68	160.752	153 097
9	0.93	144.380	137 505
10	0.93	135 167	128 730
11	1.19	124 680	118 743
12	1.19	119 025	113 357
13	1.38	110 207	104 959
14	1 46	111.550	106 238
15	1.57	103 151	98 239
16	1.76	98.433	93 746
17	1.79	101 039	96 228
18	2 06	93.491	89 039
19	2.08	91.664	87 299
20	2.32	88 849	84 618
21	2.40	86 422	82 307
22	2.52	84.759	80 723
23	2 53	84 719	80 685
24	2.85	80.286	76 463
25	2 93	83 265	79 300
26	3.00	79 181	75 410
27	4.85	67.079	63 885
28	6 76	59 458	56 627
29	8.65	54 141	51 563
30	10 63	50 635	48 224
31	11 84	49 191	46 810
32	13 93	46 457	44 245
33	15 67	45 165	43 014
34	17.24	43 761	41.677

35	18 85	42 879	40 837
36	19 88	42.040	40 038
37	22 52	40 742	38 802
38	22 67	40.934	38 985
39	25.16	39.533	37.650
40	26 48	39 379	37.504
41	27 80	38 635	36 795
42	29 97	38.154	36 337
43	36 42	37.463	35 679
44	61.95	33 850	32.238
45	80 94	32.357	30 816
46	92.67	30 189	28 748
47	106 50	31.031	29 553
48	125.67	29 119	27 732
49	125.67	30 408	28 960
50	151.29	29 827	28 407
51	152.22	28.652	27 288
52	170.37	29 382	27.983
53	178 62	28.317	26.969
54	189 45	29.083	27.698
55	204.99	28 090	26 752
56	214 95	28.765	27.395
57	224 91	27 955	26 624
58	233.94	28.569	27 209
59	244 74	27.838	26 512
60	253.08	28 407	27.054
61	277 68	27.723	26 405
62	299 70	27.832	26.507

0 sample, hct, plasma visc	1 shear rate (1/sec)	2 viscosity (cP)	3 relative viscosity
1 31-9	0.02	1696 386	1401.972
2 H=92	0.09	600 342	496 150
3 1.21 cP	0.15	391 849	323.842
4	0.22	318.106	262 898
5	0.28	257 725	212.996
6	0.34	233 772	193 200
7	0.41	212 841	175 902
8	0.60	168 373	139.151
9	0 79	146 268	120.883
10	0 81	150 595	124 459
11	1 04	125.381	103 621
12	1.14	124.447	102.849
13	1.30	112.248	92 767
14	1.47	108.170	89 397
15	1.49	105.344	87 061
16	1.68	99 379	82 128

17		1.73	100.346	82.931
18		1.87	94.320	77.950
19		2.06	91.471	75.596
20		2.19	87.619	72.578
21		2.33	86.852	71.779
22		2.44	84.201	69.588
23		2.53	83.197	68.758
24		2.79	79.632	65.812
25		3.00	77.545	64.087
26		3.02	77.237	63.852
27		5.57	60.857	50.295
28		8.74	52.995	43.054
29		9.95	49.693	41.036
30		12.57	46.408	38.354
31		12.57	46.779	38.660
32		15.23	44.049	36.404
33		15.76	43.993	36.358
34		17.87	42.237	34.907
35		18.95	41.917	34.642
36		20.50	40.824	33.739
37		22.14	40.487	33.460
38		23.81	39.253	32.440
39		24.68	39.325	32.500
40		27.77	38.029	31.429
41		29.97	37.608	31.081
42		36.42	37.395	31.070
43		61.98	33.340	27.554
44		87.45	31.314	25.879
45		92.10	29.498	24.379
46		112.77	29.976	24.774
47		125.25	28.340	23.421
48		144.60	28.946	23.922
49		151.71	27.819	22.991
50		182.79	28.118	23.238
51		184.71	27.267	22.535
52		208.29	27.752	22.936
53		211.17	27.004	22.317
54		237.63	26.784	22.136
55		240.00	27.340	22.595
56		250.92	26.686	22.055
57		264.15	26.630	22.008
58		265.47	27.104	22.400
59		297.24	26.463	21.870
60	31-10	0.04	987.302	815.952
61	H=92	0.10	498.827	412.254
62	1.21 cP	0.17	359.528	297.131
63		0.23	293.864	242.863
64		0.29	252.875	208.988
65		0.36	223.038	184.329
66		0.48	189.745	156.814
67		0.61	166.912	137.944
68		0.80	143.350	118.471
69		0.93	139.614	115.383
70		0.99	128.070	105.843
71		1.18	117.275	96.921
72		1.20	121.318	100.428
73		1.44	106.461	87.984
74		1.53	107.350	88.719
75		1.63	100.147	82.766
76		1.79	99.381	82.133
77		1.82	96.410	79.678
78		2.06	93.325	77.128
79		2.08	90.939	75.156
80		2.32	88.127	72.832
81		2.33	87.252	72.109
82		2.52	84.805	70.087
83		2.58	83.459	68.974
84		2.78	80.899	66.859
85		2.98	80.595	66.607
86		3.00	78.797	65.121
87		5.52	63.308	52.321
88		7.97	59.102	48.839
89		8.06	59.450	49.126
90		9.98	51.684	42.714
91		11.28	49.375	40.806
92		12.53	48.480	40.066
93		14.38	48.947	37.973
94		15.10	46.146	38.137
95		17.24	43.866	36.253
96		17.65	44.222	36.630
97		19.22	42.545	35.161
98		20.17	42.824	35.392
99		22.52	41.239	34.082
100		22.73	41.480	34.281
101		24.51	40.416	33.402
102		25.28	40.494	33.466
103		28.47	38.862	32.117
104		29.97	38.735	32.012
105		35.91	38.772	32.043
106		61.41	34.455	28.475
107		86.79	32.354	26.729
108		93.12	30.570	25.264
109		112.29	30.946	25.575
110		126.18	29.280	24.198
111		130.60	29.797	24.626
112		152.70	28.745	23.756
113		172.53	28.430	23.496
114		182.43	29.068	24.023
115		209.47	28.042	23.179

116		207.90	28.693	23.713
117		225.36	27.891	23.050
118		233.43	28.385	23.459
119		245.19	27.732	22.919
120		252.66	28.180	23.289
121		284.85	27.539	22.760
122		299.70	27.646	22.848

0 sample, hct. plasma visc	1 shear rate (1/sec)	2 viscosity (cP)	3 relative viscosity
1 30-1	0.04	1059.701	937.788
2 H=91	0.10	475.793	421.056
3 1.13 cP	0.17	334.234	295.782
4	0.23	277.143	245.259
5	0.29	233.978	207.060
6	0.36	199.079	176.176
7	0.42	182.717	161.696
8	0.49	168.850	149.425
9	0.61	146.090	129.283
10	0.80	132.657	117.396
11	0.80	122.741	108.620
12	0.99	109.469	96.875
13	1.19	101.910	90.186
14	1.25	94.957	84.033
15	1.31	87.682	77.595
16	1.59	87.427	77.369
17	1.82	77.988	69.016
18	1.86	79.800	70.619
19	2.12	74.147	65.617
20	2.14	72.606	64.253
21	2.32	70.199	62.123
22	2.46	67.771	59.974
23	2.52	67.048	59.335
24	2.71	65.300	57.788
25	2.91	62.858	55.627
26	2.97	76.438	67.644
27	3.00	62.847	55.617
28	5.52	58.474	51.747
29	8.05	50.838	44.989
30	9.34	52.473	46.436
31	11.24	44.290	39.195
32	13.79	41.581	36.797
33	13.97	44.064	38.995
34	15.69	40.422	35.772
35	17.29	40.212	35.586
36	20.15	37.459	33.146
37	20.58	37.393	33.091
38	23.22	36.408	32.219
39	23.33	35.952	31.816
40	25.74	35.310	31.248
41	25.85	35.292	31.232
42	27.14	34.610	30.628
43	28.52	34.314	30.366
44	29.97	34.184	30.251
45	30.12	29.482	26.090
46	42.78	26.999	23.893
47	68.25	24.404	21.667
48	92.49	22.251	19.691
49	100.05	22.909	20.273
50	122.09	21.111	18.682
51	138.24	21.853	19.339
52	165.12	20.394	18.225
53	176.46	21.192	18.754
54	198.15	20.257	17.927
55	214.62	20.758	18.370
56	224.64	20.085	17.774
57	250.92	19.984	17.685
58	259.08	20.432	18.081
59	277.38	19.895	17.606
60	299.70	19.995	17.695
61 31-4	0.03	1750.000	1446.281
62 H=91	0.09	638.938	544.593
63 1.21 cP	0.15	438.546	362.451
64	0.22	354.638	293.106
65	0.28	293.008	242.155
66	0.35	264.935	218.935
67	0.41	236.503	195.457
68	0.47	212.873	175.928
69	0.67	173.054	143.268
70	0.86	149.825	123.822
71	0.94	151.149	124.917
72	1.05	134.154	110.871
73	1.20	129.661	107.158
74	1.24	122.298	101.073
75	1.40	118.079	97.586
76	1.43	113.536	93.831
77	1.62	106.498	88.015
78	1.67	108.155	89.384
79	1.81	100.878	83.370
80	1.86	100.997	83.469
81	2.00	95.351	78.960
82	2.06	96.105	79.426
83	2.26	91.429	75.561
84	2.26	90.519	74.809
85	2.45	86.837	71.766
86	2.46	87.630	72.421
87	2.66	83.868	69.312
88	2.92	80.100	66.198
89	3.00	79.281	65.521

90	3.02	74.763	63 440
91	4 92	61.829	51.098
92	7.47	51.888	42.883
93	9 28	48.997	40 493
94	10.66	45.650	37.727
95	12.59	43.945	36 318
96	13.20	42.354	35.003
97	15 89	40.427	33.411
98	16.39	39.610	32.736
99	18.93	37 958	31.370
100	19 20	37.422	31.340
101	21 48	36.741	30 364
102	22.50	36.285	29 988
103	23 38	35 859	29.636
104	24 49	35.361	29.224
105	25 93	34.865	28.831
106	27.12	34 248	28 304
107	29.77	33.476	27.666
108	36.48	32 689	27.016

0 sample, hct, plasma visc	1 shear rate (1/sec)	2 viscosity (cP)	3 relative viscosity
1 30-3	0.04	1037 398	918 051
2 H=98	0.10	484 084	428.393
3 1.13 cP	0.16	360.221	318 780
4	0.23	291.029	257.548
5	0.29	256 481	226 974
6	0.35	222.589	196 981
7	0.35	222 589	196 981
8	0.42	201 935	178 704
9	0.48	185.305	163 987
10	0.67	155 372	137 497
11	0.86	136 439	120.742
12	0.94	136 337	120 652
13	1.06	122 150	108 097
14	1 20	119 770	105 991
15	1 25	112.013	99 127
16	1.44	103 735	91 801
17	1.60	101 353	89 693
18	1.63	96.409	85 318
19	1 82	92 121	81 523
20	1.86	93 763	82 976
21	2 01	87 325	77 279
22	2 13	88 655	78 456
23	2.27	83 503	73 896
24	2.39	82.498	73 007
25	2 52	79 586	70 430
26	2.79	76 467	67 670
27	3.00	74 324	65 773
28	3.51	70 445	62 341

29	6 70	53.135	47 022
30	9.32	47 989	42.468
31	9 87	45.913	40 631
32	12 62	42.906	37 970
33	13.05	41.665	36 872
34	15.28	40.143	35 525
35	16.89	38.625	34 181
36	17 93	38.050	33 673
37	20.73	36.440	32.265
38	21 88	35.947	31.812
39	23.87	34.984	30.959
40	23 90	35 053	31.020
41	27.17	33.701	29 824
42	29.16	33.114	29.304
43	29 94	34.269	30.419
44	29.97	32.943	29.153
45	48.96	30.300	26 814
46	74.43	27.670	24 487
47	92.21	25.528	22.591
48	93 42	26.557	23.502
49	118 92	25.505	22.571
50	125 49	24.384	21.579
51	150 81	24.707	21.865
52	158.67	23.700	20.973
53	169 98	24 294	21.499
54	191.67	23.227	20.555
55	201 63	23.799	21.061
56	224.64	22.923	20 286
57	227 16	23.494	20.791
58	251 07	22.751	20.134
59	252.66	23.243	20 569
60	270 96	22.669	20.061
61	290.76	22.570	19.973
62	299 73	22.700	20.088

0 sample, hct, plasma visc	1 shear rate (1/sec)	2 viscosity (cP)	3 relative viscosity
1 29-2	0.04	1063 780	1013 124
2 H=89	0.10	456 509	434 770
3 1.05 cP	0.17	322.364	307 013
4	0.23	272.405	259 433
5	0.29	232 856	221.768
6	0.36	202.277	192.645
7	0.42	185 877	177 026
8	0.48	170.329	162.218
9	0.67	142.584	135.794
10	0.93	117.200	111.619
11	0 94	124.225	118 310
12	1.12	106.056	101.006
13	1.27	103.806	98.863

14	1 31	97 458	92 817
15	1.50	90.212	85 916
16	1.93	93.410	88.962
17	1 69	85.167	81 111
18	1 80	85.903	81 812
19	2 01	78 201	74 477
20	2.06	79 444	75 661
21	2 33	74 297	70 759
22	2 33	72.725	69 262
23	2 52	70 639	67 275
24	2 52	69 574	66 261
25	2.79	67.589	64.370
26	3 00	65.259	62 151
27	3 57	58.814	56 013
28	5 48	48 020	45 733
29	6.76	44.021	41 925
30	9 30	38.451	36 620
31	9 33	39 994	38 090
32	11 85	35.310	33 629
33	11 97	36.292	34 564
34	13 76	33 622	32 021
35	14 63	33.525	31 929
36	16 61	32.054	30 528
37	16 96	31.385	29 890
38	19 26	30 369	28 923
39	20.13	29 759	28 342
40	21.25	29 449	28 047
41	22.69	28 719	27 351
42	23.89	28 403	27 050
43	25 24	27 871	26 544
44	27 86	27 150	25 857
45	29.98	26 688	25 417
46	36.15	25 768	24 541
47	55 29	23 087	21 988
48	87 03	21 010	20 010
49	92 70	20 437	19 464
50	112 53	20 008	19 055
51	125 76	19 358	18 436
52	138 00	19 391	18 468
53	152 22	18 841	17 944
54	157 02	19 049	18 142
55	178 59	18 411	17 534
56	188 91	18 500	17 695
57	205 02	18 123	17 260
58	214 41	18 315	17 443
59	224 94	17 945	17 090
60	239 76	18 106	17 244
61	251 22	17 763	16 917
62	258 90	17 966	17 110

63	271 02	17 644	16 804
64	299.70	17 613	16 774
65 31-6	0.04	877 600	725 289
66 H=89	0 10	425 000	351 240
67 1 21 cP	0 16	304 762	251 869
68	0 23	240 682	198 911
69	0 29	210 072	173 613
70	0 35	182 149	150 536
71	0 42	167 001	138 017
72	0 48	152 861	126 331
73	0 55	145 340	120 132
74	0 74	122.353	101.118
75	0 93	113 962	94 167
76	0 92	108 573	89 720
77	1 18	94 367	77 989
78	1 20	97 723	80 928
79	1 37	87 413	72 242
80	1 53	86 154	71 202
81	1 63	80 520	66 545
82	1 79	79.369	65 760
83	1 88	75 287	62 221
84	2 12	73 020	60 347
85	2 14	70.892	58 588
86	2 39	68.674	56 757
87	2 39	67.757	55 998
88	2 59	65.928	54 486
89	2 65	65.005	53 723
90	2 78	63 138	52 197
91	3 00	61 688	50 982
92	3 56	55 173	45 598
93	7 39	41 162	34 018
94	9 29	38 110	31 496
95	10 56	35 947	29 708
96	13 75	33 227	27 460
97	13 92	33 096	27 352
98	16 95	31.274	25.846
99	17 23	31 071	25 679
100	19 49	30.125	24 897
101	20 54	29 501	24 381
102	22.67	28 864	23 855
103	23 18	28 435	23 500
104	25 16	27 764	22 945
105	25 21	28 079	23 206
106	27.11	27 590	22 802
107	27 14	27 374	22 540
108	29 78	26 718	22 081
109	42.42	25 389	20 983
110	68.01	22 805	18 847
111	93 03	20 477	16 923
112	106.14	20.916	17.286

113	126.33	19.405	16 103
114	137.91	20 067	16 584
115	159 33	18.989	15 693
116	176 13	19 392	16 026
117	185 82	18.696	15 451
118	207 99	19 003	15 705
119	212.22	18.490	15 281
120	238.62	18 293	15 118
121	239.76	18 694	15 450
122	264 93	18.158	15 007
123	271.59	18.463	15 259
124	299 70	18.143	14 994

0 sample, hct, plasma visc	1 shear rate (1/sec)	2 viscosity (cP)	3 relative viscosity
1 29-8	0.05	573.718	546.398
2 H=86	0.11	332 065	316 252
3 1.05 cP	0 17	236 379	225 123
4	0.24	197 089	187.704
5	0.30	168 091	160 087
6	0.36	149 630	142 505
7	0.43	135.133	128 698
8	0.55	121.038	115 274
9	0.75	102.570	97.686
10	0 93	98 448	93.760
11	0 94	92.603	88.193
12	1.13	82.190	78 276
13	1 19	86 145	82.043
14	1.32	76.990	73 324
15	1.39	79.771	75 972
16	1.57	71.034	67.631
17	1.65	72.193	68.755
18	1.83	66.710	63 533
19	1.92	67 402	64 192
20	2.08	62 660	59 674
21	2 18	62 606	59 625
22	2.34	60 326	57 453
23	2.45	58 848	56 046
24	2 59	57 368	54 636
25	2.71	56 215	53 538
26	2 98	53 849	51 285
27	3.00	53 554	51 004
28	4 22	45 043	42 898
29	6 13	38 894	37 042
30	8 68	33 846	32 234
31	9 30	33 727	32.121
32	11.23	31.266	29 777
33	11 93	30 995	29 519
34	13 77	29 078	27 693
35	13 92	29.341	27 944
36	16.32	27.568	26 255
37	16 57	27.686	26 368
38	18 56	26.717	25 445
39	18.88	26.587	25 321
40	20 55	26.033	24 793
41	21.42	25.452	24 430
42	22 53	25.415	24 205
43	23.33	25.123	23 927
44	24 51	24.838	23 655
45	25.24	24.634	23 461
46	27 14	24 287	23 130
47	27 17	24.066	22 920
48	29 15	23.688	22 560
49	29 97	23.482	22 364
50	42.03	22.091	21 039
51	73.80	19.634	18.718
52	93 19	18.239	17 370
53	112.02	18 278	17 408
54	126 24	17.395	16 567
55	143 88	17 640	16 800
56	159.18	16.943	16 136
57	182 07	17.087	16 273
58	198 84	16.551	15 763
59	213 84	16.765	15 967
60	225 21	16 358	15 579
61	245 70	16 538	15 750
62	251 73	16.208	15 436
63	270 81	16.395	15 614
64	271 53	16.136	15 368
65	298 05	16.019	15 256

0 sample, hct, plasma visc	1 shear rate (1/sec)	2 viscosity (cP)	3 relative viscosity
1 29-10	0 03	731 332	696 697
2 H=80	0 10	322 981	307 601
3 1.05 cP	0 16	229 288	218 350
4	0 22	175 368	167 017
5	0 29	156 230	148 810
6	0.35	144 103	137 241
7	0 42	127 220	121 162
8	0.61	101 535	96 700
9	0 80	89.755	85 481
10	0.93	87.058	82.912
11	0.99	80.967	77 111
12	1.18	73.593	70 089
13	1.26	74 727	71 169
14	1 43	67.232	64.030
15	1.60	65.796	62 663
16	1.62	62.496	59 710
17	1.86	61.413	58 489
18	1 88	58 609	55 847
19	2 07	55 876	53 245
20	2.13	57.347	54 616
21	2 32	53 764	51 204
22	2 39	53 900	51 333
23	2.51	51 915	49 443
24	2 70	50 216	47 825
25	2 72	49 972	47 592
26	2 92	47 995	45 710
27	3 00	47.998	45 712
28	3.56	43 067	41 016
29	6.11	34.740	33 086
30	8.01	31.225	29 748
31	9 33	30.164	28 728
32	10 56	28 457	27 102
33	12.48	26 870	25 590
34	12.64	27.051	25.763
35	15.03	25.389	24 180
36	15 29	25 443	24 231
37	16 95	24.504	23 337
38	17.93	24.206	23 053
39	19 91	23.358	22 246
40	20 14	23.319	22 209
41	22.55	22.593	21 517
42	22 68	22 517	21 445
43	25 19	21.810	20 771
44	25 24	21.938	20 893
45	27 85	21 299	20 285
46	29 43	21.509	20 485
47	29 97	20.955	19 957
48	48 45	19.009	18 104
49	73 92	17 390	16 562
50	92.76	16 249	15 570
51	99 45	16 486	15 701
52	125 88	15 586	14 844
53	131 31	15 810	15 057
54	152.34	15 213	14 489
55	156 75	15 445	14 710
56	182 19	15 165	14 443
57	185 37	14 873	14 165
58	207.63	14 947	14 235
59	211 95	14 692	13 992
60	238.26	14 518	13 827
61	239 37	14 739	14 037
62	258 09	14 402	13 716
63	264 96	14 612	13 916
64	271 47	14 361	13 677
65	297 73	14 272	13 592

0 sample, hct, plasma visc	1 shear rate (1/sec)	2 viscosity (cP)	3 relative viscosity
1 31-8	0 04	625 185	516 682
2 H=82	0 10	300 289	248 173
3 1.21 cP	0 17	224 417	185 469
4	0.23	177 403	146 614
5	0.29	160.529	132 669
6	0 36	140.586	116 187
7	0.42	128.196	105 947
8	0 55	108 515	89 682
9	0 73	100 330	82 917
10	0 74	94 161	77 819
11	0 92	88.774	73 367
12	0 93	83 881	69 323
13	1 12	76.578	63 288
14	1.19	77 834	64 326
15	1 45	70.481	58 249
16	1.51	65.644	54 251
17	1 78	63.012	52 324
18	1.82	60.293	49 829
19	2.08	56.658	46 825
20	2 11	57.777	47 750
21	2.27	54 309	44 883
22	2.31	50 584	41 805
23	2.38	54 258	44 841
24	2 53	51.728	42 750
25	2 84	49 335	40 773
26	3 00	48 038	39 701
27	4 85	36 623	30 267
28	7.40	30.998	25 618
29	9 95	27 864	23 028
30	9 97	28 203	23 308
31	11 94	26 488	21 891
32	12 50	25 752	21 283
33	14 60	24 641	20 364
34	15 05	24 329	20 107
35	17.24	23 309	19 264
36	17 59	23 252	19 217
37	19.21	22 914	18 607
38	20 14	22 301	18 431
39	21 20	21 879	18 082
40	22 68	21 537	17.799
41	23.18	21 319	17 619
42	24 60	21 079	17 421
43	25 16	20 826	17 212
44	26 51	20.662	17 076
45	27 81	20 308	16 783
46	29 22	20 534	16 970
47	29.80	19 941	16 480
48	29.97	19 976	16 509

49	54.63	17.490	14.455
50	80.04	16.267	13.444
51	99.84	14.934	12.342
52	105.57	15.416	12.740
53	126.30	14.477	11.964
54	131.04	14.892	12.307
55	146.07	14.202	11.737
56	156.36	14.534	12.012
57	165.99	13.962	11.539
58	181.86	14.236	11.765
59	192.30	13.752	11.365
60	207.39	14.017	11.584
61	212.22	13.649	11.280
62	226.33	13.882	11.473
63	231.93	13.536	11.203
64	245.55	13.769	11.379
65	251.79	13.481	11.141
66	264.60	13.656	11.286
67	284.88	13.396	11.071
68	299.67	13.415	11.087

0 sample, hct, plasma visc	1 shear rate (1/sec)	2 viscosity (cP)	3 relative viscosity
1 31-2	0.03	1123.276	928.327
2 H=78	0.10	507.879	419.735
3 1.21 cP	0.16	300.738	248.544
4	0.23	233.201	192.728
5	0.29	197.098	162.891
6	0.35	182.073	150.474
7	0.42	162.923	134.647
8	0.61	128.416	106.129
9	0.80	105.115	86.872
10	0.94	118.269	97.743
11	1.05	91.028	75.230
12	1.20	100.100	82.727
13	1.31	84.878	70.147
14	1.47	84.677	69.981
15	1.50	78.305	64.715
16	1.69	72.869	60.222
17	1.73	75.225	62.169
18	1.93	74.825	61.839
19	1.94	70.489	58.255
20	2.13	67.287	55.609
21	2.20	64.943	53.672
22	2.33	66.241	54.745
23	2.39	62.065	51.293
24	2.53	62.870	51.959
25	2.58	60.272	49.812
26	2.79	58.624	48.450
27	2.99	56.079	46.346
28	3.55	52.646	43.509
29	5.45	42.713	35.300
30	8.00	35.096	29.666
31	9.36	34.875	28.822
32	9.91	32.889	27.181
33	12.01	31.264	25.921
34	12.45	29.942	24.745
35	14.36	28.371	23.447
36	15.31	28.425	23.492
37	16.91	26.780	22.132
38	18.63	26.270	21.711
39	19.46	25.478	21.056
40	21.28	24.971	20.637
41	22.03	24.606	20.170
42	23.92	23.877	19.733
43	23.92	23.788	19.660
44	25.85	23.249	19.214
45	27.88	22.701	18.761
46	29.97	22.265	18.401
47	36.00	21.175	17.500
48	61.50	18.220	15.058
49	86.85	16.870	13.942
50	93.09	16.378	13.536
51	112.41	15.997	13.221
52	119.55	15.591	12.885
53	138.06	15.443	12.763
54	146.07	15.089	12.470
55	169.86	14.963	12.366
56	172.59	14.799	12.231
57	201.66	14.628	12.087
58	205.56	14.409	11.908
59	227.04	14.435	11.921
60	231.96	14.228	11.759
61	251.85	14.080	11.636
62	258.87	14.223	11.755
63	271.65	13.981	11.555
64	298.09	13.872	11.464

0 sample, hct, plasma visc	1 shear rate (1/sec)	2 viscosity (cP)	3 relative viscosity
1 30-4	0.04	396.081	315.116
2 H=75	0.11	226.816	260.722
3 1.13 cP	0.17	171.228	151.529
4	0.23	138.540	122.602
5	0.30	121.169	107.229
6	0.36	113.882	100.781
7	0.42	101.909	90.185
8	0.55	90.331	79.939
9	0.74	76.212	67.444
10	0.86	73.341	65.081
11	0.93	68.391	60.523
12	1.12	65.348	57.830
13	1.19	60.878	53.874
14	1.39	59.139	52.335
15	1.44	56.075	49.624
16	1.39	55.600	49.204
17	1.76	50.962	45.099
18	1.85	51.240	45.345
19	2.05	49.070	43.425
20	2.08	47.054	41.641
21	2.27	45.504	40.269
22	2.31	45.945	40.659
23	2.58	43.451	38.452
24	2.59	42.928	37.989
25	3.04	41.448	36.680
26	3.00	40.311	35.850
27	4.93	31.832	28.170
28	8.10	25.444	22.519
29	9.24	25.000	22.124
30	10.65	23.080	20.427
31	12.55	22.151	19.603
32	12.57	21.536	19.076
33	15.76	19.977	17.679
34	15.87	20.352	18.011
35	18.32	19.060	16.867
36	19.19	18.837	16.670
37	20.87	18.218	16.122
38	21.82	18.116	16.032
39	23.40	17.705	15.668
40	24.47	17.484	15.473
41	25.31	17.307	15.316
42	27.75	16.785	14.854
43	29.97	16.437	14.546
44	42.48	15.085	13.350
45	61.65	13.752	12.170
46	87.03	12.796	11.324
47	92.40	12.422	10.993
48	112.47	12.195	10.792
49	118.89	11.870	10.504
50	138.00	11.817	10.458
51	163.56	11.537	10.210
52	165.15	11.353	10.047
53	204.75	11.059	9.787
54	208.08	11.205	9.916
55	237.78	10.898	9.644
56	239.76	11.039	9.769
57	271.62	10.923	9.666
58	297.42	10.690	9.460
59	299.70	10.761	9.523

0 sample, hct, plasma visc	1 shear rate (1/sec)	2 viscosity (cP)	3 relative viscosity
1 31-3	0.04	262.590	217.017
2 H=66	0.10	144.828	119.693
3 1.21 cP	0.17	106.798	88.263
4	0.23	89.406	73.889
5	0.30	78.362	64.762
6	0.36	70.701	58.431
7	0.42	67.472	55.762
8	0.48	63.194	52.226
9	0.55	59.148	48.883
10	0.69	54.674	45.185
11	0.93	46.658	38.560
12	0.93	46.972	38.820
13	1.19	43.119	35.636
14	1.19	42.799	35.371
15	1.46	39.773	32.870
16	1.51	38.765	32.037
17	1.65	37.781	31.224
18	1.76	36.543	30.201
19	1.92	35.453	29.300
20	2.08	34.223	28.283
21	2.18	33.828	27.957
22	2.38	32.649	26.983
23	2.40	32.426	26.807
24	2.65	31.098	25.701
25	2.78	30.391	25.083
26	3.00	29.723	24.562
27	3.58	26.711	22.075
28	5.48	23.167	18.320
29	8.67	18.345	15.161
30	9.35	17.927	14.816
31	11.84	16.317	13.485
32	11.99	16.413	13.564
33	13.98	15.446	12.765
34	14.40	15.176	12.542
35	16.61	14.496	11.980
36	16.94	14.296	11.815
37	19.26	13.752	11.365
38	20.75	13.361	11.042
39	21.25	13.262	10.960
40	23.23	12.829	10.602
41	23.30	12.860	10.628
42	25.21	12.570	10.388
43	25.85	12.504	10.334
44	28.52	12.021	9.935
45	29.97	11.876	9.815
46	41.88	10.774	8.904
47	60.90	9.680	8.000
48	86.34	8.940	7.388

49	93.00	8.810	7.281
50	111.78	8.481	7.009
51	126.12	8.259	6.826
52	143.89	8.119	6.710
53	152.58	7.998	6.610
54	169.23	7.945	6.566
55	172.50	7.850	6.488
56	192.27	7.745	6.401
57	201.09	7.773	6.424
58	212.07	7.650	6.322
59	226.59	7.674	6.342
60	231.87	7.575	6.260
61	245.79	7.611	6.290
62	251.61	7.499	6.198
63	271.02	7.549	6.239
64	278.04	7.442	6.150
65	299.70	7.448	6.155

0 sample, hct, plasma visc	1 shear rate (1/sec)	2 viscosity (cP)	3 relative viscosity
1 32-7	0.11	114.731	108.237
2 H=59	0.17	74.936	70.713
3 1.06 cP	0.30	55.388	52.250
4	0.42	46.851	44.199
5	0.55	40.457	38.167
6	0.93	28.715	27.090
7	0.93	32.712	30.860
8	1.12	27.501	25.944
9	1.12	30.547	28.818
10	1.32	28.435	26.825
11	1.39	25.335	23.901
12	1.51	26.965	25.439
13	1.59	24.546	23.157
14	1.76	25.336	23.902
15	1.85	24.960	23.547
16	1.95	24.412	23.030
17	2.05	23.917	22.563
18	2.14	23.706	22.364
19	2.25	23.249	21.933
20	2.33	22.860	21.566
21	2.45	22.568	21.291
22	2.84	21.117	19.922
23	4.19	17.022	16.058
24	6.10	14.732	13.898
25	8.66	12.815	12.090
26	9.30	12.771	12.048
27	11.84	11.518	10.866
28	12.62	11.467	10.818
29	14.38	10.761	10.152
30	15.92	10.548	9.951
31	16.94	10.188	9.611
32	18.57	9.971	9.407
33	19.47	9.740	9.189
34	21.88	9.413	8.880
35	22.02	9.409	8.876
36	23.92	9.171	8.652
37	25.83	8.966	8.458
38	27.82	8.724	8.230
39	29.81	8.511	8.029
40	30.12	8.506	8.025
41	68.16	6.721	6.341
42	93.27	6.230	5.877
43	99.99	6.184	5.834
44	126.18	5.877	5.544
45	144.63	5.829	5.499
46	152.58	5.710	5.387
47	176.24	5.686	5.364
48	179.01	5.592	5.275
49	205.50	5.509	5.197
50	208.23	5.584	5.268
51	231.90	5.450	5.142
52	239.94	5.519	5.207
53	251.67	5.419	5.112
54	291.30	5.268	5.064

0 sample, hct, plasma visc	1 shear rate (1/sec)	2 viscosity (cP)	3 relative viscosity
1 32-5	0.49	22.222	20.964
2 H=50	0.55	21.281	20.076
3 1.06 cP	0.68	20.432	19.275
4	0.87	19.290	18.198
5	0.99	18.250	17.217
6	1.13	17.920	16.906
7	1.26	17.159	16.188
8	1.32	17.058	16.092
9	1.44	17.016	16.053
10	1.46	16.581	15.642
11	1.72	15.856	14.958
12	1.76	16.295	15.373
13	1.92	15.438	14.564
14	2.14	15.379	14.508
15	2.18	14.874	14.032
16	2.45	14.594	13.768
17	2.53	14.708	13.875
18	2.84	14.109	13.310
19	3.00	14.303	13.493
20	3.62	13.292	12.540
21	6.17	11.156	10.525
22	8.07	10.301	9.718
23	9.25	9.750	9.198
24	10.63	9.506	8.968
25	11.89	9.112	8.596
26	13.17	8.943	8.437
27	14.53	8.810	8.312
28	15.71	8.505	8.024
29	17.19	8.192	7.728
30	18.90	8.063	7.607
31	19.82	7.884	7.438
32	21.44	7.789	7.348
33	22.49	7.614	7.183
34	23.98	7.578	7.149
35	24.47	7.464	7.042
36	28.43	7.152	6.747
37	29.70	7.253	6.842
38	29.97	7.149	6.744
39	55.14	6.069	5.725
40	80.52	5.518	5.206
41	92.97	5.353	5.050
42	112.32	5.131	4.841
43	126.06	5.032	4.747
44	137.94	4.939	4.659
45	152.52	4.864	4.589
46	176.22	4.755	4.486
47	179.01	4.738	4.470
48	201.66	4.675	4.410
49	212.07	4.628	4.366
50	227.22	4.617	4.356
51	231.90	4.576	4.317
52	259.11	4.559	4.301
53	278.10	4.487	4.233
54	297.84	4.459	4.207
55	299.70	4.488	4.234

0 sample, hct, plasma visc	1 shear rate (1/sec)	2 viscosity (cP)	3 relative viscosity
1 32-4	0.00	12.805	12.080
2 H=44	0.93	12.589	11.876
3 1.06 cP	1.12	11.896	11.223
4	1.33	11.599	10.942
5	1.37	11.342	10.700
6	1.63	10.945	10.325
7	1.73	10.812	10.200
8	2.01	10.412	9.823
9	2.19	10.273	9.692
10	2.26	10.208	9.630
11	2.52	10.049	9.480
12	2.52	9.999	9.433
13	2.64	9.993	9.427
14	2.78	9.976	9.411
15	3.00	10.028	9.460
16	4.97	8.731	8.237
17	6.15	7.739	7.301
18	11.89	6.928	6.536
19	12.60	7.029	6.631
20	16.50	6.464	6.098
21	17.06	6.349	5.990
22	20.47	6.244	5.891
23	20.88	6.298	5.942
24	24.45	6.004	5.664
25	24.70	6.062	5.719
26	28.41	5.809	5.480
27	29.97	5.801	5.473
28	36.15	5.693	5.371
29	67.98	4.949	4.669
30	92.76	4.607	4.346
31	106.14	4.532	4.275
32	123.94	4.374	4.126
33	137.85	4.331	4.086
34	158.94	4.213	3.975
35	182.52	4.158	3.923
36	196.72	4.077	3.846
37	220.62	4.038	3.809
38	238.32	3.980	3.755
39	258.84	3.989	3.763
40	277.95	3.914	3.692
41	299.73	3.912	3.691

0 sample, hct, plasma visc	1 shear rate (1/sec)	2 viscosity (cP)	3 relative viscosity
1 32-1	1.99	5.074	4.787
2 H=34	2.15	5.135	4.844
3 1.06 cP	2.18	4.853	4.578
4	2.40	5.079	4.792
5	2.45	5.074	4.787
6	2.59	4.879	4.603
7	2.78	4.700	4.434
8	3.00	4.624	4.362
9	4.32	3.720	3.509
10	6.24	3.709	3.499
11	8.78	3.638	3.432
12	9.94	3.702	3.492
13	11.96	3.786	3.572
14	13.90	3.629	3.424
15	16.42	3.791	3.576
16	16.55	3.646	3.440
17	19.17	3.569	3.367
18	20.88	3.557	3.356
19	21.81	3.524	3.325
20	24.46	3.430	3.236
21	24.70	3.554	3.353

22	28.43	3.426	3.232
23	29.97	3.487	3.290
24	30.03	3.801	3.586
25	35.41	3.433	3.239
26	73.11	3.131	2.954
27	87.18	3.212	3.030
28	106.05	3.041	2.869
29	119.04	3.097	2.922
30	139.20	2.988	2.819
31	157.20	3.024	2.853
32	165.48	2.955	2.788
33	192.06	2.924	2.758
34	195.39	2.976	2.808
35	218.43	2.903	2.739
36	227.28	2.944	2.777
37	238.26	2.892	2.728
38	259.11	2.917	2.752
39	277.80	2.867	2.705
40	299.76	2.876	2.713

0 sample, hct. plasma visc.	1 shear rate (1/sec)	2 viscosity (cP)	3 relative viscosity
1 32-2	3.00	3.513	3.314
2 H=24	5.56	2.218	2.092
3 1.06 cP	10.01	2.245	2.118
4	11.91	2.162	2.040
5	14.46	2.234	2.108
6	14.95	2.068	1.951
7	18.28	2.235	2.108
8	18.51	2.159	2.037
9	21.47	2.227	2.101
10	22.47	2.134	2.013
11	24.02	2.219	2.093
12	26.50	2.195	2.071
13	29.07	2.143	2.022
14	36.78	2.334	2.202
15	68.64	2.228	2.102
16	92.61	2.082	1.964
17	106.83	2.175	2.052
18	125.67	2.103	1.984
19	144.96	2.169	2.046
20	158.91	2.107	1.988
21	191.94	2.111	1.992
22	195.84	2.154	2.032
23	224.91	2.113	1.993
24	240.27	2.156	2.034
25	251.37	2.112	1.992
26	265.83	2.157	2.035
27	297.75	2.119	1.999

0 sample, hct. plasma visc.	1 shear rate (1/sec)	2 viscosity (cP)	3 relative viscosity
1 32-3	8.72	1.170	1.104
2 H=11	11.27	1.289	1.216
3 1.06 cP	12.61	1.359	1.282
4	14.45	1.287	1.214
5	15.91	1.328	1.253
6	17.63	1.329	1.254
7	19.20	1.308	1.234
8	20.82	1.340	1.264
9	22.50	1.367	1.290
10	23.36	1.362	1.285
11	25.90	1.387	1.308
12	27.76	1.366	1.289
13	29.98	1.413	1.333
14	36.78	1.431	1.350
15	68.67	1.429	1.348
16	92.70	1.311	1.237
17	106.83	1.416	1.336
18	125.61	1.337	1.261
19	145.02	1.422	1.342
20	158.67	1.356	1.279
21	189.57	1.424	1.343
22	191.82	1.371	1.293
23	224.73	1.387	1.308
24	227.67	1.437	1.356
25	251.25	1.401	1.322
26	259.56	1.444	1.362
27	297.42	1.422	1.342

REFERENCES

Batchelor, G. K. In *Theories of Applied Mechanics*, edited by W. T. Koites. North Holland Pub., 1976. p. 33.

Bayliss, L. E. In *Rheology of Blood and Lymph: Deformation and Flow in Biological Systems*, edited by A. Frey-Wyssling. New York: Interscience Publishers, 1952. p. 354.

Beck, W. S. "Hematopoiesis and introduction to the anemias." In *Hematology*, 3rd edition, edited by W. S. Beck. Cambridge, Ma.: M.I.T. Press, 1981, p. 1.

Berczeller, L. and Wastl, H. "Uber die Viskositat von Blutkorperchensuspensionen II." *Biochem. Z.* **167**:195 (1924).

Benis, A. M. and Lacoste, J. "Study of erythrocyte aggregation by blood viscometry at low shear rates using a balance method." *Circ. Res.* **22**:29 (1968).

Bingham, E. C. and Roepke, R. R. "The rheology of blood. III." *J. gen. Physiol.* **28**:79 (1944a).

Bingham, E. C. and Roepke, R. R. "The rheology of blood. IV. The fluidity of whole blood at 37 °C." *J. gen. Physiol.* **28**:131 (1944b).

Bird, R. B.; Stewart, W. E.; and Lightfoot, E. N. *Transport Phenomena*. New York: John Wiley & Sons, Inc, 1960.

Bloor, M. I. G. "An analysis of blood flow at low shear rates in a concentric cylinder viscometer." *Biorheology* **19**:681 (1982).

Burton-Opitz, R. "The effect of changes in temperature upon the viscosity of the 'living' blood." *J. exp. Med.* **8**:59 (1906).

Burton-Opitz, R. "The viscosity of the blood." *J. Am. med. Ass.* **57**:353 (1911).

Casson, N. "A flow equation for pigment-oil suspensions of the printing ink type." In *Rheology of Disperse Systems*, edited by C. C. Mill.

New York: Pergamon Press, 1958. p. 84.

Castaneda, A. R.; Bernstein, E. F.; and Varco, R. L. "The effect of polyvinylprotedone, mannitol, dextrose, and of various dextrans on red cell charge." *Third European Conference on Microcirculation*, Jerusalem. *Bibl. Anat.* **7**:262 (1965).

Cerny, L. C.; Cook, F. B.; and Walker, C. C. "Rheology of blood." *Am. J. Physiol.* **202**:188 (1962).

Charm, S. E. and Kurland, G. S. "The flow behaviour and shear stress-shear rate characteristics of canine blood." *Am. J. Physiol.* **203**:417 (1962).

Charm, S. E. and Kurland, G. S. "Static method for determining blood yield stress." *Nature.* **216**:1121 (1967).

Charm, S. E. and Kurland, G. S. *Blood Flow and Microcirculation.* New York: John Wiley & Sons, 1974.

Chien, S. "Shear dependence of effective cell volume as a determinant of blood viscosity." *Science* **168**:977 (1970).

Chien, S.; Dellenback, R. J.; Usami, S.; and Gregersen, M. I. "Plasma trapping in hematocrit determination." *Proc. Soc. Exp. Biol. Med.* **119**:1155 (1965).

Chien, S.; Usami, S.; Taylor, H. M.; Lundberg, J. L.; and Gregersen, M. I. "Effects of hematocrit and plasma proteins on human blood rheology at low shear rates." *J. Appl. Physiol.* **21**:81 (1966).

Chien, S.; Usami, S.; Dellenback, R. J.; and Gregersen, M. I. "Shear-dependent deformation of erythrocytes in rheology of human blood." *Am. J. Physiol.* **219**:136 (1970).

Chien, S.; Usami, S.; Dellenback, R. J.; Bryant, C. A.; and Gregersen, M. I. "Change of erythrocyte deformability during fixation in actealdehyde." In *Theoretical and Clinical Hemorheology,* edited by H. H. Hartert and A. L. Copley. Heidelberg: Springer-Veilag Berlin, 1971. p. 136.

Chmiel, H. "New experimental results in haemorheology." *Biorheology* **11**:87 (1974).

Chmiel, H. and Walitza, E. *On the Rheology of Blood and Synovial Fluids.* Research Studies Press, 1980.

Cokelet, G. R. *The Rheology of Human Blood.* Sc.D. thesis. Cambridge, Mass.: M.I.T., 1963.

Cokelet, G. R. and Smith, J. H. "The effect of concentric cylinder viscometer gap size on the experimental rheological properties of human blood." *Biorheology* **10**:51 (1973).

Cokelet, G. R.; Merrill, E. W.; Gilliland, E. R.; and Shin, H. "The rheology of human blood--measurement near and at zero shear rate." *Trans. Soc. Rheol.* **7**:303 (1963).

Copley, A. L. "Non-newtonian behavior of surface layers of human plasma protein systems and a new concept of the initiation of thrombosis." *Biorheology* **2**:79 (1971).

Copley, A. L. and King, R. G. "Viscous resistance of thromboid (thrombus-like) surface layers in systems of plasma proteins including fibrinogen." *Thromb. Res.* **1**:1 (1972).

Copley, A. L.; Krchma, L. C.; and Whitney, M. E. "Humoral rheology. I. Viscosity studies and anomalous flow properties of human blood systems with heparins and other anticoagulants." *J. gen. Physiol.* **26**:49 (1942).

Copley, A. L.; Glover, F. A.; and Thorley, R. S. "Capillary flow and wall adherance of bovine blood, plasma, and serum in contact with glass and fibrin surfaces." *Kolloidzeitschrift* **168**:101 (1960)

Dintenfass, L. "Thixotropy of blood at very low rates of shear." *Kolloidzeitschrift* **180**:160 (1962a).

Dintenfass, L. "Considerations of the internal viscosity of red cells and its effects on the viscosity of whole blood." *Angiology* **13**:33 (1962b).

Dintenfass, L. "Viscosity of the packed red and white blood cells." *Exp. Molec. Path.* **4**:597 (1965a).

Dintenfass, L. "Some observations on the viscosity of pathological human blood plasma." *Throm. Diath. haemorrh.* **1**:492 (1965b).

Dintenfass, L. "A preliminary outline of the blood high viscosity syndromes." *Arch. intern. Med.* **118**:427 (1966).

Dintenfass, L. "Viscosity of blood at high haematocrits measured in microcapillary (parallel-plate) viscometers of r=3-30 microns." In *Proceedings of the 1st International Conference on Haemorheology*, edited by A. L. Copley. Oxford: Pergamon Press, 1968a. p. 197.

Dintenfass, L. "Internal viscosity of the red cell and a blood viscosity equation." *Nature* **219**:956 (1968b).

Dintenfass,L. "Considerations of the internal viscosity of the red cell and of the rheology of the red cell membrane and of the effects of these factors on blood flow." In *Theoretical and Clinical Hemorheology*, edited by H. H. Hartert and A. L. Copley. Heidelberg: Apringer-Veilag Berlin, 1971. p. 174.

duPre'Denning, A. and Watson, J. H. "The viscosity of blood." *Proc. Roy. Soc. Ser. B* **78**:328 (1906).

Eagle, H. "Amino acid metabolism in mammalian cell cultures." *Science* **130**:432 (1959).

Eastham, R. D. and Morgan, E. H. "Plasma viscosity in clinical laboratory practice." *J. med. Lab. Technol.* **22**:70 (1965).

Einstein, A. "Eine neue Bestimmung der Molekul-dimensionen." *Ann. der Physik.* **19**:289 (1906).

Erslev, A. J. and Atwater, J. "Effect of MCHC on viscosity." *J. Lab. Clin. Med.* **62**:401 (1963).

Evans, E. A. and Hochmuth, R. M. "A solid-liquid composite model of the red cell membrane." *J. Membrane Biol.* **30**:351 (1977).

Evans, E. A. and Hochmuth, R. M. "Mechanochemical properties of membranes." In Vol. 10 of *Current Topics in Membranes and Transport*, edited by A. Kleinzeller and F. Bonner. Academic Press, 1978. p. 1.

Evans, E. A.; Waugh, R.; and Melnik, L. "Elastic area compressibility modulus of red cell membrane." *Biophys. J.* **16**:585 (1976).

Ewald, C. "Uber die Transpiration des Blutes." *Arch. Anat. Physiol.* **208**:32 (1877).

Fahraeus, R. and Lindqvist, T. "The viscosity of blood in narrow capillary tubes." *Am. J. Physiol.* **96**:562 (1931).

Freund, R. J. and Minton P. D. *Regression Methods: A Tool for Data Analysis.* New York: Marcel Dekker, Inc., 1979.

Goldsmith, H. L. and Mason, S. G. "The microrheology of dispersions." In *Rheology: Theory and Applications*, Vol. 4, edited by F. R. Eirich. New York and London: Academic Press, 1967. p. 85.

Goodeve, C. F. and Whitfield, G. E. "The measurement of thixotropy in absolute units." *Trans. Faraday Soc.* **34**:511 (1938).

Guyton, A. C. *Textbook of Medical Physiology*, 6th edition. Philadelphia: W. B. Saunders Company, 1981.

Hagenbach, E. "Uber die Bestimming der Zahigkeit einer Flussigkeit durch Ausfluss aus Rohren." *Pogg. Ann.* **109**:42 (1860).

Harris, J. W. and Kellermeyer, R. W. "Polycythemia." In *The Red Cell--Production, Metabolism, Destruction: Normal and Abnormal*, 2nd edition. Cambridge, Ma.: Harvard University Press, 1970. p. 661.

Haynes, R. H. "Physical aspects of the mammalian circulatory system." *Trans. Soc. Rheology* **7**:19 (1963).

Hess, W. "Blutviskositat und Blutkorperchen." *Pflugers Arch. ges. Physiol.* **140**:354 (1911).

Hess, W. "Beitrag zum Theorie der Viskositat heterogener Systeme." *Kolloidzeitschrift* **27**:1 (1920).

Hiemenz, P. C. *Principles of Colloid and Surface Chemistry.* New York: Marcel Dekker, Inc., 1977.

Himmelblau, D. M. *Process Analysis by Statistical Methods.* New York: John Wiley & Sons, 1970.

Jeffrey, G. B. "The motion of ellipsoidal particles immersed in a

viscous fluid." *Proc. Roy. Soc. Ser. A* **102**:161 (1923).

Jerrard, H. G. "Turbulence in apparatus for measurement of streaming double refraction." *J. Appl. Physics* **21**:1007 (1950).

Karnis, A.; Goldsmith, H. L.; and Mason, S. G. "Axial migration of particles in Poiseuille flow." *Nature* **200**:159 (1963).

Langstroth, L. "Blood viscosity. I. Conditions affecting the viscosity of blood after withdrawal from the body." *J. exp. Med.* **30**:597 (1919).

Lewry, B. "Die Reibung des Blutes." *Pflugers Arch. ges Physiol.* **65**:26 (1897).

Lux, S. "Hemolytic anemias. III. Membrane disorders." In *Hematology*, 3rd edition, edited by W. S. Beck. Cambridge, Ma.: M.I.T. Press, 1981. p. 197.

MacKenzie, M. R.; Fudenberg, H. H.; and O'Reilly, R. A. "The hyperviscosity syndrome. I. In IgG myeloma. The role of protein concentration and molecular shape." *J. clin. Invest.* **49**:15 (1970).

Mayer, G. A. "Relation of the viscosity of plasma and whole blood." *Am. J. Clin. Path.* **45**:273 (1966).

Mayer, G. A.; Fridrich, J.; Newell, J.; and Szivek, J. "Plasma components and blood viscosity." *Biorheology* **3**:177 (1966).

Meiselman, H. J. *Some Physical and Rheological Properties of Human Blood.* Sc.D. thesis. Cambridge, Mass.: M.I.T., 1965.

Meiselman, H. J.; Merrill, E. W.; Gilliland, E. R.; Pelletier, G. A.; and Salzman, E. W. "Influence of plasma osmolarity on the rheology of human blood." *J. Appl. Physiol.* **22**:772 (1967).

Meiselman, H. J. and Cokelet, G. R. "Blood rheology: Instrumentation and techniques." In *Advances in Microcirculation*, vol. 5, edited by H. Harders. Basil: S. Karger, 1973. p. 32.

Merrill, E. W. "Rheology of blood." *Physiol. Rev.* **49**:863 (1969).

Merrill, E. W.; Gilliland, E. R.; Cokelet, G. C.; Shin, H.; Britten, A.; and Wells, R. E. "Rheology of human blood near and at zero flow. Effects of temperature and hematocrit level." *Biophys. J.* **3**:199 (1963a).

Merrill, E. W.; Cokelet, G. R.; Britten, A.; and Wells, R. E. "Non-Newtonian rheology of human blood: Effect of fibrinogen deduced by 'subtraction'." *Circ. Res.* **13**:48 (1963b).

Merrill, E. W.; Benis, A. M.; Gilliland, E. R.; Sherwood, T. K.; and Salzman, E. W. "Pressure-flow relations of human blood in hollow fibers at low flow rates." *J. Appl. Physiol.* **20**:954 (1965a).

Merrill, E. W.; Margetts, W. G.; Cokelet, G. R.; and Gilliland, E. R. "The Casson equation and rheology of blood near zero shear." In *4th Int. Congress on Rheology, Part 4: Symposium on Biorheology*, edited by A. L. Copley. New York: Interscience Publishers, 1965b. p. 135.

Merrill, E. W.; Margetts, W. G.; Cokelet, G. R.; Britten, A.; Salzman, E. W.; Pennell, R. B.; and Melin, M. "Influence of plasma proteins on the rheology of human blood." In *4th Int. Congress on Rheology, Part 4: Symposium on Biorheology*, edited by A. L. Copley. New York: Interscience Publishers, 1965c. p. 601.

Merrill, E. W.; Gilliland, E. R.; Lee, T. S.; and Salzman, E. W. "Blood rheology: Effect of fibrinogen deduced by addition." *Circ. Res.* **22**:29 (1968).

Moll, K. "Vergleichende Blutuntersuchungen. Viskositats und refraktometrische Bestimmungen des Blutes, Plasmas, und Serums von Hunden, Ratten, Gansen, und Enten, und vergleichen in menschlichen Blut nebst Hamoglobinbestimmungen." *Pflugers Arch. ges. Physiol.* **247**:74 (1943).

Nygaard, K. K.; Wilder, M.; and Berkson, J. "The relation between viscosities of the blood and the relative volume of erythrocytes." *Am. J. Physiol.* **114**:128 (1935).

Oldroyd, J. G. "The elastic and viscous properties of emulsions and suspensions." *Proc. Roy. Soc. Ser. A* **218**:122 (1953).

Oldroyd, J. G. "The effect of interfacial stabilizing film on the elastic and viscous properties of emulsions." *Proc. Roy. Soc. Ser. A* **232**:567 (1955).

Poiseuille, J. L. M. "Recherches experimentales sur le mouvement des liquides dans les tubes de tres-petits diametres." *Compt. Rend. d. Seances de l'Acad. d. Sci.* **16**:60 (1843).

Princen, H. M. "Rheology of foams and highly concentrated emulsions. I. Elastic properties and yield stress of a cylindrical model system." *J. Colloid. Int. Sci.* **91**:160 (1983).

Quemada, D. "Rheology of concentrated disperse systems and minimum energy dissipation principle. I. Viscosity-concentration relationship." *Rheol. Acta* **16**:82 (1977).

Quemada, D. "Rheology of concentrated disperse systems. II. A model for non-newtonian shear viscosity in steady flows." *Rheol. Acta* **17**:632 (1978a).

Quemada, D. "Rheology of concentrated disperse systems. III. General features of the proposed non-newtonian model. Comparison with experimental data." *Rheol. Acta* **17**:643 (1978b).

Quemada, D. "A rheological model for studying the hematocrit dependence of red cell-red cell and red cell-protein interactions in blood." *Biorheology* **18**:501 (1981).

Rand, P. W.; Lacombe, E.; Hunt, H. E.; and Austin, W. H. "Viscosity of normal human blood under normothermic and hypothermic conditions." *J. appl. Physiol.* **19**:117 (1964).

Rand, P. W.; Barker, N.; and Lacombe, E. "Effects of plasma viscosity and aggregation in whole blood viscosity." *Am. J. Physiol.* **218**:681 (1970).

Rand, R. P. "Mechanical properties of the red cell membrane. II. Viscoelastic breakdown of the membranes." *Biophys. J.* **4**:303 (1964).

Rand, R. P. and Burton, A. C. "Mechanical properties of the red cell membrane." *Biophysics J.* **4**:115 (1964).

Riehl, J. "Vergluchende Blutuntersuchungen. Viskositats-und refraktometrische Bestimmungen des Blutes, Plasma, und Serums von Pferden, Rinderu, Schweinen, Schafen, Ziegen und Kaninchen nebst Hamoglobinbestimmungen." *Pflugers Arch. ges. Physiol.* **246**:709 (1943).

Riha, P. "The quantitative description of the viscoelastic properties of human blood." In *Rheology, Proc. of the 8th Int. Congress on Rheology*, Vol. 3. New York: Plenum Press, 1980. p. 575.

Reiner, M. and Scott-Blair, G. "The flow of blood through narrow tubes." *Nature* **184**:354 (1959).

Rosenblum, W. I. "*In vitro* measurements of the effects of anticoagulants on the flow properties of blood: The relationship of these effects to red cell shrinkage." *Blood* **31**:234 (1968).

Rumscheidt, F. D. and Mason, S. G. "Particle motions in sheared suspensions. XI. Internal circulation in fluid drops." *J. Colloid Sci.* **16**:210 (1961a).

Rumscheidt, F. D. and Mason, S. G. "Particle motions in sheared suspensions. XII. Deformation and burst of fluid drops in shear and hyperbolic flow." *J. Colloid Sci.* **16**:238 (1961b).

Saltzman, W. M. *An Investigation of the Hydrodynamic Resistance of Concentrated Layers of Erythrocytes.* S.M. thesis. Cambridge, Mass.: M.I.T., 1984.

Schmid-Schonbein, H.; Wells, R. E.; and Goldstone, J. "Model experiments in red cell rheology: The mammalian red cell as a fluid drop." In *Theoretical and Clinical Hemorheology*, edited by H. H. Hartert and A. L. Copley. Heidelberg: Springer-Veilag Berlin, 1971a. p. 233.

Schmid-Schonbein, H.; Wells, R. E.; and Goldstone, J. "Fluid dop-like behavior of erythrocytes--disturbance in pathology and its quantification." *Biorheology* **7**:227 (1971b).

Secomb, T. W.; Fischer, T. M.; and Skalak, R. "The motion of closed-packed red blood cells in shear flow." *Biorheology* **20**:283 (1983a).

Secomb, T. W.; Chien, S.; Jan, K.-M.; and Skalak, R. "The bulk rheology of close-packed red blood cells in shear flow." *Biorheology* **20**:295 (1983b).

Sherwood, G. K. "Blood groups. II. Transfusion therapy." In *Hematology*, 3rd edition, edited by W. S. Beck. Cambridge, Ma.: M.I.T. Press, 1981. p. 197.

Skalak, R.; Zarda, P. R.; Jan, K.-M.; and Chien, S. "Theory of rouleau formation." In *Cardiovascular and Pulmonary Dynamics*, edited by M. Y. Jaffrin. *Institut National de la Sante et de la Recherche Medical (INSERM)* **77**:299 (1977).

Skalak, R.; Keller, S. A.; and Secomb, T. W. "Mechanics of blood flow." *J. Biomech. Eng.* **103**:102 (1981a).

Skalak, R.; Zarda, P. R.; Jan, K.-M.; and Chien, S. "Mechanics of rouleau formation." *Biophys. J.* **35**:771 (1981b).

Smoluchowski, M. von. "Versuch einer mathematischen Theorie der Koagulationskinetik Kollorder Losunger." *Z. Phys. Chem.* **92**:129 (1917).

Taylor, G. I. "The viscosity of fluid containing small drops of another fluid." *Proc. Roy. Soc. Ser. A* **138**:41 (1932).

Thomas, H. W. and Janes, D. E. "The trapped supernatant in the packed red cell column on centrifugation of bovine red cell suspensions and its relations to the deformability of the red cell." In *Proceedings of the First International Conference on Hemorheology*, edited by A. L. Copley. Oxford: Pergamon Press, 1968. p. 569.

Thurston, G. B. "Viscoelasticity of blood." *Biophysics J.* **12**:1205 (1972).

Thurston, G. B. "Effects of hematocrit on blood viscoelasticity and in establishing normal values." *Biorheology* **15**:239 (1978).

Tolle, H. *Optimization Methods*. New York: Springer-Veilag, Inc., 1975.

Trevan, J. W. "The viscosity of blood." *Biochem. J.* **12**:60 (1918).

Usami, S.; Chien, S.; and Gregersen, M. I. "Viscometric behavior of young